THE AMINO TERMINUS OF MUTANT HUNTINGTIN CAUSES TRANSCRIPTIONAL DYSREGULATION

by

Geraldine Titus Gomez

Submitted in partial fulfillment of the requirements
for the degree of Doctor of Philosophy

at

Dalhousie University
Halifax, Nova Scotia
December 2006

Your file Votre référence
ISBN: 978-0-494-27194-0
Our file Notre référence
ISBN: 978-0-494-27194-0

DALHOUSIE UNIVERSITY

To comply with the Canadian Privacy Act the National Library of Canada has requested that the following pages be removed from this copy of the thesis:

Preliminary Pages

Examiners Signature Page (pii)

Dalhousie Library Copyright Agreement (piii)

Appendices

Copyright Releases (if applicable)

to the memory of David Rodgerson

and

to all families affected by hereditary diseases

TABLE OF CONTENTS

LIST OF FIGURES

LIST OF TABLES

ABSTRACT

Huntington's disease (HD) is a progressive neurodegenerative disorder caused by a mutation in the gene that encodes huntingtin. Although mutant huntingtin is widely expressed throughout the brain and body, the most pronounced neuropathology of HD is of the eventual loss of GABAergic medium spiny neurons in the caudate and putamen. Prior to cell death, intranuclear mutant huntingtin decreases mRNA levels of a small percentage of genes expressed in the caudate and putamen of HD patients and in the striatum of several different models of transgenic HD mice. The mechanism of this mutant huntingtin-induced decrease in selected mRNAs has not yet been defined. It has been hypothesized that mutant huntingtin interacts with transcription factors, sequesters these proteins from active transcriptional complexes thereby leading to the observed decrease in steady-state mRNA levels. The goal of this research was to study the effect of the N-terminal fragment of mutant huntingtin on the expression of the dopamine- and cAMP-regulated phosphoprotein (DARPP-32) and preproenkephalin (ppENK) genes to define the mechanism by which mutant huntingtin down-regulates steady-state mRNA levels of specific genes. The N-terminal fragment of mutant huntingtin lowered steady-state levels of DARPP-32 and ppENK mRNA in the brains of R6 transgenic HD mice to ~ 40-50% of the levels observed in young R6 and wild-type mice. Steady-state levels of DARPP-32 mRNA were not affected in the kidneys of these mice even though the N-terminal fragment of mutant huntingtin was also expressed in the kidney. The N-terminal fragment of mutant huntingtin altered transcription from all start sites of the proximal DARPP-32 and the ppENK promoters. The activity of DARPP-32 and ppENK promoter deletion constructs was lower in the presence of the N-terminal fragment of mutant huntingtin in immortalized striatal cell lines but no difference in transcription factor binding to these promoters were detected. Transient transfection experiments demonstrated that short-term expression of the N-terminal fragment of mutant huntingtin exerted cell- and promoter-specific transcriptional repression of the DARPP-32, ppENK and cytomegalovirus (CMV) promoters. The effects of the N-terminal fragment of mutant huntingtin on transcription were also observed *in vitro* in the presence of purified N-terminal fragment of mutant huntingtin and nuclear proteins isolated from R6 transgenic HD mice. The presence of the amino terminus of huntingtin protein with an expanded polyglutamine repeat in combination with factors present in the wild-type forebrain nuclear extracts decreased the stability of the proteins that interacted with the CMV promoter. Dysregulation of transcription is an early step in HD pathogenesis that likely causes a cascade of changes throughout the brain, neuronal dysfunction and eventually death of susceptible neurons. The N-terminal fragment of mutant huntingtin in concert with tissue- and promoter-specific neuronal factors induce gene-specific transcriptional dysregulation. The N-terminal fragment of mutant huntingtin decreased transcription, not by sequestering proteins away from the promoter, but by directly interacting with the proteins that form the preinitiation complex, altering the stability of the preinitiation complex, which reduced the rate of transcription.

LIST OF ABBREVIATIONS USED

μCi	microcurrie
x *g*	centrifugal force
3-NP	3-nitropropionic acid
5'RLM-RACE	5' RNA ligase-mediated rapid amplification of cDNA ends
A	adenosine
AHRR	aryl hydrocarbon receptor
AMPA	α-amino-3-hydroxyl-5-methyl-4-isoxazolepropionate
ANOVA	analysis of variance
ANS	autonomic nervous system
ATG	translation initiation codon
ATP	adenosine triphosphate
BCA	bicinchoninic acid
BDNF	brain-derived neurotrophic factor
BLAST	basic local alignment search tool
bp	basepair
BSA	bovine serum albumin
C	cytosine
$CaCl_2$	calcium chloride
CAG	glutamine
Camk2a	α-calcium/calmodulin-dependent protein kinase II gene
cAMP	cyclic AMP
CB1	cannabinoid receptor 1
CBP	CREB binding protein
CDEF	cell cycle-dependent element
cDNA	complementary DNA
CIP	calf intestinal phosphatase
CMV	cytomegalovirus
CNS	central nervous system
CREB	cAMP response element binding protein
CRF	corticotrophin releasing factor

CtBP	C-terminal binding protein
CTP	cytosine triphosphase
D_1	dopamine D_1 receptor
D_2	dopamine D_2 receptor
DAB	diaminobenzidine
DARPP-32	dopamine- and cAMP-regulated phosphoprotein M_r 32 kDa
dATP	2'-deoxyadenosine 5'-triphosphate
DMEM	Dulbecco's modified Eagle medium
DNA	deoxyribonucleic acid
dNTPs	deoxynucleotide triphosphates
DTT	dithiothreitol
E2F	elongation factor-2
EDTA	ethylenediaminetetraacetic acid
ESTs	expressed sequence tags
G	guanine
GABA	gamma-aminobutyric acid
GAPDH	glyceraldehyde 3-phosphate dehydrogenase
GFAP	glial fibrillary acidic protein
GFP	green fluorescent protein
GST	glutathione S-transferase
GTP	guanine triphosphate
H_2O	water
H_2O_2	hydrogen peroxide
HAPs	huntingtin-associated proteins
HATs	histone acetyltransferases
HBSS	Hank's buffered salt solution
HCl	hydrogen chloride
HD	Huntington's Disease
HDACs	histone deacetylases
HEAT	Huntingtin, Elongation factor 3, protein phosphatase 2A, Tor1
HEK	human embryonic kidney
HELT	hey-like bHLH-transcriptional repressor

HIPs	huntingtin-interacting protein
HPA	hypothalamo-pituitary-adrenal
HPRT	hypoxanthine phosphorribosytransferase
hr	hour
HYP	huntingtin-yeast partner
IE	immediate-early
IPTG	isopropyl-β-D-thiogalactopyranoside
IT15	Interesting Transcript 15 gene
K+	potassium
KA	kainic acid
kb	kilobase
KCl	potassium chloride
kDa	kilodalton
KID	kidney
KO	knockout
KOH	potassium hydroxide
M	molar
M1F1	MIBP-1/RFX1 complex
MAP2	microtubule-associated protein-2
$MgCl_2$	magnesium chloride
mGluR1	metabotropic glutamate receptor-subtype 1
MIBP-1/RFX1	c-myc intron 1 binding protein 1/ regulatory factor that bind to the X box 1
min	minutes
mM	millimolar
MMLV	Moloney Murine Leukemia Virus
MMLV-RT	mMLV-Reverse Transcriptase
MOK2	ribonucleoprotein associated zinc finger protein
MPC	magnetic particle concentrator
mRNA	messenger ribonucleic acid
MZF-1	myeloid zinc finger protein
Na+	sodium

NAA	*N*-acetylaspartate
NaCl	sodium chloride
NCoR	nuclear corepressor
NE	nuclear extract
NFAT	nuclear factor of activated T-cells
NFKB	NF-KappaB
ng	nanogram
NH_4	ammonium
NIIs	neuronal intranuclear inclusions
nM	nanomolar
NMDA	*N*-methyl-D-aspartate
NP-40	nonidet P-40
NR1	NMDA receptor 1
NR2	NMDA receptor 2
NRSF	neuron restrictive silencer factor
nts	nucleotides
NUDR	nuclear deformed epidermal autoregulatory factor-1 related transcriptional regulatory protein
OD	optical density
OLF1	olfactory neuron-specific factor 1
P/CAF	p300/CBP-associated factor
p53	tumor protein 53
PAGE	polyacrylamide gel electrophoresis
PBS	phosphate buffered saline
PCR	polymerase chain reaction
PDE10A	phosphodiesterase 10A
pg	picogram
PKA	protein kinase A
PKC	protein kinase C
pmol	picomole
PMSF	phenylmethylsulphonyl fluoride
PNK	T4 polynucleotide kinase

PO_4	phosphate
PP-1	protein phosphatase 1
ppENK	preproenkephalin
PPT	preprotachykinin
PQBP	polyglutamine binding protein-1
PVN	paraventricular nucleus
qRT-PCR	quantitative RT-PCR
RAP30	RNA polymerase II associating protein 30
RAP74	RNA polymerase II associating protein 74
REST	repressor element-1 silencing transcription factor
RLM-RACE	RNA ligase mediated rapid amplification of cDNA ends
RNA	ribonucleic acid
RNase	ribonuclease
rNTPs	ribonucleotides
RPA	RNase protection assay
RREB1	ras-responsive element binding protein 1
RT	reverse transcriptase
RT-PCR	reverse transcriptase polymerase chain reaction
RXR	retinoid x γ receptor
SAHA	suberoylanilide hydroxamic
SDH	succinate dehydrogenase
SDS	sodium dodecyl sulfate
SDS-PAGE	sodium dodecyl sulfate-polyacrylamide gel electrophoresis
sec	second
SEM	standard error of the mean
SFM	serum free media
siRNA	small interfering RNA
Sp1	specificity protein 1
SSC	sodium chloride-sodium citrate
SSRIs	selective serotonin reuptake inhibitors
STAT	signal transducers and activators of transcription
T	thymidine

TAFs	TBP-associated factors
TAP	tobacco acid pyrophosphatase
TBE	tris-borate-EDTA
TBP	TATA binding protein
TBS	tris-buffered saline
TBS-T	tris-buffered saline- Tween
TdT	terminal deoxynucleotide transferase
TE buffer	Tris-HCl and EDTA
TFIIA	general transcription factor IIA
TFIIB	general transcription factor IIB
TFIIC	general transcription factor IIC
TFIID	general transcription factor IID
TFIIE	general transcription factor IIE
TFIIF	general transcription factor IIF
TFIIG	general transcription factor IIG
TFIIH	general transcription factor IIH
TK	thymidine kinase
tRNA	transfer RNA
U	uracil
UTP	uridine 5'-triphosphate
UTR	untranslated regions
UV	ultraviolet
v/v	volume/volume
w/v	weight/volume
WT	wild-type
YAC	yeast-derived artificial chromosome

ACKNOWLEDGEMENTS

I would like to acknowledge my supervisor Dr. Eileen Denovan-Wright for her guidance, encouragement and endless support. I thank her for taking me under her wing and teaching me the ABCs of performing research in molecular biology. She has encouraged me to think critically and challenged me to become a better researcher. I am extremely grateful for her support over the past four years, especially while I was writing this thesis. I will always have fond memories of running into her office with a "quick question" only to still be there twenty minutes later talking science. I will greatly miss those discussions not to mention all the morning and afternoon "pep-talk and shoulder massage" sessions.

I wish to thank Dr. Elena Cattaneo for the gift of the immortalized ST14A cells and their derivatives; Dr. Beverly Davidson for the gift of the shRNAvec and shHD2.1 vectors; Dr Xiao-Jiang Li for the gift of the vectors that generated His-23Q and His-87Q and Dr. Mark Nachtigal for the gift of the pCMV-Luc vector. I am grateful to Michael Fitzgerald for his assistance with the densitometric analysis of data presented in figures 3-9 and 3-10. I thank Min Huang, Kathleen Murphy and Janette Nason for the technical help they have provided over the course of my degree. I would also like to acknowledge the Canadian Institutes of Health Research (CIHR), National Science and Engineering Research Council (NSERC) and the Killam Trust for funding.

I thank the past and present members of the EDW lab especially Andrea, Elizabeth, Marissa, Matt and Mike for making the last four and half years very enjoyable. A special thank you goes to Haibei my "lab buddy" from the very beginning. I would also like to acknowledge the Department of Pharmacology and the members of 15 East for their assistance and companionship.

My heartfelt thanks go to my family. None of this would have been possible without their love and support. Mom and Dad, thank you for everything you have done for me especially while I was busy writing this thesis. Thank you for the packed lunches and suppers, for the laundry, but most importantly for all the prayers. Simon, Valentine and Alwyn you guys are the best!! Thank you for the prayers, the hugs (just when I needed them) and for keeping me company at 12:30 am while I ate supper. I love you all very much. Dad, I'm finally done!!

I would like to thank my friends at St. Ignatius Parish in Bedford, Catholic Christian Outreach (Halifax) and the St. Joseph's Newman Centre at Dalhousie University. They have been an integral part of the past four years of my life and I thank them for all their prayers and support.

I thank God for giving me the opportunity to pursue my graduate degree and for the strength to complete this task. All that I am and all that I can accomplish is because of Him.

"For I know well the plans I have in mind for you' says the Lord, 'plans for your welfare, not for woe – plans to give you a future full of hope."~ Jeremiah 29:11

CHAPTER 1

Introduction

1.1 Huntington's Disease

In April 1872, George Huntington made a major contribution to medical research by publishing a detailed report in the Medical and Surgical Reporter (Philadelphia) on an inherited form of chorea. The disease he described eventually came to bear his name, Huntington's chorea, now called Huntington's Disease (HD). Huntington came from several generations of physicians and as a young child accompanied his father and grandfather on medical rounds. Based on his own observations of patients, as well as the observations of his father and grandfather, he was able to obtain a crucial longitudinal point of view that spanned 78 years and gave him a unique perspective on this hereditary disease [Huntington (1872) as republished in Huntington (2003)]. In his publication, Huntington defined the essential features of this disorder as "1, its hereditary nature; 2, a tendency to insanity and suicide; 3, its manifesting itself as a grave disease only in adult life." (Huntington, 2003)

HD is currently characterized by the clinical triad of movement disorder, dementia and psychiatric disturbances. HD typically develops in the fourth or fifth decade of life. In the early stages of the disease patients develop minor involuntary movements of the face, fingers, feet or thorax (Folstein *et al.*, 1986; Vonsattel & DiFiglia, 1998). The patient population is heterogeneous with respect to psychiatric disturbances including depression, anxiety, apathy and irritability and these aspects of the disease can occur prior to the onset of the choreiform movements (Craufurd *et al.*, 2001). As HD progresses, the affected person develops overt choreiform movements of the head, neck, arms and legs. Patients also show cognitive deficits such as impairments of memory and language comprehension, the severity of which parallels disease progression

(Bachoud-Levi *et al.*, 2001). In the late stages of the disease patients become severely rigid and akinetic. They also have severe dementia, eventually ceasing to talk and becoming unable to care for themselves. The duration of the disease ranges from 10 to 20 years after the first symptoms appear and inevitably ends in death (Borrell-Pages *et al.*, 2006).

Pathologically, HD is characterized by the selective loss of efferent medium spiny neurons in the caudate nucleus and the putamen and, to a lesser extent, other neurons within the basal ganglia (Vonsattel *et al.*, 1985). In humans, the caudate nucleus and putamen are mainly comprised of GABAergic (gamma-aminobutyric acid) medium spiny projection neurons that either express enkephalin or substance P and dynorphin (Gerfen, 1992). The GABA/enkephalin-positive neurons that project to the lateral globus pallidus are lost early in the progression of HD (Ferrante *et al.*, 1986). Subsequently, the GABA/substance P-positive efferent neurons that terminate in the internal pallidal region and the substantia nigra are also lost (Ferrante *et al.*, 1986). Unlike the medium-spiny projection neurons, interneuron populations within the caudate and putamen are relatively spared in HD (Dawbarn *et al.*, 1985; Ferrante *et al.*, 1985). Although the caudate and putamen are the regions most affected by atrophy and neuronal loss in HD, degeneration of neurons in the cortex, thalamus and subthalamic nucleus have also been reported in HD (Cudkowicz & Kowall, 1990; Hedreen *et al.*, 1991) implying that the caudate and putamen are selectively vulnerable to cell death (Leegwater-Kim & Cha, 2004). The Vonsattel scale is commonly used to grade the severity of HD pathology into five grades (0-4). Patients classified as grade 0 do not have any apparent pathology in post-mortem observations but have been described as symptomatic suggesting that early neuronal

dysfunction induces behavioural changes and that this neuronal dysfunction precedes neurodegeneration.

HD is the most common inherited neurodegenerative disorder worldwide wih a single genetic cause. It has a prevalence of 4 to 7 per 100,000 (Landles & Bates, 2004). It afflicts 30,000 people in the US and another 250,000 people are at risk to develop the disease based on the known inheritance patterns within families with affected family members (Leegwater-Kim & Cha, 2004). HD varies in prevalence between ethnic groups with a prevalence of 1 in 10,000 in the UK compared to a prevalence of 1 in 1,000,000 in Japanese and African populations (Rubinsztein, 2002). HD was originally described in North America in families of British descent; it is found in all major regions of the world whose population is predominantly of European origin including North and South America and Australia (Harper, 1992). The largest and concentration of patients with HD inhabit the region around Lake Maracaibo in Venezuela. In this region there is a very high frequency of HD. The high incidence of this disease in Venezuela is explained by the founder effect. In the 19th century a single woman who developed HD moved into the area and had a large number of descendents. Today, the prevalence of HD in the Lake Maracaibo region of Venezuela is 700 per 100,000.

In 1983, the gene that causes HD was first mapped by linkage to the tip of the short arm of chromosome 4 (Gusella *et al.*, 1983). The *HD* gene, also known as Interesting Transcript 15 (*IT15*), was not isolated until 1993 (The Huntington's Disease Collaborative Research Group, 1993). In 1993, following a large collaborative effort it was determined that HD is caused by an expansion of a CAG trinucleotide repeat in a polymorphic region of exon 1 of the *HD* gene. Individuals that have between 6-35 CAG

repeats at this position in both copies of the *HD* gene do not develop Huntington's disease, while individuals that have CAG repeat lengths of 40-50 units in one *HD* gene develop Huntington's disease between 30 and 40 years of age (Gusella *et al.*, 1993). Individuals with CAG repeats over 60 in one copy of the *HD* gene have severe juvenile HD with an appearance of symptoms before the age of 20 (Snell *et al.*, 1993). Individuals with one copy of *HD* with a CAG repeat length ranging from 36-39 have an increased risk of developing HD (Rubinsztein *et al.*, 1996). There is an inverse correlation with the length of the repeat and the age of onset. It should be noted that this correlation is strongest for repeat lengths greater than 70 CAG repeats (Telenius *et al.*, 1993). The correlation is less robust for the majority of patients that have less than 70 reiterations of the CAG repeat (Duyao *et al.*, 1993; Telenius *et al.*, 1993; The Huntington's Disease Collaborative Research Group, 1993; Ho *et al.*, 2001). The CAG repeat size is not the only determining factor of the age of onset of HD symptoms. Recently, it was determined that the variability in age of onset is also familial and can be attributed to genetic or shared environmental factors or both (Li *et al.*, 2003; Wexler *et al.*, 2004). The CAG repeat length is unstable and changes size from one generation to the next particularly when passed through the male germline where expansions tend to occur more frequently than contractions (Duyao *et al.*, 1993; Telenius *et al.*, 1995). Thus the CAG repeat numbers tend to increase and the age of onset tends to decrease in successive generations in families (Ho *et al.*, 2001).

1.2 Current Treatments

Currently, there is no effective therapeutic option for HD and there are no therapies which significantly slow the progression of the disease or delay its onset. Current therapies are aimed at treating disease symptoms. Fluphenazine, tetrabenazine, and haloperidol are used to treat choreic movements associated with HD (Terrence, 1976; Asher & Aminoff, 1981; Bonelli *et al.*, 2004b). Tricyclic antidepressants and selective serotonin reuptake inhibitors (SSRIs) are used to treat depression (Handley *et al.*, 2006). Chlorpromazine, clozapine, risperidone, quetiapine are used to treat psychological disturbances (Bonelli *et al.*, 2004b; Handley *et al.*, 2006). Many potential therapies have been tested in genetic models of HD (Li *et al.*, 2005). Many clinical trials have already occurred or are currently underway. These include Dimebon, minocycline, ethyl-epicosapentaenoic acid, phenylbutyrate, coenzyme Q10, remacemide, riluzole and creatine. Clinical trials have determined that minocycline treatment stabilizes general motor and neuropsychological function and improves psychiatric symptoms in HD patients (Denovan-Wright *et al.*, 2002; Bonelli *et al.*, 2004a). Alternatively, fetal tissue transplantation to the striatum has been attempted to treat HD in humans and has a favorable effect (Bachoud-Levi *et al.*, 2000; Hauser *et al.*, 2002; Gaura *et al.*, 2004). These therapies may delay the progression of the disease but are not effective in preventing or treating all symptoms of HD.

1.3 Wild-type Huntingtin

The *HD* gene encodes a transcript containing the sequence of 67 exons, which is translated into a protein of 348 kDa called huntingtin (The Huntington's Disease

Collaborative Research Group, 1993; Ambrose *et al.*, 1994). This protein is a widely expressed in the human body and homologs of huntingtin are found in all vertebrates and in *Drosophila* (Li *et al.*, 1993; DiFiglia *et al.*, 1995; Sharp *et al.*, 1995; Bhide *et al.*, 1996; Li *et al.*, 1999b). There is little conserved sequence similarity between huntingtin and other proteins other than a region of contiguous glutamine residues (polyQ) and HEAT repeats (Andrade & Bork, 1995). The HEAT acronym refers to the first four proteins in which these motifs were detected (Huntingtin, Elongation factor 3, protein phosphatsase 2A, Tor1 rapamycin target protein). HEAT repeats are 40 amino acid motifs that normally appear in tandem arrays. HEAT repeats are evenly distributed in the huntingtin protein (Andrade & Bork, 1995; Takano & Gusella, 2002). The huntingtin protein is thought to contain 40-66 repeats encompassing about 80% of the protein (Takano & Gusella, 2002; Truant, 2003). The function of HEAT repeats is currently unknown but they may play a scaffolding role in the formation of particular protein-protein interactions (Takano & Gusella, 2002).

Despite 15 years of research, there is still no concensus regarding the primary function of normal huntingtin (Cattaneo *et al.*, 2005). Huntingtin is essential for embryonic development, as its inactivation in huntingtin-knockout mice causes embryonic death before day 8.5 (Duyao *et al.*, 1995; Nasir *et al.*, 1995; Zeitlin *et al.*, 1995). Huntingtin is also important in adulthood since 12 week-old heterozygous knockout mice displayed increased motor activity and significant neuronal loss in the subthalamic nucleus (Nasir *et al.*, 1995). Huntingtin is enriched in membrane-containing cell fractions and has been implicated in vesicle transport and synaptic function as it is known to associate with clathrin through huntingtin-interacting protein (Engqvist-

Goldstein *et al.*, 2001; Metzler *et al.*, 2001; Waelter *et al.*, 2001b). It has also been suggested that huntingtin might be an anti-apoptotic protein as abnormally high levels of apoptosis were observed in HD-knockout embryos (Zeitlin *et al.*, 1995) and over expression of wild-type huntingtin protects cells against a variety of apoptotic stimuli (Rigamonti *et al.*, 2000). Huntingtin may also facilitate gene transcription. Mice that express full-length wild-type human huntingtin following inheritance of a yeast-derived artificial chromosome (YAC) in addition to the two copies of mouse huntingtin have increased brain-derived neurotrophic factor (BDNF) protein levels in the cortex due to up regulation of *BDNF* transcription by wild-type huntingtin (Zuccato *et al.*, 2001). Wild-type huntingtin promotes *BDNF* transcription by sequestering the available repressor element 1-silencing transcription factor (REST; also known as neuronal restrictive silencing factor, NRSF) in the cytoplasm, thereby preventing it from forming a repressor complex in the nucleus and thus allowing transcription to occur (Zuccato *et al.*, 2003).

1.4 Gain-of-function of Mutant Huntingtin

Several considerations suggest that the pathogenesis of HD involves a gain of function for the mutant protein and that the human huntingtin gene product with an expanded polyglutamine region has a function distinct from that encoded by the wild-type huntingtin gene (Ross, 1995a). Huntington's disease has a dominant inheritance which suggests that the mutation leads to a novel function of the encoded protein. HD patients that are homozygous for two copies of *HD* with CAG repeats longer than 40 are clinically indistinguishable from individuals that are heterozygous for the gene suggesting that the normal allele in heterozygote individuals does not attenuate the

disease phenotype (Wexler *et al.*, 1987; Myers *et al.*, 1989). The inheritance patterns also suggest that mutant huntingtin maintains the normal function of huntingtin in addition to having the toxic effect associated with development of HD (Everett & Wood, 2004). Homozygous knock-in mice with expanded CAG repeats in the homolog of the human huntingtin gene in mice develop normally indicating that mutant huntingtin retains the developmental functions of wild-type huntingtin (White *et al.*, 1997). Furthermore, individuals that have Wolf-Hirschhorn syndrome have a deletion of the short arm of chromosome 4 containing the huntingtin allele. These individuals do not have HD symptoms (Ambrose *et al.*, 1994; Housman, 1995). They display symptoms including mental retardation, epilepsy, growth delay and cranio-facial dysgenesis (Bergemann *et al.*, 2005). In addition, mice that were heterozygous for huntingtin inactivation are phenotypically normal (Duyao *et al.*, 1995; Zeitlin *et al.*, 1995). A knockout mouse model was created by a targeted disruption in exon 5 of the homolog of the human huntingtin gene in mice (Nasir *et al.*, 1995). These mice produce a truncated N-terminal fragment of the huntingtin protein. They have significant neuronal loss in the subthalamic nucleus and increased motor activity. These studies demonstrated that huntingtin plays an essential role during development and that a loss of function of the huntingtin protein, by itself, does not account for the HD pathology.

A conditional knock-out model of huntingtin using the Cre-loxP site-specific recombination system to generate mice in which the *Cre* gene is expressed under the neuron-specific promoter of the *Camk2a* gene (α-calcium/calmodulin-dependent protein kinase II) was developed (Dragatsis *et al.*, 2000). These conditional knockout mice exhibit a progressive motor phenotype, which is evident by 10-12 months and have a

reduced life-span. Neurodegeneration of the striatum and cortex is also observed in these conditional knockout mice, implying that loss of huntingtin function may contribute to the pathology of the HD phenotype. The loss of normal huntingtin function, due to the presence of mutant huntingtin, could contribute to pathogenesis of the disease. Huntingtin plays a role in up regulating *BDNF* transcription (Zuccato *et al.*, 2001). Striatal neurons require cortical BDNF for their survival. However, in the presence of mutant huntingtin this effect is lost (Zuccato *et al.*, 2001). Mutant huntingtin may sequester wild-type huntingtin and alter its normal function.

The expansion of the polyglutamine region confers a novel deleterious effect on the mutant huntingtin protein. Although previous work had shown that inactivation of the hypoxanthine phosphoribosytransferase (HPRT) gene does not cause deleterious effects, mice in which a 146 CAG repeat was inserted into the HPRT gene, produce a polyglutamine-expanded form of the HPRT protein and develop a late-onset neurological phenotype (Ordway *et al.*, 1997). This provides further evidence that HD is caused by a gain of function rather than only by a loss of wild-type huntingtin function.

1.5 Proteolytic Cleavage of Huntingtin by Caspases

Proteolytic cleavage of mutant huntingtin has been proposed to play a role in the pathogenesis of HD. The huntingtin protein undergoes proteolytic cleavage by caspase-3 at amino acids 513 and 552, by caspase-2 at amino acid 552 and by caspase-6 at amino acid 586 (Goldberg *et al.*, 1996; Wellington *et al.*, 1998; Wellington *et al.*, 2000). Cleavage of normal huntingtin and huntingtin with an expanded polyglutamine region preferentially occurs at amino acid 552 of human huntingtin *in vivo* (Wellington *et al.*,

2002). This cleavage produces an N-terminal huntingtin fragment containing the polyglutamine region and is observed in wild-type and YAC transgenic HD mice expressing full-length human huntingtin with 72 CAG repeats prior to the onset of neurodegeneration (Wellington *et al.*, 2002).

Huntingtin does not have an evident nuclear localization signal, however, both full-length and the amino terminus of wild-type huntingtin have been detected in nuclei of normal human fibroblasts and mouse clonal striatal cells (Kegel *et al.*, 2002). The carboxy-terminus of huntingtin contains a nuclear export signal and the levels of full-length huntingtin in the nucleus are lower than levels observed in the cytoplasm (Kegel *et al.*, 2002; Xia *et al.*, 2003). In the diseased state, N-terminus fragments of mutant huntingtin with an expanded polyglutamine repeat accumulate in the nucleus (Davies *et al.*, 1997; DiFiglia *et al.*, 1997; Hackam *et al.*, 1998). There is clear evidence that the N-terminal mutant huntingtin fragment containing an expanded polyglutamine region is toxic to cells (Cooper *et al.*, 1998; Hackam *et al.*, 1998; Martindale *et al.*, 1998) especially when targeted to the nucleus of cultured striatal neurons (Saudou *et al.*, 1998; Li *et al.*, 1999a; Peters *et al.*, 1999). Furthermore, blocking nuclear localization of mutant huntingtin by adding a nuclear export signal to the protein suppressed the ability of the amino terminus of mutant huntingtin to form intranuclear inclusions and to induce neurodegeneration (Saudou *et al.*, 1998).

1.6 Neuronal Intranuclear Inclusions in HD

Neuronal intranuclear inclusions (NIIs) have been reported in the neurons of HD patients (DiFiglia *et al.*, 1997; Becher *et al.*, 1998). Aggregates are also found in post-

mortem human HD brains in cortical and striatal neurons and in dystrophic neurites (Vonsattel & DiFiglia, 1998; Ho *et al.*, 2001). These NIIs react with N-terminal huntingtin antibodies but not antibodies to the C-terminal region of the protein (DiFiglia *et al.*, 1997; Becher *et al.*, 1998). Moreover, a 40 kDa polypeptide that contains the polyglutamine tract is enriched in nuclear fractions taken from homogenates of human HD brains indicating that NIIs contain N-terminal fragments of huntingtin (DiFiglia *et al.*, 1997; Ross, 1997). Furthermore, co-localization of ubiquitin with NIIs suggests that the cell targets misfolded and aggregated huntingtin to an ineffective proteasome degradation pathway, as the presence of the N-terminal fragment of mutant huntingtin inhibits proteasome function (Bence *et al.*, 2001).

The role of these neuronal aggregates in the pathology of HD is controversial. It has been suggested that NIIs could play a causative role in the pathology of HD (Davies *et al.*, 1997; DiFiglia *et al.*, 1997). Initial data pointed towards a pathogenic effect of the aggregates as they appear prior to onset of symptoms of disease in a transgenic mouse model expressing exon 1 of the HD gene with an expanded polyglutamine region (Davies *et al.*, 1997). Knock-down of huntingtin expression in a conditional mouse model eliminated both the behavioural phenotype and inclusions (Yamamoto *et al.*, 2000) reinforcing the idea that NII formation and changes in phenotype were linked. Nevertheless, some studies have argued against a direct association between NIIs and cell death and suggested that NIIs are protective (Lunkes & Mandel, 1998; Saudou *et al.*, 1998; Lunkes *et al.*, 1999). Blocking nuclear accumulation of the N-terminal of mutant huntingtin *in vitro* suppress the ability of the protein to form NIIs and result in an increase in mutant huntingtin-induced death (Saudou *et al.*, 1998). This implies that the

aggregates are part of a cell detoxifying mechanism and that free mutant huntingtin is more toxic than mutant huntingtin fragments within nuclear inclusions. Finally, it is also possible that NII formation is a secondary phenomenon. Formation of NIIs reduced the intracellular levels of diffuse mutant huntingtin and prolonged survival in transient transfections of rat primary striatal cultures (Arrasate *et al.*, 2004). This indicated that NIIs form from soluble huntingtin and that NIIs lessen the toxicity of soluble mutant huntingtin. Despite all of the controversy, there is abundant data in both animal and cell culture models to indicate that a key property distinguishing mutant and wild-type huntingtin N-terminal fragments is the tendency for the mutant protein to aggregate (Cooper *et al.*, 1998; Hackam *et al.*, 1998).

1.7 Excitotoxicity of Neurons

Chronic exposure of neurons to excitatory amino acids like glutamate leads to neurodegeneration (Lipton & Rosenberg, 1994). As the striatum receives large glutamatergic input from corticostriatal afferents, the structure is at risk of glutamate-mediated excitotoxic injury. Glutamate is released by cortical efferents in the striatum, where it activates *N*-methyl-D-aspartate (NMDA), α-amino-3-hydroxyl-5-methyl-4-isoxazolepropionate (AMPA) and kainic acid (KA) subtypes of glutamate receptors, as well as the metabotropic glutamate receptors. A disproportionate loss of glutamate receptors, particularly NMDA receptors, is observed in symptomatic and pre-symptomatic HD patients (Greenamyre *et al.*, 1985; Young *et al.*, 1988; Albin *et al.*, 1990) implying that these receptors may play a role in the pathogenesis of the disease. In addition, intrastriatal injections of glutamate agonists, such as the NMDA agonist

quinolinic acid has been shown to closely mimic in rats the neuropathology observed in HD patients by causing selective degeneration of medium spiny neurons but not interneurons (Beal *et al.*, 1986; Beal *et al.*, 1989; Beal *et al.*, 1991). The excitotoxic hypothesis, although persuasive, does not explain certain features of HD. Glutamate receptors are also expressed in similar or even higher levels in the hippocampus, cortex and cerebellum yet there is selective loss of striatal neurons in HD. Furthermore, the selective loss of medium spiny neurons but sparing of the interneurons in the striatum also remains unexplained. The NMDA receptors are composed of two NR1 subunits and two of the NR2A, NR2B, NR2C or NR2D subunits (Dingledine *et al.*, 1999). Although NR1 subunits are widely distributed throughout the brain, each of the NR2 subunits shows a more discrete distribution. Therefore, it has been hypothesized that mutant huntingtin selectively enhances function of the neuronal NR2B-type NMDA receptors contributing to the selective vulnerability of striatal medium spiny neurons to NMDA-induced cell death in HD (Zeron *et al.*, 2001; Raymond, 2003).

1.8 Animal Models of HD

Prior to the development of transgenic models, excitotoxic lesions by intrastriatal injections of quinolinic acid and metabolic impairments by administration of 3-nitropropionic acid (3-NP) were the only means of reproducing a pattern of striatal neurodegeneration resembling human HD in animals (Beal *et al.*, 1986; Brouillet *et al.*, 1995). However, HD is caused by the expression of mutant huntingtin in viable cells that continue to survive for extended periods of time. Neurodegeneration is only the end result of the effects of mutant huntingtin in these cells. Furthermore, the effects of

mutant huntingtin by the end-stages of the disease are not specific to the striatum. Although there is severe atrophy in the striatum, there is also degeneration of neurons in other areas of the brain (Cudkowicz & Kowall, 1990; Hedreen *et al.*, 1991). Thus the excitotoxic model was not an appropriate model to analyze disease progression.

The development of transgenic mice has allowed for the more precise reproduction of the pathology of HD and analysis of changes that occur during disease progression. Several HD models have been generated and each model has strengths and limitations. No single model can recapitulate the human pathology entirely since this disease develops over decades in humans. An analysis of complementary data from different models may provide a global picture of HD pathogenesis.

There are two general types of HD models in mice. These include knock-in models where one of the copies of the mouse huntingtin gene has an extended CAG repeat and transgenic HD mice. The transgenic animals have a full complement of normal mouse huntingtin genes and protein and express either full-length human mutant huntingtin or the N-terminal region of human mutant huntingtin.

1.8.1 Knock-in Models of HD

The knock-in models of HD are created by the insertion of an expanded CAG repeat into the endogenous mouse huntingtin gene. Currently there are five knock-in mouse models of HD (Sipione & Cattaneo, 2001). They differ with respect to the length of the CAG that are inserted into the mouse homolog of the human huntingtin gene. In the models, the size of the repeat ranges from 50 to 150 CAG units. The knock-in mouse models also differ with respect to the genetic background of the mouse strain. In two

knock-in mouse models, the mice displayed an early onset of aggressive behaviour from approximately 3 months of age onwards and abnormal paw clasping from 5 months of age onwards (Shelbourne *et al.*, 1999; Lin *et al.*, 2001). The knock-in mouse model in which 150 CAG repeats have been inserted in the homolog of the human huntingtin gene in mice display behavioural and neurological features resembling HD (Lin *et al.*, 2001). However, no gross neurological phenotype has been observed in this knock-in mouse model when compared to wild-type littermates. The N-terminal fragments of the mutant huntingtin protein accumulate in the nucleus as nuclear aggregates in four of the five knock-in models (White *et al.*, 1997; Shelbourne *et al.*, 1999; Wheeler *et al.*, 1999; Lin *et al.*, 2001).

1.8.2 Full-length Mutant Huntingtin Models of HD

Transgenic mice expressing full-length mutant human huntingtin cDNA under the control of the cytomegalovirus (CMV) promoter have been developed (Reddy *et al.*, 1998). In these transgenic mice, huntingtin is widely expressed in the brain and in the periphery. Neuronal loss is observed in the striatum and to a lesser extent in the cortex, hippocampus and thalamus of these transgenic mice. The entire human huntingtin gene cloned into a YAC has also been used to generate a transgenic mouse model expressing full-length mutant huntingtin under the control of the human huntingtin promoter (Hodgson *et al.*, 1999). These mice express huntingtin in a pattern that is similar to those of HD patients with the highest levels of expression in the brain and in the testes (Hodgson *et al.*, 1999). In these mice, translocation of the N-terminal portion of mutant huntingtin to the nucleus selectively occurs in the medium spiny neurons, where these

fragments aggregate and form NIIs (Hodgson *et al.*, 1999). The full-length models of HD allow for the study of the over-expression of mutant huntingtin, independent of the loss of function of the wild-type huntingtin protein. This provides an advantage over knock-in models where effects of both the gain of function of mutant huntingtin and loss of function of wild-type huntingtin are observed.

1.8.3 Truncated N-terminal Mutant Huntingtin Models of HD

There are several transgenic mouse models that express N-terminal truncated mutant huntingtin. Transgenic mice that express an N-terminal truncated huntingtin cDNA that contains 82 glutamines and encompasses the first 171 amino acids of human huntingtin (N171-82Q) were developed (Schilling *et al.*, 1999). The expression of the transgene was directed by the mouse prion protein promoter vector that drives the expression of foreign genes in virtually every neuron in the CNS. Behavioural and pathological abnormalities and formation of NIIs are observed in this transgenic mouse model. Another N-terminal transgenic HD mouse model is the conditional mouse model using the tetracycline-responsive gene system that contains a chimeric mouse/human exon 1 of huntingtin with 94 glutamine repeats (Yamamoto *et al.*, 2000). These HD 94 mice showed the typical behaviour and progressive neurodegenerative features observed in other models including clasping, reduction in striatum size and reactive gliosis. However, upon suppression of mutant huntingtin expression by administration of the tetracycline homolog, doxycycline, the progressive neurodegeneration was stopped. The NIIs that were present in the striatum and cortex of these mice disappeared and the motor dysfunction was reversed (Yamamoto *et al.*, 2000). Another transgenic HD model that

expresses the N-terminus of mutant huntingtin is the R6 model. This was the first transgenic model of HD developed and different lines of the R6 mice express exon 1 of the human *HD* gene with 115-150 glutamine repeats under the control of the endogenous human huntingtin promoter (Mangiarini *et al.*, 1996). The R6 transgenic mice express the truncated N-terminal fragment of mutant huntingtin containing the first 89 amino acids of mutant huntingtin with 115-150 glutamine repeats (N89-115Q or N89-150Q). The resulting levels of transgene expression are ~ 31% and 75% of the endogenous huntingtin in the R6/1 and R6/2 mice, respectively (Mangiarini *et al.*, 1996). Behavioural changes in the R6/1 and R6/2 mice develop over time. The changes that occur in the R6/2 mice occur in the R6/1 mice model, however the onset of changes is delayed by several weeks in the R6/1 mice and there is a slower progression of the disease (Fig. 1-1). The rotarod is frequently used to monitor progressive decline in motor coordination in mice. The R6/2 mice start having difficulties maintaining their balance on the rotarod at 5-6 weeks of age prior to the onset of overt phenotypical signs (Carter *et al.*, 1999). At approximately 8 weeks of age, the R6/2 mice have reduced motor activity and become hypoactive (Carter *et al.*, 1999; Luesse *et al.*, 2001). Starting at ~8 weeks of age, these mice also begin to show abnormal rear paw clasping. The pathophysiology of this abnormal response is not fully understood but when R6 mice are suspended by the tail they clasp their hind- and forelimbs tightly to their thorax and abdomen. When placed in the same suspended position, wild-type mice spread their four limbs and actively look for a surface to land on. Typically, R6/2 mice are severely impaired by 8-12 weeks of age, whereas R6/1 mice have experienced a profound decline in motor coordination at ~ 13-20 weeks of age. The brains of 12 week-old R6/2 mice weigh ~ 20% less than brains from

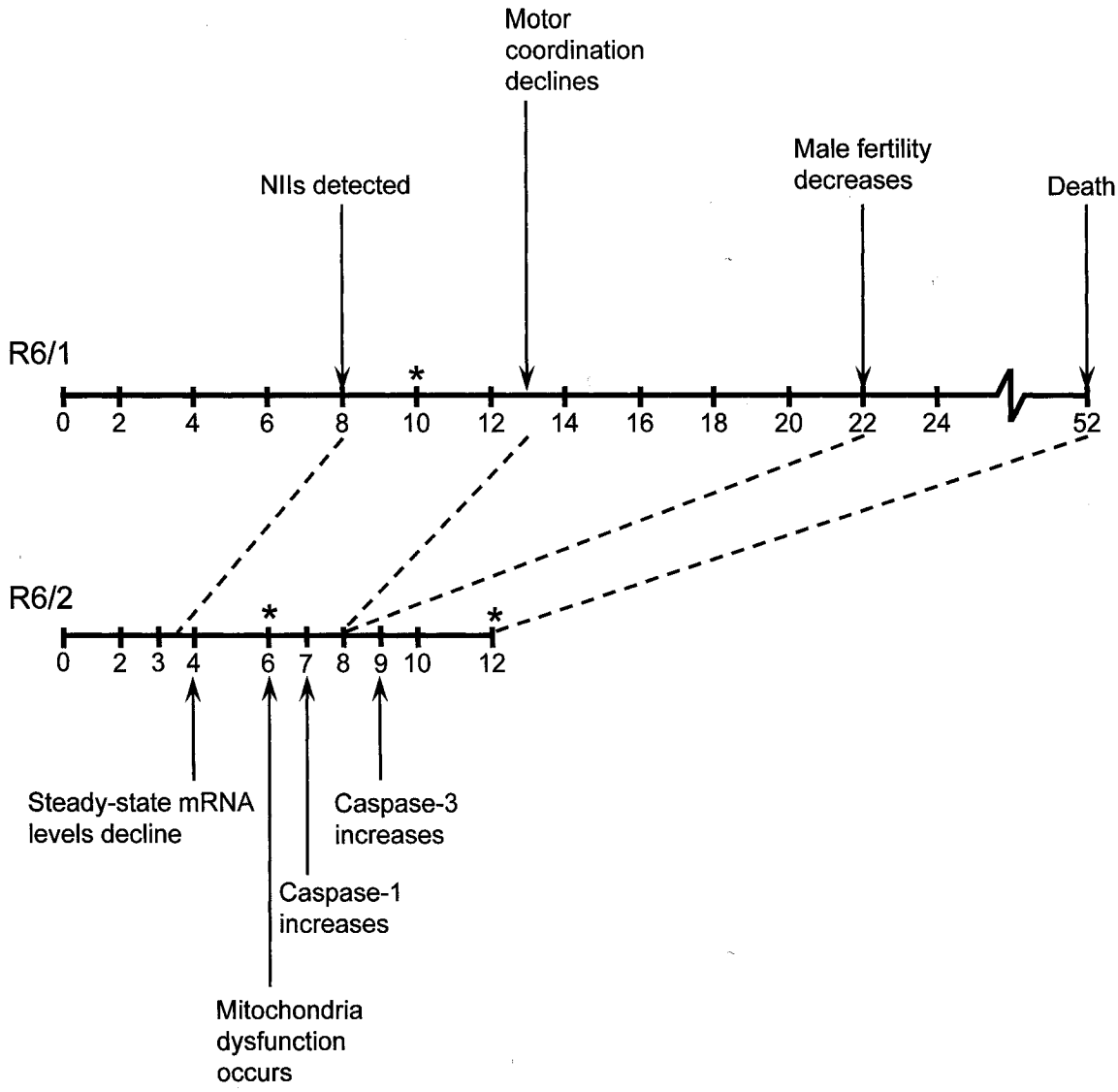

Figure 1-1. The temporal progression of changes at earliest observed time points in the R6/1 and R6/2 transgenic HD mice. The lines indicate the lifespan of the R6/1 and R6/2 mice, respectively. The age of the mice in weeks is indicated by the numbers under each line. Various changes that occur at different ages in the R6/1 and R6/2 mouse models are indicated by arrows. The times that comparable changes occur in the R6/2 model are indicated by the dotted lines. The asterisk (*) indicates time points at which microarray studies show changes in steady-state mRNA levels.

wild-type controls and the reduction in size of the brain was consistent throughout all CNS structures. The neuronal density did not change indicating that cell volume and mass declined but cell number was preserved (Davies *et al.*, 1997). The volume of the striatum of R6/1 mice is also reduced by 17% in 18 week-old R6/1 mice (Hansson *et al.*, 1999).

R6 mice exhibit neuronal loss and degeneration only at very late time points, 14-16 weeks in the R6/2 mice (Turmaine *et al.*, 2000) and 20 weeks in the R6/1 mice (Iannicola *et al.*, 2000). In R6/2 mice, aggregates first appear in the striatum around 3-4 weeks of age. NIIs do not appear in the R6/1 mice until approximately 8 weeks of age (Morton *et al.*, 2000; Hansson *et al.*, 2001). The R6/2 mice die at approximately 13-16 weeks of age, while the R6/1 model can live for more than one year.

The R6 model has been employed in a large number of studies resulting in a thorough characterization of the changes that occur in this model (Mangiarini *et al.*, 1996; Naver *et al.*, 2003; Li *et al.*, 2005). Out of all the existing models of HD, the R6/2 mice develop symptoms most rapidly and have the most widespread occurrence of NIIs in the brain (Li *et al.*, 2005). R6/2 mice mimic features of human HD with respect to sequence of symptom onset as well as the progression of the disease in tests for motor coordination, visuospatial learning and spontaneous locomotion (Sipione & Cattaneo, 2001; Li *et al.*, 2005). The R6 transgenic HD mouse model has an earlier onset of symptoms and a shorter life-span compared to transgenic animals expressing full-length huntingtin, making them relatively easy and inexpensive to use. This N-terminal model of HD does not recapitulate the proteolytic cleavage of huntingtin and, therefore, may not reproduce the same cell-specificity and temporal evolution of the degeneration seen in

HD. The R6/2 mice accumulate aggregates in several non-CNS tissues such as the skeletal muscle, heart, liver, adrenal glands, pancreas and kidney (Sathasivam *et al.*, 1999). In humans, aggregates are only known to be present in the brain.

1.9 Cellular Models of HD

Several neuronal-like cells which stably express either full-length or N-terminal mutant huntingtin under the control of various promoters are currently available. They can be grouped into those that over express exogenous mutant huntingtin and those that express the mutant protein at the same levels as the mouse huntingtin protein. PC12 cells that stably over express exon 1 of huntingtin with either 20 or 150 glutamines were established (Li *et al.*, 1999a). The molecular and biological properties of these PC12 cells are well known (Greene & Tischler, 1976). In the presence of nerve growth factor, PC12 cells differentiate into neuronal-like cells. Cellular deficits and altered gene expression have been observed in stably transfected rat pheochromocytoma PC12 cells that express the N-terminal portion of huntingtin with 20 or 150 glutamine residues (Li *et al.*, 1999a). In these cells, the truncated N-terminal fragment of mutant huntingtin was found to localize to the nucleus. Differential display polymerase chain reaction (PCR) analyses showed that PC12 cells expressing the N-terminal of mutant huntingtin with 150 glutamine repeats had altered gene expression compared to cells expressing the N-terminal of huntingtin with 20 glutamine repeats. Another cellular model of HD is derived from neuroblastoma cells, which are also able to differentiate into neuronal-like cells. The mouse-rat neuroblastoma-glioma hybrid cell line, NG108-15, has been stably transfected with either truncated N-terminal or full-length huntingtin under the control of

the tetracycline-inducible transactivator (Lunkes & Mandel, 1998). This model is useful in studying the processing mechanism of normal and mutant huntingtin, as well as aggregate formation and localization over time.

Neuroblastoma cells and the PC12 cells originate from tumors and the genetic events that lead to their continuous growth are unknown. Conditionally immortalized cells derived from the mouse embryonic striatum immortalized with a temperature-sensitive variant of the large-T antigen were established (Trettel *et al.*, 2000). This cellular model of HD is based on conditionally immortalized striatal cells obtained from the Hdh^{Q111} knockin HD mice and their wild-type littermates (Wheeler *et al.*, 2000). The ST14A model cells were derived from conditionally immortalized embryonic rat striatal neurons (Cattaneo & Conti, 1998). ST14A cells divide *in vitro* at 33°C but stop dividing at 39°C or when the serum is removed. Removal of growth factors from the culture medium halts the proliferation of progenitor cells, which then differentiate and exhibit neuronal markers like nestin, microtubule-associated protein-2 (MAP2), dopamine- and cAMP-regulated phosphoprotein M_r 32 kDa (DARPP-32) but not glial fibrillary acidic protein (GFAP) (Cattaneo & Conti, 1998). ST14A cells were stably transfected to over express the first 548 amino acids of human huntingtin with either 15 (N548wt) or 128 (N548mu) glutamines (Rigamonti *et al.*, 2000). The expression of the N-terminus of mutant huntingtin in ST14A cells accelerates apoptotic cell death in serum-free media (Cattaneo & Conti, 1998). The N548mu cells like R6 transgenic HD mice have a full complement of normal huntingtin protein and express the N-terminal fragment of human huntingtin with an expanded polyglutamine region. In the ST14A-derived cells and the R6 transgenic HD mouse models the truncated fragment of the human huntingtin gene is

under the control of the endogenous human huntingtin promoter (Mangiarini *et al.*, 1996; Rigamonti *et al.*, 2000). Furthermore, the ST14A cells are immortalized striatal cells and numerous studies have shown that cell lines obtained after immortalizing rodent CNS primary cells retain some of the properties of the immature progenitors from which they were derived (Cattaneo & Conti, 1998). Therefore, these striatal cells were an appropriate cellular model to study the striatal-specific effects of the truncated N-terminal fragment of mutant huntingtin.

1.10 Activation of Caspases

Apoptosis may be also involved in HD pathogenesis. Studies performed on post-mortem brains from HD patients revealed DNA fragmentation within degenerating neurons (Dragunow *et al.*, 1995; Portera-Cailliau *et al.*, 1995; Saudou *et al.*, 1998). Mutant huntingtin is cleaved by caspases, which generates N-terminal fragments that translocate to the nucleus (Goldberg *et al.*, 1996; Wellington *et al.*, 1998; Wellington *et al.*, 2000). In a cellular model of HD, 150Q-E PC12, and an N-terminal animal model of HD, R6/2, that express exon 1 of human huntingtin with 150 CAG repeats, the presence of these N-terminal fragments in the nucleus in the form of NIIs increases the expression of caspase-1 at the transcriptional level (Ona *et al.*, 1999; Li *et al.*, 2000) and also increases the activity of caspase-8 (Sanchez *et al.*, 1999). As the disease progresses in this cellular model, cytochrome *c* and caspase-3 levels increase (Li *et al.*, 2000). Furthermore, the over expression of anti-apoptotic molecules like $BclX_L$ was shown to be neuroprotective in primary cultures that express the N-terminal fragment of mutant huntingtin indicating that mutant huntingtin may induce neurodegeneration of striatal

neurons by an apoptotic mechanism (Saudou *et al.*, 1998). The increase in caspase-1 mRNA levels in the R6/2 transgenic HD mice were observed in 7 week-old mice and the increase in caspase-3 mRNA levels were observed in 9 week-old mice (Chen *et al.*, 2000). The exact role of caspase activation as a cause or secondary effect in HD pathogenesis is yet to be fully determined.

1.11 Mitochondria Dysfunction

The administration of 3-NP in non-human primates produced striatal lesions with selective loss of medium spiny neurons, movement disorder and cognitive deficits similar to HD (Brouillet *et al.*, 1995; Palfi *et al.*, 1996). 3-NP irreversibly inhibits succinate dehydrogenase (SDH) leading to energy deficiency *in vivo* with ATP depletion followed by the activation of excitatory amino acid receptors (Beal *et al.*, 1993). This led to the "weak excitotoxic hypothesis" for HD. This hypothesis proposes that mitochondrial dysfunction leads to excitotoxicity and neuronal loss in HD (Albin & Greenamyre, 1992). According to this hypothesis loss of ATP would lead to partial cell membrane depolarization, removal of the voltage-dependent Mg^{2+} block of the NMDA receptor and activation of the NMDA receptors, calcium overload in the cell and eventually neuronal cell death (Beal, 1992). Support for the hypothesis that this mechanism results in loss of medium spiny neurons came from the observation that the administration of NDMA receptor antagonists attenuate the lesions produced by 3-NP and malonate, another mitochondrial toxin (Beal *et al.*, 1993; Greene *et al.*, 1993). The similarity of the neuropathological lesions produced by 3-NP and those observed in HD suggested that

striatal neurons are sensitive to mitochondrial damage and indicated that mitochondrial dysfunction may cause neuronal death in HD.

Mitochondria dysfunction and impaired energy production are well documented in HD in both symptomatic and pre-symptomatic HD patients (Beal, 2000). Using magnetic resonance spectroscopy, it was observed that glucose metabolism is decreased in the brains of HD patients (Antonini *et al.*, 1996), lactate levels are increased in areas of the HD brain like the occipital cortex and the basal ganglia (Jenkins *et al.*, 1993) and the ratio of lactate to pyruvate in the cerebral and spinal fluid is increased in HD patients (Koroshetz *et al.*, 1997). These deficiencies in energy metabolism occur in the brain and in the periphery, as metabolic defects in skeletal muscle tissue are also observed (Lodi *et al.*, 2000). Decreases in mitochondrial-synthesized *N*-acetylaspartate (NAA) are observed prior to cell loss in 6 week-old R6/2 transgenic HD mice (Bates *et al.*, 1996; Jenkins *et al.*, 2000) indicating that mitochondrial energy production is impaired in relatively young R6/2 mice (Beal, 2000). Mitochondria isolated from HD patient lymphoblasts have reduced calcium buffering capacity and are relatively depolarized (Panov *et al.*, 2002). The N-terminal mutant huntingtin protein has also been identified on neuronal mitochondrial membranes (Panov *et al.*, 2002). However, the activity of mitochondrial complexes I-IV that are involved in the electron transport chain activity are not decreased in tissue from the brains of presymptomatic and Grade 1 HD patients (Guidetti *et al.*, 2001). The mechanism by which mutant huntingtin disrupts mitochondrial function and energy metabolism remains unclear.

Recent studies have suggested that peroxisome proliferator-activated receptor gamma co-activator-1 α (PGC-1α) may be involved in HD (Lin *et al.*, 2004; Cui *et al.*,

2006; St-Pierre *et al.*, 2006; Weydt *et al.*, 2006). PGC1α, a transcriptional co-activator, plays an important role as the regulator of metabolic pathways such as mitochondrial biogenesis and respiration and lipid homeostasis (Puigserver & Spiegelman, 2003). PGC1α knockout mice display deficits in oxidative metabolism and striatal lesions reminiscent of characteristics that are observed in HD patients (Lin *et al.*, 2004; Leone *et al.*, 2005). Levels of PGC1α are decreased in presymptomatic HD patients and in knock-in HD mice medium spiny neurons (Cui *et al.*, 2006). Therefore, it has been proposed that the decrease in PGC-1α levels leads to mitochondrial abnormalities such as deficits in energy metabolism and dysfunction of neurons, which ultimately results in neurodegeneration (Cui *et al.*, 2006).

1.12 Abnormal Protein Interactions

Mutant huntingtin with an expanded polyglutamine repeat may form aggregates through an enzymatic reaction catalyzed by transglutaminase and through the formation of hydrogen-bonded β-sheet rich fibrils termed "polar zippers" (Perutz, 1995; Kahlem *et al.*, 1998). This led to the hypothesis that mutant huntingtin exerts its pathological effects by interacting with various proteins through abnormal protein interactions. Huntingtin-interacting proteins (HIPs) and huntingtin-associated proteins (HAPs) have been identified by yeast two-hybrid analysis, affinity chromatography, glutathione S-transferase (GST)-pull down and co-immunoprecipitation assays (Cattaneo *et al.*, 2001). These proteins can be grouped into four main categories including proteins involved in 1) membrane trafficking and endocytosis, 2) signaling, 3) metabolism and 4) transcription (Sipione & Cattaneo, 2001; Li & Li, 2004). Huntingtin-interacting proteins included in

the category of proteins involved in membrane trafficking also include proteins that are involved in clathrin-mediated endocytosis and in the recycling of synaptic vesicles (Kalchman *et al.*, 1997; Wanker *et al.*, 1997; Sun *et al.*, 2001). Huntingtin-interacting proteins involved in transcription have functional roles as transcription factors, transcription co-activators, transcription repressors and components of the basal transcriptional machinery. The identified huntingtin-interacting proteins mostly interact with the N-terminus or the polyproline region of the huntingtin protein. The transcription factor NF-κB, however, interacts with the HEAT repeat region of the mutant huntingtin protein (Cattaneo *et al.*, 2001; Sipione & Cattaneo, 2001; Takano & Gusella, 2002; Li & Li, 2004). These studies have identified proteins that interact with huntingtin using *in vitro* binding and co-localization assays and yeast two-hybrid analysis.

1.13 Transcriptional Dysregulation

Transcriptional dysregulation is currently thought to be a central mechanism in the pathogenesis of HD (Luthi-Carter & Cha, 2003). It has been hypothesized that transcription factors containing glutamine-rich domains (Courey & Tjian, 1988; Courey *et al.*, 1989) can interact with intranuclear N-terminal mutant huntingtin and that such interactions would affect gene transcription (Li *et al.*, 1999a). Altered levels of mRNA in the presence of N89-150Q were first observed in 4 week-old R6/2 transgenic mouse models (Cha *et al.*, 1998). Changes in gene expression were also observed in stably-transfected PC12 cells that express exon 1 of huntingtin with 150 CAG glutamine residues (Li *et al.*, 1999a). Since then many studies have determined changes in the steady-state mRNA levels of various genes in the brains of HD mouse models and human

subjects with HD. A partial list of specific mRNA changes in different HD models is presented in Table 1-1.

Microarray studies were performed on RNA from cell culture HD models, transgenic HD mouse models and brain tissue from human HD brain to identify the functional classes of genes affected by mutant huntingtin. Expression profiling was performed on various cell models of HD including PC12 cells that express exon 1 of mutant huntingtin with varying CAG repeats under the control of the inducible doxycycline-sensitive promoter (Wyttenbach *et al.*, 2001; Kita *et al.*, 2002) and the immortalized striatal-derived cells that express the first 548 amino acids of mutant huntingtin with varying glutamine repeats under the control of the doxycycline-regulated promoter (Sipione *et al.*, 2002). mRNA levels of proteins involved in lipid metabolism, cell signaling, vesicle trafficking, RNA processing and apoptosis are altered by the presence of the truncated N-terminal fragment of mutant huntingtin in these cell lines.

Microarray analysis performed on striatal RNA from 6 week-old early symptomatic and 12 week-old late symptomatic R6/2 transgenic HD mice indicated that, of nearly 6000 mRNAs that were measured, the steady-state levels mRNA levels of 104 genes are decreased and 22 genes are increased (Luthi-Carter *et al.*, 2000). The steady-state mRNA levels of genes involved in neuronal signaling such as neurotransmitter receptors, neurotransmitters and neuropeptides, as well as calcium signaling pathway components are less abundant in R6/2 compared to wild-type mice while the steady-state mRNA levels of a few genes associated with inflammation are more abundant in R6/2 compard to wild-type mice (Luthi-Carter *et al.*, 2000). Early gene expression changes

Table 1-1. A partial list of mRNA changes in human HD brains or in HD model systems.

mRNA	Proposed function	Change detected (reference)
DARPP-32	Modulates cAMP signaling cascade	Decreased in human HD caudate nucleus (Hodges *et al.*, 2006) Decreased in R6/1 mouse striatum (Desplats *et al.*, 2006) Decreased in R6/2 mouse striatum (Bibb *et al.*, 2000; Luthi-Carter *et al.*, 2000; van Dellen *et al.*, 2000) Decreased in N171-82Q mouse striatum (Luthi-Carter *et al.*, 2000) Decreased in YAC128 mouse striatum (Van Raamsdonk *et al.*, 2005)
ppENK	Neuropeptide	Decreased in human HD caudate nucleus (Albin *et al.*, 1991; Richfield *et al.*, 1995; Hodges *et al.*, 2006) Decreased in R6/1 mouse striatum (Desplats *et al.*, 2006) Decreased in R6/2 mouse striatum (Bibb *et al.*, 2000; Luthi-Carter *et al.*, 2000; Sun *et al.*, 2002) Decreased in R6/2 mouse cortex and cerebellum (Luthi-Carter *et al.*, 2002a) Decreased in N171-82Q mouse striatum (Luthi-Carter *et al.*, 2000) Decreased in knock-in HD mouse striatum (Menalled *et al.*, 2000) No change in YAC72 at 12 months (Chan *et al.*, 2002)
D_1 dopamine receptor	G-protein-coupled receptor (activation increases cAMP)	Decreased in human HD caudate nucleus (Augood *et al.*, 1997; Hodges *et al.*, 2006) Decreased in R6/1 mouse striatum (Desplats *et al.*, 2006) Decreased in R6/2 mouse striatum (Cha *et al.*, 1998; Luthi-Carter *et al.*, 2000)
D_2 dopamine receptor	G-protein-coupled receptor (activation decreases cAMP)	Decreased in human HD caudate nucleus (Augood *et al.*, 1997; Hodges *et al.*, 2006) Decreased in R6/1 mouse striatum (Desplats *et al.*, 2006) Decreased in R6/2 mouse striatum (Cha *et al.*, 1998; Cha *et al.*, 1999) Decreased in N171-82Q mouse striatum (Luthi-Carter *et al.*, 2000) No change in YAC72 at 12 months (Chan *et al.*, 2002)

Table 1-1. (continued)

Cannabinoid receptor 1 (CB1)	G-protein-coupled receptor (activation decreases cAMP)	Decrease in human HD caudate nucleus (Glass *et al.*, 1993) Decreased in R6/1 mouse striatum (McCaw *et al.*, 2004) Decreased in R6/2 mouse striatum (Denovan-Wright & Robertson, 2000; Luthi-Cater *et al.*, 2000; McCaw *et al.*, 2004) Decreased in HD94 mouse striatum (Lastres-Becker *et al.*, 2002)
Phosphodiesterase 10A (PDE10A2)	Regulates intracellular concentration of cyclic nucleotides.	Decrease in human HD caudate nucleus (Hodges *et al.*, 2006) Decreased in R6/1 mouse striatum (Hebb *et al.*, 2004) Decreased in R6/2 mouse striatum (Hebb *et al.*, 2004, Hu *et al.*, 2004)
Phosphodiesterase 1B (PDE1B)	Regulates intracellular concentration of cyclic nucleotides	Decrease in human HD caudate nucleus (Hodges *et al.*, 2006) Decreased in R6/1 mouse striatum (Desplats *et al.*, 2006) Decreased in R6/2 mouse striatum (Luthi-Carter *et al.*, 2002a; Hebb *et al.*, 2004)
Adenosine A_{2a} receptor	G-protein-coupled receptor (activation increases cAMP)	Decrease in human HD caudate nucleus (Glass *et al.*, 2000; Hodges *et al.*, 2006) Decreased in R6/1 mouse striatum (Desplats *et al.*, 2006) Decreased in R6/2 mouse striatum (Cha *et al.*, 1998; Cha *et al.*, 1999) Decreased in N171-82Q mouse striatum (Luthi-Carter *et al.*, 2000) No change in YAC72 at 12 months (Chan *et al.*, 2002)
BDNF	Neuronal differentiation and survival	Decreased in human HD cortex (Zuccato *et al.*, 2001) Decreased in R6/2 striatum, cerebellum and cortex (Luthi-Carter *et al.*, 2002a) Decreased in YAC72 cortex and hippocampus (Zuccato *et al.*, 2001)
RNA polymerase II large subunit	Component of the basal transcriptional machinery	Increased in R6/2 striatum, cortex and cerebellum (Luthi-Carter *et al.*, 2002a)

occur in the 6 week-old early symptomatic R6/2 transgenic HD mice and similar pathways are affected in the 12 week-old late symptomatic R6/2 mice, indicating that altered expression of this set of genes remain stable. Microarray analysis performed on striatal, cortical and cerebellar RNA from 12 week-old R6/2 mice surveying nearly 11,000 genes indicated that the number and magnitude of mRNA changes caused by the expanded polyglutamine in exon 1 of mutant huntingtin were similar in all three brain regions examined (Luthi-Carter *et al.*, 2002a). Furthermore, steady-state mRNA and protein levels of BDNF are decreased in the cortex of various mouse models of HD as well as in post-mortem cortical tissue from patients that have HD (Zuccato *et al.*, 2001; Luthi-Carter *et al.*, 2002a; Duan *et al.*, 2003; Zuccato *et al.*, 2005). This indicated that N89-150Q affects gene expression in transgenic mice.

Microarray analysis comparing mRNA profiles of human HD brains (Grades 0-2) to those from unaffected controls show that the greatest number and magnitude of differentially expressed mRNAs has a distinct regional pattern that parallels the known pattern of degeneration. Changes first appear in cells of the caudate, followed by changes in the motor cortex and the cerebellum (Hodges *et al.*, 2006). Similar to the microarrays on the R6/2 transgenic mouse model, the highest proportion of mRNA changes in the caudate in human HD patients is also related to neuronal signaling.

Recently, microarray analysis in 10 week-old R6/1 transgenic HD mice showed that the transcripts of 39 of 48 genes that have enriched expression in the striatum are affected indicating that these genes are preferentially affected in HD mice (Desplats *et al.*, 2006). They defined striatal-enriched genes as those that have predominant expression in the striatum, with some genes being expressed at lower levels in the cortex,

hippocampus or thalamus. The mRNA levels of 8 of the 39 genes identified in this study were reported in earlier microarray experiments to be decreased in the striatum of 6 week-old R6/2 mice (Luthi-Carter *et al.*, 2000) and in human HD brains (Hodges *et al.*, 2006). They are DARPP-32, preproenkephalin (ppENK), adenosine A_{2a} receptor, dopamine D_1 and D_2 receptors, adenyly cyclase V, α-actinin 2 and the retinoid x (RXR) γ receptor (Thomas, 2006). The analysis of all these microarrays suggests that the steady-state levels of transcripts are affected throughout the brain in HD. The relationship between transcription and the selective vulnerability of striatal neurons to death is currently unknown. Neuronal death occurs late in HD pathogenesis and is possibly a consequence of early changes. Some of the changes in steady-state transcript levels occur early in HD and could be attributed to a direct effect of mutant huntingtin that initiates disease progression.

1.14 Current Hypothesis of Transcriptional Dysregulation

The eukaryotic transcriptional apparatus consists of sequence-specific activators, co-activators or co-repressors and components of the basal transcriptional machinery (Fig. 1-2). The sequence-specific activators recognize specific short consensus elements and act by increasing the efficiency with which the basal transcriptional machinery binds to the promoter. The sequence-specific transcription factors can be divided into several classes on the basis of the activation domains they possess, including those that are glutamine-rich, proline-rich and acidic (Tjian, 1996). The co-activators and the co-repressors do not themselves bind DNA. They work by protein-protein interactions and provide a connection between the DNA-bound activators and the basal transcriptional

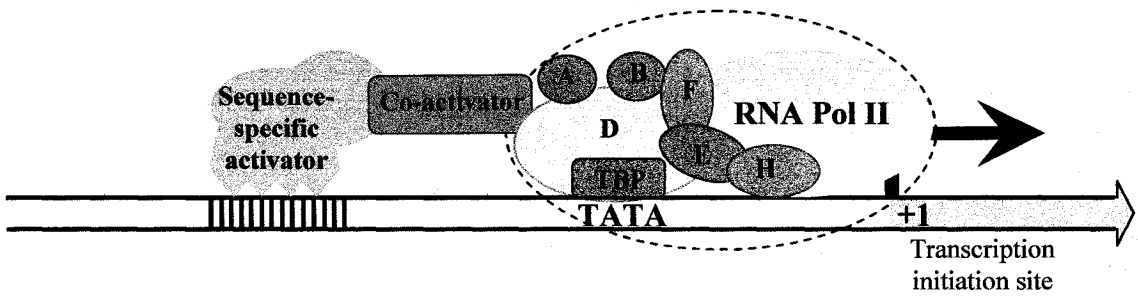

Figure 1-2. Fundamental elements of eukaryotic transcriptional initiation. The eukaryotic transcriptional apparatus consists of sequence-specific activators, co-activators and components of the core basal transcriptional machinery.

machinery. Some activators, like cyclic AMP (cAMP) response element binding protein (CREB) binding protein (CBP), also act as acetylases to alter the conformation of chromatin. The basal transcriptional machinery consists of RNA polymerase II and the general transcription factors TFIIA, TFIIB, TFIID, TFIIE, TFIIF and TFIIH, which are all required to form the active initiation complex (Orphanides *et al.*, 1996). It was hypothesized that mutant huntingtin with its expanded polyglutamine region interacts with various sequence-specific transcription factors like specificity protein 1 (Sp1), CREB and p53, co-activators like CBP or components of the basal transcriptional machinery like TFIID and TFIIF sequesters the proteins via insoluble complexes and disrupts transcription (Cha, 2000; Sugars & Rubinsztein, 2003; Thomas, 2006). It has also been proposed that mutant huntingtin itself, with its expanded polyglutamine region acts as a transcription factor, interacts with the DNA and disrupts transcription (Luthi-Carter & Cha, 2003).

1.14.1 Sequence-specific Activators

Sp1 is a ubiquitous sequence-specific transcriptional activator whose major function is the recruitment of the general transcription factor TFIID to DNA (Pugh & Tjian, 1990). It mediates transcriptional activation through its glutamine-rich activation domain that targets components of the basal transcriptional machinery (Freiman & Tjian, 2002). Sp1 interacts with a component of the basal transcriptional machinery. If mutant huntingtin binds to Sp1 and prevents it from interacting with DNA and $TAF_{II}130$, it would be predicted that the activity of Sp1-dependent genes would be decreased. Full length mutant huntingtin interacts with Sp1 *in vitro* and in the caudate of grade 1 human

HD brain tissue (Dunah *et al.*, 2002; Li *et al.*, 2002). Soluble levels of Sp1 are increased in primary striatal neuronal cultures from R6/2 transgenic HD mice, in R6/2 transgenic mice brains (Qiu *et al.*, 2006) and in human HD brains (Dunah *et al.*, 2002). Sp1 protein and DNA-binding activity are increased in 15 week-old R6/1 and 12 week-old R6/2 transgenic HD mice, when compared to age-matched wild-type littermates (Hu *et al.*, 2004; Chen-Plotkin *et al.*, 2006). The increases in Sp1 occur weeks after steady-state mRNA levels are affected by the expression of N89-115Q in the R6 transgenic HD mice (Hu *et al.*, 2004). It has recently been hypothesized that enhancement of the Sp1 transcription factor activity contributes to the pathology of HD (Qiu *et al.*, 2006). Sp1-driven gene expression can be inhibited using mithramycin A, which blocks Sp1 binding to the promoters or Sp1 RNA interference. Reducing or blocking Sp1 levels is neuroprotective in the presence of mutant huntingtin (Qiu *et al.*, 2006). This is contrary to findings that the presence of mutant huntingtin *in vitro* inhibits the binding of Sp1 to DNA (Li *et al.*, 2002) and decreases *in vitro* transcription from naked DNA (Zhai *et al.*, 2005).

1.14.2 Transcriptional Co-activators

The sequence-specific activator CREB along with its co-activator CBP have been implicated in mutant huntingtin-induced gene repression. CREB is able to directly activate $TAF_{II}130$ to induce gene transcription or interacts with CBP which acts as a bridge between CREB and the basal transcriptional machinery (Lonze & Ginty, 2002). CBP is also an acetyltransferase enzyme with an 18 CAG repeats. Acetyltransferases promote transcription by acetylating histones. Decreasing acetyltransferase activity

results in decreased transcription of genes that are under the control of CBP. If CBP were sequestered by mutant huntingtin, it would be unable to fulfill either its function as a bridge between CREB and the basal transcriptional machinery or its function as an acetyltransferase. CBP has been shown to co-aggregate with huntingtin *in vitro* (Kazantsev *et al.*, 1999; Steffan *et al.*, 2000), in the R6/2 transgenic HD mouse model (Steffan *et al.*, 2000), in the Htt-N171-82Q transgenic mouse model and in post-mortem HD brains (Nucifora *et al.*, 2001). The presence of truncated mutant huntingtin in primary rat cortical neurons decreases CBP-mediated transcription and leads to cell death. Moreover, CBP over expression in primary cultures rescues the cells from toxicity meditated by truncated mutant huntingtin (Nucifora *et al.*, 2001). The transcriptional activity of CBP is repressed in the early time points by soluble N-terminal fragments of mutant huntingtin. Decreases in transcriptional activity occur prior to the time that aggregates are detectable in the PC12 cell model of HD that express exon 1 of mutant huntingtin under the control of the inducible doxycycline-sensitive promoter (Cong *et al.*, 2005). However, there is no observed decrease in the soluble levels of CBP in primary striatal neurons that expresses exon 1 of mutant huntingtin (Chiang *et al.*, 2005).

1.14.3 Histone Acetyltransferases

The acetyltransferase domain of CBP interacts with the truncated N-terminal fragment of mutant huntingtin (Steffan *et al.*, 2000). This interaction between the acetyltransferase domain of CBP and the polyglutamine region of the N-terminal fragment of mutant huntingtin is enhanced by the expansion of the polyglutamine region in mutant huntingtin (Steffan *et al.*, 2000) and this interaction interferes with the

acetyltransferase activity of CBP (Cong *et al.*, 2005). This led to the hypothesis that interactions between the N-terminal fragment of mutant huntingtin and histone acetyltransferases (HATs) leads to a decrease in histone acetylation and results in a decrease in gene transcription. Histone acetylation and deacetylation are modulated by the interplay between HATs and histone deacetylases (HDACs), which work in concert to modify chromosome structure and regulate transcription (Vogelauer *et al.*, 2000). HDACs are involved in removing the acetyl group from the core histones of the nucleosomes resulting in transcriptional repression. In PC12 cells that express exon 1 of mutant huntingtin with either 25 or 103 glutamine repeats, there is a reduction in the acetylation of histones (Steffan *et al.*, 2001). HDAC inhibitors act as inducers of cell growth, arrest, differentiation and cause death both *in vitro* and *in vivo* (Marks *et al.*, 2001). HDAC inhibitors work by increasing the acetylation of histones, thereby increasing transcription of genes that have been silenced. HDAC inhibitors like sodium butyrate and suberoylanilide hydroxamic (SAHA) alleviated the repression caused by huntingtin in PC12 cells that express exon 1 of mutant huntingtin with either 25 or 103 glutamine repeats (Steffan *et al.*, 2001). Moreover, in transgenic *Drosophila* that expresses exon 1 of huntingtin with 93 glutamines, a decrease in rhabdomere degeneration and early adult death are observed if the flies are reared on SAHA and sodium butyrate. These results indicated that decreased acetyltransferase activity might be an important component in HD pathogenesis or that the effects of the HDAC inhibitors compensate for some of the effects of the N-terminal fragment of mutant huntingtin.

The effects of the HDAC inhibitors SAHA and sodium butyrate on the clinical and neuropathological phenotype of R6/2 transgenic mice were also studied (Ferrante *et al.*, 2003; Hockly *et al.*, 2003). Sodium butyrate treatment prolonged the survival of the R6/2 mice. Both SAHA and sodium butyrate improved performance on a rotarod test, and the sodium butyrate-treated mice had decreased gross brain atrophy while the SAHA-treated mice showed a reduction in neuronal atrophy indicating that it was neuroprotective. In both studies, administration of SAHA and sodium butyrate corrected global hypoacetylation of histones. However, microarray analysis of sodium butyrate-treated R6/2 transgenic HD mice demonstrated selective changes in gene expression but there was no uniform correction of the expression of genes that were decreased by N89-150Q. Alternatively it should be noted that HDAC inhibitors may globally increase gene transcription, thereby leading to the alleviation of symptoms in transgenic HD mice. This implies that acetylation and deacetylation of histones may not be the mechanism by which mutant huntingtin alters gene expression in HD but increased transcription may ameliorate some of the effects of mutant huntingtin.

1.14.4 Basal Transcriptional Machinery

The N-terminal fragment of mutant huntingtin interacts with polyglutamine binding protein-1 (PQBP) (Waragai *et al.*, 1999). This protein is localized primarily in the nucleus and binds to other polyglutamine containing proteins (Okazawa *et al.*, 2001). PQBP-1 can also interact with the C-terminal region of RNA Pol II large subunit, which regulates RNA termination and splicing (Okazawa *et al.*, 2001). The RNA Pol II subunits can be recruited to polyglutamine inclusions in cell lines that stably express the

N-terminus of mutant huntingtin with 82 polyglutamine repeats (Luthi-Carter *et al.*, 2002b). However, it is not yet known whether the sequestration of RNA Pol II subunit occurs in *in vivo* models of HD or in HD patients. Another link between mutant huntingtin and the basal transcriptional machinery is the TFIID multisubunit complex which is made up of TATA box-binding protein (TBP) and multiple TBP-associated factors (TAFs), like $TAF_{II}130$ (Albright & Tjian, 2000). Full length mutant huntingtin interacts with $TAF_{II}130$ *in vitro* and in the caudate of grade 1 human HD brain tissue (Dunah *et al.*, 2002). $TAF_{II}130$ acts as a bridge between various sequence-specific transcription factors like Sp1 and CREB, and the basal transcriptional machinery. Therefore, $TAF_{II}130$ is an essential component for gene transcription by RNA polymerase II and if sequestered by mutant huntingtin would alter gene expression. It should also be noted that the TFIID subunit TBP is also detected in huntingtin aggregates in post-mortem human HD brains and in a transiently transfected cell culture model expressing exon 1 of huntingtin with 96 polyglutamine repeats (Huang *et al.*, 1998; Suhr *et al.*, 2001). Recently, TFIIF was identified as a novel direct target of the N-terminal fragment of mutant huntingtin (Zhai *et al.*, 2005). TFIIF consists of two subunits, RAP30 and RAP74. The N-terminal fragment of mutant huntingtin had a strong affinity for RAP30. Since RAP30 lacks a polyglutamine domain, it was proposed that contact between the N-terminal fragment of mutant huntingtin and RAP30 involves β sheet structures (Zhai *et al.*, 2005). An intact TFIIF complex containing RAP30 and RAP74 is required for transcription initiation and elongation. Therefore, it was hypothesized that TFIIF dissociation would contribute to transcriptional dysregulation in HD.

1.15 Gene Expression in HD

The presence of the N-terminal of huntingtin with an expanded polyglutamine region decreases the expression of genes in the striatum, cortex, cerebellum and muscle of the R6 transgenic mouse model of HD (Luthi-Carter *et al.*, 2000; Luthi-Carter *et al.*, 2002a). The mRNA levels of DARPP-32 and ppENK are decreased in various models of HD like the R6 and the N171-82Q transgenic HD models (Luthi-Carter *et al.*, 2000; Luthi-Carter *et al.*, 2002a; Desplats *et al.*, 2006). Furthermore, DARPP-32 and ppENK mRNA levels are also decreased in the brains of HD patients (Augood *et al.*, 1996; Hodges *et al.*, 2006). These genes are enriched in the striatum and are also expressed in other areas of the brain like the cortex allowing us to further examine changes in steady-state mRNA levels in different parts of the brain.

1.15.1 Dopamine- and cAMP-regulated Phosphoprotein M_r 32 kDa

DARPP-32 was initially thought to be a neuronal phosphoprotein concentrated in parts of the brain that receive dopaminergic input, like the caudate and putamen, nucleus accumbens, olfactory tubercle and a portion of the amygdaloid complex (Ouimet *et al.*, 1984). However, DARPP-32 was eventually identified in a number of non-neuronal tissues including porcine brown fat adipocytes, bovine adipose tissue, ciliary epithelium of the eye and rat renal tubule cells (Hemmings *et al.*, 1992). DARPP-32 is highly expressed in the caudate and putamen and the renal tubule cells (Walaas & Greengard, 1984; Meister *et al.*, 1989). In the caudate and putamen, DARPP-32 is present in almost all medium spiny neurons. These include the striato-nigral projection neurons from the caudate putamen to the substantia nigra and the globus pallidus internal part as well as

the striatopallidal projection neurons from the caudate putamen to the globus pallidus external part (Walaas & Greengard, 1984). DARPP-32 is also expressed in the renal tubule cells of the medullary thick ascending limb of the Loop of Henle and at lower concentrations in the proximal convoluted tubes (Meister *et al.*, 1989).

DARPP-32 plays a major role in mediating the effects of dopamine in the dopamine signaling pathway and the activity of the protein is normally regulated by altering the proportion of phosphorylated and de-phosphorylated DARPP-32 following receptor activation. DARPP-32 was initially identified as a major target of dopamine and protein kinase A (PKA) but recently it was observed that the regulation of the phosphorylation state of DARPP-32 provides a mechanism for integrating information from the various neurotransmitters (dopamine and serotonin), neuromodulators (glutamate and GABA) and steroid hormones (opioids and neurotensin). In the striatum, dopamine interacting with D_1 receptors of striatonigral neurons leads to an increase in cAMP, activation of protein kinase A and phosphorylation of DARPP-32. However, dopamine interacting with D_2 receptors of the striatopallidal neurons leads to a decrease in the levels of phosph-DARPP-32 by two synergistic mechanisms: inhibition of cAMP formation, which inhibits PKA activation and increased levels of intracellular calcium, which activates calcineurin, a protein phosphatase. Phospho-DARPP-32 is an inhibitor of protein phosphatase-1 (PP-1), which in turn inhibits the dephosphorylation of various receptors; NMDA receptors, AMPA receptors, calcium channels, CREB protein and Na^+/K^+-ATPase. Therefore, PP-1 under the control of DARPP-32 plays a critical role in regulating many biochemical, electrophysiological, gene transcriptional and behavioural responses to various stimuli.

The steady-state mRNA and protein levels of DARPP-32 are known to be decreased in the striatum of R6 (Bibb *et al.*, 2000; Luthi-Carter *et al.*, 2000; van Dellen *et al.*, 2000), N171-82Q (Luthi-Carter *et al.*, 2000) and YAC128 (Van Raamsdonk *et al.*, 2005) transgenic mouse models of HD and in rats where striatal neurons were transduced with lentiviral vectors expressing the first 171 amino acids of human huntingtin with a glutamine repeat length of 82 (de Almeida *et al.*, 2002).

1.15.2 Preproenkephalin

ppENK mRNA is ubiquitously expressed at low levels throughout the body and high constitutive levels of this mRNA are found in the striatum, heart, hypothalamus, hippocampus, adrenal medulla and testis (Udenfriend & Kilpatrick, 1983; Garrett et al., 1989; Weisinger et al., 1990). ppENK is the precursor for the six copies of the small neuropeptide met-enkephalin and one copy of the neuopeptide called leu-enkephalin. ppENK produces the endogenous opioid neuropeptides involved in cell signaling and modulates pain, immune and stress responses (Salzet *et al.*, 2000; Drolet *et al.*, 2001). Enkephalins have the greatest affinity for the δ opioid receptors. Immune cells such as macrophages, T cells and B cells are also modulated by opioids (Salzet *et al.*, 2000). Enkephalins stimulate the release of pro-inflammatory cytokines such as interlukin-6 (Zhong *et al.*, 1998), influence intracellular signaling transduction in T-cells (Sorensen & Claesson, 1998) and stimulate B and T cell proliferation (Kowalski, 1998). There is also strong evidence indicating that opioids are involved in the mediation, modulation and regulation of stress responses. Enkephalins may exert their action on the hypothalamo-pituitary-adrenal (HPA axis) and the autonomic nervous system (ANS), which are the

two major systems that serve to maintain homeostasis during exposure to stressors (Howlett & Rees, 1986; Katoh *et al.*, 1990; Szekely, 1990; Pechnick, 1993). Enkephalin is able to modify the synthesis and release of corticotrophin releasing factor (CRF), a releasing hormone produced by the hypothalamus and involved in the HPA axis (Szekely, 1990; Borsook & Hyman, 1995).

ppENK is normally regulated at the level of gene expression by cAMP, calcium and protein kinase C (PKC) levels. The protein kinases or second messengers translocate to the nucleus and phophorylates CREB that is bound to its regulatory elements on the ppENK gene and alters gene transcription. Diverse neural and neuroendocrine stimuli have been shown to increase levels of ppENK mRNA including electrical stimulation and seizures in the hippocampus (Hong *et al.*, 1980; Iadarola *et al.*, 1986; Gall, 1988), stressors such as hypertonic saline in the paraventricular nucleus (PVN) of the hypothalamus (Lightman & Young, 1987) and chronic treatment with haloperidol, a D_2-dopamine receptor antagonists (Sabol *et al.*, 1983; Tang *et al.*, 1983).

Steady-state ppENK mRNA levels are reduced in brains from HD patients (Albin *et al.*, 1991; Richfield *et al.*, 1995; Hodges *et al.*, 2006). *In situ* hybridization analysis showed that there was a significant reduction in the density of striatal neurons expressing ppENK messenger RNA in the patients with symptomatic HD (Ferrante *et al.*, 1986; Albin *et al.*, 1991). ppENK mRNA levels are decreased per neuron in post-mortem HD brains (Richfield *et al.*, 1995). Symptomatic R6/2 transgenic HD mice and knock-in mice with an expanded CAG repeat have decreased ppENK mRNA levels compared to age-matched wild-type littermates (Menalled *et al.*, 2000; Sun *et al.*, 2002). N171-82Q transgenic HD mice that express the N-terminal of mutant huntingtin with an expanded

glutamine region also have decreased ppENK mRNA levels at 4 months of age when compared to age-matched littermates (Luthi-Carter *et al.*, 2002b). However, no differences in the levels of ppENK mRNA were observed in 12 month-old YAC72 mice when compared to wild-type littermates (Chan *et al.*, 2002).

1.15.3 Hypoxanthine Phosphoribosyltransferase

HPRT is a cytoplasmic enzyme that catalyzes the conversion of hypoxanthine and guanine to their respective 5'-mononucleotides and plays a crucial role in the metabolic salvage of purines in mammalian cells. Although constitutively produced, the HPRT enzyme is not essential as purines can be created *de novo* (DeMars, 1971). Even though HPRT is dispensable at the cellular level, germinal HPRT deficiency does lead to human disease. A partial deficiency of the enzyme in humans causes gouty arthritis, whereas a complete deficiency of HPRT leads to a devastating neurological disorder, Lesch-Nyhan syndrome (Lesch & Nyhan, 1964). The HPRT enzyme is approximately 24.5 kDa and is highly conserved among hamsters, mice and humans. Studies of tissue distribution of the enzyme in mammals have indicated that the enzyme activity is expressed in low levels in virtually all tissues, with a higher expression in the testes, and approximately sevenfold higher expression in the brain (Melton *et al.*, 1981; Chinault & Caskey, 1984; Watts *et al.*, 1987). HPRT steady-state mRNA levels are not affected in the R6 transgenic HD model (Luthi-Carter *et al.*, 2000). In our studies, we employed HPRT as a negative control since this gene is expressed in the cells that also express DARPP-32 and ppENK in the brain but the steady-state levels of HPRT mRNA are not decreased in the presence of the N-terminal fragment of mutant huntingtin with an expanded polyglutamine region.

1.15.4 Cytomegalovirus

Human cytomegalovirus (CMV) is a member of the herpesvirus classification group. CMV has a large double-stranded DNA genome of 240 kb. CMV is infectious in a wide range of tissues and independent of specific virus-receptor interactions (Beck & Barrell, 1988). The immediate-early (IE) region of the CMV genome have been defined and encode three immediate-early genes, IE gene 1, IE gene 2 and IE gene 3 (Stinski *et al.*, 1982; Stinski *et al.*, 1983). Based on the high steady-state levels of 1.9 kb viral mRNA and the abundance of its translation product in infected cells, IE gene 1 is the major immediate early gene (Stinski *et al.*, 1982). The structure of the gene coding the CMV major IE 72 kDa protein including the promoter-regulatory region and the single transcription initiation site have been defined (Stenberg *et al.*, 1984; Thomsen *et al.*, 1984). There is a strong enhancer located upstream of the CMV IE gene 1 and *in vitro* studies have indicated that it has strong promoter activity (Boshart *et al.*, 1985). This CMV enhancer is a pan-active enhancer and drives strong expression in the heart, kidney, brain and testis of transgenic mice (Schmidt *et al.*, 1990).

The CMV IE1 promoter is widely used in expression vectors in mammalian cells. The CMV promoter has been used as a control promoter to normalize luciferase activity in several HD studies involving transient transfections of the truncated N-terminal fragment of mutant huntingtin into PC12 cells (Yohrling *et al.*, 2003; Cong *et al.*, 2005). The CMV promoter is also used to drive the expression of the truncated N-terminal fragment and full-length huntingtin in various animal models (Reddy *et al.*, 1998) and cellular models of HD (Cooper *et al.*, 1998; Waelter *et al.*, 2001a; de Almeida *et al.*, 2002; Arrasate *et al.*, 2004; Charvin *et al.*, 2005; Poirier *et al.*, 2005).

1.16 Overall Objective

The overall goal of this research was to define the mechanism whereby the N-terminual fragment of mutant huntingtin decreases steady-state mRNA levels in a gene- and tissue-specific manner. Huntington's disease is currently believed to be caused by a gain-of-function of the mutant huntingtin protein. The presence of this N-terminal fragment of mutant huntingtin in the nucleus is thought to alter the expression of specific genes. One of the changes that occur during HD pathogenesis is the observed decrease in expression of specific genes in the striatum. We hypothesized that mutant huntingtin directly affects the transcription of specific genes in a promoter- and tissue-specific manner. We studied model genes in *in vivo, ex vivo* and *in vitro* models of HD to examine the gene-specific effects of the N-terminal fragment of mutant huntingtin. These genes included DARPP-32 and ppENK, which are highly expressed in the striatum and affected by the presence of mutant huntingtin, and HPRT, which is also highly expressed in the striatum but not affected by the presence of mutant huntingtin. DARPP-32 is also expressed in the kidney and comparison of expression of DARPP-32 in the striatum and kidney enabled us to study the tissue-specific effects of mutant huntingtin.

CHAPTER 2

Materials and Methods

2.1 Animals

R6/1 [B6CBA-Tg(HDexon1)61Gpb/2J] and R6/2 [B6CBA-Tg(HDexon1)62Gpb/1J] transgenic mice and wild-type littermates were used in this study (Mangiarini *et al.*, 1996). Mice were originally obtained from Jackson Laboratories (Bar Harbour, ME). Two colonies were maintained by crossing B6CBA-Tg(HDexon1)61Gpb/1J and B6CBA-Tg(HDexon1)62Gpb/1J hemizygous males with C57BL/6J females. The genotype of each mouse was determined when the mice were weaned at 3 weeks of age and again when each animal was sacrificed. DNA was extracted from ear-punch tissue samples for each animal used in this study by digestion of the tissue with Proteinase K (200 μg; Promega) in buffer containing 10 mM Tris-HCl (pH 8.0), 5 mM ethylenediaminetetraacetic acid [EDTA (pH 8.0; Sigma)], 50 mM sodium chloride (NaCl; EMD Biosciences) and 0.5% (v/v) Tween-20 (Sigma). The extracted DNA was used as a PCR substrate using the REDExtract-N-Amp Ready Mix for Blood (Sigma). A region of the integrated human HD exon 1 transgene was PCR amplified using primers (5'-AGG GCT GTC AAT CAT GCT GG-3' and 5'-GGA CTT GAG GGA CTC GAA-3') that correspond to nucleotides 77-96 and 347-364, respectively of the human huntingtin cDNA (GenBank accession number XM_003405) and the following PCR cycling conditions: 94°C for 1 min, followed by 40 repeated cycles of 94°C for 30 sec, 50°C for 30 sec and 72°C for 30 sec and a final extension at 72°C for 10 min. All primers mentioned were obtained from Sigma-Genosys unless otherwise noted. All animal protocols were in accordance with the guidelines from the Canadian Council on Animal Care and approved by the Carleton Animal Care Committee

at Dalhousie University. All efforts were made to minimize the number of animals used in this study.

2.2 Genomic DNA Isolation, Total RNA Extraction and cDNA Synthesis

Genomic DNA was isolated following the standard protocol described in Sambrook *et al.* (2000). DNA was extracted from fresh frozen tissue by placing tissue in lysis buffer [10 mM Tris-HCl (pH 8.0), 0.1 M EDTA (pH 8.0; Sigma), 0.5% (w/v) sodium dodecyl sulfate (SDS; Sigma) and 20 μg/ml of RNase A (Promega)] and rocking gently for 20 min. EDTA (Sigma) and proteinase K (Promega) were added to a final concentration of 15 mM and 100 μg/ml, respectively, and incubated at 30°C for 2 hours with occasional swirling. The reactions were allowed to cool to room temperature, an equal volume of buffered phenol (pH 8.0) was added and the cell lysates were inverted gently for 10 min on a rocking platform. Samples were subjected to centrifugation at 1,500 x *g* for 10 min to separate the two phases and the upper aqueous phase was removed. The aqueous phase was phenol-extracted a second time to remove any residual protein and lipid. Three volumes of cold 100% (v/v) ethanol were added and the solution was inverted 20 times. The DNA that precipitated was removed by spooling around a glass J hook and briefly dried. The DNA was dissolved in TE buffer [10 mM Tris-HCl, 1 mM EDTA (pH 8.0)]. Sodium acetate (pH 5.2; Sigma) was added to a final concentration of 0.3 M and 100% (v/v) ethanol was added to a final concentration of 66% (v/v). The solution was mixed well and incubated on ice for 10 min to precipitate the DNA. DNA was pelleted by centrifugation at 12,000 x *g* for 10 min, washed with 70% (v/v) ethanol and dissolved overnight at 4°C in TE buffer (pH 8.0). The DNA was

quantified at 260 nm using a GeneQuant II (Pharmacia Biotech) spectrophotometer and stored at -20°C.

RNA was isolated from fresh frozen brains of wild-type and R6 transgenic HD mice using the Trizol™ (Invitrogen) reagent and the procedure described by the manufacturer. All buffers, solutions, glassware, plasticware and equipment were treated to be RNase-free as described in Sambrook *et al.* (2000). Striata dissected from the brains (11-14 mg/mouse) of two mice per group were homogenized in 200 µl of Trizol reagent using a pellet pestle cordless motor (Kontes). Trizol reagent (800 µl) was added to the homogenized tissue and mixed well. The homogenate was incubated at room temperature for 5 min. Chloroform (200 µl; Fisher Scientific) was added to the homogenate, mixed vigorously by hand for 15 sec and incubated at room temperature for 3 min. The homogenate was centrifuged at 12,000 x *g* for 15 min at 4°C. The aqueous layer was transferred to a clean microfuge tube and 500 µl of isopropyl alcohol (Fisher Scientific) was added. The solution was inverted several times and incubated at room temperature for 10 min to precipitate the RNA. The mixture was centrifuged at 12,000 x *g* for 10 min at 4°C and the supernatant was discarded. The pellet was washed twice with 75% (v/v) ethanol and centrifuged at 7,500 x *g* for 5 min at 4°C. The pellet was air dried for 10 min at room temperature and dissolved in RNase-free H_2O by placing on ice for 10 min, followed by 10 min at 55°C. The RNA was quantified using spectrophotometric analysis (at 260 nm) and stored at -70°C.

To synthesize cDNA, 1 µg of RNA was incubated with random primers (0.3 µg/µl; GibcoBRL) at 72°C for 5 min. The solution was placed on ice and Moloney Murine Leukemia Virus (MMLV; Promega) buffer (1X), dNTPs (0.5 mM; Fermentas), RNasin

(50 U, Promega) and MMLV-Reverse Transcriptase (MMLV-RT, 200 U, Promega) were added. The reaction was incubated at 37°C for 1hr and inactivated by heating at 95°C for 5 min. The reactions were stored at -20°C before use.

2.3 Northern Blot Analysis

A Northern blot was prepared by fractionating 10 μg of total RNA, isolated using Trizol™ (Invitrogen), from the striata and cortex of 10 week-old wild-type and R6/2 transgenic HD mice on a 1% (w/v) denaturing formaldehyde agarose gel and transferring to Hybond N+ membrane (Amersham Biosciences) following the standard protocol described in Sambrook *et al.* (2000). The DARPP-32 *in situ* probe 2 (see section 2.4) was used as a hybridization probe. Following hybridization of the DARPP-32-specific probe, the blot was stripped and a 371 bp cloned PCR product of the mouse cyclophilin cDNA (43-413 nts; GenBank accession number X52803) was allowed to anneal with the same Northern blot to determine the amounts of mRNA present in each lane. The following primer combination: 5'-TGG TCA ACC CCA CCG TGT TCT T-3' (43-64 nts; GenBank accession number X52803) and 5'-GCC ATC CAG CCA CTC AGT CTT G-3' (392-413 nts; GenBank accession number X52803), and the PCR cycling conditions, 94°C for 1 min, followed by repeated cycles of 94°C for 1 min, 50°C for 1 min and 72°C for 1 min and a final extension at 72°C for 10 min, were used to amplify the mouse cyclophilin cDNA.

Methods for radiolabeling the probes, hybridization and post-hybridization washes are described in Denovan-Wright *et al.*, 1998. The 371 bp cyclophilin cDNA fragment was radio-labeled by random priming. Ten pmol of the DARPP-32 *in situ*

probe 2 oligonucleotide was 3' end-labeled with 3000 μCi [α-^{32}P] dATP for 90 min at 37°C using 30 U of terminal deoxynucleotide transferase (TdT, Amersham). Unincorporated radionucleotides in the random priming and 3' end-labeling reactions were removed from labeled probes using a Sephadex G-25 spin column (Pharmacia). The blot was pre-hybridized for 4 hr [50% (v/v) formamide (Invitrogen), 5X sodium chloride-sodium citrate (SSC), 1X Denhardt's reagent (Sigma), 20 mM sodium phosphate (pH6.8; EMD Biosciences), 0.2% (w/v) SDS (Sigma), 5 mM EDTA (Sigma), 10 mg/ml poly A (Sigma), 50 mg/ml sheared salmon sperm DNA (Sigma), 50 mg/ml yeast RNA (Sigma)] at 42°C. The blot was allowed to anneal with the radio-labeled cDNA or 3' end-labeled oligonucleotide probe ($5x10^6$ cpm/ml) in hybridization buffer [50% (v/v) formamide (Invitrogen), 5X SSC, 10% (w/v) dextran sulfate (Chemicon), 1X Denhardt's reagent (Fisher Scientific), 20mM sodium phosphate (pH 6.8; EMD Biosciences), 0.2% (w/v) SDS (Sigma), 5 mM EDTA (Sigma), 10 mg/ml poly A (Sigma), 50 mg/ml sheared salmon sperm DNA (Sigma), 50 mg/ml yeast RNA (Sigma)] overnight at 42°C. The blot was washed for 15 min each, four times in 1X SSC at 55°C, four times in 0.5X SSC at 55°C, two times in 0.25X SSC at 55°C, two times in 0.25X SSC at room temperature and exposed to Hypermax (Kodak) film at -70°C. DARPP-32-specific hybridization probe was removed from the blot by incubating the membrane in 50% (v/v) deionized formamide (Invitrogen), 0.1X SSC, 0.1% (w/v) SDS at 68°C for 1 hr. The blot was re-probed with the radio-labeled 371 bp mouse cyclophilin cDNA. Densitometric analysis of autoradiographs was performed using Kodak 1D Image Analysis Software. Levels were subjected to two-way analysis of varience (ANOVA) and the 0.05 level of significance was adopted for all comparisons.

2.4 *In Situ* Hybridization Analysis

Three synthetic oligonucleotide probes were obtained from Sigma-Aldrich Canada (Ontario, Canada). DARPP-32 *in situ* probe 1 (5'-CCA GAA CTC GGC GTT GTA TTA TTA ATG AAG TCC-3') is complementary to the 5' untranslated region (UTR) of the DARPP-32 mRNA (1723-1755 nts; GenBank accession number MMU23160). DARPP-32 *in situ* probe 2 (5'-TCC ACT TGG TCC TCA GAG TTT CCA TCT CTC-3') is complementary to the coding sequence of the mouse DARPP-32 cDNA (899-928 nts; GenBank accession number XM_109714). The ppENK *in situ* probe (5'-ATC TGC ATC CTT CTT CAT GAA ACC GCC ATA CCT CTT GGC AAG GAT-3') is complementary to the coding sequence of the mouse ppENK cDNA (693-737 nts; GenBank accession number BC049766). The oligonucleotides were 3′ end-labeled with 3000 μCi [α-^{33}P]dATP for 90 min at 37°C using 30 U of TdT (Promega) in terminal transferase buffer (1X). Unincorporated radionucleotides were removed from the labeled probes using a Sephadex G-25 spin column (Pharmacia).

In situ hybridization was performed on coronal forebrain (Bregma +1.70 to –0.50; Franklin and Paxinos, 1997) and kidney sections of 3 to 29 week-old mice and emulsion autoradiography was performed on selected slides as described previously (Denovan-Wright & Robertson, 2000). Tissue sections, 14 μM in thickness, were cut from the fresh frozen brains and kidneys using the Microm HM 500 O cyrostat and stored at -70°C. These tissue sections were allowed to reach room temperature, fixed in 4% (w/v) paraformaldehyde in 0.1 M phosphate-buffer for 5 min, rinsed twice in phosphate-buffered saline [PBS (pH7.4); 137 mM NaCl (EMD Biosciences), 2.7 mM KCl (BDH), 10 mM Na_2HPO_4 (EMD), 2 mM KH_2PO_4 (BDH)] for 5 min, once in 2X SSC for 20 min

and air dried for 30 min. Each slide was covered with hybridization buffer containing $1x10^6$ cpm/ml of labeled probe, coverslipped with parafilm and incubated overnight at 42°C in a humidified chamber. Following hybridization, the slides were washed four times in 1X SSC, four times in 0.5X SSC and four times in 0.25X SSC. All washes were 30 min long and were carried out at 55°C. The slides were rinsed briefly in double distilled H_2O, dried overnight at room temperature and exposed to BioMax MR (Kodak) film for 1-3 weeks at room temperature. The film was developed using the Kodak X-OMAT 1000A processor. Densitometric analysis of autoradiographs was performed using Kodak 1D Image Analysis Software. Statistical analysis of the optical density of the hybridization signal is described in Hebb *et al.*, 2004. The optical densities were subjected to a two-way ANOVA (genotype x age). The overall ANOVA was followed by one-way ANOVA (gene) performed at independent ages. Tukey's honestly significant multiple comparisons were employed where appropriate and the 0.05 levels of significance was adopted for all comparisons. The rate of decline in DARPP-32 and ppENK mRNA levels in R6/2 and R6/ 1 mice was fit using Sigma plot software with the equation $y = y^0 + ae^{-bx}$, where y^0 is the horizontal asymptote. Following, *in situ* hybridization, in the darkroom the slides were immersed in autoradiographic emulsion (Kodak NTB2), allowed to dry and exposed for four weeks at 4°C in a light-tight case and the emulsion-coated tissue sections were developed using Kodak D19 developer and fixer. Following this the sections were counter-stained for Nissl substance using cresyl violet (ICN Biochemicals). Brightfield micrographs of the sections were taken using the Zeiss Axioplan upright microscope and a Nikon Coolpix 995 camera.

2.5 Immunohistochemical Analysis

Immunohistochemistry for neuronal intranuclear inclusions in the striatum and renal medulla of wild-type and R6/1 mice using anti-ubiquitin antibody were performed on coronal brain and kidney sections as described in Rodriguez-Lebron *et al.*, 2005. Fresh-frozen coronal brain sections were allowed to reach room temperature fixed with 4% (w/v) paraformaldehyde for 15 min and rinsed three times for 10 min with 0.01 M PBS and. The tissue was incubated in 0.1% (v/v) H_2O_2 (Fisher Scientific) and 10% (v/v) methanol (Fisher Scientific) in 0.01 M PBS for 10 min and rinsed three times for 10 min each in 0.01 M PBS. The tissue was incubated in a solution of 5% (v/v) normal goat serum (Calbiochem) and 0.25% (v/v) Triton X-100 (Sigma) in 0.01 M PBS for 1 hr at room temperature to block non-specific binding sites. Immunostaining was performed overnight at 4°C using a 1:4000 dilution of polyclonal rabbit anti-ubiquitin (IgG) antibody (DakoCytomation) in 1% (v/v) normal goat serum (Vector Laboratories), 0.25% (v/v) triton X-100 in 0.01 M PBS. The next day the tissue was incubated in a 1:500 dilution of biotinylated anti-rabbit (IgG) antibody (Vector Laboratories) for 2 hr at room temperature and rinsed three times for 10 min each in 0.01 M PBS. Interaction between the primary and the secondary antibodies were detected using the Vectastain Elite ABC kit (Vector Laboratories) and diaminobenzidine (DAB, Sigma) according to manufacture's instructions.

2.6 Quantitative RT-PCR

Quantitative RT-PCR (qRT-PCR) (LightCycler, Roche) was used to determine the number of copies of DARPP-32 and ppENK mature and unspliced primary transcript

in cDNA samples derived from the striatum of wild-type and R6/1 transgenic HD mice as described in Hu *et al.*, 2004. Striatal RNA was extracted from 3-, 5-, 6-, and 12 week-old wild-type and R6/1 transgenic HD mice. Five gene-specific primers and 200 U of MMLV-RT (Promega) were used to generate first-strand cDNA using 1 μg total RNA as the template. These primers included HPRT AS a primer complementary to HPRT 5'-CAC AGG ACT AGA ACA CCT GC-3' (750-769 nts; GenBank accession number BC083145), DARPP-R-Intron 5'-CTC CCT GCC TCT GGA AAC CTA AAA AG-3', which is complementary to sequence in intron 4 (154077-154102 nts; GenBank accession number AL591390), DARPP-R-Exon 5'-ACC TCC GCC TGG CTG TCT TCT T-3' (781-802 nts; GenBank accession number XM_109714), ppENK-R-Intron 5'-CCT CAC CGC AAA TTC AAC TCA CC-3' (785-807 nts; GenBank accession number AK047709) and ppENK-R-Exon 5'-CTC TCA TCC TGT TTG CTG CTG TCT TT-3' (555-580 nts; GenBank accession number BC049766). Negative control RT reactions, which included all components except MMLV-RT for each sample, were also analyzed by qRT-PCR to determine levels of genomic DNA that was present in total RNA samples prior to cDNA synthesis.

The HPRT AS primer was used with the HPRT-F- primer, 5'-GCT GGT GAA AAG GAC CTC T-3' (521-539 nts; GenBank accession number BC083145) to amplify a 249 bp product from cDNA corresponding to mature HPRT transcripts. The qRT-PCR conditions to amplify HPRT were as follows; 95°C for 10 min, followed by 45 repeated cycles of 95°C for 15 sec, 63°C for 5 sec and 72°C for 10 sec. The DARPP-32-specific sense primer used in qRT-PCR reactions was 5'-AAG AGA CCC AAC CCC TGT GCC TAT-3' (DARPP-F, 600-623 nts; GenBank accession number XM_109714). This primer

was used in conjunction with the coding region-specific antisense primer (DARPP-R-Exon) to amplify a 203 bp product from cDNA corresponding to mature DARPP-32 transcripts. The DARPP-F primer was also used with the DARPP-R-Intron primer to amplify a 194 bp product from unspliced DARPP-32 primary transcript. The PCR conditions to amplify the mature and primary DARPP-32 transcripts included 95°C for 10 min, followed by 45 repeated cycles of 95°C for 15 sec, 55°C for 5 sec and 72°C for 15 sec. The PCR reactions contained 1μl of cDNA or no RT negative control, 0.2 μM sense and antisense primers, 3 mM (for DARPP-32) or 5 mM (for HPRT) $MgCl_2$ and 2 μl of LightCycler-DNA FastStart SYBR Green 1 Mix (Roche) containing nucleotides, buffer and hot start *Taq* DNA polymerase. Low levels of product were observed in the no RT negative control PCR reactions containing the DARPP-32 primary transcript-specific primers, which correspond to genomic DNA. The amount of product in the no RT negative control PCR reactions were subtracted from the copy number of the DARPP-32 primary product. The copy number of DARPP-32 primary and mature products in each sample was normalized using the copy number of HPRT products. Normalized cDNA levels were subjected to two-way ANOVA and the 0.05 level of significance was adopted for all comparisons.

The number of copies of DARPP-32 mRNA levels in the differentiated N548wt and N548mu cells were also quantified using qRT-PCR. RNA was extracted from the cells using Trizol™ (Invitrogen) at 0, 24, 48, 72 and 96 hr following serum-withdrawal. First-strand cDNA was generated by 200 U of M-MLV reverse transcriptase (Promega) and DARPP-R-Exon and HPRT AS primers and 1 μg of total RNA. The DARPP-32-rat-specific sense primer used in qRT-PCR reactions was 5'-AAG AGA CCC AAC CCC

TGT GCC TAC-3' (DARPP-F-2, 622-645 nts; GenBank accession number AY601872). This primer in conjunction with DARPP-R-Exon was used to amplify a 224 bp product from cDNA corresponding to the mature DARPP-32 transcripts. cDNA at each time point was normalized first to HPRT and then to the levels of transcripts at 0 hr to correct for variability between the N548wt and N548mu cell lines. Levels were subjected to two-way ANOVA and the 0.05 level of significance was adopted for all comparisons.

2.7 5' RNA Ligase-Mediated Rapid Amplification of cDNA Ends

5' RNA ligase-mediated rapid amplification of cDNA ends (5'RLM-RACE) was performed to identify DARPP-32 and ppENK transcription sites using the first-choice RLM-RACE kit (Ambion) as described in McCaw *et al.*, 2004. RNA was isolated using Trizol™ (Invitrogen) from the striatum of 23 week-old wild-type and R6/1 mice. The extracted RNA was treated with calf intestinal phosphatase (CIP) to remove 5'-phosphate from uncapped RNA (degraded mRNA, rRNA, tRNA and genomic DNA). Half of the CIP-treated RNA was treated with tobacco acid pyrophosphatase (TAP) to remove 7-methylguanosine caps from the 5'end of full-length mRNAs, leaving 5'-monophosphate groups. The other half of the CIP-treated RNA served as a control for the effectiveness of CIP treatment in removing the 5' PO_4 groups from other nucleic acids in the sample. This method allows for the amplification of full-length mature transcripts and excludes truncated messages from the amplification process. A 45 bp RNA adapter oligonucleotide (5' GCU GAU GGC GAU GAA UGA ACA CUG CGU UUG CUG GCU UUG AUG AAA 3') was ligated to RNA (samples and controls) that contained a

5'-phosphate and random-primed MMLV reverse transcription (200 U, Promega) was performed to obtain a library of mature full-length cDNAs.

PCR amplification of the 5' ends of DARPP-32 cDNA included the 5' RACE outer and inner adapter primers and the DARPP-32 outer gene-specific primer 5'-CGG GCA CAG AGA ACT GAA TCT TCT T-3' (420-444 nts; GenBank accession number XM_109714) and the DARPP-32 inner gene-specific primer 5'-GAG CGT TCT TGG GGT GTC TGG CTG AG-3' (2288-2313 nts; GenBank accession number S80640). PCR amplification of the 5' ends of ppENK cDNA included the 5' RACE outer and inner adapter primer and the ppENK outer gene-specific primer 5'-CCT GGA GGT ATC CTA TCT TCC CAC G-3' (402-426 nts; GenBank accession number AK047709) and the ppENK inner gene-specific primer 5'-CCT GAT GAC ATC CTG TCC TTC CG-3' (365-387 nts; GenBank accession number AK047709). The reactions were run for 30 cycles in the first round of PCR using the outer primers and for 40 cycles in the second, nested PCR amplification, using the inner primers. For the above mentioned PCR amplifications, cycling conditions included 94°C for 3 min, followed by repeated cycles of 94°C for 30 sec, 55°C for 30 sec and 72°C for 30 sec. The final extension was at 72°C for 10 min.

An aliquot of each reaction was fractionated on a 1.5% (w/v) agarose gel, gel-purified using the GenElute™ Gel Extraction Kit (Sigma), ligated into pCR®-Blunt II TOPO® vector (Invitrogen) and transformed into One Shot® TOP10 Electrocompotent™ *E. coli* cells (Invitrogen). Several independent clones that were positive for inserts of different sizes were identified by *EcoR*I digestion, which released the insert from the pCR®-Blunt II TOPO® vector. The sequences of these independent

clones were determined by T7 dideoxy chain termination method using the T7 Sequencing™ Kit (Amersham Biosciences), [α^{33}P]dATP (3000 Ci/mmol), M13 universal forward and reverse primers and following manufacture's instructions.

2.8 RNase Protection Assay

To quantify and determine the 5' ends of DARPP-32 mRNA, ribonuclease protection assays (RPA) were performed using a 465 bp RPA probe spanning the region that included the transcription start sites in the proximal promoter region identified in GenBank and by 5' RLM-RACE. A sense DARPP-32 primer 5'-TGC TCA TTG GCC GCT TTC CCC TA-3' (1843-1865 nts; GenBank accession number S80640) and antisense DARPP-32 primer 5'-GAG CGT TCT TGG GGT GTC TGG CTG AG-3' (2288-2313 nts; GenBank accession number S80640) were used to amplify a DARPP-32-specific product from mouse genomic DNA. Cycling conditions for the PCR were as follows, initial denaturation 94°C for 3 min, followed by repeated cycles of 94°C for 30 sec, 58°C for 30 sec and 72°C for 30 sec, final extension was 72°C for 10 min. Similarly, to determine the relative amount of transcripts that initiated within the ppENK promoter, a 625 bp ppENK-specific fragment of mouse genomic DNA was generated using a sense ppENK primer 5' AAG CAG TTT CCC CTT CGT GTC CT-3' (4492-4514 nts; GenBank accession number U20894) and a ppENK-specific antisense primer (5'-CCT GAT GAC ATC CTG TCC TTC CG-3') (5095-5117 nts; GenBank accession number U20894). PCR amplification conditions were as follows: 94°C for 3 min, followed by repeated cycles of 94°C for 30 sec, 56°C for 1 min and 72°C for 30 sec. The final extension was 72°C for 10 min. The amplified products were fractionated on a 1.5%

(w/v) agarose gel and the band was excised. The PCR amplified product was extracted from the gel using GenElute™ Gel Extraction Kit (Sigma). The DARPP-32- and ppENK-specific products were ligated into the pCR®II-TOPO vector (Invitrogen), cloned and sequenced. The inserts in plasmids from a selected clone were PCR amplified using gene-specific primers, and an adapter sequence containing the T7 promoter was ligated to the PCR product using the Lig'nScribe kit (Ambion). *In vitro* transcription of the PCR amplified product was performed using the T7 RNA polymerase and trinucleotides including Biotin-14-CTP (Invitrogen). Full-length biotin-labeled ribonucleotide probes were fractionated on a 5% polyacrylamide gel, visualized by ultraviolet (UV) shadowing under 254 nm, excised and eluted from the gel overnight at 37°C in elution buffer containing 0.5 M NH_4 acetate, 1 mM EDTA and 0.2% (w/v) SDS. The probe was ethanol precipitated, resuspended in RNase-free H_2O, quantified by spectrophotometric analysis (at 260 nm) and stored at -70°C.

RNase protection assays were performed using the Supersignal RPA III kit (Pierce). The assays were performed on striatal RNA isolated from 9 week-old wild-type and R6/2 transgenic HD mice, striatal and cortical RNA from 12 week-old wild-type and R6/1 transgenic HD mice, and RNA isolated from the kidney of 10 week-old wild-type mice. Control reactions included probe only samples and probe with excess yeast RNA in the absence of mouse RNA. Specified concentrations of probe were combined with 1, 10 or 20 μg of wild-type, R6/1 or R6/2 RNA, precipitated, resuspended in hybridization III buffer (Ambion) and allowed to hybridize overnight at 42°C. After hybridization each of the samples except those containing probe only, were subjected to a 30 min RNase digestion at 37°C using 1:100 dilution of RNase A/T1. The digested products and a

biotinylated RNA ladder (Ambion) were fractionated on a 5% polyacrylamide gel and transferred to Hybond N+ membrane (Amersham Pharmacia). Bands were visualized using the chemiluminescent detection kit (Pierce) after exposing the membrane to high performance chemiluminescent film (Amersham Pharmacia).

2.9 Cell Culture

ST14A and derivatives of this cell line that were stably transfected to express the first 548 amino acids of huntingtin with 15 CAG repeats (N548wt) or 128 CAG repeats (N548mu) were kindly provided by Dr. Elena Cattaneo (Cattaneo & Conti, 1998; Rigamonti *et al.*, 2000). Cells were cultured at the permissive temperature of 33°C in Dulbecco's modified Eagle medium (DMEM, Invitrogen) supplemented with 10% (v/v) fetal calf serum (Hyclone), sodium bicarbonate (3.7 mg/ml; Hyclone), sodium pyruvate (0.11 mg/ml; Hyclone), glutamine (0.29 mg/ml; Hyclone); HEPES (238.8 mg/ml; Hyclone) and penicillin-streptomycin (100 U/ml; Hyclone) as previously described (Cattaneo & Conti, 1998). To induce differentiation, cells were grown at the permissive temperature in the absence of serum and antibiotics. HEK293 cells were cultured in DMEM supplemented with 10% (v/v) horse serum (Sigma). Cells were grown in an incubator at 37°C with humidified 5% CO_2 and 95% air.

The number of live and dead cells at 0, 24, 48, 72 and 96 hr post-serum-withdrawal was determined using the Live/Dead Viability/Cytotoxicity Kit (Molecular Probes) as per manufacture's instructions. Cells were plated at $5x10^4$ cells per well on coverslips in a poly-d-lysine coated 4-well plates. The cells were rinsed three times with 0.01 M PBS at room temperature. Ethidium homodimer-1 and calcein AM were added to

each well at a final concentration of 4 μM and 2 μM, respectively, and incubated at room temperature for 30 min. Calcein produces an intense green fluorescence in live cells (emission ~515 nm) which exclude the ethidium homodimer-1. Ethidium homodimer-1 produces a bright red fluorescence in cells that are dead or in the process of dying (emission ~635 nm). Fluorescence was visualized using a Zeiss Axiovert 100 microscope. The average number of living and dead cells at each time point was determined (n=4 wells per time point). Data was subjected to two-way ANOVA and the 0.05 level of significance was adopted for all comparisons.

2.10 Transfections and Luciferase Assay

A 1.4 kb *Bgl*II-*Hind*III fragment of the DARPP-32 promoter was PCR amplified from mouse genomic DNA using the sense primer 5'-AGA TCT CGA GAG ACT CAA GGG CTT GGA-3', (911-931 nts; GenBank accession number S80640) and the antisense primer 5'-AAG CTT GAG CGT TCT TGG GGT GTC TGG CTG AG-3' (2288-2313 nts; GenBank accession number S80640). The cycling conditions were 95°C for 15 min, followed by 35 cycles of 94°C for 30 sec, 52°C for 30 sec, 72°C for 90 sec, followed by a final extension of 72°C for 10 min. A 637 bp *Bgl*II-*Hind*III fragment of the ppENK promoter was amplified from mouse genomic DNA using the sense primer 5'-AGA TCT AAG CAG TTT CCC CTT CGT GTC CT-3', (4492-4514 nts; GenBank accession number U20894) and the antisense primer 5'-AAG CTT CCT GAT GAC ATC CTG TCC TTC CG-3'(5095-5117 nts; GenBank accession number U20894). The cycling conditions were 95°C for 15 min, followed by 35 cycles of 94°C for 1 min, 56°C for 1 min, 72°C for 1 min, followed by a final extension of 72°C for 10 min. Both fragments

were cloned into the pCR®-Blunt II TOPO® vector (Invitrogen) and digested with restriction enzymes to identify positive clones and release the fragments. The fragments was then cloned into pGL3-Basic vector (Promega) at the *Bgl*II/*Hind*III site [pGL3-DARPP(-1414/-11; pGL3-ENK(-524/+101)]. To prepare a series of 5' deletion constructs of the DARPP-32 and the ppENK promoters, pGL3-DARPP(-1414/-11) and pGL3-ENK(-524/+101) were digested with *Bgl*II (10 U, Fermentas) and with *Kpn*I (10 U, Fermentas) at the pGL3 vector arm, and subjected to the Exonuclease III/Mung Bean nuclease deletion as described Denovan-Wright & Lee, 1994. Two μg of *Bgl*II/*Kpn*I double-digested pGL3-DARPP(-1414/-11) or pGL3-ENK(-524/+101) were digested with ExoIII (200 U, MBI) at 37°C for 5 min. Every 30 sec, 200 ng of DNA was removed from the reaction and placed in a microfuge tube containing ice-cold 5X Mung Bean buffer. The digested DNA was heated at 68°C for 15 min and placed back on ice. The pooled ExoIII deletions were cleaved with 10 U of Mung Bean nuclease for 30 min at 30°C. Two μl of 1.0 M Tris Base (EMD Biosciences), pH 7.5 was added to each reaction and the samples were heated for 5 min at 70°C. The Exonuclease III/Mung Bean nuclease deletion reaction products were phenol:chloroform extracted. Sodium acetate (0.3 M, pH 5.2) and 66% (v/v) ethanol was added to the aqueous phase. The solution was mixed well and incubated at -20°C for 1 hr to precipitate the DNA. DNA was pelleted by centrifugation at 12,000 x *g* for 30 min at 4°C, washed with 70% (v/v) ethanol and dissolved in RNase-free H_2O. The Exonuclease III/Mung Bean nuclease deletions were re-ligated using the T4 Ligase (1 U, MBI) in the T4 DNA ligation buffer. The DNA sequences of several independent clones for each promoter were determined using the dideoxy method as described in 2.7. Six different promoter deletion constructs

were identified for pGL3-DARPP(-1414/-11) and one promoter deletion construct was identified for pGL3-ENK(-524/+101).

Vectors used in transfection experiments included pEGFP-N1 (Clontech), phRL-TK (Promega), pGL3-HPRT(-795/+97), pCMV-Luc, pCMV-22Q and pCMV-115Q, in addition to the DARPP-32- and ppENK-specific promoter constructs. pGL3-HPRT(-795/+97) was constructed by PCR amplifying a 904 bps *Xho*I-*Hind*III fragment of the HPRT promoter from mouse genomic DNA using the sense primer 5'-CTC GAG GTG TCG CCA CAC CTG ACT AAA ATC A-3' (51-75 nts; GenBank accession number K01507) and antisense primer 5'-AAG CTT GCA AAA AGC GGT CTG AGG AGG AA-3' (920-942 nts; GenBank accession number K01507). Final concentration of 2 mM $MgCl_2$ was added to the PCR reaction and cycling conditions were 95°C for 15 min, followed by 35 cycles of 94°C for 1 min, 56°C for 1 min, 72°C for 1 min, with a final extension at 72°C for 10 min. The amplified HPRT promoter fragment was cloned into the pCR®-Blunt II TOPO® vector (Invitrogen) and digested with restriction enzymes. The fragment was then cloned into the *Xho*I/*Hind*III sites of pGL3-Basic (Promega). A plasmid that expressed firefly luciferase under the control of the immediate early human cytomegalovirus (CMV) promoter region (pCMV-Luc) was kindly provided by Dr. Mark Nachtigal. Construction of pCMV-115Q encoding part of the 5'-UTR, the coding region within exon 1 with ~115 CAG repeats, and part of intron 1 of human huntingtin is described in Rodriguez-Lebron *et al.*, 2005. pCMV-115Q was digested with *Blp*I (Fermentas) and *BstE*II (Fermentas) to remove the 115 CAG repeats and was replaced with a *Blp*I and *BstE*II digested fragment containing 22 CAG repeats. The resulting

vector (pCMV-22Q) was identical to pCMV-115Q but had 22 instead of 115 CAG repeats.

ST14A, HEK293, N548wt and N548mu cells were transfected using Lipofectamine (Invitrogen) and Plus reagent (Invitrogen) with pEGFP-N1, phRL-TK and pGL3-DARPP(-1414/-11), pGL3-DARPP deletion constructs, pGL3-ENK(-524/+101), pGL3-ENK deletion constructs, pGL3-HPRT(-795/+97), pCMV-Luc or pGL3-Basic, following the manufacture's protocol (Invitrogen). Briefly, fifty thousand cells were plated in poly-d-lysine (Sigma) coated 4-well plates and incubated at 33°C overnight. The next day, 0.2 μg of the vector being tested [pGL3-DARPP(-1414/-11), pGL3-DARPP deletion constructs, pGL3-ENK(-524/+101), pCMV-Luc or pGL3-Basic], 0.2 μg of pEGFP-N1, which served as an internal control and 0.05 μg phRL-TK, which was the normalizing control, were diluted to a final volume of 25 μl in serum-free media (SFM). A plasmid that expresses a 21-nt antisense strand complementary to 416-436 nts (GenBank accession number NM_002111) of human huntingtin mRNA (shHD2.1) and an empty vector control (shRNAvec) were kindly provided by Dr. Beverly Davidson (Harper *et al.*, 2005). For the knockdown experiments, 0.20 μg of the vector being tested [pGL3-DARPP(-1414/-11), pGL3-ENK(-524/+101) or pGL3-HPRT(-795/+97)], 0.3 μg of a shHD2.1 or shRNAvec and 0.025 μg phRL-TK were diluted to a final volume of 25 μl in SFM. Alternatively, for transient transfections, 0.2 μg of the vector being tested [pGL3-DARPP(-1411/-11), pGL3-DARPP(-171/-11), pGL3-ENK(-524/+101), pGL3-ENK(-220/+101), pGL3-HPRT(-795/+97) or pCMV-Luc], 0.2 μg of pCMV-22Q or pCMV-115Q, 0.05 μg pEGFP-N1 and 0.05 μg phRL-TK were diluted to a final volume of 25 μl in SFM. Four microliters of Plus reagent was added to the DNA and incubated

at room temperature for 15 min. One microliter of Lipofectamine reagent was diluted to a final volume of 25 µl in SFM. The diluted Lipofectamine reagent was added to the DNA/Plus reagent mix and incubated at room temperature for 15 min. Cells were rinsed twice with SFM and the media was replaced with 200 µl of SFM. Fifty microliters of the DNA/Plus reagent/Lipofectamine mix was added to each well and incubated at 33°C for four hours. After four hours, fetal bovine serum (40 µl; Hyclone) and SFM (160 µl) were added to each well and the cells were incubated at 33°C overnight. The next morning, the cells were rinsed twice with Hank's buffered salt solution (HBSS; Invitrogen) and the media was replaced with ST14A growth media. Cells were harvested 48 hr post-transfection for Dual Luciferase assays (Promega), following manufacture's instructions. The media was removed from each well and the cells were rinsed with 0.01 M PBS. 1X passive lysis buffer (100 µl) was added to each well and the cells were covered to prevent light exposure and slowly shaken at room temperature for 15 min. The cells were scraped from the wells, transferred to a microfuge tube, frozen in dry ice/ethanol mix and thawed at room temperature. The freeze/thaw cycle was repeated twice for a total of three cycles and the cellular debris was pelleted by spinning the lysates at 12,000 x *g* for 30 sec. The supernatant was removed and placed in a clean tube. Ten microlitres of cell lysate was added to 50 µl of the Luciferase Assay Reagent II (Promega) and mixed by pipetting. The firefly lucifease activity was quantified using a 20/20m luminometer (Turner Biosystems), 50 µl of the Stop & Glo reagent (Promega), which contains the Stop & Glo substrate, was added to the tube and the *Renilla* luciferase activity was measured. Firefly luciferase activity was normalized to *Renilla* luciferase activity expressed from pRL-TK. Each experiment was repeated 12 times over three days.

Normalized data was subjected to one-way or two-way ANOVA and the 0.05 level of significance was adopted for all comparisons.

2.11 *In Vitro* DNase I Footprinting

Nuclear protein extracts were prepared from the forebrain of 5 week-old wild-type and R6/1 transgenic HD mice as described in Sambrook *et al.* (2000). Briefly, forebrains from three 5 week-old wild-type mice were pooled and three 5 week-old R6/1 mice were pooled and minced in 3 ml of ice-cold tissue homogenization buffer [10 mM Hepes-KOH (pH 7.6; Sigma), 25 mM KCl (BDH), 0.15 mM spermine (Sigma), 0.5 mM spermidine (Sigma), 1 mM EDTA (pH 8.0; Sigma), 2 M sucrose (EMD Biosciences), 10% (v/v) glycerol (Fisher Scientific), 0.5 mM phenylmethylsulphonyl fluoride (PMSF; Sigma) 1 μg/μl leupeptin (Sigma) and 1 μg/ml pepstatin (Sigma)] in a tight-fitting Dounce homogenizer until 80%-90% of the cells are broken. The lysed cells were subjected to centrifugation at 103,900 x *g* for 40 min at 4°C. The supernatants were discarded and the pellets were resuspended in ice-cold tissue resuspension buffer [5 mM Hepes-KOH (pH 7.9), 1.5 mM $MgCl_2$ (Sigma), 0.5 mM dithiothreitol (DTT; Sigma), 0.5 mM PMSF and 26% (v/v) glycerol]. 5M NaCl (EMD Biosciences) was added to a final concentration of 300 mM and the suspension was incubated on ice for 30 min. The suspensions were centrifuged at 103,900 x *g* for 20 min at 4°C. The supernatants, which contained 300 mM NaCl-soluble nuclear proteins, were collected and the concentration of total protein was determined using the BCA (bicinchoninic acid) protein assay (Pierce Biotechnology).

A 471 bp DARPP-32 promoter fragment was generated by PCR amplification using the sense DARPP-32 primer 5'-TGC TCA TTG GCC GCT TTC CCC TA-3' (1843-1846 nts; GenBank accession number S80640) and the antisense DARPP-32 primer 5'-AAG CTT GAG CGT TCT TGG GGT GTC TGG CTG AG-3' (2288-2313 nts; GenBank accession number S80640) which amplifies the -481 to -11 region of the DARPP-32 promoter, upstream of the first coding nucleotide. Cycling conditions for the above mentioned PCR were as follows: 95°C for 15 min, followed by repeated cycles of 94°C for 30 sec, 55°C for 30 sec and 72°C for 30 sec. The final extension was 72°C for 10 min. A 637 bps *Bgl*II-*Hind*III fragment of the ppENK promoter was amplified with the sense primer 5'-AGA TCT AAG CAG TTT CCC CTT CGT GTC CT-3', (4492-4514 nts; GenBank accession number U20894) and the antisense primer 5'-AAG CTT CCT GAT GAC ATC CTG TCC TTC CG-3'(5095-5117 nts; GenBank accession number U20894) and the following cycling conditions 95°C for 15 min, followed by repeated cycles of 94°C for 30 sec, 55°C for 30 sec and 72°C for 1 min. The final extension was 72°C for 10 min. The antisense DARPP-32 and ppENK primers (5 pmol) and 2 μg of the PhiX174 DNA/*Hinf*I ladder (Fermentas) were end-labeled using 3000 μCi [γ-^{32}P] dATP and 10 U of T4 polynucleotide kinase (PNK, Fermentas) in PNK buffer A. The reactions were stopped by the addition of 25 mM EDTA (pH 8.0) and unincorporated nucleotides were removed using a Sephadex G-25 column (Amersham Biosciences).

Ten μg of striatal nuclear protein extract from 5 week-old wild-type or R6/1 transgenic HD mice was incubated for 20 min at room temperature with 50,000 cpm of labeled DARPP-32 or ppENK promoter fragment in binding buffer [25 mM Tris-HCl (pH 8.0), 50 mM KCl (BDH), 6.25 mM $MgCl_2$ (Sigma), 0.5 mM EDTA (Sigma), 10%

(v/v) glycerol (Fisher Scientific) and 0.5 mM DTT (Sigma)]. $CaCl_2$ (EMD Biosciences) and $MgCl_2$ (Sigma) were added to a final concentration of 2.5 mM and 5 mM, respectively. DNase 1 (0.15 U, Promega) was added and the reactions were incubated at room temperature for 2 min and 30 sec followed by the addition of 100 mM NaCl (EMD Biosciences), 15 mM EDTA (Sigma), 0.5% (w/v) SDS (GibcoBRL) and 50 μg/ml yeast RNA (Sigma). Samples were extracted with phenol:chloroform:isoamyl alcohol (Invitrogen), precipitated with ethanol and resuspended in 10 μl of 10 mM EDTA (pH 7.5; Sigma) and 97.5% (v/v) deionized formamide (Invitrogen). The samples were heated at 95°C for 3 min to denature the DNA and placed on ice. The denatured samples were fractionated on 5% denaturing polyacrylamide gel electrophoresis (PAGE) gels with 1X Tris-borate-EDTA (Sigma) [TBE; 90 mM Tris-borate and 2 mM EDTA (pH 8.0)] buffer run at 2500 V for 2 hours. The gel was dried and exposed to X-ray film (Kodak).

2.12 *In Vitro* Transcription Assay

In vitro transcription and product analysis was performed using HeLaScribe Nuclear Extract *In Vitro* transcription system (Promega). Bovise serum albumin (BSA), striatal nuclear protein extracts from 5 week-old wild-type or R6/1 transgenic HD mice, kidney nuclear protein extracts from 5 week-old wild-type mice and 5 pmol of His-23Q or His-87Q fusion proteins were added to *in vitro* transcription reactions containing 8 U of HeLa nuclear extract, 20 mM HEPES (pH 7.9 at 25°C), 100 mM KCl (BDH), 0.2 mM EDTA (Sigma), 0.5 mM DTT (Sigma), 20% (v/v) glycerol (Fisher Scientific) with 400 μM each of rCTP, rATP, rUTP and 16 μM rGTP, 3 mM $MgCl_2$ (Sigma), 100 ng of DNA and 10 μCi of 3000 μCi [α-^{32}P]rGTP at 30°C for 60 min. Effects of the truncated N-

terminal fragment of mutant huntingtin on *in vitro* transcription from the control template [CMV IE gene 1 promoter isolated by *Eco*R1 and *Bam*H1 double-digestion of the 3.8 kb pMK11 plasmid] provided with the HeLaScribe™ nuclear extract *in vitro* transcription kit (Promega) was observed. *In vitro* transcription from the *Kpn*1/*BstB*I digested fragment of the pGL3-DARPP (1644 bps) and pGL3-HPRT (1129 bps) plasmids and the *Kpn*1/*Not*I (336 bps) and *Not*1/*BstB*I (530 bps) digested fragment of the pGL3-ENK(-524/+101) plasmid were also observed. For the *in vitro* transcription assays the components of the reaction were pre-incubated for 30 min at 30°C in the absence of rNTPs. Following addition of rNTPs, the reaction was incubated at 30°C for 30 min. To stop the transcription reaction, 175 µl of room temperature HeLa Extract stop solution (Promega) [0.3M Tris-HCl (pH 7.4), 0.3 M sodium acetate, 0.5% (w/v) SDS, 2 mM EDTA and 3 µg/ml of tRNA] was added to each reaction. RNA was isolated from each reaction following phenol:chloroform:isoamyl alcohol. Two hundred µl of phenol:chloroform:isoamyl alcohol (Invitrogen) was added to each reaction and vortexed for 1 min. The samples were subjected to centrifugation for 5 min at 13,000 x *g* and the upper, aqueous phase was transferred to a clean microfuge tube. Ethanol was added to a final concentration of 75% (v/v) and the RNA was allowed to precipitate overnight at -70°C. RNA was pelleted by centrifugation at 13,000 x *g* for 10 min at 4°C. The RNA pellets were air dried for 10 min at room temperature and dissolved in RNase-free H_2O by placing the solution on ice for 10 min, mixing and incubation for 10 min at 55°C. Formamide [49% (v/v); Invitrogen], 0.05% bromophenol blue (w/v; Sigma), 0.05% xylene cyanol (w/v; Sigma) and 5 mM EDTA (Sigma) were added to the resuspended samples. The samples were heated at 95°C for 10 min to denature the RNA and placed

on ice. The denatured samples were fractionated on a 5% denaturing PAGE gel with 1X TBE buffer. Gels were dried and exposed to BioMax MS film (Kodak) overnight in the -70°C. After developing the film, densitometric analysis of autoradiographs was performed using Kodak 1D Image Analysis Software. Each experiment was repeated three times, using independently derived protein samples. The average optical densities normalized to the optical density of the product obtained in the presence of BSA were subjected to one-way or two-way ANOVA and the 0.05 level of significance was adopted for all comparisons.

2.13 Production of Histidine-tagged Huntingtin Fusion Proteins

Vectors that generate the first 171 amino acids of huntingtin with a six histidine tag fused to the N-terminus were kindly provided by Dr. Xiao-Jiang Li (Li *et al.*, 2002). These fusion proteins contained either 23 (His-23Q) or 87 (His-87Q) glutamines in the repeat region. Proteins were produced and purified as described in Li *et al.*, 2002. BL21 bacteria were transformed with the constructs and grown at 37°C to an optical density of 0.6 at 600 nm. Expression of the fusion proteins was induced by adding isopropyl-β-D-thiogalactopyranoside (IPTG; Invitrogen) to a final concentration of 1 mM in the bacterial culture broth for 2 hr. The bacteria were harvested by centrifugation and resuspended in 8 ml of binding buffer [5 mM imidazole (Sigma), 500 mM NaCl (EMD Biosciences), 20 mM Tris-HCl (pH 8.0), 25 mM β-mercapthoethanol (Sigma), 0.1% (v/v) Nonidet P-40 (NP-40; Sigma) and 1 mM PMSF (Sigma)] and lysed with 8 mg of lysozyme (Sigma) for 30 min on ice. The solution was sonicated on ice using six 10 sec bursts with 10 sec cooling periods in between each period of sonication. The lysate was

drawn through an 18 gauge needle several times to ensure that the cell lysate was dispersed throughout the solution. The lysate was centrifuged at 14,500 x *g* (11,000 rpm; SS-34 rotor, Sorvall RC-5B centrifuge, DuPont Instruments) for 30 min to pellet the cellular debris. The Ni-NTA purification system (Invitrogen) was used to isolate the histidine-tagged proteins from the *E. coli* bacterial lysate. The supernatant was added to a prepared Ni-NTA agarose column and allowed to bind for 60 min using gentle agitation to keep the resin suspended in the lysate solution. The resin was settled by centrifugation at 800 x *g* for 1 min and the supernatant was removed. The resin was washed 4 times with wash buffer [50 mM imidazole (Sigma), 500 mM NaCl (EMD Biosciences), 20mM Tris-HCl (pH 8.0), 25 mM β-mercapthoethanol (Sigma), 0.1% (v/v) NP-40 (Roche) and 1mM PMSF (Sigma)] and the proteins bound to the column were eluted with elution buffer containing 400 mM imidazole (Sigma), 500 mM NaCl (EMD Biosciences), 20 mM Tris-HCl (pH 8.0), 20 mM β-mercapthoethanol (Sigma), 0.1% (v/v) NP-40 and 1mM PMSF. Eluate fractions were collected, microdialyzed using a 1 ml Float-A-Lyzer (Spectrum Laboratories Inc.) against 1X transcription buffer [20 mM Hepes (pH 7.9), 100 mM KCl (BDH), 0.2 mM EDTA (Sigma), 0.5 mM DTT (Sigma), 20% (v/v) glycerol 0.2 mM PMSF] and analyzed by 10% (w/v) SDS polyacrylamide gel electrophoresis (SDS-PAGE). The SDS-PAGE gel was silver stained to examine and quantify the purified protein. The gel was washed twice in 50% (v/v) methanol for 20 min each wash and left overnight in 50% (v/v) methanol. The next day the gel was rehydrated in two 30 min washes in RNase-free H_2O and returned to 50% (v/v) methanol for 1 hr. The gel was rinsed with RNase-free H_2O and stained for 1 hr with 0.2% (w/v) silver nitrate (Sigma), 0.075% (w/v) sodium hydroxide, 0.207 M ammonium hydroxide. The gel was rinsed

twice with RNase-free H_2O for 5 min each rinse and developed in 0.005% (w/v) citric acid (Sigma) and 0.019% (v/v) formaldehyde (Fisher Scientific). After one rinse with RNase-free H_2O the developing reaction was stopped by placing the gel in 45% (v/v) methanol (Fisher Scientific) and 10% (v/v) acetic acid (Fisher Scientific). The purified protein was quantified by comparison to a standard curve of known concentrations of BSA on the same gel. Densitometric analysis of silver-staining intensity was performed using Kodak 1D Image Analysis Software and the concentration of the purified protein was calculated.

2.14 Streptavidin-coupled Dynabeads

The CMV IE gene 1 promoter, isolated by *Eco*R1 and *Bam*H1 double-digestion of the 3.8 kb pMK11 plasmid and provided with the HeLaScribe™ nuclear extract *in vitro* transcription kit (Promega) was PCR amplified using the 5' biotin-labeled sense primer, (5'-GCA GAA CTG GTA GGT ATG GAA G-3') and the antisense primer (5'-CAC AGG ACG GGT GTG GTC-3') and the following cycling conditions: 95°C for 15 min, followed by 35 cycles of 94°C for 30 sec, 55°C for 30 sec, 72°C for 90 sec, followed by a final extension of 72°C for 10 min. The biotin-labeled product was fractionated on a 1.5% (w/v) agarose gel, gel-purified using the GenElute™ Gel Extraction Kit (Sigma) and quantified using the quantitative GeneRuler DNA ladder mix (Fermentas). 1 mg Dynabeads M-280 Streptavidin were washed 2 times with 1X binding and wash buffer [10 mM Tris-HCl (pH 7.5), 1mM EDTA (Sigma), 2.0 M NaCl (EMD Biosciences)], 2 times with 0.1 M NaOH (Fisher Scientific) and 0.05 M NaCl (EMD Biosciences), once with 0.1 M NaCl (EMD Biosciences) and resuspended in 100 µl of binding and wash

buffer. Five pmoles of biotin-labeled 1.2 kb CMV IE gene 1 promoter was incubated with 1 mg of prepared Dynabeads in a final volume of 100 µl RNase-free H_2O for 30 min at room temperature with gentle rotation. The beads coupled to biotin-labeled DNA were washed three times with 1X binding and wash buffer and resuspended in 100 µl of 1X transcription buffer [20 mM HEPES (pH 7.9 at 25°C), 100 mM KCl (BDH), 0.2 mM EDTA (Sigma), 0.5 mM DTT (Sigma), 20% (v/v) glycerol (Fisher Scientific)].

To isolate the proteins that interacted with the Dynabead-coupled CMV promoter, 5 µg of BSA, striatal nuclear protein extracts from 5 week-old wild-type or R6/1 transgenic HD mice, kidney nuclear protein extracts from 5 week-old wild-type mice or His-23Q or His-87Q (1 or 5 pmol) fusion proteins were added to *in vitro* transcription reactions containing 8 U of HeLa nuclear extract, 1X transcription buffer, 3 mM $MgCl_2$ (Sigma) and 100 ng of Dynabead-coupled CMV promoter and incubate at 30°C for 30 min. The Dynabead-coupled CMV promoter and the proteins that interact with it were isolated from the *in vitro* transcription reaction, by placing the tube on a Dynal magnetic particle concentrator (MPC). The isolated Dynabead-coupled CMV promoter and interacting proteins were rinsed twice with 100 µl of 1X transcription buffer. The beads were resuspended in sample buffer [10% (v/v) glycerol (Fisher Scientific), 5% (v/v) β-mercaptoethanol (Sigma), 3% (w/v) SDS (GibcoBRL) and 62.5 mM Tris-HCl (pH 6.8)] heated at 95°C for 10 min and fractionated on 7.5% SDS-PAGE gel. The gel was either silver stained to visualize the proteins as described in section 2.13 or the proteins were transferred to an Immobilon-P transfer membrane (Millipore) at 100 V for 1 hr and blocked for 1 hr at room temperature in 5% (w/v) milk powder dissolved in 1X Tris-buffered saline (TBS; Sigma) with 0.1% (v/v) Tween-20 (TBS-T; Sigma). Histidine-

tagged proteins were detected by probing the blot with the mouse anti-histidine tagged antibody (1:50; Calbiochem) in 5% (w/v) milk powder dissolved in 1X TBS-T overnight at 4°C. Following 1 hr incubation at room temperature with peroxidase anti-mouse IgG (1:1000, Vector Laboratories), the peroxidase labeled antibody was detected using the enhanced chemiluminescent detection kit (Amersham Biosciences) as per manufacture's instructions and visualized after exposing the membrane to high performance chemiluminesence film (Hyperfilm ECL, Amersham Biosciences).

2.15 Statistics

Statistical analysis was performed using SPSS software. All data are reported as the mean ± the standard error of the mean (SEM). One-way or two-way ANOVA with the statistical significance set at 0.05 were performed. Tukey's honestly significant multiple comparisons were employed where appropriate.

CHAPTER 3

Expression of the DARPP-32 and ppENK Genes *In Vivo*

Portions of this chapter appeared in the following publication:

Gomez, G.T., Hu, H., McCaw, E.A. & Denovan-Wright, E.M. (2006) Brain-specific factors in combination with mutant huntingtin induce gene-specific transcriptional dysregulation. *Molecular and Cellular Neuroscience*, **31**, 661-675. Reprinted with permission from Elsevier.

3.1 Introduction

Normal and mutant huntingtin are both widely expressed in the brain and body but, for reasons that are currently unknown, there is selective degeneration of GABAergic medium spiny projection neurons in the caudate and putamen of HD patients (Vonsattel *et al.*, 1985; Schilling *et al.*, 1995; Sharp *et al.*, 1995). It is known that early neuronal dysfunction induces behavioural changes prior to any apparent neurodegeneration. In humans, there is a rough correlation between the age of onset of the disease and the CAG repeat size. This is also observed in transgenic HD mouse models such as the R6 model, where the R6/2 transgenic HD mice with 150 CAG repeats shows overt movement abnormalities starting at 8 weeks of age, while the R6/1 transgenic HD mice with 115 CAG repeats shows the same movement abnormalities starting at 13 weeks of age (Mangiarini *et al.*, 1996; Carter *et al.*, 1999; Hansson *et al.*, 2001). However, this difference in the relative time of HD-like symptom onset can not be solely attributed to the length of the CAG repeat as the R6/2 mice have a higher expression of the N89-150Q protein and a longer CAG repeat compared to R6/1 mice (Mangiarini *et al.*, 1996).

NIIs that contain the N-terminal portion of mutant huntingtin protein are present in neurons throughout the brain and in dystrophic neurites (DiFiglia *et al.*, 1997; Becher *et al.*, 1998). The N-terminal fragment of mutant huntingtin is present in the nucleus of striatal and cortical neurons and the expression of truncated mutant huntingtin has been associated with changes in the expression of a small number of the genes in the striatum in a number of different cellular and animal models of HD (Cha, 2000; Luthi-Carter *et al.*, 2000; Sipione *et al.*, 2002; Sugars & Rubinsztein, 2003; Desplats *et al.*, 2006). In addition, the N-terminal fragment of mutant huntingtin affects expression of specific

genes that are expressed in other brain regions including the cortex and hippocampus (Cattaneo *et al.*, 2005).

The goal of this study was to determine when the temporal and spatial distribution of the steady-state mRNA levels of various transcripts were first altered by N89-115Q or N89-150Q in the R6/1 and R6/2 transgenic HD mouse models. We reasoned that changes in mRNA levels that occur in young mice are more likely to be altered directly by the N-terminal fragment of mutant huntingtin, while changes that occur as the mice age may be changes that are induced due to altered cellular function. DARPP-32 is highly expressed in 96% of the striatal medium-spiny neurons, the nucleus accumbens and olfactory tubercle as well as the thick ascending limb of the loop of Henle in the kidney in adult rats (Ouimet *et al.*, 1984; Walaas & Greengard, 1984; Meister *et al.*, 1989). Steady-state mRNA and protein levels of DARPP-32 are known to be decreased in the striatum of R6 (Bibb *et al.*, 2000; Luthi-Carter *et al.*, 2000; van Dellen *et al.*, 2000), N171-82Q (Luthi-Carter *et al.*, 2000) and YAC128 transgenic mouse models of HD (Van Raamsdonk *et al.*, 2005) and in rats where striatal neurons were transduced with lentiviral vectors expressing the first 171 amino acids of human huntingtin with a polyQ repeat length of 82 (de Almeida *et al.*, 2002). It appears that regulation of DARPP-32 mRNA levels, in the absence of cell death, is restricted to HD as there are no other reports of DARPP-32 mRNA levels being altered in the brain during different pathological processes or drug administration. The ppENK gene is also highly expressed the in the striatum and mRNA levels of ppENK are known to be lower in symptomatic HD patients and several transgenic HD models (Albin *et al.*, 1991; Richfield *et al.*, 1995; Luthi-Carter *et al.*, 2000; Menalled & Chesselet, 2002; Sun *et al.*, 2002). As both of

these genes are highly expressed in the striatum and transcript levels of DARPP-32 and ppENK are decreased in various models of HD, we chose to describe the temporal and spatial changes in mRNA of these two genes as a first step in characterizing the effects of N89-115Q and N89-150Q on the steady-state mRNA levels of a subset of genes that are expressed in the striatum.

3.2 Results

Microarray and previous *in situ* analysis using cDNA probes complementary to the coding region of DARPP-32 have shown a decrease in the steady-state DARPP-32 mRNA levels in the striatum of 6 and 12 week-old R6/2 mice (Bibb *et al.*, 2000; Luthi-Carter *et al.*, 2000) and 20 week-old R6/1 mice (van Dellen *et al.*, 2000). We used the *in situ* probe 2 that was complementary to the coding regions of DARPP-32 to determine if transcripts that are normally abundantly expressed in the striatum were lower in symptomatic R6/2 transgenic HD mice compared to age-matched wild-type mice. Northern blot analysis demonstrated that the DARPP-32 *in situ* probe 2 annealed with a 1.7 kb mRNA in RNA samples derived from the striatum of wild-type mice. This mRNA was less abundant in RNA samples derived from the striatum and cortex of symptomatic 10 week-old R6/2 mice and the cortex of the wild-type mice compared to the levels observed in striatal RNA of wild-type mice (Fig. 3-1A). This probe did not detect other isoforms encoded by the DARPP gene. The levels of 1.7 kb DARPP-32 mRNA and cyclophilin mRNA were quantified by densitometry. Microarray analysis comparing wild-type and R6/2 mice at 6 and 12 weeks of age included probes against cyclophilin mRNA and no difference in cyclophilin mRNA levels were observed (Luthi-Carter *et al.*,

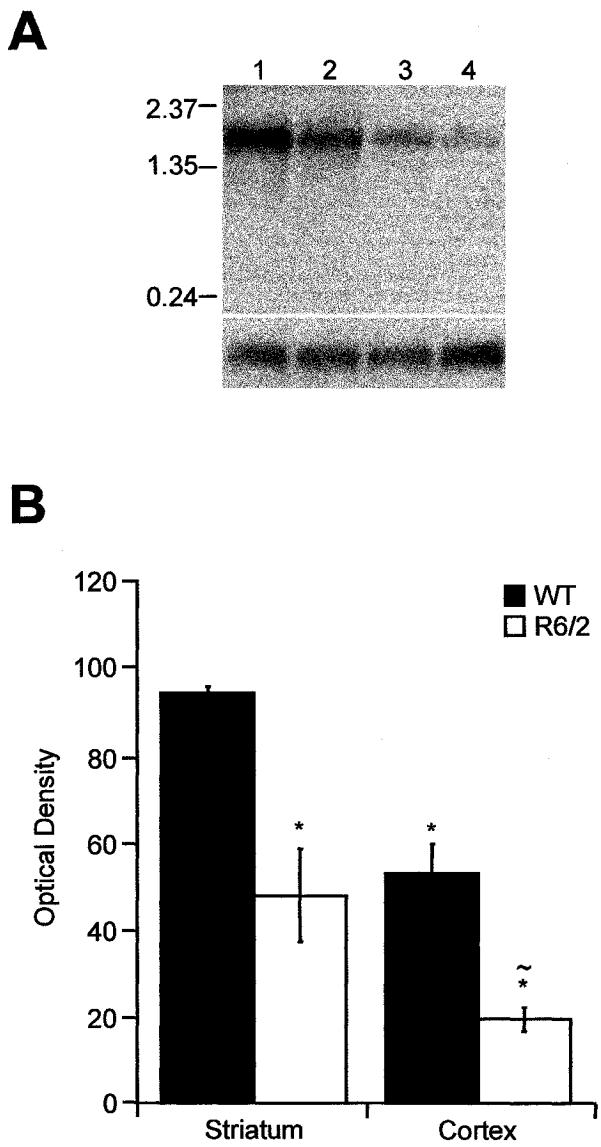

Figure 3-1. DARPP-32 mRNA levels are lower in the striatum and cortex of R6/2 transgenic HD mice compared to wild-type mice. A representative Northern blot analysis is shown (A). The blot was allowed to anneal with a DARPP-32-specific probe (top). After removal of the DARPP-32-specific probe, a cyclophilin-specific probe (bottom) was allowed to hybridized with the blot and used as a loading control. The RNA was isolated from the striatum (1, 2) and cortex (3, 4) of 10 week-old wild-type (1, 3) and R6/2 transgenic HD (2, 4) mice. The relative mobility of molecular weight markers (Gibco BRL, 9.5-0.24 RNA ladder) is shown on the left of the blot. Histogram showing the average optical density (± SEM; n=3/group) of DARPP-32 mRNA levels, normalized to cyclophilin mRNA levels, in the striatum and cortex of 10 week-old wild-type (solid black bars) and R6/2 (solid white bars) mice; *$P < 0.05$, significantly different from levels in wild-type striatum, ~$P < 0.05$, significantly different from levels in R6/1 striatum (B) (two-way ANOVA).

2000). Similarly, cyclophilin levels did not appear to differ among lanes that were loaded with equivalent mass amounts of total RNA. Levels of DARPP-32 mRNA were normalized to the levels of cyclophilin mRNA in each lane and the mean levels of normalized DARPP-32 mRNA for each tissue and genotype were calculated (Fig. 3-1B). The levels of DARPP-32 mRNA in the striatum of 10 week-old R6/2 mice were approximately 50% of the levels observed in the striatum of wild-type mice (n=3, $P < 0.05$) (Fig. 3-1B). The levels of DARPP-32 mRNA are known to be lower in the cerebral cortex compared to the caudate/putamen in rats (Schalling *et al.*, 1990). Therefore as expected, the levels of DARPP-32 mRNA in the cortex of 10 week-old wild-type mice were approximately 50% of the levels observed in the striatum of wild-type mice (n=3, $P < 0.05$) (Fig. 3-1B). There was a significant decrease in the DARPP-32 mRNA levels in the cortex of R6/2 mice compared to the cortex of wild-type mice (n=3, $P < 0.05$). The levels of DARPP-32 mRNA in the cortex of 10 week-old R6/2 were approximately 21% of the levels observed in the wild-type striatum. The observed decrease in the steady-state levels of DARPP-32 mRNA in the striatum and cortex of R6/2 compared to wild-type mice was due to the specific reduction in levels of the 1.7 kb mRNA encoded by the DARPP-32 gene. Because DARPP-32 levels are higher in the striatum than in other brain regions, the decrease in DARPP-32 in this tissue was readily observed. DARPP-32 mRNA levels, however, appear to decrease proportionately in the striatum and cortex of R6/2 compared to wild-type mice indicating that expression of the amino terminus of human huntingtin with ~ 150Q affects DARPP-32 levels in areas of the brain that express this gene.

In order to describe the temporal and spatial expression of DARPP-32 mRNA in the wild-type and R6 transgenic HD mice, we performed *in situ* hybridization on coronal brain sections of wild-type, R6/1 and R6/2 mice ranging in age from 3 to 29 weeks using *in situ* probe 2 (Fig. 3-2 and 3-3), which is complementary to the coding region of DARPP-32 and specific to the 1.7 kb DARPP-32 mRNA. DARPP-32 mRNA was detected in the striatum of wild-type, R6/1 and R6/2 mice and the intensity of the DARPP-32-specific hybridization signal decreased in the striatum of older R6/1 and R6/2 mice (Fig 3-2). DARPP-32-specific hybridization was also observed in layers II, III, V and VI of the parietal cortex and in the piriform cortex and the relative intensity of the hybridization signal, although lower than that observed in striatal tissue, also appeared to decrease in older R6/1 and R6/2 mice. The optical density of the hybridization signal in the striatum of four mice per age and genotype were averaged (Fig. 3-3A). The DARPP-32-specific hybridization signal in the striatum was normalized to the medial septum for each animal. There was no difference in DARPP-32 mRNA levels among 3 and 4 week-old wild-type, R6/1 and R6/2 mice. In R6/2 mice, the steady-state DARPP-32 mRNA levels decreased from 5 to 8 weeks of age and then remained constant at ~ 40% of the levels observed in wild-type mice in 8 to 12 week-old R6/2 mice. DARPP-32 mRNA levels decreased in 6 to 21 week-old R6/1 mice. At later time points, the levels of DARPP-32 mRNA in R6/1 mice remained constant at ~ 50% of the levels observed in wild-type mice. Comparison of the exponential curves of best fit revealed that the rate of decrease of steady-state DARPP-32 mRNA levels was faster in the R6/2 mice than in the R6/1 mice (Fig. 3-3B). The rate of decline in the steady-state levels of DARPP-32 mRNA was dependent on the age and genotype of the mice. We did not quantify

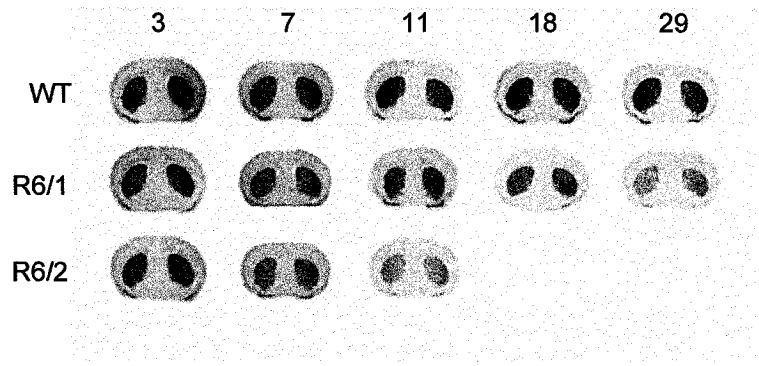

Figure 3-2. *In situ* hybridization analysis was used to determine the temporal and spatial distribution of DARPP-32 mRNA in the brains of wild-type and transgenic HD mice. Representative *in situ* hybridization analysis of coronal brain sections from wild-type (WT), R6/1 and R6/2 mice using the DARPP-32 *in situ* probe 2 as a hybridization probe. Numbers above columns of sections indicate the age of the mice in weeks.

Figure 3-3. DARPP-32 mRNA levels in the striatum of R6/1 and R6/2 mice older than 4 weeks of age are lower than levels observed in age-matched wild-type mice. Histogram showing the average optical density (± SEM; n=4/group) of DARPP-32-specific hybridization (*in situ* probe 2) in the striatum, normalized to hybridization signal in the medial septum (A). Optical density of wild-type (solid black bars), R6/1 (striped bars) and R6/2 (spotted bars) are shown and the age of the group is indicated on the x-axis (*$P < 0.05$, significantly different from age-matched wild-type; ~$P < 0.05$, significantly different from age-matched R6/1; two-way ANOVA). SIGMA PLOT was used to fit the data to a curve that best described the rate of change in DARPP-32 mRNA levels in the striatum of wild-type (closed triangles), R6/1 (open circles) and R6/2 (closed circles) mice (B). The optical density values of the levels of DARPP-32 mRNA in the R6/1 and R6/2 mice fit an exponential decay curve with a coefficient of determination (R2) value of 0.87 and 0.98 for R6/1 and R6/2 mice, respectively. The variables that describe the exponential decay in DARPP-32 mRNA levels in R6/1 mice include $y^0 = 49.34$, $a = 72.26$ and $b = 0.19$ ($P < 0.01$). For R6/2 mice, the variables that describe the exponential decay in DARPP-32 mRNA levels are $y^0 = 37.27$, $a = 264.49$ and $b = 0.49$ ($P < 0.01$).

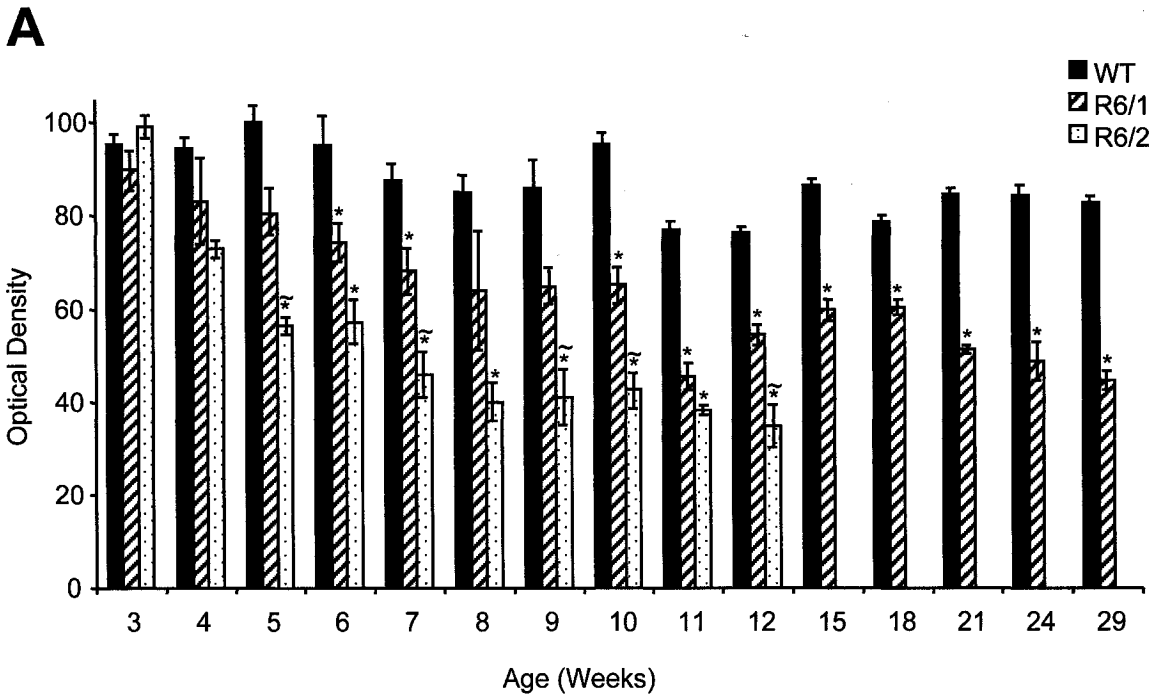
A
WT
R6/1
R6/2
Optical Density
100
80
60
40
20
0
3
4
5
6
7
8
9
10
11
12
15
18
21
24
29
Age (Weeks)

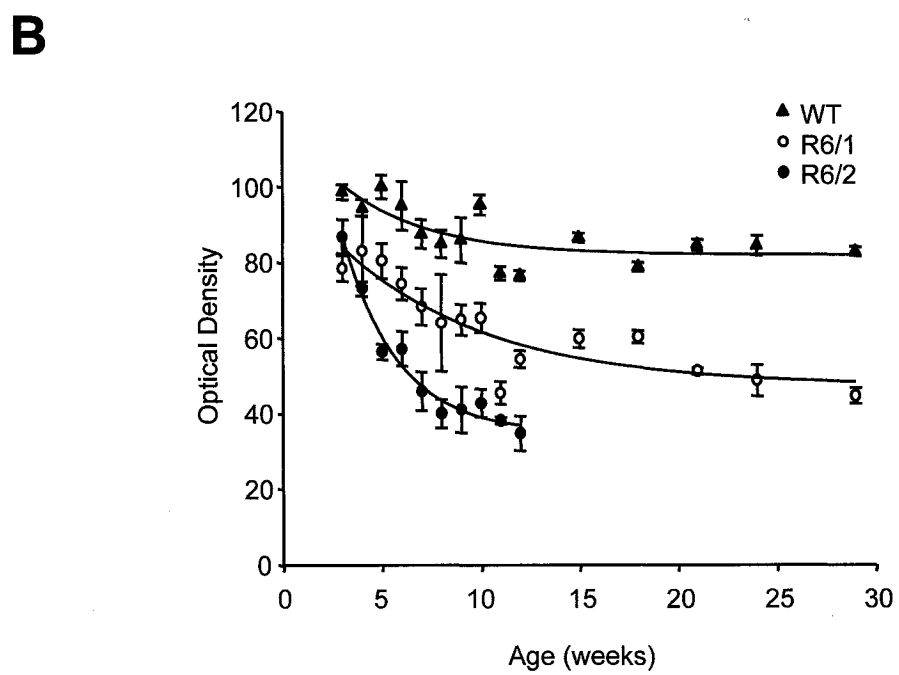
B
WT
R6/1
R6/2
Optical Density
120
100
80
60
40
20
0
0
5
10
15
20
25
30
Age (weeks)

differences in the levels of DARPP-32 mRNA in brain regions outside of the striatum following *in situ* hybridization.

The decrease in steady-state levels of DARPP-32 mRNA in the striatum could be caused by a loss of DARPP-32-expressing neurons, a loss of expression of the DARPP-32 gene in a subset of neurons or a general decrease in the number of DARPP-32 transcripts per striatal neuron. As it has been reported that there is no significant loss of striatal neurons in 3-12 week-old R6/2 or 3-29 week-old R6/1 transgenic HD mice (Mangiarini *et al.*, 1996; Hansson *et al.*, 1999; Bibb *et al.*, 2000; Turmaine *et al.*, 2000; van Dellen *et al.*, 2000), we wished to determine which of the other two possibilities led to the reduced DARPP-32 mRNA levels in these mice. Emulsion autoradiography was performed on coronal brain sections of R6/2 transgenic HD and wild-type mice that had been subjected to *in situ* hybridization using *in situ* probe 2 (Fig. 3-4). In both the R6/2 and wild-type mice, there was an even distribution of silver grains corresponding to DARPP-32-specific hybridization over all striatal neurons. In 10 week-old R6/2 mice, there was a decrease in the relative number of silver grains per neuron when compared to age-matched wild-types. In sections derived from DARPP-32 knockout mice (Fienberg & Greengard, 2000), there were a few silver grains and the grains that were present were dispersed randomly throughout the striatum. The silver grains observed following emulsion autoradiography of DARPP-32 knockout mice indicated the level of background signal. This analysis demonstrated that the decrease in the steady-state levels of DARPP-32 was due to a loss in the number of DARPP-32 transcripts per striatal neuron in HD and was not caused by altered DARPP-32 gene expression in a subset of striatal neurons.

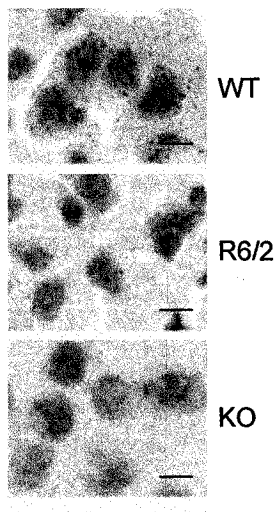

Figure 3-4. Autoradiographic emulsion of mouse striatal sections hybridized to the DARPP-32 probe. Brightfield micrographs of emulsion autoradiography of the striatum of 10 week-old WT, R6/2 and DARPP-32 knockout (KO) mice counterstained with cresyl violet. Scale bars represent 10 μm.

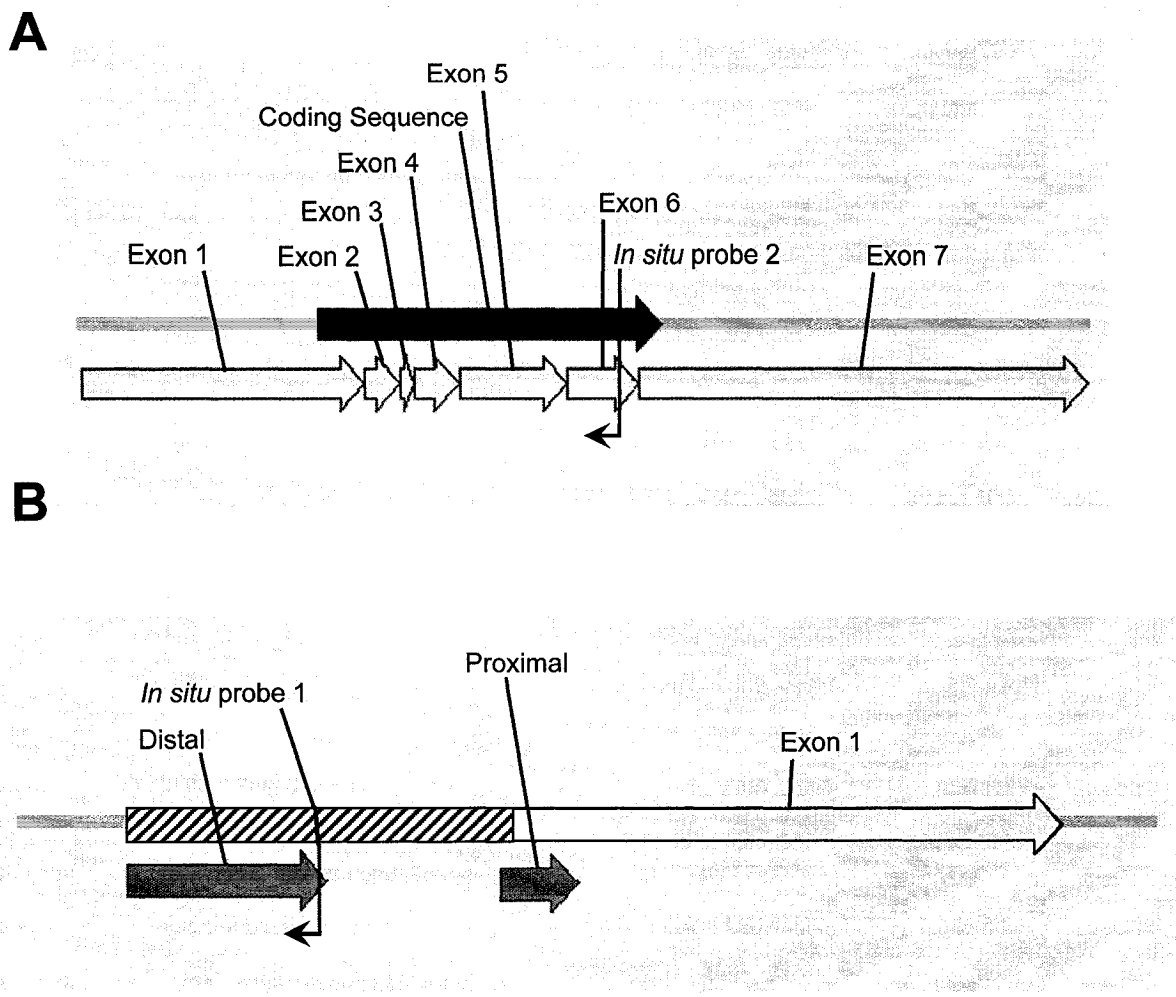

Figure 3-5. Schematic representation of the *Mus musculus* DARPP-32 mRNA, the promoter region and the relative positions of *in situ* probes. The mRNA structure of DARPP-32 is shown in A. The coding sequence (solid black) spans part of exon 1 and exon 2 to exon 7. The arrows indicate 5' to 3' organization of mRNA sequences corresponding to exons and the *in situ* hybridization probes. *In situ* probe 2 (black arrow) is complementary to the sequence in exon 6 at the 3' end of the coding region. The proximal and distal (gray arrows) regions of DARPP-32 transcript initiation in relation to the 5' end of exon 1 are shown in B. *In situ* probe 1 (black arrow) is complementary to transcripts that initiate at the distal transcription initiation region. The 5' boundary of exon 1 (white) is as defined by GenBank, (Accession number XM_19714). The hatched 5' extension includes that part of exon 1 encoding transcripts that initiate at the distal transcription initiation region.

The DARPP-32 mRNA is encoded by seven exons and the protein coding sequence spans the 3' end of exon 1 through to the 5' end of exon 7 (Fig. 3-5A). Previously, two transcription initiation regions referred to as the distal and proximal transcription initiation regions relative to the translation initiation codon were identified in the DARPP-32 gene by low resolution RPA and primer extension (Blau *et al.*, 1995; Fig. 3-5B). We wanted to determine if the transcripts that initiate from both the distal and the proximal transcription imitation regions were decreased in R6 transgenic HD mice. Because *in situ* probe 1 can anneal with transcripts that initiate only from the distal transcription start sites while *in situ* probe 2 can anneal with transcripts that initiate from both the distal and proximal promoters, comparison of the relative hybridization of these probes can indicate whether levels of transcripts that initiate from the proximal, the distal or both transcription start sites were affected by expression of N89-115Q. *In situ* hybridization was performed on brain sections of 10 week-old wild-type and R6/2 mice using *in situ* probe 1 to determine if the loss in the number of DARPP-32 transcripts was due to loss of transcripts from the distal transcription initiation region (Fig. 3-6). The hybridization signal from *in situ* probe 1 was specific for DARPP-32 mRNA as only background levels of signal were observed in sections derived from the DARPP-32 knockout mice (Fig 3-6A). The transcripts that initiate from this region were present at low levels in the striatum but there was no difference in DARPP-32 mRNA levels detected using *in situ* probe 1 among wild-type and R6 mice. DARPP-32 is also expressed in the thick ascending loop of Henle in the kidney (Meister *et al.*, 1989). We wanted to determine if transcripts that initiate from the proximal and the distal transcription initiation region were expressed in the kidney and if both sets of transcripts

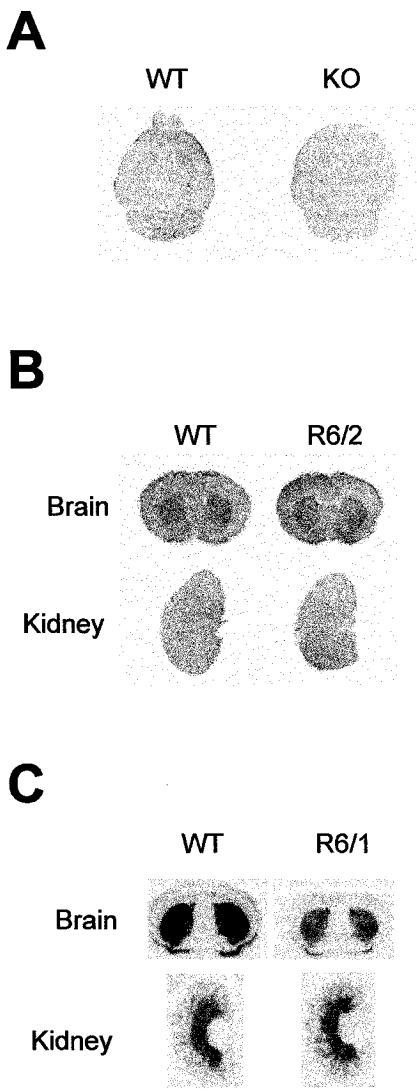

Figure 3-6. *In situ* hybridization analysis showing promoter-specific DARPP-32 expression in the brain and kidney of wild-type and transgenic HD mice. Representative *in situ* hybridization analysis using DARPP-32 *in situ* probe 1 on longitudinal brain sections of 10 week-old wild-type (WT), but not DARPP-32 knockout (KO) mice (A). Representative *in situ* hybridization analysis using DARPP-32 *in situ* probe 1 on coronal brain and kidney sections from 10 week-old wild-type (WT) and R6/2 transgenic HD mice (B). Representative *in situ* hybridization analysis using DARPP-32 *in situ* probe 2 on coronal brain and kidney sections from 30 week-old wild-type (WT) and R6/1 transgenic HD mice (C).

were lower in the kidney of R6 transgenic HD mice compared to wild-type littermates. *In situ* hybridization using *in situ* probe 2 on coronal brain and kidney sections from 30 week-old wild-type and R6/1 mice demonstrated that DARPP-32 mRNA could be detected in the renal medulla (Fig. 3-6C). Transcripts that initiate from the distal promoter were not detected in kidney (Fig. 3-6B). There was no difference in the mean intensity of the DARPP-32-specific hybridization signal in the renal medulla of 15 and 30 week-old wild-type and R6/1 mice (n=3; Fig. 3-7). The levels of DARPP-32 mRNA transcripts that initiated within the proximal, but not the distal, transcription initiation region were affected by the expression of N89-115Q in the striatum, but not the kidney.

It was possible that N89-115Q in the kidney was not expressed at high enough levels or that the protein was not in a conformation that would alter the steady-state mRNA levels of DARPP-32 in this tissue. The rate of formation of NIIs is largely dependent upon the expression levels of truncated N-terminal mutant huntingtin (Davies *et al.*, 1997; Kosinski *et al.*, 1997). Despite the controversy regarding the exact role of NIIs in HD progression (Ross, 1997; Sisodia, 1998), NIIs can serve as a marker for the presence of the amino terminus of mutant huntingtin. They contain numerous proteins in addition to the truncated N-terminal fragment of mutant huntingtin. The presence of NIIs indicate that mutant huntingtin is present in a protein conformation that can form abnormal protein complexes. These abnormal protein complexes are present in all models of HD. Therefore, we determined when NIIs could be detected in the brain and kidney of R6 transgenic HD mice and correlated these observations to the timing of the

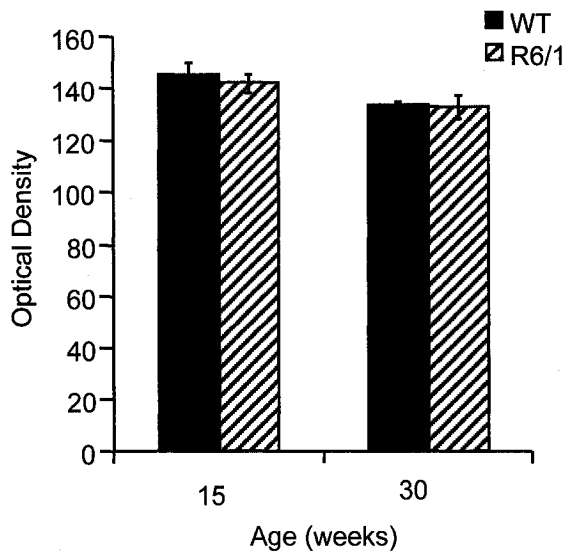

Figure 3-7. DARPP-32 mRNA levels are not changed in the kidneys of wild-type and transgenic HD mice. Histogram showing the average optical density (±SEM; n=4/group) of DARPP-32 *in situ* probe 2 hybridization in the renal medulla of kidneys derived from 15 and 30 week-old wild-type (WT) (solid black bar) and R6/1 (striped bars) mice.

decrease in DARPP-32 mRNA in the striatum but not the kidney. Ubiquitin is a highly conserved 76 amino acid polypeptide with a role in protein degradation. Immunocytochemistry analysis using antibodies against ubiquitin and the N-terminal fragment of mutant huntingtin indicates that these proteins are co-localized in NIIs (Davies *et al.*, 1997). Analysis of 5 sections per animal and 3 animals per age and genotype were performed. Ubiquitin-positive NIIs were present in the striatum of 7 week-old and older R6/1 mice and 4 week-old and older R6/2 mice (Table 3-1; Fig. 3-8). NIIs were not observed in the kidneys of 15 week-old R6/1 mice, but were observed in the kidneys of 22 and 30 week-old R6/1 mice (Fig. 3-8). These observations indicated that N89-115Q was expressed in the kidneys at lower levels than in the brain or that accumulation of mutant huntingtin in ubiquitin-positive aggregates was slower in the kidney than in the brain. Steady-state levels of DARPP-32 mRNA started to decrease in the striatum of 5 week-old R6/1 mice, two weeks prior to the time that ubiquitin-positive NIIs could be detected in the striatum and throughout the brain. However, DARPP-32 mRNA levels in the kidneys were unchanged in 30 week-old R6/1 mice, which was eight weeks after ubiquitin-positive NIIs were first detected in the kidney of R6/1 mice. This immunohistochemical analysis, in conjunction with *in situ* hybridization analysis, indicated that the expression of N89-115Q exerted a tissue-specific effect on the levels of DARPP-32 mRNA. The level of DARPP-32 mRNA in the striatum, but not the kidney, were affected despite the fact that NIIs containing N89-115Q were present in both the brain and kidney.

DARPP-32 mRNA is only one of many mRNAs that are affected by the expression of N89-115Q in the striatum (Luthi-Carter *et al.*, 2000). We wanted to

Table 3-1. Ubiquitin-positive NIIs are present in brain sections of R6/1 and R6/2 transgenic HD mice older than 6 and 3 weeks of age, respectively.

Age (weeks)	Wild-type	R6/1	R6/2
3	-§	-	-
4	-	-	++‡
5	-	-	++
6	-	-	++
7	-	+†	++
8	-	++	
9	-	++	
10	-	++	
11	-	++	
12	-	++	++
14	-	++	
15	-	++	
22	-	++	
30	-	++	

§ - No NIIs observed.

† + Few randomly dispersed small NIIs observed.

‡ ++ NIIs clearly visible.

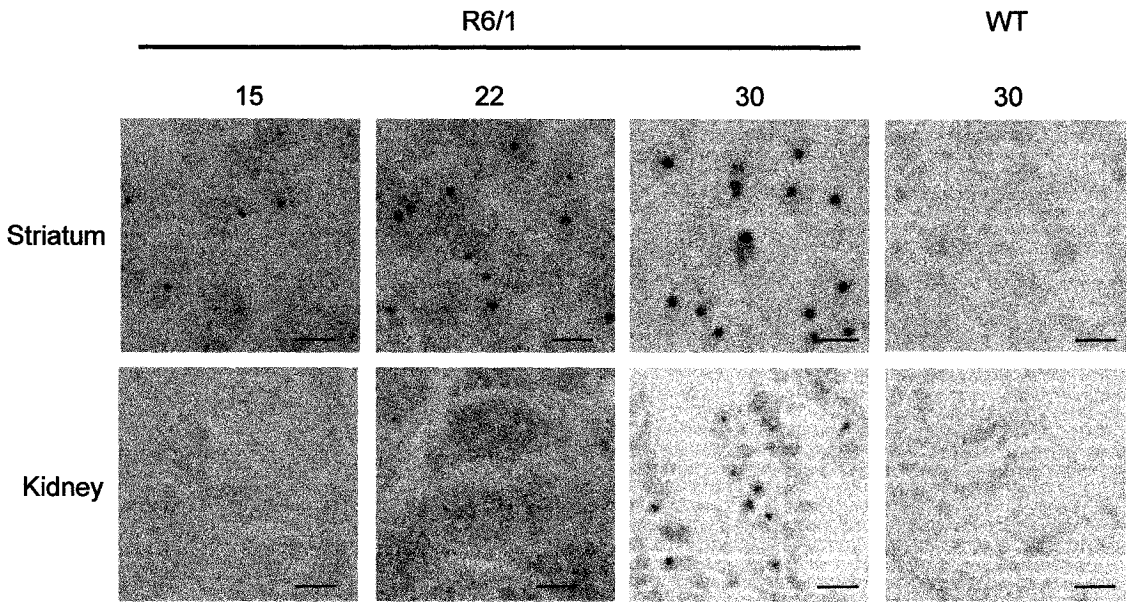

Figure 3-8. NIIs are present in the striatum of 15, 22 and 30 week-old R6/1 transgenic HD mice and the kidneys of 22 and 30 week-old R6/1 transgenic HD mice. Representative photomicrographs of the immunohistochemical analysis using the anti-ubiquitin antibody to detect the presence of NIIs in 15, 22 and 30 week-old R6/1 striatum and kidneys. Scale bars represent 10 μm.

compare the changes that occur in the temporal and spatial patterns of expression of the DARPP-32 gene in the R6 model to another gene (ppENK) whose mRNA levels are known to be affected by the expression of N89-115Q in this and other transgenic mouse models of HD (Luthi-Carter *et al.*, 2000; Menalled *et al.*, 2000; Sun *et al.*, 2002). *In situ* hybridization was performed on coronal brain sections of wild-type, R6/1 and R6/2 mice ranging in age from 3 to 28 weeks using a ppENK-specific *in situ* probe (Fig. 3-9 and 3-10). The ppENK *in situ* probe is complementary to the coding region of ppENK mRNA. The specificity of the probe for ppENK was verified by basic local alignment search tool (BLAST) analysis. ppENK was detected in the striatum of wild-type, R6/1 and R6/2 mice and the intensity of the ppENK-specific hybridization signal decreased in the striatum of older R6/1 and R6/2 mice (Fig 3-9). The optical densities of the ppENK-specific hybridization signal in the striatum normalized to the medial septum of four mice per age and genotype were averaged (Fig. 3-10A). There was a significant decrease in the ppENK-specific hybridization signal in R6/2 and R6/1 transgenic mice over time. At three weeks of age, there was no difference in the optical densities of the ppENK-specific hybridization signal among wild-type, R6/1 and R6/2 mice. However, in all R6 mice older than 4 weeks of age, ppENK mRNA levels were significantly lower than levels observed in wild-type mice. In both R6/1 and R6/2 mice, the steady-state ppENK mRNA levels decreased rapidly from 4 to 6 weeks of age and then remained constant at ~ 30% of the levels observed in wild-type mice. There was no difference in the steady-state ppENK mRNA levels between age-matched R6/1 and R6/2 mice. Comparison of the exponential curves of best fit revealed that the rate of decrease of steady-state ppENK mRNA levels were similar in the R6/2 and R6/1 transgenic HD mice (Fig. 3-10B). The

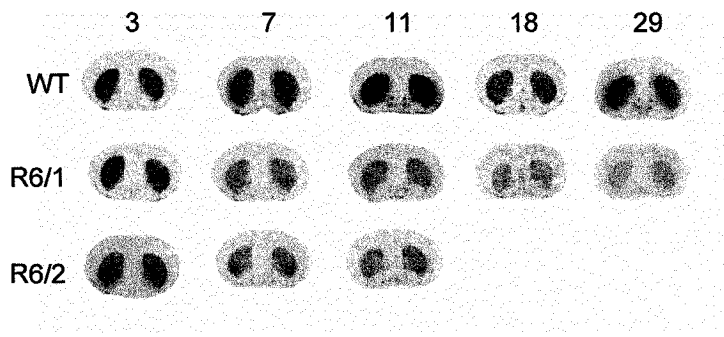

Figure 3-9. *In situ* hybridization analysis was used to determine the temporal and spatial distribution of ppENK mRNA in the brains of wild-type and transgenic R6/1 and R6/2 mice. Representative *in situ* hybridization analysis of coronal brain sections of wild-type (WT), R6/1 and R6/2 mice using the ppENK *in situ* probe as a hybridization probe. Numbers above columns of sections indicate the age of the mice in weeks.

Figure 3-10. ppENK mRNA levels in the striatum of R6/1 and R6/2 mice older than 3 weeks of age are lower than levels observed in age-matched wild-type mice. Histogram showing the average optical density (± SEM; n=4/group) of ppENK-specific hybridization in the striatum, normalized to the hybridization signal in the medial septum (A). Optical density levels of wild-type (solid black bars), R6/1 (striped bars) and R6/2 (spotted bars) are shown and the age of the group is indicated on the x-axis (*$P < 0.05$, significantly different from age-matched wild-type; two-way ANOVA). SIGMA PLOT was used to fit the curve that best described the rate of change in ppENK mRNA levels in the striatum of wild-type (closed triangles), R6/1 (open circles) and R6/2 (closed circles) mice (B). The optical density values of the levels of ppENK mRNA in the R6/1 and R6/2 mice fit an exponential decay curve with a coefficient of determination (R^2) value of 0.91 and 0.99 for R6/1 and R6/2 mice, respectively. The variables that describe the exponential decay in ppENK mRNA levels in R6/1 mice include $y^0 = 18.24$, $a = 105.40$ and $b = 0.29$ ($P < 0.01$). For R6/2 mice, the variables that describe the exponential decay in ppENK mRNA levels are $y^0 = 26.46$, $a = 991.33$ and $b = 0.97$ ($P < 0.01$).

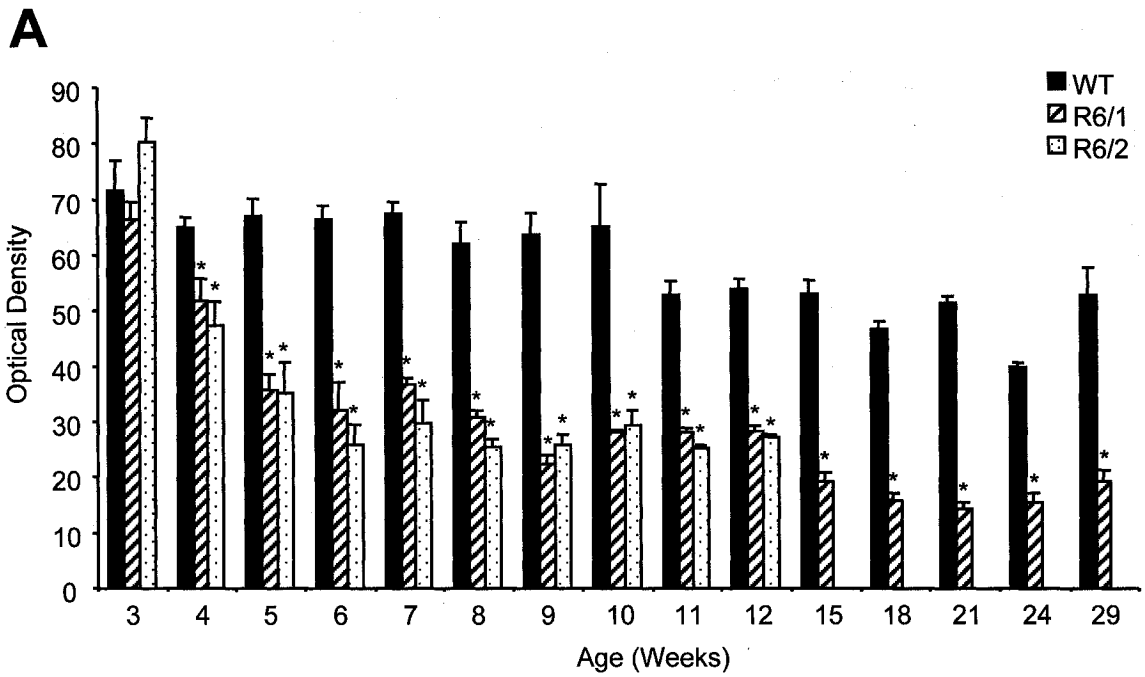
A
WT
R6/1
R6/2
Optical Density
0
10
20
30
40
50
60
70
80
90
3
4
5
6
7
8
9
10
11
12
15
18
21
24
29
Age (Weeks)

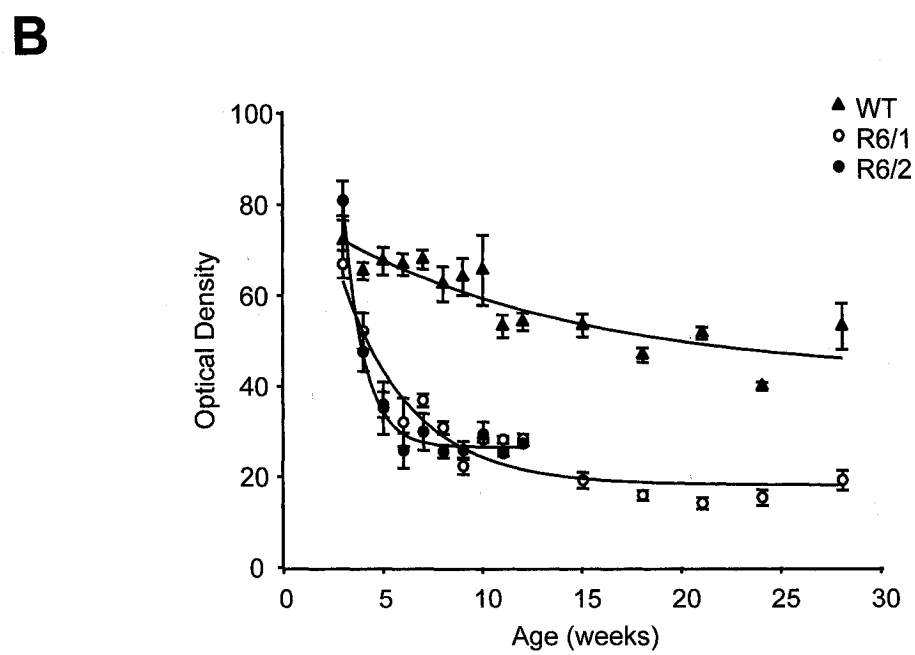
B
WT
R6/1
R6/2
Optical Density
0
20
40
60
80
100
0
5
10
15
20
25
30
Age (weeks)

rate of decline in the steady-state levels of ppENK mRNA was dependent on the age, but not the genotype, of the R6 transgenic HD mice.

3.3 Discussion

The most pronounced early neuropathological feature of HD is the progressive loss of GABAergic medium spiny projection neurons in the caudate and putamen (Vonsattel *et al.*, 1985). There is also neuronal cell death in other regions of the brain including the cortex, thalamus and subthalamic nucleus (Cudkowicz & Kowall, 1990; Hedreen *et al.*, 1991). It has been thoroughly documented that mutant huntingtin is expressed throughout the brain and that levels of mutant huntingtin are not significantly higher in the neurons of the caudate and putamen compared to levels in other regions of the brain (Aronin *et al.*, 1995; Bhide *et al.*, 1996). As such, the selective cell loss has drawn considerable attention to the effect of mutant huntingtin in the caudate and putamen. In rodents, the striatum is functionally equivalent to the caudate and putamen and much of the research on the effects of mutant huntingtin in cellular and animal models of HD focus on the striatum. Of the neurons that are affected by mutant huntingtin in the caudate and putamen, the D_2/enkephalin-positive medium spiny GABAergic projection neurons appear to be more vulnerable to effects of mutant huntingtin as these neurons are lost earlier in HD progression than the D_1/substance P-positive neurons (Ferrante *et al.*, 1986). Eventually, both types of medium spiny projection neurons are lost (Richfield *et al.*, 1995). The brains of 12 week-old R6/2 mice and 18 week-old R6/1 mice weigh ~ 20% and 18% less respectively, than the brains age-matched wild-type littermates (Davies *et al.*, 1997). The reduction in size was constant

throughout all CNS structures, which had an apparently normal neuronal density (Davies *et al.*, 1997). These R6 mice exhibit neuronal loss and degeneration only at very late time points. It has been reported that the survival of R6/2 mice can be extended if mice are housed under enriched conditions. Under such conditions neurodegeneration can be observed in 14-16 week-old R6/2 mice (Turmaine *et al.*, 2000) and in 20 week-old in the R6/1 mice (Iannicola *et al.*, 2000). However, the percentage of cresyl violet-stained striatal neurons that expressed ppENK are significantly decreased in 12 week-old, but not 8 week-old, R6/2 transgenic HD mice (Sun *et al.*, 2002). There is also a small significant decrease in the percentage of cresyl violet-stained striatal neurons that expressed preprotachykinin (PPT), a peptide product of substance P in 12 week-old R6/2 transgenic HD mice. This indicates that the ppENK-positive neurons in the striatum, when compared to the substance P-positive neurons in the striatum, are preferentially affected earlier by the amino terminus of mutant huntingtin in this transgenic model of HD and that the changes in protein levels precede neurodegeneration.

ppENK is expressed in the D_2 positive medium spiny neurons, while DARPP-32 is expressed in both the D_1- and D_2- positive medium spiny neurons. In this study, we observed that ppENK mRNA levels were significantly decreased from age-matched wild-types at 4 weeks of age in the R6/1 and R6/2 transgenic HD. This decrease in ppENK mRNA levels preceded the time that DARPP-32 mRNA levels began to decline, which was at 5 weeks of age in R6/2 and 6 weeks of age in R6/1 mice. This decrease in steady-state mRNA levels of DARPP-32 and ppENK preceded the loss of D_1- and D_2- positive medium spiny neurons in the striatum of the R6 transgenic HD mice (Davies *et al.*, 1997; Sun *et al.*, 2002). In agreement with previous reports, *in situ* hybridization analysis on

coronal brain sections of whole brains from 10 week-old wild-type and R6/2 mice showed an even distribution of the DARPP-32 hybridization signal in the striatum (Walaas & Greengard, 1984). Emulsion autoradiography of the DARPP-32-specific hybridization signal demonstrated that the decrease of DARPP-32 mRNA levels in the striatum occurred throughout all striatal neurons, and did not occur within a selective subpopulation of striatal neurons. There was a decrease in the DARPP-32 mRNA levels per neuron. Similarly, immunohistochemical studies on coronal brain sections of whole brains from 6 week-old R6/2 transgenic HD mice showed a decrease in DARPP-32 protein levels and the morphology of DARPP-32-positive medium spiny neurons appears to be unaffected in R6/2 transgenic HD mice (Bibb *et al.*, 2000). Steady-state mRNA levels of ppENK were decreased in the striatum and nucleus accumbens of 6 week-old R6/2 mice (Bibb *et al.*, 2000) and it has previously been shown that the loss of ppENK transcripts in the 8 week-old R6/2 mice is due to a decrease in the ppENK mRNA levels per neuron (Sun *et al.*, 2002).

There are many genes expressed in the striatum that are not altered in the R6 transgenic HD mice (Bibb *et al.*, 2000; Luthi-Carter *et al.*, 2000; Luthi-Carter *et al.*, 2002a; Desplats *et al.*, 2006). Because there is no detectable loss of neurons in the R6 model at the age at which ppENK and DARPP-32 mRNA levels started to decrease and because there are many genes whose mRNA expression levels are unaffected by the presence of N89-115Q or N89-150Q, the decrease in steady-state mRNA levels of ppENK and DARPP-32 mRNA may reflect gene-specific changes that occur relatively early in the progression of the disease in these mice.

DARPP-32 and ppENK mRNA levels were the same in 3 week-old wild-type, R6/1 and R6/2 mice. However, as the mice aged, the levels of DARPP-32 and ppENK mRNA declined in the R6 mice. This indicated that all the factors necessary for the full expression of DARPP-32 and ppENK mRNA are initially expressed in striatal neurons of R6 and wild-type mice and that at some time after three weeks a change occurs in the R6 mice that alters steady-state mRNA levels. It has previously been shown that increasing levels of insoluble ubiquitinated N-terminal fragments of mutant huntingtin accumulate in the cortex and the striatum of R6/2 transgenic HD mice starting at 3.5 weeks (Meade *et al.*, 2002). The amount of detectable amino terminus human huntingtin protein increases starting at ~ 4 weeks of age in the R6/1 mice (Hu and Denovan-Wright, unpublished data). The final levels of N89-150Q appear to be higher in R6/2 compared to levels of N89-115Q in the R6/1 mice and the length of the CAG repeat length is lower in R6/1 compared to R6/2 mice (Mangiarini *et al.*, 1996; Hu and Denovan-Wright, unpublished data). It seems likely that when N89-150Q and N89-115Q levels reach a particular concentration the levels of DARPP-32 and ppENK mRNA begin to decrease. Steady-state levels of DARPP-32 mRNA decreased in the striatum and cortex of the R6/1 and R6/2 transgenic mouse models in a manner that was inversely dependent on the length of the polyglutamine-encoding CAG repeat in exon 1 of the transgene or the relative expression of the transgene or both. It was not possible to correlate effects on mRNA levels solely with CAG repeat length in the R6 lines of transgenic HD mice because the detectable levels of the amino terminus of mutant huntingtin and the length of the CAG repeat length are both lower in R6/1 compared to R6/2 mice (Mangiarini *et al.*, 1996; Hu and Denovan-Wright, unpublished data). The difference in relative expression levels of

the amino terminus of mutant human huntingtin is likely due to differences in the site of integration of the transgene, which affects transcription of the transgene and levels of the N-terminus of mutant huntingtin. The sites of integration for the transgene into the R6/2 and R6/1 mice genomes have not been defined (Mangiarini *et al.*, 1996).

The rate of decline of DARPP-32 mRNA levels in the R6/2 transgenic HD model, which has a longer CAG repeat length and a higher level of expression of N89-150Q, was faster than in the R6/1 model. Alternatively, steady-state ppENK mRNA levels decrease in the striatum of R6/1 and R6/2 mice in a manner that was independent of the length of the polyglutamine region or the expression of the transgene. After the period of mRNA decline, the new steady-state level of DARPP-32 mRNA levels in the R6/1 and R6/2 mice was ~ 40 - 50% of the levels observed in age-matched wild-type mice, while the new ppENK mRNA steady-state level was ~ 30% of the level observed in age-matched wild-type mice. Similarly, cannabinoid receptor type-1 (CB1; McCaw *et al.*, 2004) and phosphodiesterase 10A (PDE10A; Hu *et al.*, 2004) mRNA levels undergo a period of decline and then remain constant in older R6 transgenic HD mice compared to age-matched wild-type mice. These observations suggest that the N-terminal fragments of mutant huntingtin differentially affects individual genes within the same cells and that ppENK mRNA levels may be more sensitive to the effects of N89-115Q and N89-150Q than the DARPP-32 mRNA levels. It is possible that levels of N89-115Q and N89-150Q or length of the CAG repeat expressed in either strain has a maximal adverse effect on the steady-state levels of ppENK mRNA. Such differences in the sensitivities of individual gene products may explain the temporal order in which mRNAs appear to decline in various models of HD. The description of the temporal and spatial distribution of mRNA

in R6 HD mice highlighted important similarities and differences between DARPP-32 and ppENK. These studies, therefore, have extended previous observations that examined isolated time points in RNA that was extracted from tissue.

N89-115Q affects the steady-state levels of DARPP-32 in a transcription initiation site-specific manner. *In situ* hybridization analysis showed that transcripts that initiate from the proximal, but not the distal transcription initiation region of the DARPP-32 promoter, were less abundant in the brains of R6 transgenic HD mice. This raises the possibility that N89-115Q may affect the factors that control expression of certain genes from specific promoters. A more precise definition of transcription initiation sites that are used to express N89-115Q-affected genes may indicate whether there are differences in the selection of start sites in R6 compared to wild-type mice.

N89-115Q affects the steady-state levels of DARPP-32 mRNA in a tissue-specific manner. *In situ* hybridization and Northern blot analysis showed that within the brain, DARPP-32 was expressed at lower levels in the cortex than in the striatum but N89-115Q and N89-150Q caused levels to decrease by ~ 50% in the striatum and cortex of R6/2 and R6/1 mice. It appeared that mutant huntingtin exerted the same relative effect on expression of DARPP-32 in two different cells within the brain. However, *in situ* hybridization analysis showed that DARPP-32 mRNA levels were not decreased in the renal medulla in the kidneys of older R6 transgenic HD mice compared to age-matched wild-type even eight weeks after NIIs were first detected in the kidneys of these mice. The role of NIIs in the pathology of HD is controversial. It has been suggested that NIIs could play a causative role in the pathology of the disease as they occur prior to the onset of disease symptoms in transgenic HD mice and the knockdown of huntingtin in a

conditional mouse model eliminated inclusions as well as the behavioural phenotype in (Davies *et al.*, 1997; Yamamoto *et al.*, 2000). Conversely, it has also been suggested that NIIs formation are protective as the suppression of NII formation resulted in an increase in mutant huntingtin-induced death *in vitro* (Saudou *et al.*, 1998). Ubiquitin-positive NIIs were first detected in 4 week-old R6/2 mice and ppENK mRNA levels started to decline in 4 week-old R6/2 mice. We compared NII deposition and DARPP-32 and ppENK mRNA expression in R6/1 instead of R6/2 mice as the latter have changes in gene expression and development of HD-like symptoms within in a short window of time making it difficult to determine the relative order of events. In the R6/1 mice, ppENK mRNA levels were decreased at 4 weeks of age, DARPP-32 mRNA levels were decreased at 5 weeks of age and ubiquitin-positive NIIs were first detected at 7 weeks of age. This implies that NIIs are not directly involved in the initial events that contribute to decreased levels of ppENK and DARPP-32 mRNA because NIIs are detected only after changes in steady-state mRNA levels are observed. The accumulation of the insoluble form of N89-115Q and N89-150Q in NIIs is an indicator that mutant huntingtin is being produced in these cells. It seems likely that soluble N-terminal fragments of mutant huntingtin becomes incorporated into insoluble complexes in NIIs over time. NIIs continue to increase in diameter as the mice age. This indicates that soluble N-terminal fragments of mutant huntingtin rather than the insoluble aggregates may be toxic to the cells. NIIs formation reduces intracellular levels of diffuse huntingtin and prolonged neuronal survival *in vitro* (Arrasate *et al.*, 2004). NIIs might protect the neuron by decreasing the levels of toxic diffuse forms of mutant huntingtin, implying that NII

formation is a secondary phenomenon that functions as a coping response to toxic soluble mutant huntingtin (Arrasate *et al.*, 2004).

The order of events related to when DARPP-32 and ppENK mRNA steady-state levels start to decrease, when levels of these messages reach a new lower equilibrium, the time that NIIs could be detected, and the occurrence of abnormal motor symptoms are summarized in figure 3-11. Decreases in the steady-state levels of DARPP-32 and ppENK mRNA are among the first changes observed. The decrease in steady-state levels of these transcripts occurs prior to caspase-1 and -3 activation, which occur in 7 and 9 week-old R6/2 mice, respectively (Ona *et al.*, 1999; Chen *et al.*, 2000) and mitochondrial deficits which were observed in 6 week-old R6/2 transgenic HD mice (Bates *et al.*, 1996; Jenkins *et al.*, 2000). R6/2 mice develop symptoms including resting tremor, irregular gait, abrupt movements, epileptic seizures and diabetes at 9-11 weeks of age, well after the changes in DARPP-32 and ppENK transcript levels began to decline (Mangiarini *et al.*, 1996). The relative order of changes was difficult to define in R6/2 mice because they occur within a short time frame. In contrast, the R6/1 transgenic mice had a slower progression of the disease phenotype and the relative order of these events in these R6/1 transgenic HD mice could be readily determined. Therefore, the R6/1 transgenic HD model may be a good model in which to further examine the individual events that lead up to the loss of steady-state mRNA levels of DARPP-32 and ppENK. As the steady-state levels of transcripts were among the earliest changes that were observed in the R6 transgenic HD mouse model, it was most likely that these changes were due to the primary effects of N89-115Q and N89-150Q rather than secondary compensatory changes or changes involved in neuronal death.

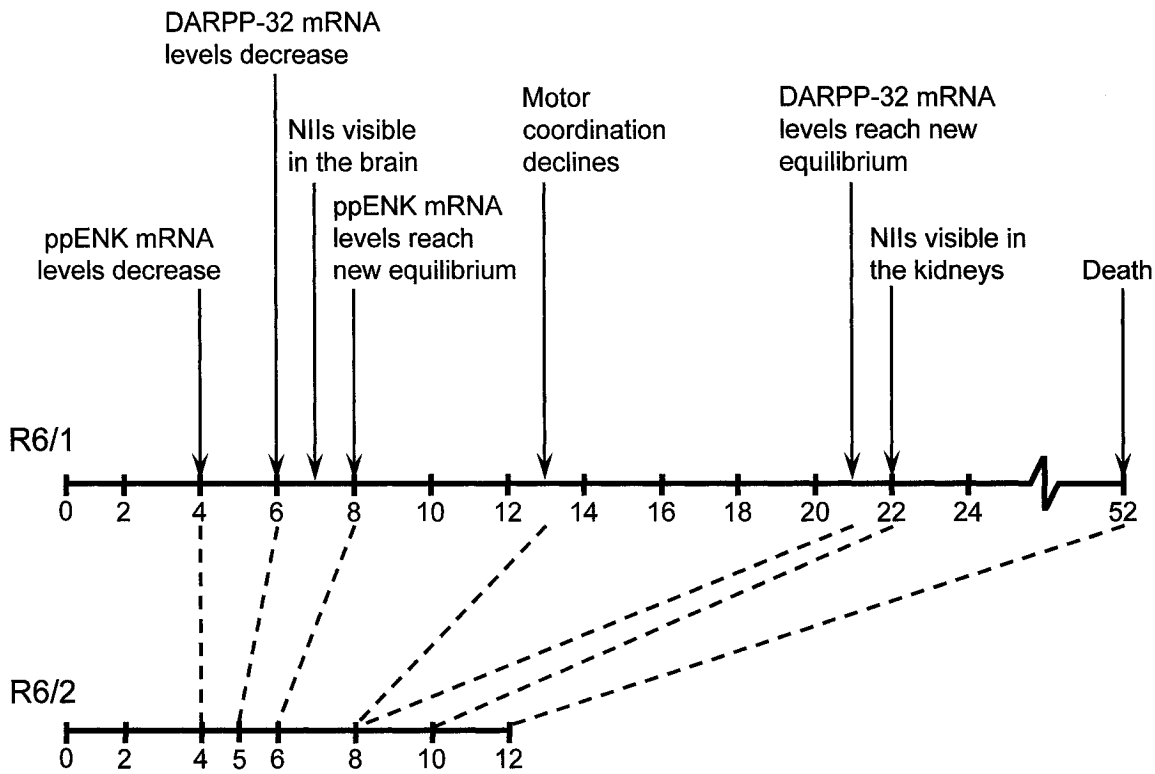

Figure 3-11. Comparison of the temporal progression of changes that occur in the R6/1 and R6/2 transgenic HD mice. The lines indicate the lifespan of the R6/1 and R6/2 mice, respectively. The age of the mice in weeks is indicated by the numbers under each line. Various changes that occur at different ages in the R6/1 mouse model are indicated by arrows. The times that these changes occur in the R6/2 model are indicated by the dotted lines.

The decrease in the steady-state levels of ppENK and DARPP-32 mRNA in the R6 transgenic HD mice with its full complement of mouse huntingtin provides evidence that the amino terminus of the huntingtin protein with its expanded polyglutamine region has an abnormal function that alters mRNA levels in models of HD. Furthermore, we have determined that the decreases in steady-state mRNA levels was not due to a loss of neurons, but was due to the gene-, tissue- and promoter-specific effects of N89-115Q and N89-150Q. Currently, there are many studies that focus on determining the mechanism by which mutant huntingtin decreases the steady-state levels of various transcripts. These studies are based on the assumption that mutant huntingtin affects transcription of these genes. It should be noted that steady-state mRNA levels could be decreased by either altering transcription of the gene or by affecting the stability of the mRNA, both of which could lead to the observed decrease in steady-state levels of the transcripts. We are studying effects that occur early in HD pathogenesis that may be directly caused by the presence of mutant huntingtin rather than resulting from secondary compensatory changes. However, the effects of mutant huntingtin on the steady-state levels of these genes could be attributed to indirect effects of mutant huntingtin, such as intracellular signaling. The differences between ppENK and DARPP-32 steady-state mRNA levels in the R6/1 and R6/2 transgenic HD mouse models indicate that comparison of these two model genes may lead to increased understanding of the abnormal function of the truncated N-terminal fragment of mutant huntingtin.

CHAPTER 4

The Amino Terminus of Mutant Huntingtin Decreases Transcription *In Vivo* and *Ex Vivo*

Portions of this chapter appeared in the following publication:

Gomez, G.T., Hu, H., McCaw, E.A. & Denovan-Wright, E.M. (2006) Brain-specific factors in combination with mutant huntingtin induce gene-specific transcriptional dysregulation. *Molecular and Cellular Neuroscience*, **31**, 661-675. Reprinted with permission from Elsevier.

4.1 Introduction

The N-terminus of mutant huntingtin has been associated with changes in the steady-state mRNA levels of a small number of genes in a number of different cellular and animal models of HD (Cha, 2000; Luthi-Carter *et al.*, 2000; Sipione *et al.*, 2002; Sugars & Rubinsztein, 2003). The observed decrease in steady-state levels of the transcripts could be attributed to a decrease in the rate of transcription or a decrease in the stability of the mRNA, which are two distinctly different processes that could lead to the observed decrease in steady-state levels of transcripts.

Transcripts from the DARPP-32 distal transcription region were not affected by the presence of N89-115Q (Chapter 3). The effects of N89-115Q and N89-150Q on the transcripts that initiated from the proximal promoter of DARPP-32 and the ppENK promoter might be caused by a loss of transcripts from a particular transcription start site(s). N89-115Q altered the steady-state levels of DARPP-32 in the brain but not in the kidney. It is possible that the tissue-specific effects of N89-115Q and N89-150Q could be caused by interactions between the N-terminal fragment of mutant huntingtin and specific transcription factors that direct the transcriptisome to unique initiation sites within the DARPP-32 proximal promoter in the brain and in the kidney.

Decreases in steady-state levels of transcripts in the striatum could be attributed to intra- or intercellular effects of the N-terminal fragment of mutant huntingtin. BDNF is synthesized in the cerebral cortex but not in the striatum and is known to support the survival of striatal neurons (Altar *et al.*, 1997; Conner *et al.*, 1997). Reduced BDNF mRNA levels have been observed in the cerebral cortex and it has been proposed that

mutant huntingtin affects the levels of BDNF in the cortex and reduced trophic factor support alters the function of striatal neurons (Zuccato *et al.*, 2001; Cattaneo *et al.*, 2005).

The N-terminal fragment of mutant huntingtin is known to interact with numerous proteins some of which are ubiquitous transcription factors such as CREB and Sp1 or widely expressed co-activators of the basal Pol II transcriptional machinery such as CBP and $TAF_{II}130$ (Sugars & Rubinsztein, 2003). It is currently hypothesized that mutant huntingtin with an expanded polyglutamine region interacts via polar zippers with other proteins that also contain polyglutamine regions. Such interactions between transcription factors and the N-terminal fragments of mutant huntingtin have been hypothesized to alter transcription of various genes (Kazantsev *et al.*, 1999; Steffan *et al.*, 2000; Nucifora *et al.*, 2001; Dunah *et al.*, 2002; Li *et al.*, 2002; Zhai *et al.*, 2005).

Steady-state DARPP-32 mRNA levels are decreased in the striatum and cortex of the R6/1 and R6/2 transgenic HD mouse model (Chapter 3; Bibb *et al.*, 2000; Luthi-Carter *et al.*, 2000; van Dellen *et al.*, 2000), in the YAC128 transgenic mouse model (Van Raamsdonk *et al.*, 2005) and in rats where striatal neurons were transduced with lentiviral vectors expressing the first 171 amino acids of human huntingtin with a polyQ repeat length of 82 (de Almeida *et al.*, 2002). ppENK mRNA levels are also decreased in the R6 mouse model (Chapter 3; Luthi-Carter *et al.*, 2000) and a knock-in HD mouse model (Menalled *et al.*, 2000). DARPP-32 and ppENK mRNA levels are also known to be decreased in human HD brains (Albin *et al.*, 1991; Richfield *et al.*, 1995; Desplats *et al.*, 2006). HPRT is a cytoplasmic enzyme that is expressed in virtually all tissues and levels of HPRT mRNA are highest in brain and testes (Watts *et al.*, 1987; Rincon-Limas *et al.*, 1991). HPRT mRNA levels are not affected in 6 and 12 week-old R6/2 mice

(Luthi-Carter *et al.*, 2000). In this study, we used DARPP-32, ppENK and HPRT as model genes to study the mechanism by which N89-115Q and N89-150Q decrease the steady-state mRNA levels in a gene-specific and tissue-specific manner.

4.2 Results

In order to quantify the levels of primary and mature transcripts in the striatum of wild-type and R6/1 transgenic HD mice, we needed to normalize the samples to an internal control to account for variability among samples due to the efficiency of reverse transcriptase reactions. The number of HPRT mature transcripts in 3, 5, 6 and 12 week-old wild-type and R6/1 striata were quantified using real-time qRT-PCR. We decided to analyze the transcript level at these time points because levels of DARPP-32 and ppENK mRNA were not affected by N89-115Q in 3 week-old R6/1 mice, started to decline and were declining in 5 and 6 week-old R6/1 mice and were at a reduced, but constant level, in 12 week-old and older R6/1 mice (Fig. 3-3 and 3-10). The levels of mature HPRT transcripts were determined in samples containing equivalent amounts of total RNA in reverse transcriptase and qRT-PCR reactions. There was no difference in HPRT mature transcript levels between age-matched wild-type and R6/1 transgenic HD mice (Fig. 4-1). There was no significant difference in HPRT mRNA levels among 3, 5, 6 and 12 week-old mice. Since HPRT mRNA levels were not altered in R6/1 compared to wild-type mice, we used HPRT cDNA levels as the internal standard for all subsequent qRT-PCR analyses.

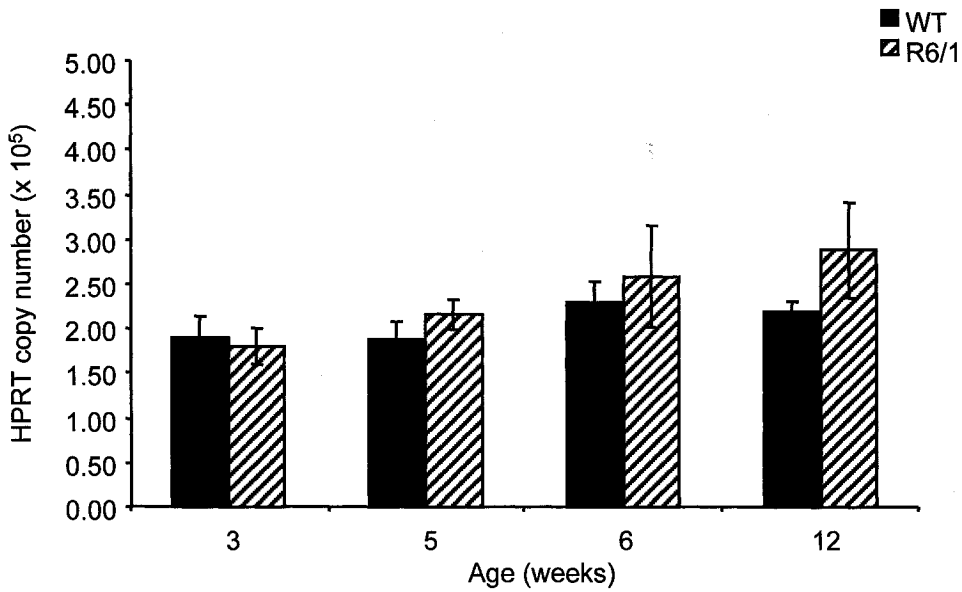

Figure 4-1. HPRT mRNA levels in the striatum were equivalent between age-matched wild-type and transgenic R6/1 HD mice. Histogram showing the average copy numbers of mature HPRT transcripts determined by qRT-PCR. 1 μg of total RNA isolated from the striatum of 3, 5, 6 and 12 week-old wild-type (WT; solid black bars) and R6/1 transgenic mice (striped bars) was reverse transcribed in the presence of gene-specific primers. The cDNA generated from 50 ng of total RNA was used as the PCR substrate in each reaction. The average number of copies of HPRT-specific PCR product is presented as the mean ± SEM (n=3 for each age and genotype).

Steady-state mRNA levels are dependent on the net difference between the rate of synthesis and decay of mRNA (Ross, 1995b). The observed decrease in steady-state DARPP-32 mRNA levels that occurred in R6/1 transgenic HD mice older than 6 weeks of age (Fig. 3-3) could be caused by a decrease in the rate of transcription of the DARPP-32 gene or a decrease in the stability of the DARPP-32 mRNA. The mechanism by which the N-terminal fragement of mutant huntingtin could alter gene transcription or mRNA stability would be fundamentally different. Therefore, it was important to clearly define whether transcription or mRNA stability was altered by the N-terminal fragment of mutant huntingtin leading to the observed decrease in steady-state DARPP-32 mRNA levels. The number of DARPP-32 primary and mature transcripts in 3, 5, 6 and 12 week-old wild-type and R6/1 striata were quantified using real-time qRT-PCR (Fig. 4-2). Because intron splicing occurs co-transcriptionally, the amount of primary transcripts at any given time reflects newly synthesized primary transcript and, indirectly, rate of transcription. The levels of primary and mature DARPP-32 transcripts were normalized to levels of mature HPRT to control for variability among samples. The ratios of primary and mature DARPP-32 transcripts to HPRT were in approximately 0.10 and 2.00, respectively, indicating that HPRT was expressed at similar levels as both the primary and mature DARPP-32 transcripts and could be used as an internal standard. qRT-PCR analysis demonstrated that there was no difference in primary and mature DARPP-32 transcript levels in RNA isolated from 3 and 5 week-old wild-type and R6/1 mice striatal tissue (Fig. 4-2A and 4-2B). There was a trend for levels of primary transcript to be decreased in 5 week-old R6/1 striatal samples compared to samples derived from 5 week-old wild-type mice. There was a significant decrease in the copy number of primary and

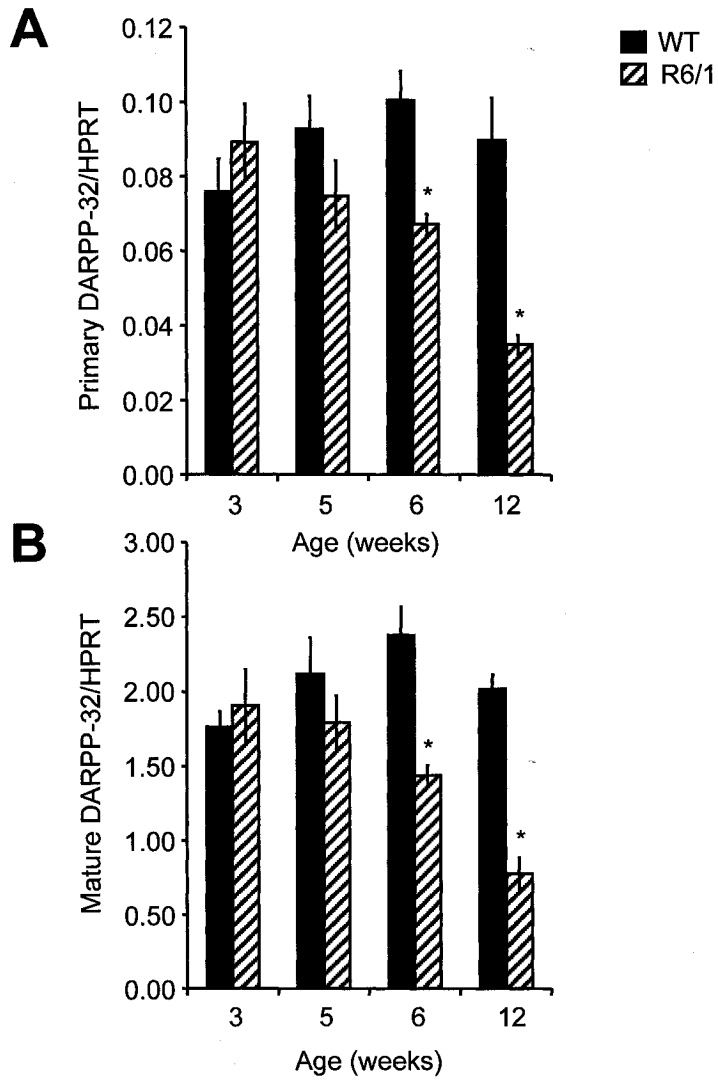

Figure 4-2. N89-115Q altered transcription of the DARPP-32 gene *in vivo*. Copy numbers of mature and primary DARPP-32 and HPRT transcripts were quantified by qRT-PCR. Total RNA isolated from the striatum of 3, 5, 6 and 12 week-old wild-type (WT; solid black bars) and R6/1 transgenic mice (striped bars) was reverse transcribed in the presence of gene-specific primers. The copy number of mature and primary DARPP-32 transcripts were normalized to the levels of HPRT in each sample. The ratio of primary (A) and mature (B) DARPP-32 cDNA to HPRT cDNA is presented as the mean ± SEM (n=6 for each age and genotype). $*P < 0.05$, significantly different from age-matched wild-type (two-way ANOVA).

mature transcripts in striatal tissue isolated from 6 ($P < 0.05$) and 12 week-old ($P < 0.05$) R6/1 mice compared to age-matched wild-types (Fig. 4-2A and 4-2B). The ratio of primary transcript levels to mature transcript levels in the striatal tissue from 3, 5, 6 and 12 week-old wild-type and R6/1 transgenic HD mice were constant indicating that the levels of primary and mature transcripts were consistently proportional in the wild-type and R6/1 mice as they aged. Based on these observations, it appears that the decrease in steady-state DARPP-32 mRNA levels was caused by a decrease in the rate of transcription beginning at ~ 5 weeks of age in R6/1 mice rather than a decrease in DARPP-32 mRNA stability in R6/1 mice older than 6 weeks of age.

Since DARPP-32 transcription was affected by the expression of N89-115Q and the steady-state mRNA levels that initiate from the distal transcription start sites were not altered by N89-115Q (Fig. 3-6), we wanted to determine if N89-115Q altered transcription initiation site selection from the proximal promoter of the DARPP-32 gene. The proximal transcription initiation region has previously been defined but, due to the complex banding pattern of the RPA, the start sites could not be resolved to the nucleotide level (Blau *et al.*, 1995). To identify the transcription start sites in the proximal promoter of the DARPP-32 gene, we employed 5'RLM-RACE, which amplifies cDNA from full-length capped mRNAs. Products of the 5' RLM-RACE derived from the capped 5' ends of DARPP-32 striatal mRNA appeared as a complex banding pattern on the agarose gel ranging in size from 350 to 450 bp (data not shown) suggesting that capped DARPP-32 mRNAs had several distinct 5' ends. This indicated that the DARPP-32 gene had multiple transcription start sites that were being utilized in the striatum. The 5' RLM-RACE products were cloned and sequenced and ten

transcription start sites within the proximal transcription initiation region were identified. These sites did not correspond to any of the 5' ends of expressed sequence tags (ESTs) found in GenBank (Fig. 4-3). It should be noted that the 5' ends of ESTs may represent full-length or incomplete cDNAs, therefore, not all cDNAs necessarily correspond to transcription initiation sites. Analysis of 5' RLM-RACE products, together with the number of different 5' ends of ESTs, indicated that there were a large number of transcription initiation sites utilized in the striatum to express DARPP-32. 5'RLM-RACE is not a quantitative technique and this approach can lead to the amplification and identification of rare cDNAs.

General transcription factors position RNA polymerase II near the transcription start site and dictate the precise location of transcription initiation. The N-terminal fragment of mutant huntingtin is known to interact with various transcription factors (Kazantsev *et al.*, 1999; Shimohata *et al.*, 2000; Steffan *et al.*, 2000; Nucifora *et al.*, 2001; Suhr *et al.*, 2001; Dunah *et al.*, 2002; Kegel *et al.*, 2002; Li *et al.*, 2002; Luthi-Carter & Cha, 2003; Zhai *et al.*, 2005). Therefore, we chose to identify whether there was loss of transcripts that originated from particular start sites in the DARPP-32 promoter in R6 transgenic HD mice. To do this, we performed RPA that enabled us to quantify the levels of transcripts that initiated from the various start sites of the DARPP-32 gene in the wild-type and R6 transgenic HD mice. The RPA probe was 465 bp in length and corresponded to the sequence spanning the proximal transcription initiation region and part of exon 1 of the DARPP-32 gene. This probe, therefore, could anneal with the 5' ends of transcripts that initiated within the proximal transcription initiation region. RPA was conducted on striatal RNA from 9 week-old wild-type and R6/2 mice

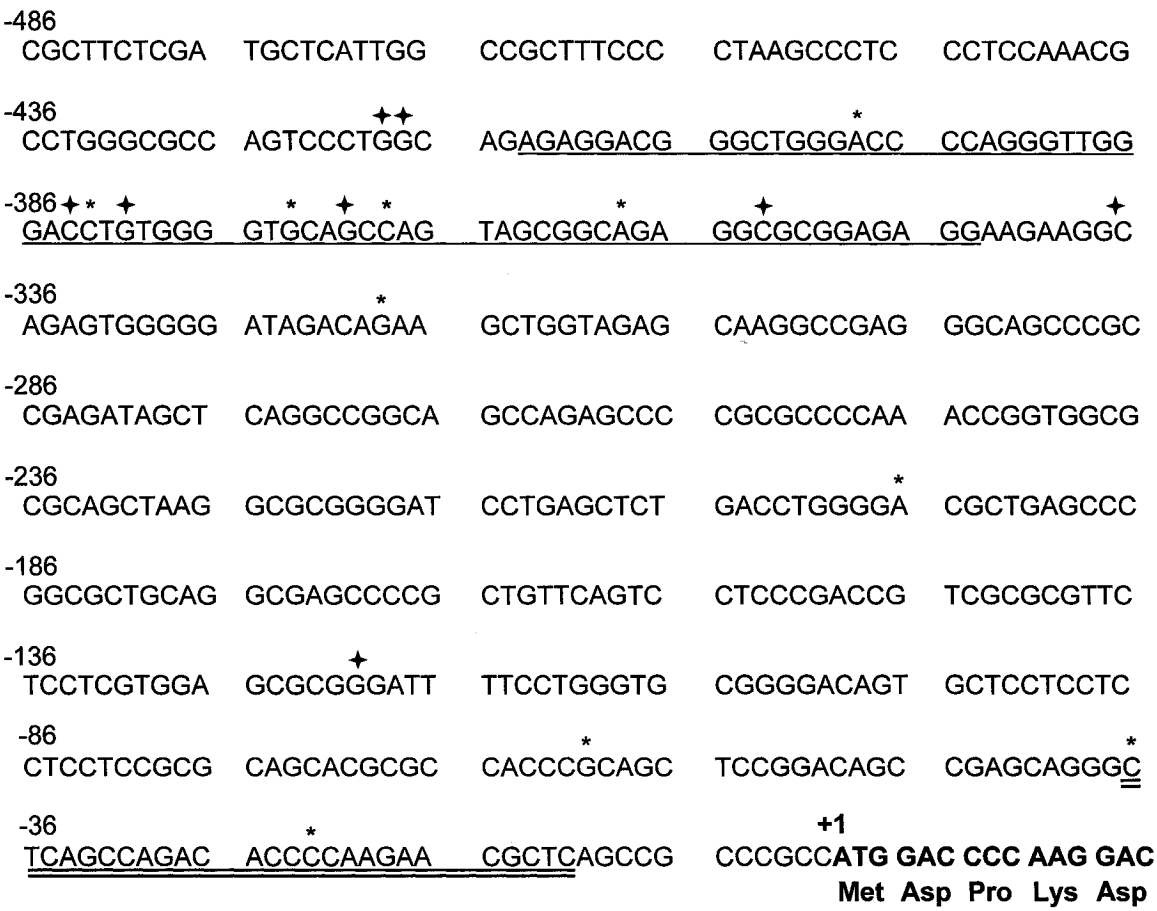

Figure 4-3. The mouse DARPP-32 gene has multiple transcription start sites. The ten transcription initiation sites identified by 5' RLM-RACE are indicated by asterisks (*) . The 5' ends of expressed sequence tags (ESTs) found in Genbank are indicated by crosses (✦). The proximal transcription initiation region as defined by Blau *et al.*, (1995) is underlined. Sequence complementary to the 5' RLM-RACE primer is double underlined. The coding and predicted amino acid sequence of the amino terminus of DARPP-32 is in bold font. The A of the methionine initiation codon was designated as +1. The numbers of the left of the DNA sequence indicate the position relative to the +1 position.

and the sizes of the probe fragments that annealed with DARPP-32 mRNA and were protected from RNase A/T1 digestion are shown (Fig. 4-4). The presence of fragments of various sizes confirmed that the DARPP-32 gene initiated at multiple transcription start sites in both wild-type and R6/1 transgenic HD mice. The most abundant protected products corresponded to mRNAs whose transcription initiated at ~ 330-300 nts and 210-190 nts upstream of the ATG initiation codon. Moreover, it appeared that the relative abundance of the DARPP-32 transcripts from each site were lower in the samples derived from R6/2 transgenic HD mice when compared to the wild-type mice. This observation indicated that N89-115Q exerted negative effects on transcription from all DARPP-32 transcription start sites. Steady-state levels of β-actin mRNA are not altered in 12 week-old R6/2 transgenic HD mice (Luthi-Carter *et al.*, 2000) and the β-actin gene has a well-defined single transcription start site (Tokunaga *et al.*, 1986). Therefore, β-actin was used as a positive control in RPA to demonstrate that equivalent amounts of total RNA were included in each sample analyzed. RPA was also performed on RNA isolated from the renal medulla of kidneys of 10 week-old wild-type mice. Transcripts that initiate from the distal transcription initiation region of the DARPP-32 gene are not present in the kidneys (Fig. 3-6). In the proximal transcription initiation region, the same transcription start sites were used in the kidney and striatum (Fig. 4-4). N89-115Q did not have an effect on DARPP-32 mRNA levels in the kidney and the resistance of DARPP-32-specific transcription in the kidney could not be attributed to alternative transcription start site use of this promoter in the kidney compared to the brain.

The ppENK transcription start sites were defined in order to determine whether N89-115Q altered transcription initiation from particular start sites for this gene.

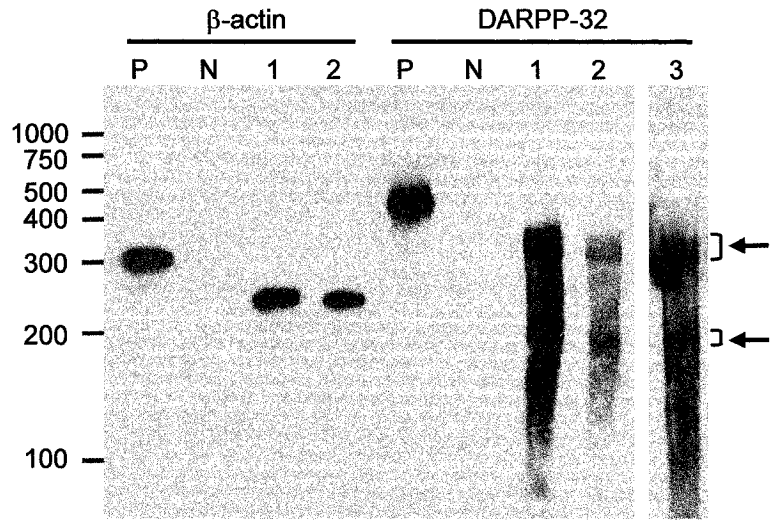

Figure 4-4. RNase protection assays demonstrated that N89-115Q affected transcription from all DARPP-32 transcription start sites and that the same transcription initiation sites were utilized in the kidney and striatum. β-actin was used as a control for the amount of RNA included in each reaction. Ten pg of undigested β-actin or DARPP-32 probe (P) and a no target control (N) which consisted of 250 pg of the specified probe, combined with yeast RNA and digested with RNase A/T1, are shown. β-actin- and DARPP-32-protected products from striatal RNA (1 and 10 μg RNA for β-actin and DARPP-32-specific reactions, respectively) isolated from 9 week-old wild-type (1) and R6/2 (2) and DARPP-32-protected products from kidney RNA (50 μg) isolated from 10 week-old wild-type mice (3) are shown. Multiple transcription initiation sites were detected. The products generated from the two major transcription initiation regions are indicated by brackets and arrows and are ~330-300 and 210-190 nts upstream of the ATG initiation codon. Other DARPP-32 5' end specific products that initiate between 350 and 100 nts upstream of the ATG initiation codon were detected in all samples. The relative mobility of biotin-labeled RNA ladder is indicated on the left of the panel.

Five distinct products were detected following 5' RLM-RACE using ppENK-specific primers located 390 bp downstream from the previously defined transcription initiation site for this gene (Fig 4-5). The products were approximately 530, 500, 470, 450 and 190 bp in length (data not shown). The ppENK-specific products were cloned and clones with five different sizes of inserts were identified. Representative clones of each size class were sequenced and compared to the ppENK genomic sequence and five ppENK transcription start sites were identified (Fig 4-5). Four ppENK transcription start sites in the rat genome have previously been identified (Weisinger *et al.*, 1990) and are 750 to 800 nts upstream of the ATG initiation codon. This corresponds to the region in the mouse ppENK gene that contains four of the five transcription start sites. The transcription start site that corresponded to the -289 site on the mouse ppENK gene was identical to one of the rat transcription start sites and has previously been identified (GenBank accession number U20894).

5' RLM-RACE can amplify rare cDNA transcripts. Thus using RPA, we confirmed the position of transcription start sites, determine the relative abundance of mRNAs that initiate at each site and identified whether there was loss of transcripts that originated from particular start sites in the ppENK promoter in R6/1 transgenic HD mice. The RPA probe was 625 nts in length and corresponded to the sequence upstream of the coding region that spanned the five transcription start sites identified by 5' RLM-RACE. RPA was performed with RNA isolated from the cortices and striata of 3 and 12 week-old wild-type and R6/1 mice. The sizes of the probe fragments that annealed with ppENK mRNA and were protected from RNase A/T1 digestion are shown (Fig. 4-6). No ppENK-specific protected products were detected in the samples containing cortical RNA

-390
TGGCGTAGGG CCTGCGTCAG CTGCAGCCCG CCGGCGATTG GGGCGCGCGC
-340
GCCTCCTTCG GTTTGGGGTT AATTATAAAG TGGCTGTGGC CGCCGCCAGC
-290
AAGGCAGGCG CACAGAGCCC CGCTGCCCAG CGACGCTGCC CGGCGCCTCG
-240
CAGAGCTCCC CGACGCGGCC GCTTTACACT TGCCTTCTTT CTTTCTCTTG
-190
CAGAGTGGCA TCTGGTACAC GCTCTTCCAG TAACCTGCGC CATCTGGAGC
-140
AACGGCAGCG TGAGTGACTT TGCCCCAAGT CGCCCGTGCC TTGGCGACCG
-90
TCGCCTGTTC CCTCGGTGCA TGCGTTCGTC CAACTTTCTC GGGGTTCCTC
-40 +1
ATTGCTTTGG GTGTCCGGGT CCTATTCCCC CAAGCGCCTG CTCCCGAGCC
+12
GCGAACTTCA GTGTTCGCTC CAGAATCTTG CCCTAAGCAA CCGACGCCAG
+62
GGAAGACAGG GCGCCCTCGG AAGGACAGGA TGTCATCAGG AAAACAGGAC
+112
TCCCCGTGGG AAGATAGGAT ACCTCCAGGA AGATAGAATA GTCCCAGGCA
+162
TCACTAGAAC AGCAGGAAAC ACTAGGGTCC AAGCTCTCAT TGAGGCACCC
+212
GGGGAGGTTG TTGGGTTGTG GGCGGGGCTC AGGAAAGACT GTCCCTGCTG
+262
GTCCTGATCC ACGACCACCC ACCCGGCAAG GTTCTCTCTA AGAGAACCTT
+312
GTCAGAGACA GAACGGGTCC CTACAGGCGC GTTCTTCTCT CCTACAGCCC
+362

ATG GCG CGG TTC CTG AGG CTT TGC ACC TGG CTG CTG GCG CTT GGG TCC TGC
Met Ala Arg Phe Leu Arg Leu Cys Thr Trp Leu Leu Ala Leu Gly Ser Cys

Figure 4-5. The mouse ppENK gene has five transcription start sites. The five transcription initiation sites identified by 5' RLM-RACE are indicated by asterisks (*). Sequence complementary to the 5' RLM-RACE primer is double underlined. The transcription start site closest to the methionine initiation codon in the ppENK coding region was defined as +1. The numbers on the left of the sequence are relative to the +1 position. The coding sequence and predicted amino acid sequence of the amino terminus of ppENK is in bold font.

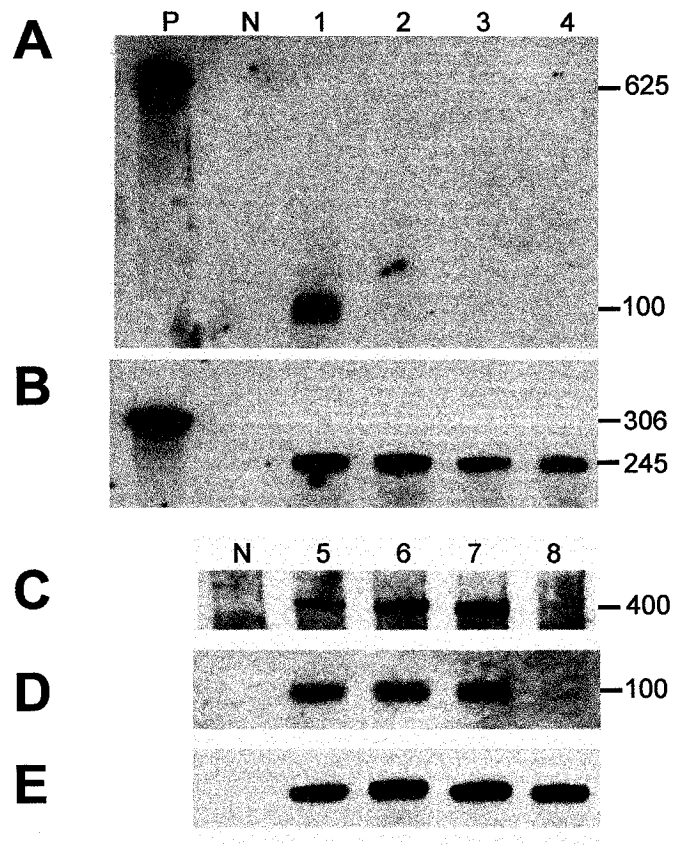

Figure 4-6. Levels of ppENK mRNA that initiate from two transcription initiation sites were reduced in R6/1 compared to WT mice. Panels A, C and D show ppENK-specific RPA products, while panels B and E show β-actin-specific products. The RPA for β-actin-specific products demonstrated that equivalent amounts of RNA were included in each reaction. Undigested ppENK (5 pg) or β-actin (20 pg) probe (P) and a no target control (N), which consisted of 500 pg of the specified probe, combined with yeast RNA and digested with RNase A/T1, are shown. Total RNA was isolated from the striatum (1, 2) and cortex (3, 4) of 12 week-old wild-type (1, 3) and R6/1 (2, 4) mice and used as the target for RPA. Total RNA was isolated from the striatum of 3 (5, 6) and 12 (7, 8) week-old wild-type (5, 7) and R6/1 (6, 8) mice and used as the target for RPA. The sizes (indicated on the right) of the undigested probe and RPA products were calculated based on the relative mobility of biotin-labeled RNA size markers. One and 20 μg of RNA was used for β-actin- and ppENK-specific reactions, respectively.

(Fig 4-6A). This was expected as ppENK is not normally expressed in cortical tissue. The most abundant protected product was 100 nts in length that was detected in the samples containing striatal RNA. This product corresponded to mRNAs whose transcription initiated at the +1 site as defined in figure 4-5. There was no difference in the relative abundance of this product in RNA derived from 3 week-old R6/1 compared to 3 week-old wild-type mice (Fig 4-6D). However, there was a decrease in the abundance of transcripts from this start site in 12 week-old R6/1 mice when compared to age-matched wild-type mice (Fig. 4-6A). An overnight exposure of the membrane to detect weak chemiluminescent signals, demonstrated that a less abundant protected product of 400 nts was present in the samples derived from 3 week-old wild-type and R6/1 mice, and 12 week-old wild-type mice, levels were very low in 12 week-old R6/1 mice (Fig 4-6C). Transcripts that initiate from the -375, -320 and -270 transcription start sites were not detected by the RPA implying that ppENK transcripts that initiate from those sites are less abundant. Transcripts that initiate from this novel ppENK transcription start site in the mouse genome were clearly more abundant than those from the other four transcription start sites, therefore we defined it as +1 in figure 4-5. β-actin was used as a positive control demonstrating that equivalent amounts of total RNA were included in each sample analyzed (Fig 4-6B and E).

Transcription of the DARPP-32 gene was decreased by the 548 amino acid N-terminal fragment of mutant huntingtin in cell culture. DARPP-32 protein levels increase in parental ST14A cells that are induced to differentiate and develop a neuron-like phenotype in serum-free media (Ehrlich *et al.*, 2001). The N548wt and N548mu cell lines, derived from ST14A cells, express equivalent amounts of the amino terminus of

truncated huntingtin protein with 15 and 128 polyglutamines that can be detected at 72 kDa and 115 kDa, respectively (Rigamonti *et al.*, 2000). In N548wt and N548mu cell lines, levels of DARPP-32 mRNA increased 24 hr after serum-withdrawal (Fig. 4-7A). DARPP-32 mRNA levels in N548wt and N548mu cell lines increased 2- and 1.6-fold, respectively, compared to levels in undifferentiated cells. Furthermore, 48 hr after serum withdrawal, the levels of DARPP-32 mRNA were still significantly higher in the N548wt cell line (1.8-fold increase), while the DARPP-32 mRNA levels in the N548mu cells had returned to levels observed in undifferentiated cells. Levels of DARPP-32 mRNA were significantly decreased at 72 and 96 hr in N548mu cells compared to levels observed at time 0. In N548wt cell, DARPP-32 mRNA levels decreased 96 hr post-serum-withdrawal. N548wt and N548mu cells showed the same pattern of transient increase and subsequent decline in DARPP-32 mRNA levels during differentiation. Comparison of the relative levels of DARPP-32 mRNA in the two cell lines at different time points demonstrated that the levels of DARPP-32 declined more rapidly in N548mu compared to N548wt cells as there was a statistically significant difference in the levels at 48 and 72 hrs following serum-withdrawal (Fig. 4-7B). The observed difference in DARPP-32 mRNA levels between the two cell lines did not result from truncated mutant huntingtin-induced cell death because, there were very few dead cells and there was no difference between cell lines in the percentage of dead cells 24 hr after serum-withdrawal (Fig. 4-8). At the last time point analyzed (96 hr), 92% of cells in the N548mu cell lines and 96% of cells in the N548wt cell lines were viable, suggesting that the presence of the N-terminal fragment of mutant huntingtin increased cell death although the percentage of dead cells was still relatively low. Furthermore, DARPP-32 mRNA levels were internally

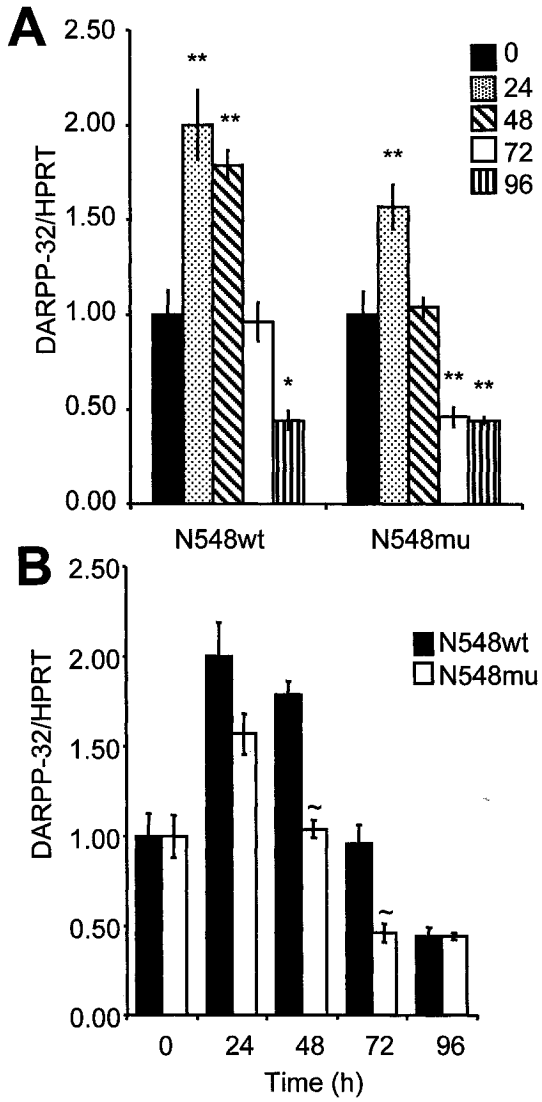

Figure 4-7. Transcription of DARPP-32 was differentially regulated in N548wt and N548mu cell lines. Total RNA was isolated from N548wt and N548mu cells 0, 24, 48, 72 and 96 h after serum-withdrawal and reverse transcribed in the presence of gene-specific primers. Copy numbers of mature DARPP-32 and HPRT transcripts were determined by qRT-PCR Within each cell line, the ratio of DARPP-32 to HPRT at each time point was normalized to the ratio at t=0 (A). Comparison of DARPP-32/HPRT ratios in N548wt and N548mu cells at each time point are shown in B. The ratio of mature DARPP-32 cDNA to HPRT cDNA is presented as mean (± SEM, n=3 for each time point). $*P < 0.05$, $**P < 0.005$ significantly different from t=0; $\sim P < 0.05$ significantly different from time-matched N548wt (two-way ANOVA).

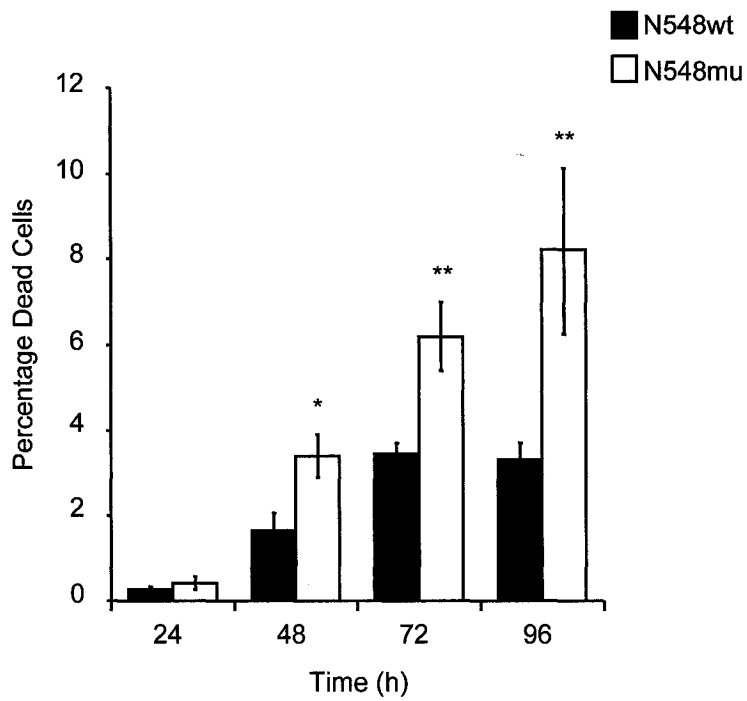

Figure 4-8. The amino terminus of mutant huntingtin increased the percentage of dead cells in N548mu compared to N548wt cells over 96 hr of serum-withdrawal. Histogram showing the average percentage (± SEM, n=3) of dead N548wt (solid black bars) and N548mu (solid white bars) cells at 24, 48, 72 and 96 h after serum withdrawal. $*P < 0.05$, $**P < 0.005$, significantly different from N548wt cells exposed to the same period of serum withdrawal (two-way ANOVA).

normalized to levels of HPRT mRNA, which would have accounted for any differences caused by cell loss. Levels of DARPP-32 mRNA declined more rapidly in immortalized striatal cells stably transfected with the 548 amino acid N-terminal fragment of mutant huntingtin than in cells expressing the same portion of huntingtin with a non-pathological number of polyglutamines when these cells differentiate. This observation suggested that the factors required to increase expression of DARPP-32 during differentiation were present in both cell lines but that the presence of the 548 amino acid N-terminal fragment of mutant huntingtin affected the rate of accumulation of DARPP-32 mRNA and led to a decreased level of this transcript over time in differentiated cells.

Mutant huntingtin with its expanded polyglutamine region can physically interact with various transcription factors that also contain polyglutamine regions and it is thought that this direct physical association blocks the function of certain transcription factors (see Sugars and Rubensztein, 2003 and references therein and Marcora *et al.*, 2003; Obrietan & Hoyt, 2004; Schaffar *et al.*, 2004; Sugars *et al.*, 2004; Bae *et al.*, 2005; Cong *et al.*, 2005; Lievens *et al.*, 2005; Mills *et al.*, 2005). Therefore, we hypothesized that sequential deletions of the DARPP-32 promoter could remove the binding site(s) of transcription factors that interact with the N-terminal fragment of mutant huntingtin and alleviate mutant huntingtin-induced transcriptional dysregulation. In order to identify a promoter that could be used as an internal control, we measured the activity of the thymidine kinase (phRL-TK), HPRT [pGL3-HPRT(-795/+97)] and cytomegalovirus (pCMV-Luc) promoters in N548wt and N548mu cells (data not shown). The activity of the TK and HPRT promoters were approximately 75% and 60% lower in N548mu compared to N548wt cells. The average activity of the CMV promoter in N548mu was

95% lower ($P < 0.05$) than the average activity of this promoter in N548wt cells. Therefore, all transfection analyses included co-transfection of phRL-TK, to correct for variability in transfection among samples and variability of expression due to differences between the ST14A-derived cell lines, which may be independent of the effect of 548 amino acid N-terminal fragment of mutant huntingtin. The TK promoter was selected as the internal control instead of the HPRT promoter. The TK promoter has been well characterized, is commercially available and is commonly used in the Dual Luciferase Reporter Assay system. The TK promoter is not endogenous to these cells and, therefore, there could not be competition between endogenous genomic sites and the plasmid for transactivating factors. Furthermore, as this gene is not endogenously expressed in these cells, feedback mechanisms that could alter the expression of endogenous genes would not be a concern.

A 1.4 kb genomic DNA fragment derived from the region upstream of the DARPP-32 translation start site was a functional promoter in N548wt, N548mu and ST14A cells (Fig. 4-9 and 4-12A). The activity of the DARPP-32 promoter was lower in N548mu compared to N548wt cells. Six promoter deletions of this 1.4 kb fragment were constructed and transfected into N548wt and N548mu cells (Fig. 4-9). The various deletion constructs supported different levels of promoter activity. Deletion of the -1346 to -1277 region, which contained three potential Sp1 binding sites, alleviated repression of the promoter. Sequential deletions from -1277 to -171 removed activator elements resulting in decreased promoter activity. The activity of each of the promoter deletion constructs was decreased it the N548mu compared to N548wt cells and the ratio of activities of each promoter construct in the two cells lines was ~ 0.7, indicating that all

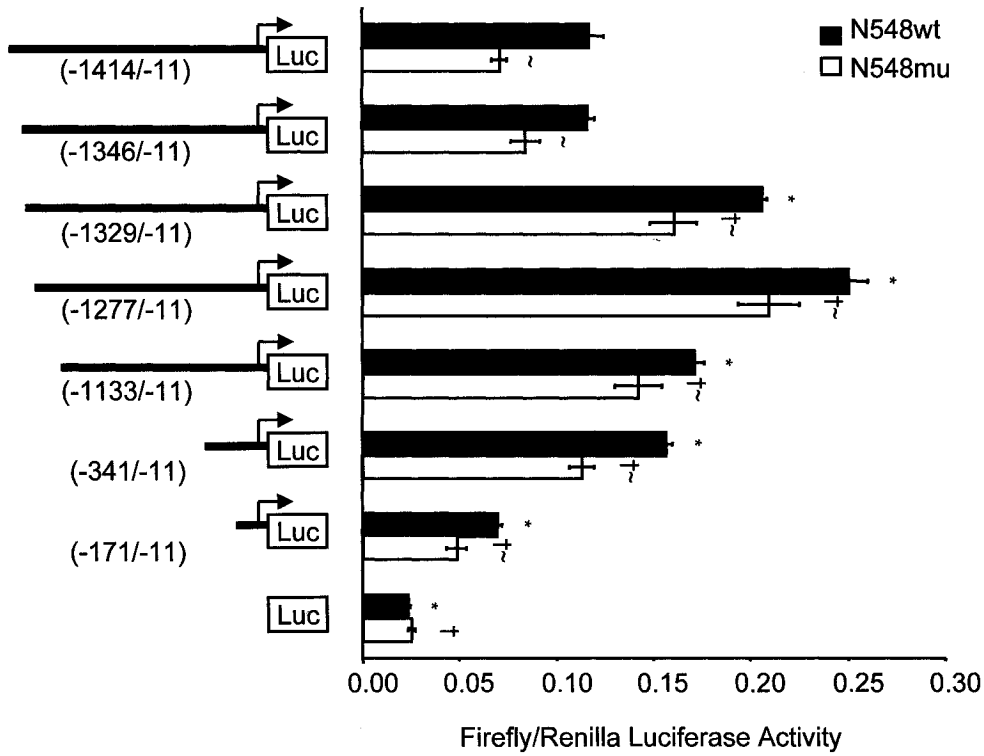

Figure 4-9. The -171/-11 region of the DARPP-32 promoter conferred sensitivity to N89-115Q. Schematic representations of deletion constructs of the DARPP-32 promoter in the pGL3 vector. Numbers indicate the region of the DARPP-32 promoter relative to the ATG start codon included in each deletion construct. A series of DARPP-32 promoter luciferase constructs and a promoter-less pGL3 vector were co-transfected with phRL-TK into N548wt cells (solid black bars) and the N548mu cells (solid white bars). Firefly luciferase activity was normalized to *Renilla* luciferase activity and the results were expressed as a mean (± SEM, n=12 for each construct per cell line). $*P < 0.05$, significant difference from pGL3-DARPP(-1414/-11) in N548wt cells. $\dagger P < 0.05$, significant difference from pGL3-DARPP(-1414/-11) in N548mu cells. $\sim P < 0.05$, significant difference between DARPP-32 deletion construct expressed in N548wt and N548mu cells (two-way ANOVA).

the constructs were equally affected by the expression of N-terminal fragment of mutant huntingtin. The promoter- less construct pGL3-Basic had some basal promoter activity, but this activity was not affected by the presence of the N-terminal fragment of mutant huntingtin protein. Therefore, *cis*-elements that may have conferred sensitivity to the N-terminual fragment of mutant huntingtin would have to be located in the -171 to -11 region of the DARPP-32 promoter relative to the adenosine of the translation initiation codon. Similarly, the -524/+101 region of the ppENK promoter is functionally active and confers sensitivity to the N-terminal fragment of mutant huntingtin. The activity of this promoter was decreased in N548mu compared to N548wt cell (Fig 4-10). The ratio of the activity of the ppENK promoter in the two cell lines was ~ 0.4, indicating that this ppENK promoter construct was more sensitive to the effects of the N-terminal fragment of mutant huntingtin than the DARPP-32 promoter deletion constructs.

The effects of mutant huntingtin in the N548mu cells could be attributed to the expanded polyglutamine region in the N548mu cells compared to the N548wt cells or to differences in the two distinct cell lines that were independent of the of the N-terminal fragment of mutant huntingtin. In order to distinguish between these two possibilities, we used the shHD2.1 vector that expresses a 21-nt antisense strand complementary to the 413-436 nts of human huntingtin mRNA to decrease levels of the wild-type or mutant huntingtin amino-terminus in N548wt or N548mu cells, respectively (Fig 4-11). This shHD2.1 vector silences endogenous human huntingtin expressed in HEK293 cells and also reduces the expression of a cloned plasmid that expresses the first 171 amino acids of mutant huntingtin with 82 CAG repeats (HD-N171-82Q) in HEK293 cells (Harper *et al.*, 2005). The expression of the shHD2.1 vector reduced the protein levels of the 548 amino

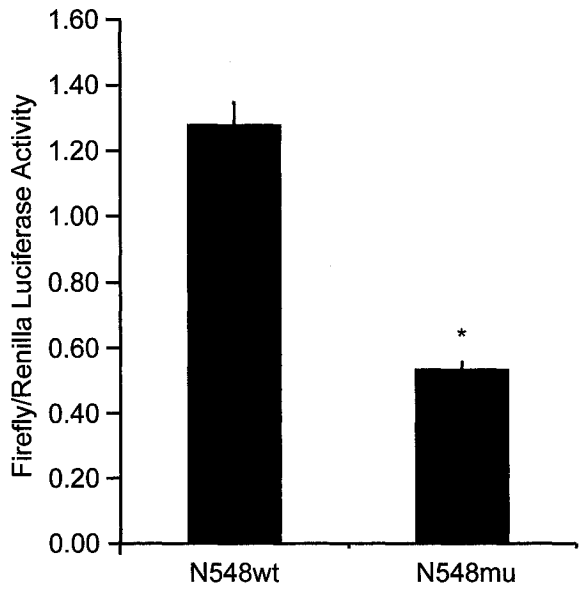

Figure 4-10. The -524/+101 region of the ppENK promoter conferred sensitivity to N89-115Q. A 625 bp ppENK promoter-containing luciferase construct, pGL3-ENK(-524/+101), was co-transfected with phRL-TK into N548wt cells and the N548mu cells. Firefly luciferase activity was normalized to *Renilla* luciferase activity and the results were expressed as a mean (± SEM, n=12 per cell line). $*P < 0.05$, significant difference from pGL3-ENK(-524/+101) in N548wt cells (one-way ANOVA).

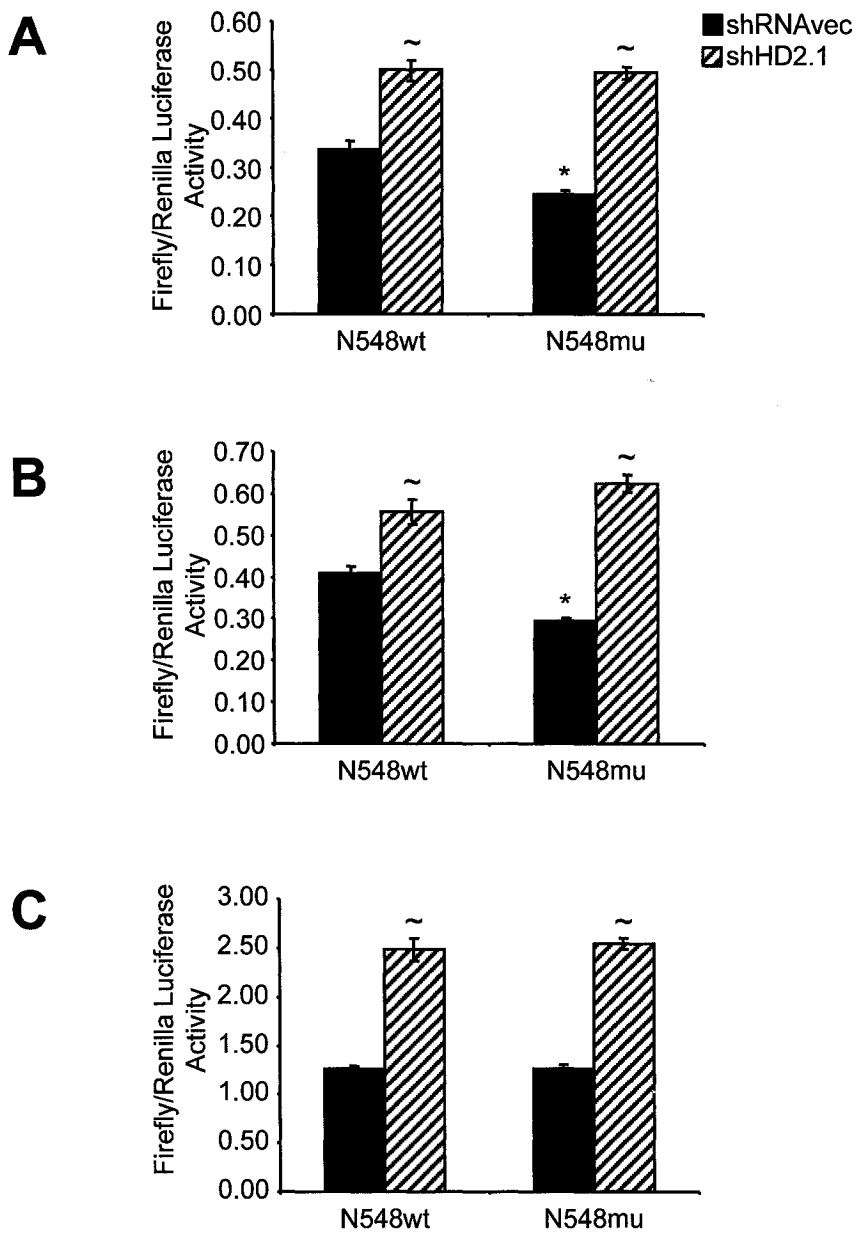

Figure 4-11. Expression of an siRNA that reduced levels of the amino terminus of human huntingtin in N548wt and N548mu cells alleviated the repression induced by the amino terminus of mutant huntingtin on the pGL3-DARPP and pGL3-ENK promoter constructs. The activity of pGL3-DARPP(-1414/-11) (A), pGL3-ENK(-524/+101) (B) and pGL3-HPRT(-795/+97) (C) promoters after co-transfection of N548wt and N548mu cells with the promoters and shHD2.1, a plasmid that expresses a 21-nt antisense strand complementary to nts 416-436 of human htt mRNA, or shRNAvec, an empty vector control was determined. Firefly luciferase activity was normalized to *Renilla* luciferase activity and the results were expressed as a mean (± SEM, n=12 per cell line). $*P < 0.05$, significant difference from promoter activity in N548wt cells; $\sim P < 0.05$, significant difference from promoter activity in the presence of shRNAvec (two-way ANOVA).

acids N-terminus of the huntingtin protein in the N548wt and N548mu cells (Hu and Denovan-Wright, unpublished data). In the presence of control vector that did not express shHD2.1, the activity of pGL3-DARPP(-1414/-11) and pGL3-ENK(-524/+101) vectors were decreased in the N548mu cells compared to N548wt cells (Fig. 4-11A and 4-11B). The expression of the shHD2.1 vector in the N548wt and N548mu cells increased the activity of the pGL3-DARPP(-1414/-11), pGL3-ENK(-524/+101) and pGL3-HPRT(-795/+97) vectors in both cells lines when compared to the control shRNA empty vector (Fig. 4-11). Furthermore, the repression on the activity of the pGL3-DARPP(-1414/-11) and the pGL3-ENK(-524/+101) vectors were alleviated in the N548mu cells.

The observed decrease in transcriptional activity from the DARPP-32 promoter deletion constructs and the ppENK promoter construct may have been caused directly by the N-terminal fragment of mutant huntingtin or by differences in the transcription factor repertoire expressed in the two ST14A cell line derivatives. We acutely expressed exon 1 of the wild-type or mutant *HD* gene in parental ST14A cells and observed the activity of the 1.4 kb DARPP-32 promoter construct [pGL3-DARPP(-1414/-11)], the smallest DARPP-32 promoter deletion construct [pGL3-DARPP (-171/-11)], the 625 bp ppENK promoter construct [pGL3-ENK(-524/+101)] and a ppENK promoter deletion construct [pGL3-ENK(-220/+101)]. There was no difference in the activity of pGL3-DARPP(-1414/-11), pGL3-DARPP(-171/-11), pGL3-ENK(-524/+101) or pGL3-ENK(-220/+101) in the presence of exon 1 of the wild-type *HD* gene and a control vector (pEGFP-N1) indicating that the product from exon 1 of the wild-type *HD* gene did not increase or decrease the activity of the pGL3-DARPP(-1414/-11), pGL3-DARPP(-171/-11), pGL3-

ENK(-524/+101) or pGL3-ENK(-220/+101) promoters in ST14A cells (Fig. 4-12A and 4-13). However, the acute expression of N89-115Q caused a significant decrease in pGL3-DARPP(-1414/-11), pGL3-DARPP (-171/-11), pGL3-ENK(-524/+101) and pGL3-ENK (-220/+101) promoter activity compared to the activity observed in the presence of wild-type huntingtin (Fig. 4-12A and 4-13). This confirmed that *cis*-elements that may confer N89-115Q sensitivity would be located in the -171/-11 region of the DARPP-32 promoter and the -220/+101 region of the ppENK promoter. Although the activity of pGL3-DARPP(-1414/-11) was higher in HEK293 cells than in the ST14A cells, there was no difference in the activity of pGL3-DARPP(-1414/-11) in the presence of exon 1 of wild-type huntingtin and the control vector pEGFP-N1 indicating that wild-type huntingtin did not increase or decrease the activity of the pGL3-DARPP(-1414/-11) in HEK293 cells (Fig. 4-12B). However, unlike the effects observed in ST14A cells, the acute expression of N89-115Q did not alter the activity of the pGL3-DARPP(-1414/-11) construct in HEK293 cells (Fig. 4-12B). The N-terminal proteins of wild-type and mutant huntingtin are equivalently expressed in the transiently transfected HEK293 cells (data not shown). These observations provided evidence that even short-term expression of N89-115Q altered transcription of the DARPP-32 promoter but that the effect was restricted to specific cells culture models just as the effect was restricted to the brain and not the kidney *in vivo*. There was also no difference in the activity of the HPRT [pGL3-HPRT(-795/+97)] or the TK (phRL-TK) promoter in the presence of exon 1 of wild-type huntingtin and the control vector pEGFP-N1 indicating that wild-type huntingtin did not increase or decrease the activity of the pGL3-HPRT(-795/+97) (Fig. 4-14A) or phRL-TK (Fig. 4-14B) in ST14A cells. The acute expression of exon 1 of the *HD* gene did not

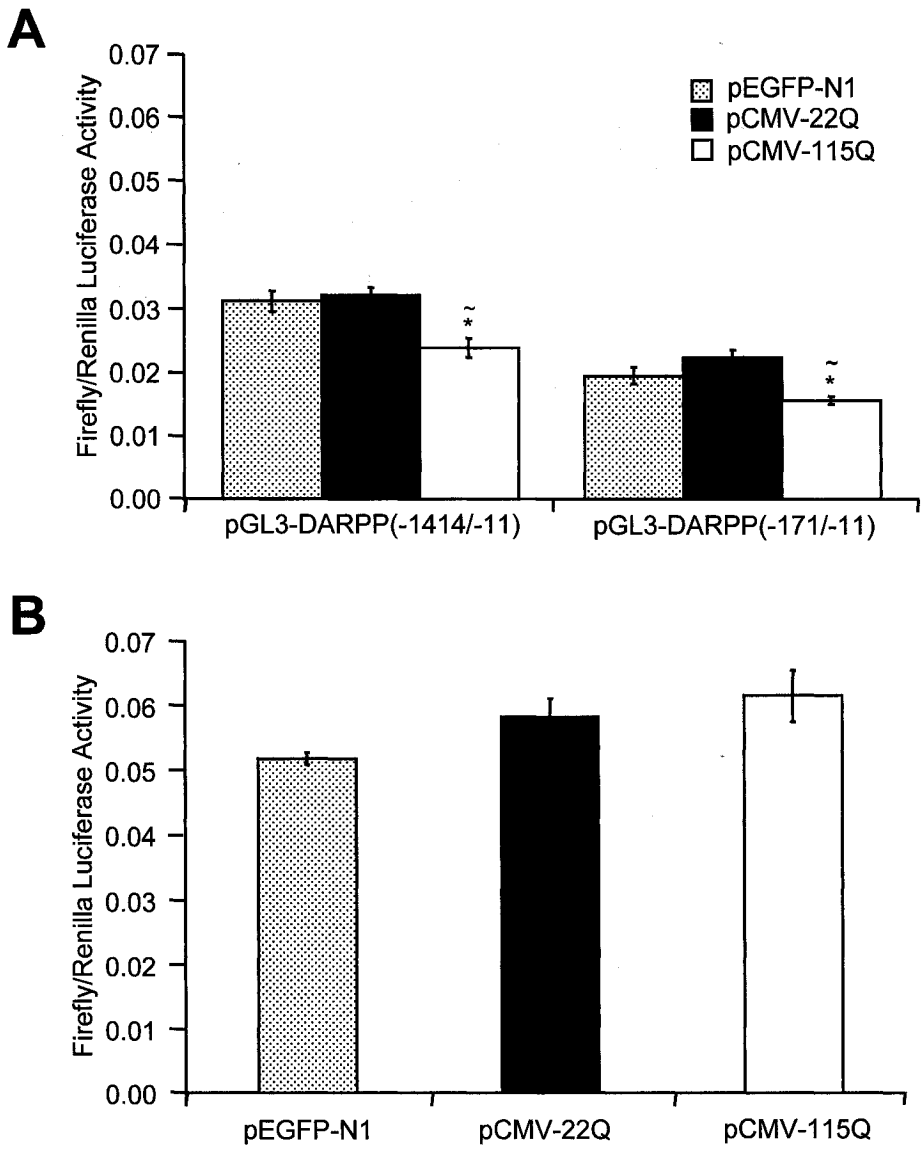

Figure 4-12. Acute expression of N89-115Q altered transcription of the DARPP-32 gene in a cell-specific manner. Luciferase activity following transient co-transfections of ST14A cells with a vector that expresses GFP (pEGFP-N1; dotted bars) or exon 1 of huntingtin with 22 CAG repeats (pCMV-22Q; solid black bars) or 115 CAG repeats (pCMV-115Q; solid white bars) and pGL3-DARPP(-1414/-11) or pGL3-DARPP(-171/-11) (A). Luciferase activity following co-transfections of HEK293 cells with pGL3-DARPP(-1414/-11) and pEGFP-N1, pCMV-22Q or pCMV-115Q (B). Firefly luciferase activity was normalized to *Renilla* luciferase activity and the results were expressed as mean (± SEM, n=12 per construct combination). $*P < 0.05$, significant difference in promoter activity in the presence of pCMV-115Q compared to pCMV-22Q; $\sim P < 0.05$, significant difference from the promoter activity in the presence of pEGFP-N1 (two-way ANOVA).

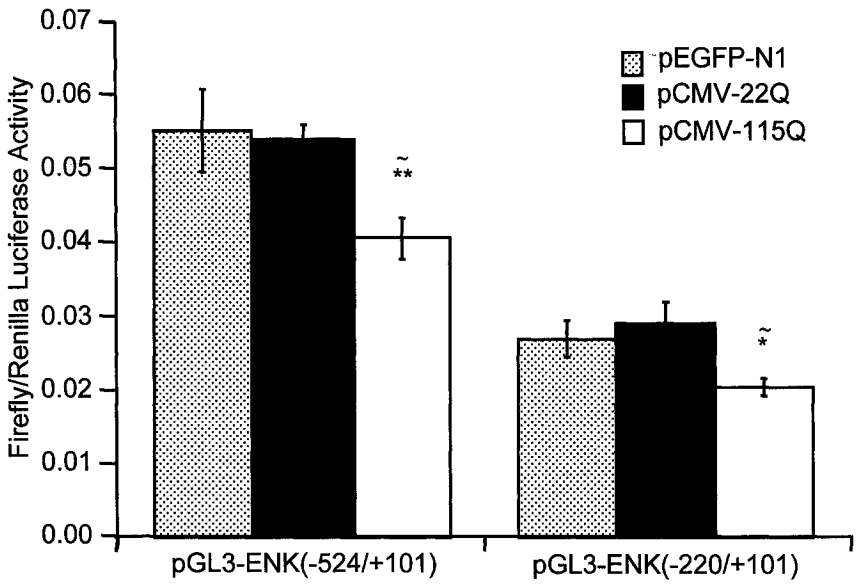

Figure 4-13. Acute expression of N89-115Q altered transcription from ppENK promoter fragments. Luciferase activity from transient co-transfections of ST14A cells with a vector that expresses GFP (pEGFP-N1; dotted bars) or exon 1 of huntingtin with 22 CAG repeats (pCMV-22Q; solid black bars) or 115 CAG repeats (pCMV-115Q; solid white bars) and pGL3-ENK(-524/+101) or pGL3-ENK(-220/+101). Firefly luciferase activity was normalized to *Renilla* luciferase activity and the results were expressed as mean (± SEM, n=12). $*P < 0.05$ and $**P < 0.005$, significant difference in promoter activity in the presence of pCMV-115Q compared to pCMV-22Q; $\sim P < 0.05$, significant difference from the promoter activity in the presence of pEGFP-N1 (two-way ANOVA).

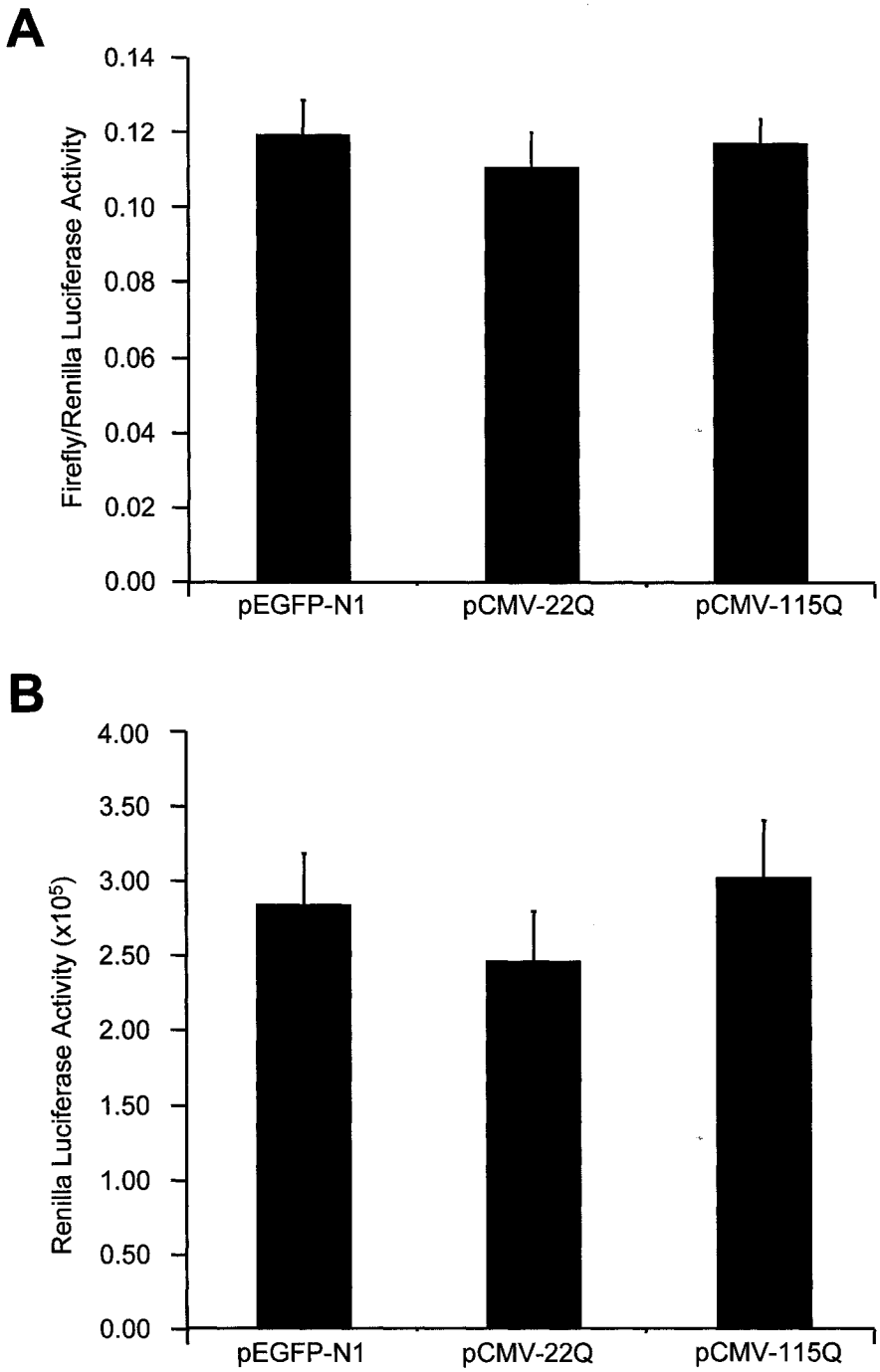

Figure 4-14. Acute expression of N89-115Q did not alter transcription of the HPRT promoter or the TK promoter. Luciferase activity following transient co-transfections of ST14A cells with pEGFP-N1 or pCMV-22Q or pCMV-115Q and pGL3-HPRT(-795/+97) or phRL-TK. Firefly luciferase activity was normalized to *Renilla* luciferase activity and the results were expressed as mean (± SEM, n=12) (A). The raw *Renilla* luciferase activity under the control of the TK promoter was expressed as mean (± SEM, n=12) (B).

affect the activity of the HPRT [pGL3-HPRT(-795/+97)] (Fig. 4-14A) or the TK (phRL-TK) promoters (Fig. 4-14B) in ST14A cells.

DNase I footprinting was employed to determine if there was a difference in protein-DNA interactions between the nuclear proteins isolated from 5 week-old wild-type and R6/1 mice and the -254/-71 region of the DARPP-32 promoter or the -142/+7 region of the ppENK promoter. Nuclear extracts were isolated from this age of mice as it had been demonstrated that transcription of the endogenous DARPP-32 and ppENK genes were affected by 5 weeks of age in R6/1 mice (Fig. 3-3A and 3-10A, respectively). This implied that at 5 weeks in the R6/1 transgenic HD mice the N-terminus of mutant huntingtin was expressed at levels that affected the transcription of the DARPP-32 and ppENK genes. The ratio of N89-115Q to other proteins in the nuclear extracts isolated from the R6/1 transgenic HD mice would be physiologically relevant. As seen in figure 4-15A and B, there were sites that were protected from DNase I digestion and sites that were hypersensitive to DNase I within the -254/-71 region of the DARPP-32 promoter and the -142/+7 region of the ppENK promoter in the presence of nuclear extracts isolated from wild-type and R6/1 forebrain. Based on sequence analysis of potential transcription factor binding sites in these GC-rich regions (http//www.genomatix.de/), there are a number of factors that could contribute to the observed footprinting pattern (Fig. 4-15A, B). However, there was no difference in the DNase I footprinting patterns in the presence of nuclear extracts isolated from wild-type or R6/1 mice demonstrating that N89-115Q did not cause a detectable gain or loss of specific transcription factor binding in this region of the DARPP-32 promoter. The -306/-142 region of the ppENK promoter was also analyzed and did not show any differences in DNase I

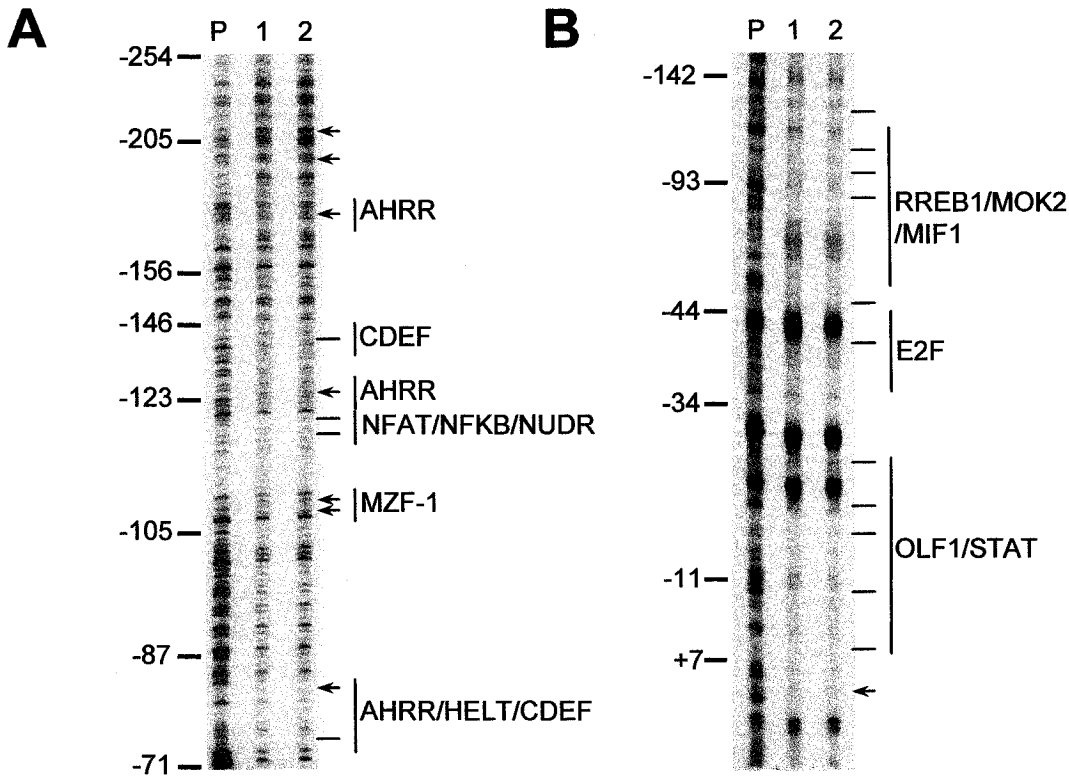

Figure 4-15. DNase 1 footprinting analysis revealed no differences in proteins bound to the -254/-71 region of the DARPP-32 or -142/+7 region of the ppENK promoter in the presence of nuclear proteins derived from R6/1 compared to wild-type mice. The 3' end-labeled probe that spanned the -11 to -476 region of the DARPP-32 promoter (A) and the -524/+101 region of the ppENK promoter (B) was incubated with bovine serum albumin (P), nuclear extracts from the striatum of 5-week old wild-type (1) and R6/1 transgenic HD (2) mice. Lines (—) indicate sites that were protected from DNase I digestion and arrows (←) indicate DNase I hypersensitive sites. The nucleotide position of DARPP-32 and ppENK promoters as defined in Fig 4-3 and Fig. 4-5, respectively and based on mobility of the [γ-32P] ATP labeled ΦX174 DNA/Hinf I markers is indicated to the left of each panel. Potential transcription factor binding sites are indicated to the right of each panel. Aryl hydrocarbon receptor [(AHRR) -165/-187, -111/-134 and -65/-81], nuclear factor of activated T-cells [(NFAT) -109/-120], NF-KappaB [(NFKB) -109/-124], nuclear deformed epidermal autoregulatory factor-1 related transcriptional regulatory protein [(NUDR) -109/-127], myeloid zinc finger protein [(MZF-1) -100/-107], Hey-like bHLH-transcriptional repressor [(HELT) -63/-77] and cell cycle-dependent element [(CDEF) -64/-81 and -135/-147] are potential DARPP-32 promoter-binding proteins. Ras-responsive element binding protein 1 [(RREB1) -117/-103], ribonucleoprotein associated zinc finger protein [(MOK2) -114/-94], MIBP-1/RFX1 complex[(MIF1) -106/-88], elongation factor 2 [(E2F) -59/-43], olfactory neuron-specific factor 1 [(OLF1) -20/+3] and signal transducers and activators of transcription [(STAT) -3/-21] are potential ppENK promoter-binding proteins.

footprinting patterns in the presence of nuclear extracts isolated from wild-type or R6/1 mice. The *in vitro* DNase 1 footprinting assays were performed in the presence of excess nuclear extract. Such *in vitro* analyses cannot indicate whether the affinity of various transcription factors for the DNA or frequency of factor association is altered in the presence of N89-115Q *in vivo*. We did not analyze the -71/-11 region of the DARPP-32 promoter and although it is possible that N89-115Q affects binding of factors to this sequence of the promoter, it seems unlikely as this region is greater than 120 bp downstream of both major transcription start sites in the proximal promoter. Functional *trans*-acting factors are generally located upstream of transcription initiation sites and components of the holoenzyme complex bind in the immediate vicinity (-30 to +30) of transcription initiation sites in Pol II promoters (Lemon & Tjian, 2000).

4.3 Discussion

Steady-state mRNA levels of DARPP-32 and ppENK were decreased in the brains of aging R6 transgenic mice (Chapter 3). The levels of both the primary and the mature DARPP-32 transcripts decreased in R6/1 transgenic HD mice older than 6 weeks of age. This demonstrated that transcription of the DARPP-32 gene, and not stability of the DARPP-32 mRNA, was altered by the expression of N89-115Q *in vivo* and that the change occurred in young presymptomatic mice. Similarly, the rate of transcription of the CB1 and PDE10A genes are decreased in the striatum of transgenic R6/1 mice starting at ~ 5-6 weeks of age (Hu *et al.*, 2004; McCaw *et al.*, 2004). N89-115Q decreased steady-state mRNA levels by altering transcription of selective genes.

N89-115Q did not alter transcription of the DARPP-32 and ppENK genes by altering transcription start site selectivity. Both the DARPP-32 and ppENK genes have multiple transcription start sites. DARPP-32 transcripts initiate from a multitude of individual transcription initiation sites, which have been grouped into the proximal and distal transcription start site regions of the DARPP-32 gene (Fig. 4-3, 4-4 and Blau *et al.*, 1995). We have demonstrated that transcripts that initiate at the distal transcription initiation region were expressed in the brain, but not in the kidney, and steady-state levels of these transcripts in the brains were not affected by N89-115Q (Chapter 3). The decrease in steady-state DARPP-32 mRNA levels was specifically associated with decreases of the transcripts that initiated from the proximal transcription initiation region (Fig 3-6). However, the loss of mRNA was not due to a decrease in transcripts from particular start sites within the proximal transcription initiation region, but was associated with a general decrease in transcripts from all start sites in the proximal transcription initiation region. Similarly, five transcription start sites of the ppENK mouse gene were identified by 5'RLM-RACE. ppENK transcripts that initiate from two of these transcription start sites were detected by RPA in the striatum and transcripts that initiate from both start sites were decreased in R6/1 transgenic HD mice. This provides evidence that the decrease in ppENK steady-state mRNA levels was also not caused by effects of N89-115Q on a particular transcription start site, but rather by an affect on transcription from both initiation sites. Similarly, the CB1 gene has multiple transcription start sites and the levels of transcripts initiating at each of the different sites of the CB1 promoter decreases in R6 mice (McCaw *et al.*, 2004). In contrast, transcripts that initiate from three distinct transcription start sites of the PDE10A2 gene have been identified in the

striatum, but the levels of transcripts that initiate from only two of these sites are decreased in R6/1 transgenic HD mice. For PDE10A2, N89-115Q alters transcription in a start site-specific manner (Hu *et al.*, 2004).

Since N89-115Q altered transcription in R6/1 transgenic HD mice and is known to interact with various transcription factors, we adopted an *ex vivo* system to analyze the effects of the N-terminal fragment of mutant huntingtin on the promoter regions of the DARPP-32 and ppENK genes. This *ex vivo* system employed immortalized rat striatal neurons (ST14A) and derivatives expressing the amino terminus of wild-type (N548wt) or mutant (N548mu) huntingtin. The R6 transgenic mice carry the mutant huntingtin transgene through development. DARPP-32 and ppENK transcript levels were normal in younger transgenic HD mice indicating that all factors necessary for the synthesis of these transcripts were available in the R6 transgenic HD mice. As the R6 transgenic HD mice get older, transcript levels start to decrease. We wanted to determine if transcription of DARPP-32 and ppENK were effected as soon as the promoters were exposed to a given concentration of the truncated N-terminal fragment of mutant huntingtin or whether the changes were occurring over considerable periods of time because of long-term adaptive changes in cells or in the signaling between neurons. It has been suggested that the lack of BDNF-trophic support from cortical projection neurons could alter gene expression in the striatum (Zuccato *et al.*, 2001). By using a cell culture model of HD, we determined that the N-terminal fragments of mutant huntingtin exerted its effects on these promoters via an intracellular mechanism and not an intercellular signaling mechanism. It should also be noted that the N548wt cells are not a true representation of the form of huntingtin in wild-type animals as the 548 amino acids at the N-terminus of

the huntingtin protein is over expressed in these cells. The N548wt cells served as an important control in order to determine which effects could be caused by the first 548 amino acids of huntingtin and which effects could be caused by the expanded polyglutamine region of mutant huntingtin within the first 548 amino acids. The polyproline and the HEAT repeat regions of mutant huntingtin are known to interact with various proteins such as NK-κB, huntingtin-yeast partner (HYP) A, HYP-B, HYP-C, p53, glyceraldehyde 3-phosphate dehydrogenase (GAPDH; Burke *et al.*, 1996; Faber *et al.*, 1998; Steffan *et al.*, 2000; Takano & Gusella, 2002; Li & Li, 2004). We transiently transfected ST14A cells with the first 89 amino acids of human huntingtin containing either 22 or 115 CAG repeats. This fragment of mutant huntingtin corresponds to the transgene that is expressed in the R6 transgenic HD mice. We also observed the promoter activity in the ST14A cells in the absence of transiently transfected N-terminal fragments of huntingtin as this state is comparable to wild-type mice.

DARPP-32, but not ppENK, was endogenously expressed in the ST14A cells (Ehrlich *et al.*, 2001). In the ST14A cell derivatives the transcript levels of the DARPP-32 gene was lower in the N548mu cells compared to the N548wt cells when the cells were induced to differentiate. The difference in DARPP-32 transcript levels in the N548mu cells compared to N548wt cells could not be attributed to cell loss as there was only modest cell loss in both cell lines and variability in the number of viable cells among samples were internally normalized to levels of HPRT mRNA. The N-terminal fragment of mutant huntingtin exerted its effects on the DARPP-32 promoter via an intracellular mechanism, rather than an intercellular mechanism, that was recapitulated in these immortalized striatal neuronal cultures.

The N548wt and the N548mu are two independent cell lines and differences in promoter activities could reflect basic differences between the transformed N548wt and N548mu cells lines that are unrelated to the N-terminal fragment of mutant huntingtin. In fact the HPRT promoter activity was decreased in the N548mu cells even though we did not observe any difference in the HPRT mRNA copy number in quantitative RT-PCR analysis of RNA isolated from striatal tissue of wild-type and any age of R6/1 mice relative to total RNA. Therefore, we assumed that the N548wt and N548mu cell lines differ with respect to CAG repeat length in the stably expressed truncated human huntingtin transgene and may differ by other components controlling transcription.

Knockdown of the N-terminal fragment of huntingtin in the N548wt and N548mu cells revealed that there were two components of repression on the activity of the DARPP-32(-1414/-11) and ppENK(-524/+101) promoters in these cell lines. One component of repression could be attributed to the N-terminus of huntingtin or an effect of shHD2.1 on a component of the cells that has not been previously identified and is independent of over expression of the first 548 amino acids of huntingtin. Expression of shHD2.1 resulted in increased activity of DARPP-32, ppENK and HPRT in the N548wt and N548mu cell lines. However, we have clearly demonstrated that the N terminus of huntingtin expressed in parental ST14A cells did not activate or repress DARPP-32, ppENK or HPRT promoter activities. This suggested that the component of repression in both the N548wt and N548mu cells, is more likely due to a non-specific shHD2.1 effect that is present in both the N548wt and N548mu cells. It should be noted that a sequence-specific knockdown of an unintended target cannot be controlled for by adding vector without siRNA, vector expressing a scrambled form of shHD2.1 or vector expressing a

siRNA against another target such as LacZ. The other component of the repression specifically in the N548mu cells could be attributed to the expanded polyglutamine region at the N-terminus of the huntingtin protein as knockdown of huntingtin in these cells results in an alleviation of the repression on the activities of the DARPP-32(-1414/-11) and ppENK(-524/+101) promoters in the N548mu cells. As such, the combined effects of derepression via shHD2.1 resulted in equivalent promoter activity of the DARPP-32 and ppENK promoters in N548wt and N548mu cells.

In order to confirm that the repression on the DARPP-32 and ppENK promoter activities were due to the expanded polyglutamine region at the N-terminus of mutant huntingtin, we needed to test the effects of the expanded polyglutamine region in the N-terminus of mutant huntingtin on the DARPP-32 and ppENK promoter activities within one cell line. In parental ST14A cells we observed that the DARPP-32 and ppENK promoters were sensitive to transcriptional repression via short-term expression of exon 1 of mutant huntingtin indicating that the expanded polyglutamine region at the N-terminus of mutant huntingtin caused the decrease in transcription from the DARPP-32 and ppENK promoters. Furthermore, the decrease in transcription of the ppENK and the DARPP-32 promoters were observed 48 hours after transfection, suggesting that these changes in transcription in the ST14A cells were most likely due to the direct effects of the N-terminus of mutant huntingtin rather than secondary compensatory changes within the cell caused by long-term expression of mutant huntingtin. Since transcription from the DARPP-32 and ppENK promoters within an extrachromosomal plasmid were affected by the truncated N-terminual fragment of mutant huntingtin, it did not appear that chromatin structure or blockade of chromatin remodeling by factors such as CBP

(Steffan *et al.*, 2000; Steffan *et al.*, 2001) was a crucial factor in the mechanism by which the N-terminus of mutant huntingtin exerted its effects on transcription in this experimental model. In addition, the activities of the TK and HPRT promoters in ST14A cells and the DARPP-32 promoter in HEK293 cells were not affected by the short-term expression of the mutant huntingtin transgene indicating that the gene-specific and tissue-specific effects of N89-115Q were still observed in this *ex vivo* model of HD.

Mutant huntingtin interacts with, and in some cases, alters the activity of transcription factors and co-activators such as Sp1, CBP, $TAF_{II}130$, p53, p300, P/CAF (p300/CBP-associated factor), CtBP (C-terminal binding protein), NCoR (nuclear corepressor) and NRSF (Dunah *et al.*, 2002; Sugars & Rubinsztein, 2003; Zuccato *et al.*, 2003). The sequential promoter deletion analysis of the DARPP-32 and ppENK promoters demonstrated that, if the N-terminal fragment of mutant huntingtin was interacting with a specific factor or factors, the *cis*-binding site would have to reside within the smallest promoter deletion fragments analyzed. Similarly, Chiang *et al.* (2005) found that the activity of the core promoter of the A_{2A} adenosine receptor gene was decreased in the presence of the N-terminal fragment of mutant huntingtin, and they attributed this effect to alterations in the activity of CREB/CBP. The GC-rich 180 bp region of the DARPP-32 promoter, which is downstream of the majority of transcription initiation sites, and the 310 bp region of the ppENK promoter, which spans the major transcription start site were analyzed and several potential transcription factor binding sites were identified. Some of these transcription factors, such as Sp1 and NF-κB have been shown to interact with mutant huntingtin (Dunah *et al.*, 2002; Li *et al.*, 2002; Takano & Gusella, 2002). The binding sites for other mutant huntingtin-interacting

transcription factors such as CREB, NRSF, TBP, RXR, NCoR, and p53 were not found in this region of the DARPP-32 or ppENK promoters. There was no difference in the DNase I footprints in this region of the ppENK and DARPP-32 promoters using nuclear proteins extracted from wild-type mice and R6/1 transgenic HD mice. In these nuclear extracts N89-115Q and other nuclear proteins are present in physiologically relevant ratios. Transcriptional activators were not excluded from the promoter and no novel factors acting as repressors were recruited to the promoter in the presence of N89-115Q. These observations do not support the hypothesis that N89-115Q sequesters transcription factors and prevents them from interacting with *cis*-elements (Cha, 2000; Steffan *et al.*, 2000; Luthi-Carter & Cha, 2003; Sugars & Rubinsztein, 2003). It also does not provide any evidence for the theory that N89-115Q itself is a DNA binding protein that acts directly as a transcription factor (Luthi-Carter & Cha, 2003).

N89-115Q with its expanded polyglutamine region leads to altered DARPP-32 and ppENK transcription in a promoter- and cell-specific manner. The basis for susceptibility or resistance of these and other promoters to the action of N89-115Q remains to be determined. N89-115Q did not alter binding of transcription factors to the DNA and did not act as a DNA binding protein when it was present in physiologically relevant concentrations within nuclear protein. Therefore, we propose that N89-115Q in combination with a factor present in the brain rendered the DARPP-32 and ppENK promoters sensitive to N89-115Q by altering components of the transcriptional machinery that do not interact directly with the DNA. It is also possible that these promoters are protected from N89-115Q induced transcriptional dysregulation by the presence of specific factors in other tissues that are not present in the brain.

CHAPTER 5

The Amino Terminus of Mutant Huntingtin Decreases Transcription *In Vitro*

Portions of this chapter appeared in the following publication:

Gomez, G.T., Hu, H., McCaw, E.A. & Denovan-Wright, E.M. (2006) Brain-specific factors in combination with mutant huntingtin induce gene-specific transcriptional dysregulation. *Molecular and Cellular Neuroscience*, **31**, 661-675. Reprinted with permission from Elsevier.

5.1 Introduction

N89-115Q and N89-150Q altered transcription of the DARPP-32, PDE10A and CB1 genes *in vivo* (Chapter 4; Hu *et al.*, 2004; McCaw *et al.*, 2004) and DARPP-32 and ppENK, but not HPRT, promoter activity in cell culture models of HD (Chapter 4). These observations indicated that N89-115Q exerted its effects on transcription via intracellular mechanisms. We did not find evidence of changes in DNA-protein interactions at the DARPP-32 or ppENK promoters suggesting that sequestration of transcription factors could not account for transcriptional dysregulation of these promoters. N89-115Q affects transcription of the DARPP-32 promoter in a tissue- and cell-specific manner. It appeared that a specific factor present in the brain rendered the DARPP-32 promoter sensitive to N89-115Q, or that a kidney-specific factor protected DARPP-32 transcription from the effects of N89-115Q.

In order to study the mechanism of action of the N-terminual fragment of mutant huntingtin, we developed an *in vitro* transcription system in which we could study the effects of the N-terminal fragment of mutant huntingtin protein in a cell-free system apart from cellular processes and the effects of chromatin. From a practical point of view *in vitro* transcription has an advantage over transfection or transgenic mouse studies since it is easily amendable to the addition of purified proteins.

The human cytomegalovirus (CMV) is a member of the herpesvirus classification group. CMV has a large double-stranded DNA genome of 240 kb. The first viral genes expressed in cells infected with the virus do not require prior viral protein synthesis for efficient transcription and have been referred to as immediate-early genes. Upstream of the major immediate-early gene of CMV is a strong promoter regulatory region and *in*

vitro transcription analysis indicates that this regulatory sequence competes efficiently for RNA polymerase II and other factors of the transcription complex present in transcriptionally competent cell lysate derived from HeLa cells (Stenberg *et al.*, 1984; Thomsen *et al.*, 1984; Boshart *et al.*, 1985).

The transcription cycle involves preinitiation complex formation, initiation, promoter clearance, elongation and termination. If the N-terminal fragment of mutant huntingtin interfered with any of these phases, production of mRNA would be decreased. The abnormal function of the amino terminus of mutant huntingtin with respect to transcription must account for gene-specific, as well as, tissue-specific effects. Since the formation of the preinitiation complex is the first step in the transcription cycle, we initiated our analysis by testing whether the N-terminal fragment of mutant huntingtin altered preinitiation complex formation or the constituents of the preinitiation complex.

In cell culture systems, the effects of the amino terminus of mutant huntingtin on transcription were observed 48 hr after ST14A cells were transiently transfected (Chapter 4). In cell culture, however, the N-terminal fragment of mutant huntingtin could alter the relative abundance or state of other proteins that in turn altered transcription of the genes of interest. To determine if the N-terminual fragment of mutant huntingtin exerts its effects via a direct rather than an indirect mechanism, we purified huntingtin protein comprising the first 171 amino acids from the N-terminus with either 23 or 87 polyglutamines and observed the effects of the addition of these purified proteins on the transcription cycle.

5.2 Results

We adopted an *in vitro* transcription system to study the mechanism by which the truncated N-terminus of mutant huntingtin alters transcription in a cell-free system. First, we attempted *in vitro* transcription from linearized fragments of the DARPP-32 and HPRT promoters. The DARPP-32 promoter (-1414/-11) and the HPRT promoter (-795/+97) are active in cell culture and both have multiple transcription start sites (Chapter 4 and Melton *et al.*, 1986; Blau *et al.*, 1995). HeLa nuclear extract is a well-characterized system for *in vitro* transcription of eukaryotic genes. It is prepared from human HeLa cells and contains all components required to support transcription initiation by RNA polymerase II (Dignam *et al.*, 1983). It is also a source of transcription factors, DNA binding proteins and the enzymatic machinery involved in RNA processing. The positive control provided with the HeLa Scribe *in vitro* transcription kit (Promega) consisted of a 1.2 kb fragment containing the strong CMV promoter and 363 nts of the tetracycline gene. This positive control template produced large amounts of a single 363 nts transcript in *in vitro* reactions using the HeLa extract and the manufacture's recommended conditions. This demonstrated that the HeLa nuclear extract was transcriptionally active *in vitro* (Fig. 5-1). Multiple smaller products were also generated from the CMV promoter although these products were considerably less abundant than the major 363 nts product. In contrast, the -1414/-11 region of the DARPP-32 promoter did not produce any distinct transcripts using the same molar equivalent of template, HeLa nuclear extract and reaction conditions (Fig. 5-1). Similarly, *in vitro* transcription from the -795/+97 region upstream of the HPRT coding sequence with active HeLa nuclear extract did not produce any distinct transcripts. Alteration of the concentration of

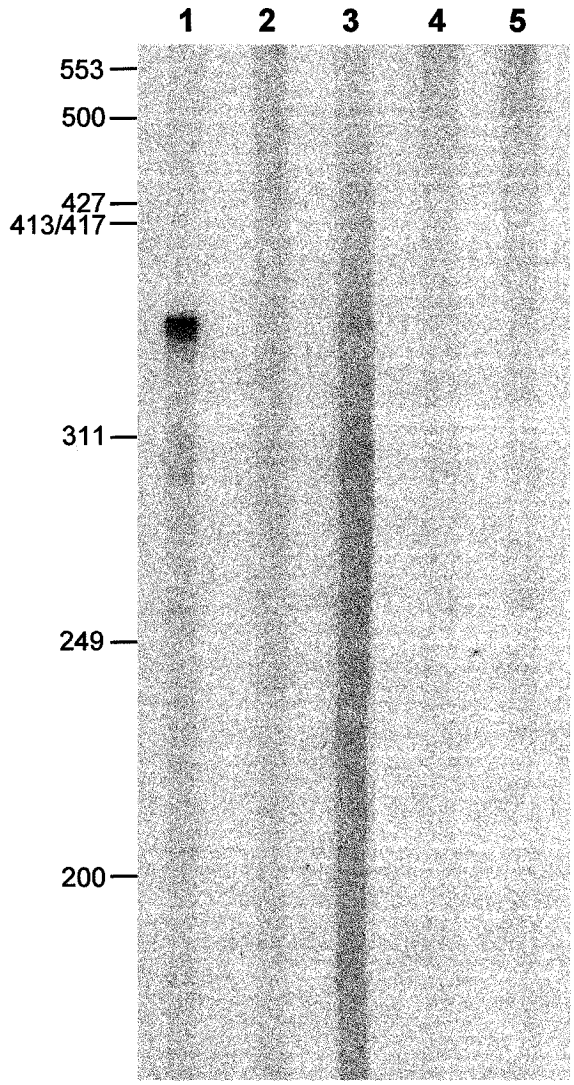

Figure 5-1. *In vitro* transcription reactions from the CMV promoter produced abundant transcripts that were 363 nts in size, unlike the DARPP-32 and HPRT promoters that only generated low abundant products. Products generated from 100 ng of the CMV promoter in the presence of HeLa nuclear extract are shown in lane 1. Reaction products from the 1.4 kb DARPP-32 (2, 3) or the 0.9 kb HPRT promoters (4, 5) in the presence of HeLa nuclear extract (2, 4) or HeLa nuclear extract supplemented with 5 μg of wild-type forebrain nuclear extract (3, 5) are shown. Products were fractionated on a 5% denaturing PAGE gel and exposed to autoradiographic film overnight. The relative mobility of the PhiX174 DNA/*Hinf*I markers are shown on the left of the panel.

Mg^{2+} in the *in vitro* transcription reaction did not increase transcription from the DARPP-32 or HPRT promoters (data not shown). We hypothesized that transcription from the DARPP-32 and HPRT promoters might require transcriptionally active HeLa nuclear extract supplemented with factors from mouse forebrain nuclear extract. *In vitro* transcription reactions that included the DARPP-32 and active HeLa nuclear extract supplemented with wild-type forebrain nuclear extract produced multiple low abundance products (Fig. 5-1). *In vitro* transcription reactions from the HPRT promoter using HeLa nuclear extract supplemented with wild-type forebrain nuclear extract produced a single low abundance product at approximately 265 nts (Fig. 5-1) and corresponds to a main transcription initiation site (Melton *et al.*, 1986). Increasing the amount of DNA template in reactions did not increase the abundance of transcripts. In fact, increasing the copy number of templates in the reactions resulted in limiting nuclear extract proteins and a decrease in the amount of transcript produced (data not shown).

The ppENK promoter contained five transcription start sites (Chapter 4). Of these five sites, one start site produced the majority of transcripts *in vivo* (+1 in Fig. 4-5). The start site at position -289 produced transcripts that could be detected by RPA (Fig. 4-6). Sites -375, -320 and -270 produced mRNAs that could only be detected by PCR amplification of 5' RLM-RACE suggesting that they were relatively rare transcripts in total striatal RNA. *In vitro* transcription reactions from the -524/+101 fragment of the ppENK promoter and active HeLa nuclear extract supplemented with wild-type forebrain nuclear extract did not produce any products (data not shown). The ppENK promoter was restriction digested into two fragments spanning the -224/+101 and the -524/-225 regions and the two DNA fragments were purified. The -524/-225 linearized fragments

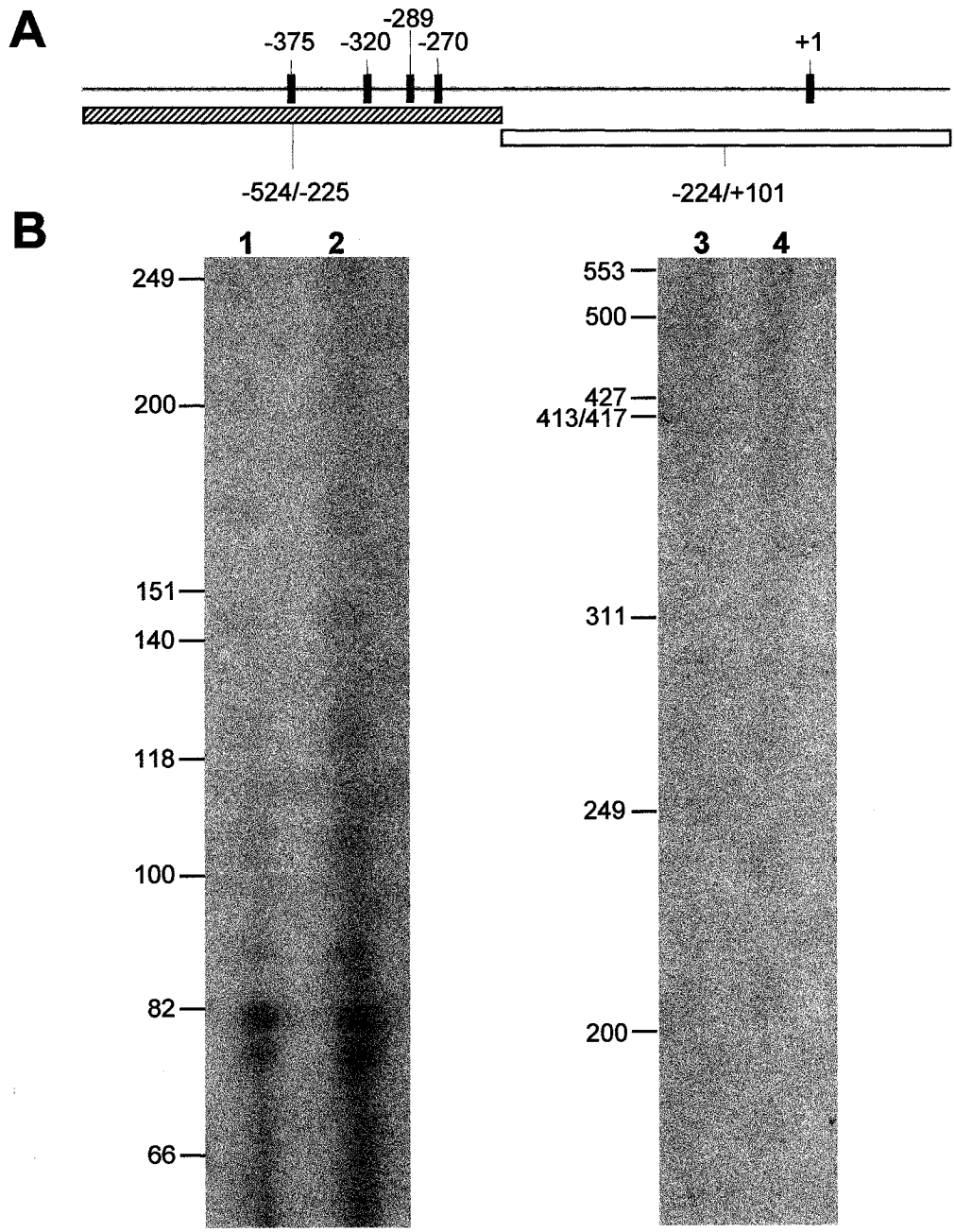

Figure 5-2. The -524/-225 region of the ppENK promoter, but not the -224/+101 region of the ppENK promoter produced distinct transcripts in *in vitro* transcription reactions. Panel A shows a schematic representation of the ppENK promoter region. The five transcription start sites are indicated (black bars). The -524/-225 region (hatched bar) and the -224/+101 region (open bar) of the ppENK promoter are shown. *In vitro* transcription products generated from the -224/+101 region of the ppENK promoter (1, 2) and the -524/-225 region of the ppENK promoter (3, 4) in the presence of HeLa nuclear extract (1, 3) or HeLa nuclear extract supplemented with 5 μg of wild-type forebrain nuclear extract (2, 3) are shown in panel B. Products were fractionated on a 5% denaturing PAGE gel and exposed to autoradiographic film overnight. The relative mobility of the PhiX174 DNA/*Hinf*I markers are indicated to the left of each panel.

of the ppENK promoter spanned the four minor transcription start sites and, based on the relative position of these sites, we expected to observe transcripts of approximately 46, 65, 96 and 151 nts (Fig 5-2A). *In vitro* transcription of the -524/-225 region of the ppENK promoter with active HeLa nuclear and active HeLa extract supplemented with wild-type forebrain nuclear extract produced transcripts of approximately 78 and 82 nts. The size of these transcripts was calculated based on the relative mobility of radio-labeled and denatured double-stranded DNA markers. These products were only detected after an extended period of exposure of the gel to autoradiography film in the presence of an intensifying screen (Fig 5-2B). We could not detected distinct products for the DARPP-32 and HPRT promoters after similar extended periods of exposure of reaction products (data not shown). The 78 and 82 nts ppENK transcripts that were detected corresponded approximately to sites -289 and -320 (Fig. 4-5). The -224/+101 linearized fragment spanned the +1 transcription initiation site of the ppENK promoter (Fig. 5-2A). Transcripts that initiated from this transcription start site were the most abundant *in vivo* (Fig. 4-6). If transcription initiated from the +1 site, we expected to observe transcripts of approximately 305 nts. However, *in vitro* transcription of the -224/+101 region of the ppENK promoter with active HeLa nuclear extract and active HeLa extract supplemented with wild-type forebrain nuclear extract did not produce any detectable transcripts (Fig 5-2B). Thus, the ppENK promoter was transcribed from distinct start sites *in vitro* using active HeLa nuclear extract but, in this system, this region of the ppENK promoter was a relatively weak promoter. Based on the low level of products produced from the ppENK and DARPP-32 promoters, these promoters were not suitable to study the effects of the N-terminal fragment of mutant huntingtin using the *in vitro* transcription system.

The CMV promoter was a positive control for the *in vitro* transcription system. It was a strong promoter that produced large amounts of a product from a single transcription start site. Activity from a plasmid containing the CMV promoter (pCMV-Luc) in N548mu was decreased when compared to the activity of this promoter in N548wt cells (Fig. 5-3A). We transiently transfected ST14A cells with a control vector (pEGFP-N1) or constructs expressing exon 1 of wild-type huntingtin or mutant huntingtin and observed the activity of the pCMV-Luc vector. There was a significant increase in the activity of the CMV promoter in the presence of both wild-type huntingtin and N89-115Q when compared to the control vector (Fig. 5-3B). However, the acute expression of the N-terminal fragment of mutant huntingtin caused a significant decrease in the activity of the CMV promoter compared to the activity of the promoter in the presence of exon 1 of wild-type huntingtin (Fig. 5-3B). This indicated that the presence of the N-terminal of the huntingtin protein increased that activity of the CMV promoter, but that expansion of the polyglutamine region in the N-terminus significantly decreased this effect. We reasoned that the CMV promoter could be used as a model promoter to study the effects of the N-terminal fragment of mutant huntingtin in *in vitro* transcription reactions because 1) the CMV promoter was transcribed using transcriptionally active HeLa nuclear extract, 2) transcription from the CMV promoter, like other promoters affected by N89-115Q such as DARPP-32 and ppENK, was decreased by the acute expression of exon 1 of mutant huntingtin in ST14A cells and 3) the CMV promoter has a single transcription initiation site in the *in vitro* transcription system. Importantly, the amount of the single product produced from the CMV promoter in the presence of HeLa nuclear extract and HeLa nuclear extract supplemented with nuclear extracts derived

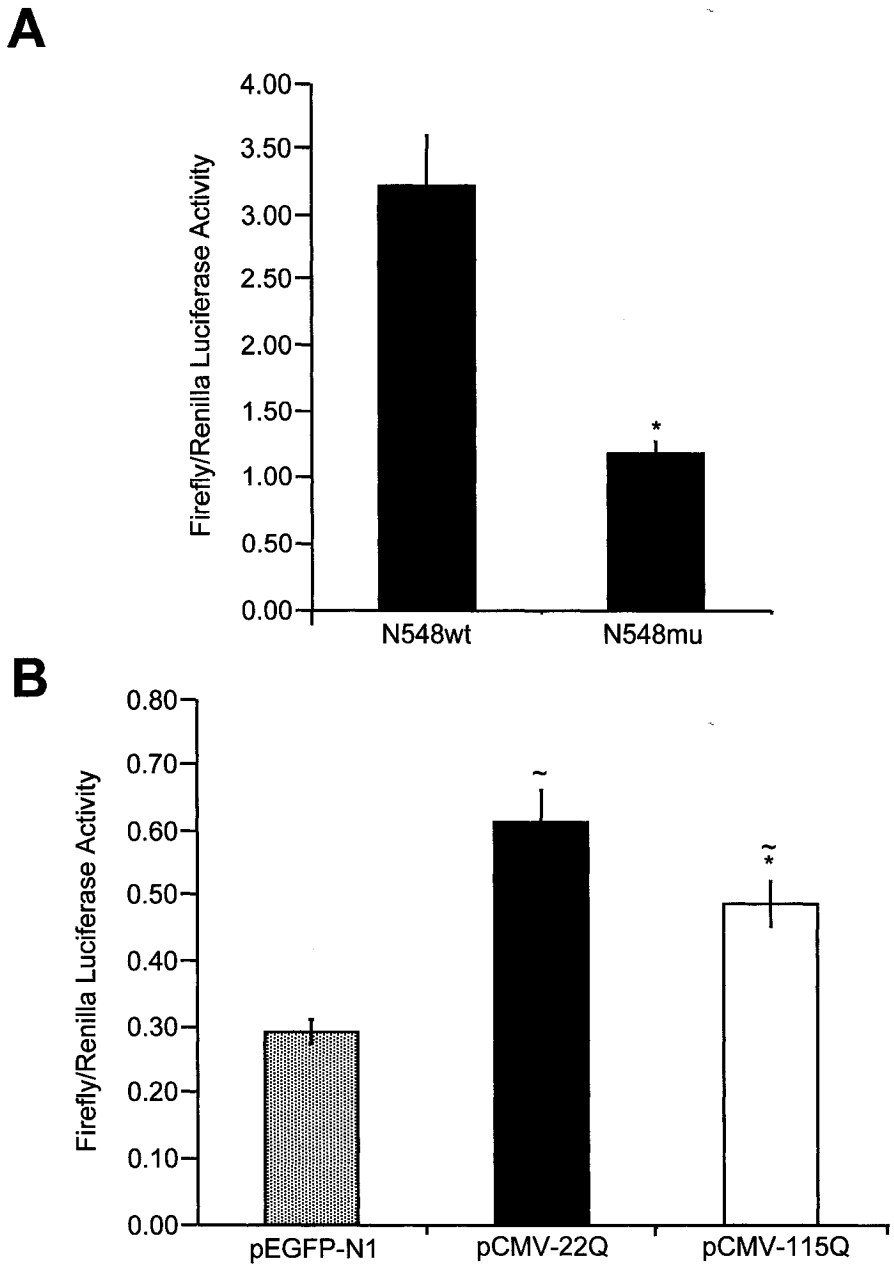

Figure 5-3. Expression of the amino terminus of mutant huntingtin in cell culture models decreased transcription from the CMV promoter. A CMV promoter-containing luciferase construct (pCMV-Luc) was co-transfected with phRL-TK into N548wt and N548mu cells (A). Luciferase activity following transient co-transfections of ST14A cells with a vector that expresses GFP (pEGFP-N1; dotted bar) or exon 1 of huntingtin with 22 CAG repeats (pCMV-22Q; solid black bar) or 115 CAG repeats (pCMV-115Q; solid white bar) and pCMV-Luc (B). Firefly luciferase activity was normalized to *Renilla* luciferase activity and the results were expressed as mean (± SEM, n=12). $*P < 0.05$, significant difference in promoter activity in the presence of pCMV-115Q compared to pCMV-22Q; $\sim P < 0.05$, significant difference from the promoter activity in the presence of pEGFP-N1 (one-way ANOVA).

from different tissues and genotypes of mice or recombinant protein could be quantified. In contrast, the low abundance and multiplicity of products produced from the DARPP-32 and ppENK promoters precluded accurate comparisons of product accumulation among reactions.

The HeLa nuclear extract was transcriptionally active and produced a 363 ntsproduct from a 1.2 kb fragment containing the CMV immediate-early gene promoter (Fig. 5-4). We first demonstrated that transcription was dependent on the HeLa extract and that none of the DNA or protein components to be added to reactions had any inherent ability to form products. No products were produced from the *in vitro* transcription reactions containing only the 1.2 kb fragment of the CMV promoter. No products were generated from the CMV promoter in the presence of wild-type or R6/1 forebrain or kidney nuclear extracts. This indicated that the wild-type and R6/1 forebrain or kidney nuclear extracts did not support transcription in the absence of HeLa extract.

Comparison of the relative amount of product generated from the reaction containing CMV promoter and HeLa extract to the reaction containing CMV promoter, HeLa extract and 5 μg of forebrain nuclear extract derived from wild-type mice demonstrated that the presence of mouse nuclear extract enhanced the transcriptional activity of the HeLa nuclear extract. We observed an increase in the amount of the 363 nts transcript as well as the multiple smaller transcripts produced during the transcription reaction. Since the forebrain nuclear extracts were not transcriptionally active in the absence of HeLa proteins, this increase in transcripts produced suggested that factors in the mouse brain nuclear extract could enhance the activity of the polymerase complex in the HeLa extract. To test whether the increase in *in vitro* transcription from the CMV

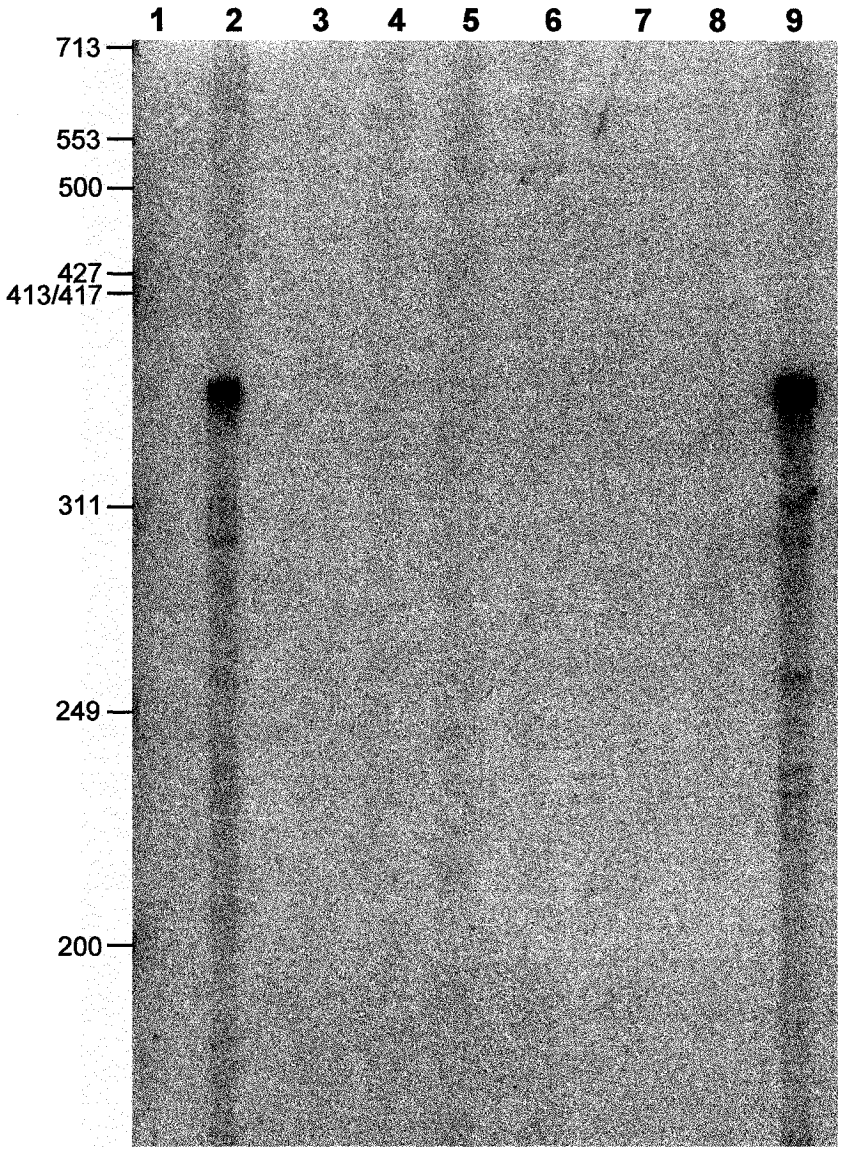

Figure 5-4. HeLa nuclear extract is active *in vitro* and the transcriptional activity of the extract is enhanced by the presence of wild-type forebrain nuclear extract. *In vitro* transcription reactions in the presence of the CMV promoter were assembled, incubated at 30°C for 30 min and the products were fractionated on a denaturing 5% PAGE gel. Products generated from the CMV promoter in the presence of HeLa nuclear extract (2) or HeLa nuclear extract supplemented with 5 μg of wild-type forebrain nuclear extract (9) are shown. No products were generated in the presence of the CMV promoter alone (1) or 5 μg of wild-type forebrain nuclear extract alone (3). No products were generated when the CMV promoter was incubated with 50 μg of wild-type forebrain nuclear extract (4), 5 μg of wild-type forebrain nuclear extract (5), 5 μg of R6/1 forebrain nuclear extract (6) and 5 μg of wild-type (7) and R6/1 (8) kidney nuclear extract. The relative mobility of the PhiX174 DNA/*Hinf*I markers are indicated to the left of the panel.

promoter in the presence of HeLa extract and mouse brain nuclear protein could be attributed to a non-specific increase in protein concentration in the reaction, we added increasing amounts of BSA to parallel reactions. The addition of 5, 10, 15, 20 or 25 μg of BSA did not change the amount of product produced from the CMV promoter during the *in vitro* transcription reaction (Fig 5-5). Therefore, the observed increase in transcripts produced from the CMV promoter in the presence of wild-type mouse forebrain nuclear extract was most likely due to specific factor(s) present in the mouse forebrain nuclear extract that enhanced the activity of the transcriptional machinery provided by the HeLa cell nuclear extract.

The addition of 5 and 10 μg of forebrain nuclear extract isolated from 5 week-old wild-type or R6/1 mice increased the amount of product produced from the CMV promoter in a 30 min period by 1.5 fold. It appeared that the factors that enhanced the activity of the HeLa extract were present at the same concentration in nuclear extracts isolated from wild-type and R6/1 mice. There was no further increase in HeLa activity in the presence of 10 μg compared to 5 μg of forebrain extract suggesting that the maximal rate of HeLa-driven transcription had been reached or that the factor(s) that enhanced the activity of the HeLa extract were present at saturating concentrations after the addition of 5 μg of forebrain extract (Fig. 5-6A). Compared to reactions which included nuclear extract from wild-type mice, there was a statistically significant decrease in the CMV promoter activity when 15, 20 and 25 μg of R6/1 forebrain nuclear extract was added to the *in vitro* transcription reactions (n=4, $P < 0.05$ Fig. 5-6A). As increasing amounts of R6/1 forebrain nuclear extracts were added to the reactions, the rate of transcription from the CMV promoter decreased (Fig. 5-6B). The mean relative activity of the CMV

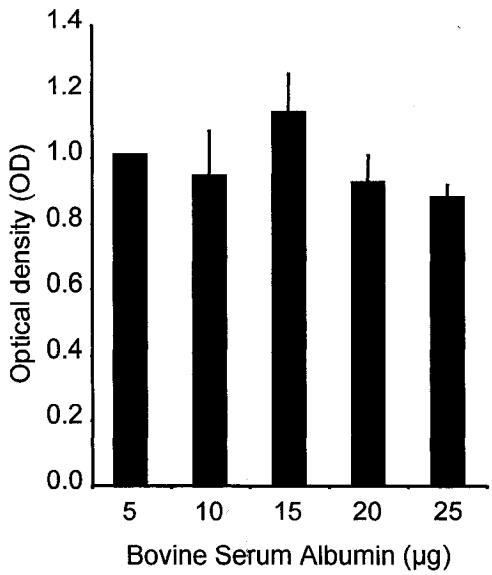

Figure 5-5. Increasing concentrations of BSA did not alter *in vitro* transcription of the CMV promoter. Histogram shows the mean optical density (± SEM, n = 4) of the amount of product generated from *in vitro* run-off transcription of the CMV promoter (100 ng) incubated with active HeLa nuclear extract and increasing concentrations of BSA (as indicated on the x-axis), normalized to the optical density of the product obtained in the presence of active HeLa nuclear extract and 5 µg of BSA.

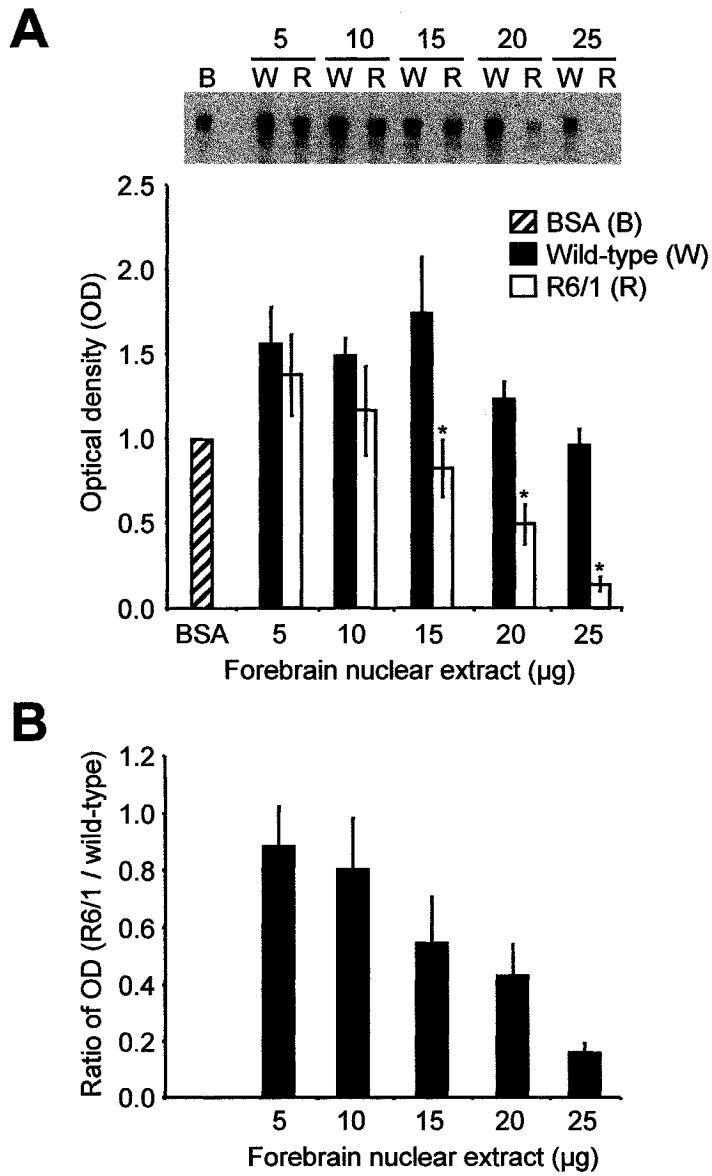

Figure 5-6. Increasing concentrations of R6/1 forebrain nuclear extract decreased *in vitro* transcription of the CMV promoter in the presence of HeLa nuclear extract. Panel A shows a representative autoradiogram of the 363 nt product generated from *in vitro* run-off transcription of the CMV promoter when incubated with active HeLa nuclear extract supplemented with BSA (B) or 5, 10, 15, 20 or 25 µg (as indicated above each set of lanes) of wild-type (W) and R6/1 (R) forebrain nuclear extracts. The histogram shows the mean optical density (± SEM, n=4) of the amount of transcription product produced in the presence of wild-type (solid black bars) or R6/1 (solid white bars) forebrain nuclear extract normalized to the optical density of the product obtained in the presence of BSA. $*P < 0.05$, significant difference between the amount of CMV transcription product formed in the presence of equivalent concentrations of wild-type and R6/1 nuclear extract (two-way ANOVA). The ratios of the mean OD (R6/1/wild-type; ± SEM, n=4) in the presence of 5-25 µg of forebrain nuclear extract are shown in panel B.

promoter in the presence of HeLa and R6/1 nuclear extract compared to reactions containing HeLa and wild-type nuclear extract decreased from ~0.8 when 5 or 10 μg of protein were added to 0.2 when 25 μg of protein were added (Fig. 5-6B). These data indicate that nuclear extracts isolated from 5 week-old R6/1 mice directly affected activity of the basal transcription machinery supplied by the HeLa nuclear extract in a dose-dependent manner. This suggested that increasing concentrations of the amino terminus of mutant huntingtin expressed in the R6/1 mice could directly affect transcription. We could not demonstrate, however, that the nuclear extracts derived from wild-type and R6/1 mice differed only by the presence of the amino terminus of mutant huntingtin.

We had demonstrated that DARPP-32 mRNA levels did not decrease in the kidneys of R6/1 mice even 8 weeks after N89-115Q-containing NIIs were observed in kidney tissue (Fig 3-6C and 3-8). We had also determined that the DARPP-32 promoter was not affected in HEK293 cells by transient co-transfection of this promoter and constructs expressing exon 1 of the *HD* gene with 115 CAG. These observations contrasted with effects of the N-terminal fragment of mutant huntingtin on DARPP-32 promoter activity in the striatum and cell-lines derived from the striatum. We hypothesized that either there was a specific factor in the brain which facilitated the repression of transcription by N89-115Q or that a factor present in the kidney could block N89-115Q-induced transcriptional dysregulation. We tested whether kidney-specific factors could prevent N89-115Q from affecting transcription of the CMV promoter *in vitro*. When wild-type kidney nuclear extract was added to *in vitro* transcription reactions containing 15 μg of 5 week-old wild-type or R6/1 forebrain nuclear extracts, the

activity of the CMV promoter decreased (Fig. 5-7). We chose to add the kidney nuclear extract to this concentration of forebrain extract as the relative activity level was decreased by ~ 40% in the presence of 15 μg of R6/1 compared to wild-type nuclear extract (Fig. 5-6A and B). A reversal of the N89-115Q effect would have increased the relative ratio of activity in these extracts whereas a further repression of transcription would have decreased the observed relative ratio of activity. We observed that there was no change in the relative ratio of the CMV promoter activity in the presence of R6/1 compared to wild-type forebrain extracts in the presence of BSA or two concentrations of wild-type kidney nuclear extract (Fig. 5-7). Therefore, kidney-specific factors did not prevent transcriptional repression induced by nuclear extracts isolated from the brains of R6/1 mice.

The transcription cycle starts with the assembly of the preinitiation complex at the promoter. We wanted to determine if the decrease in transcripts produced from the CMV promoter in the *in vitro* transcription system could be caused by a decrease in the formation of preinitiation complex. To determine if N89-115Q decreased transcription by altering the formation of the preinitiation complex, we used a magnetic Dynabead-coupled template to isolate the proteins from the transcriptionally active HeLa nuclear extract that form the preinitiation complex on the CMV promoter. The biotin-labeled CMV promoter was attached to streptavidin-coated magnetic Dynabeads. The Dynabead-coupled CMV promoter was then used as a template in *in vitro* transcription reactions. Using a magnet, the Dynabead-coupled CMV promoter and the interacting proteins were then isolated and the proteins that did not specifically interact with the CMV promoter were removed. A detailed flow scheme depicting the steps involved in

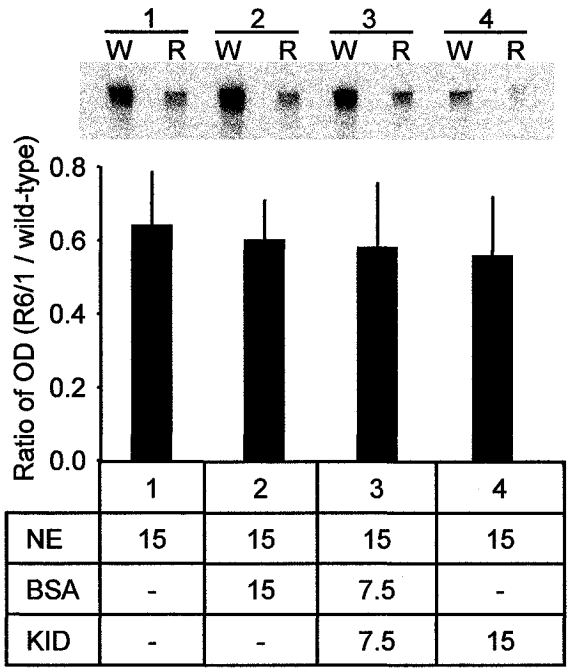

	1	2	3	4
NE	15	15	15	15
BSA	-	15	7.5	-
KID	-	-	7.5	15

Figure 5-7. Kidney nuclear extract did not alleviate the repression caused by R6/1 forebrain nuclear extract on *in vitro* transcription of the CMV promoter. A representative autoradiogram of the 363 nt product generated from *in vitro* run-off transcription of the CMV promoter (100 ng) when incubated with active HeLa nuclear extract supplemented with 15 µg of wild-type (W) or R6/1 (R) forebrain nuclear extracts (NE) (1), active HeLa nuclear extract supplemented with 15 µg of wild-type (W) or R6/1 (R) forebrain nuclear extract and 15 µg BSA (2), 7.5 µg each of BSA and kidney (KID) nuclear extract (3) or 15 µg of kidney nuclear extract (4) is shown. The histogram below shows the ratios (R6/1/wild-type) of the mean OD (± SEM, n=4) of the products of 1, 2, 3 and 4.

isolating the proteins that interact with the Dynabead-coupled CMV promoter is shown in figure 5-8. There were unique proteins that were enriched or reduced in the samples derived from the HeLa nuclear extract proteins that were isolated from the Dynabead-couple CMV promoter compared to total HeLa nuclear extract proteins (Fig. 5-9). This indicated that there was a specific complement of proteins from the active HeLa nuclear extract that interacted with the Dynabead-coupled CMV promoter.

The active HeLa nuclear extract and the inactive wild-type and R6/1 forebrain nuclear extracts contained proteins that could interact with the Dynabead-coupled CMV promoter. There was a different complement of proteins that bound to the Dynabead-coupled CMV promoter from the transcriptionally active HeLa nuclear extract compared to proteins in the wild-type and R6/1 forebrain nuclear extracts that could interact with the CMV promoter in the absence of HeLa extract (Fig. 5-10A). However, there were no obvious differences in the complement of proteins from the wild-type and R6/1 forebrain nuclear extracts that interacted with the CMV promoter. Transcriptionally active HeLa proteins bound to the CMV promoter even when mouse nuclear extract proteins were present.

We have shown that the forebrain nuclear extracts contained factors that altered the activity of the transcription complex provided by the HeLa cell extract (Fig. 5-6). Therefore, we isolated the protein complexes that interacted with the Dynabead-coupled CMV promoter after incubation with the transcriptionally active HeLa nuclear extract supplemented with BSA, wild-type forebrain nuclear extract or R6/1 forebrain nuclear extract. Silver-staining analysis of the proteins indicated that BSA interacted with the Dynabead-coupled CMV promoter (Fig. 5-10B). However, there was no difference in

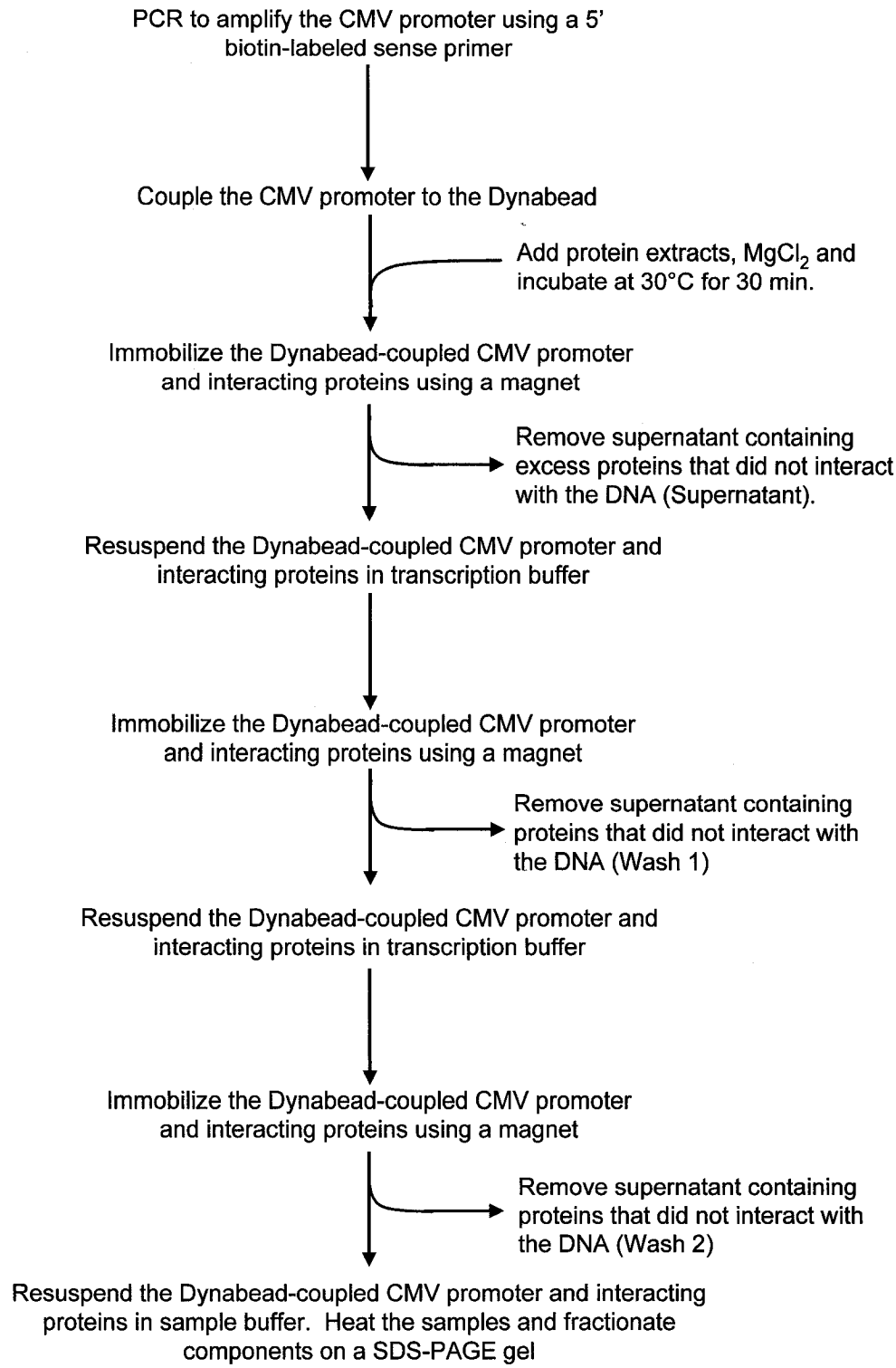

Figure 5-8. Flow scheme indicating the steps involved in isolating the proteins that interact with the Dynabead-coupled CMV promoter.

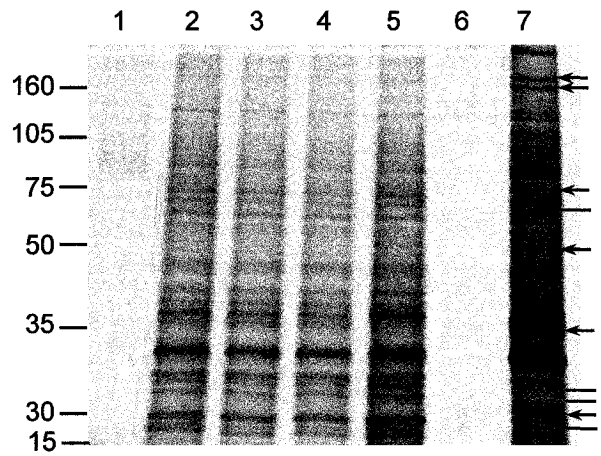

Figure 5-9. Specific proteins interacted with the Dynabead-coupled CMV promoter. Proteins were separated on a 7.5% SDS-PAGE gel and then silver-stained. The Dynabead-coupled CMV promoter (1) and 1.0 ug of HeLa nuclear extract (2) were controls. The equivalent of 1.0 ug of the total *in vitro* transcription reaction containing HeLa nuclear extract and the Dynabead-coupled CMV promoter, after 30 mins of incubation at 30°C (3), supernatant (4), wash 1 (5) and wash 2 (6) as defined in figure 5-8 are shown. Proteins that interacted with the Dynabead-couple CMV promoter are shown (7). Arrows and lines to the right of the panel indicate proteins that were enriched and not present, respectively. The relative mobility of the Full Range Rainbow™ Molecular Weight markers are indicated to the left of the panel.

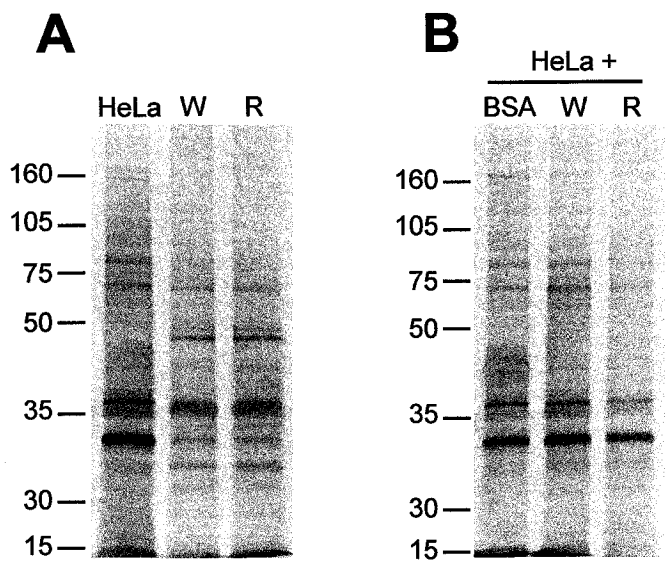

Figure 5-10. In active *in vitro* transcription reactions the proteins that were isolated from the Dynabead-coupled CMV promoter in the presence of nuclear extracts from R6/1 mice were decreased when compared to proteins isolated in the presence of wild-type nuclear extract. Proteins from 30.6 μg of HeLa nuclear extract, 15 μg of wild-type (W) and 15 μg of R6/1 (R) forebrain nuclear extract that interacted with the Dynabead-coupled CMV promoter were isolated, separated on a 7.5% SDS-PAGE gel and then silver-stained (A). Proteins from 15 μg of BSA, wild-type (W) and R6/1 (R) forebrain nuclear extract that interacted with the Dynabead-coupled CMV promoter in the presence of HeLa nuclear extract were isolated, separated on a 7.5% SDS-PAGE gel and then silver-stained (B). The relative mobility of the Full Range Rainbow™ Molecular Weight markers are indicated to the left of the panels.

the complement of proteins bound to the Dynabead-coupled CMV promoter in the presence of active HeLa nuclear extract supplemented with wild-type forebrain nuclear extract or R6/1 forebrain nuclear extract (Fig. 5-10B). There was a general decrease in the amount of proteins that interacted with the Dynabead-coupled CMV promoter after incubation with active HeLa nuclear extract supplemented with R6/1 forebrain nuclear extracts. This was in comparison to proteins that were isolated from the Dynabead-coupled CMV promoter after incubation with active HeLa nuclear extract supplemented with wild-type forebrain nuclear extract (Fig. 5-10B). We did not observe specific loss of individual proteins, however, the banding pattern was fairly complex and the presence or absence of individual proteins may have been masked. Because it appeared that the amount of protein that interacted with the promoter were decreased overall in the presence of the R6/1 forebrain nuclear extract, we hypothesized that the decrease in transcripts formed in the *in vitro* transcription system could be attributed to a decrease in the formation of the preinitiation complex in the presence of the R6/1 forebrain nuclear extract.

The effects of the R6/1 forebrain nuclear extract on the *in vitro* transcription system and the formation of the preinitiation complex could be attributed to N89-115Q itself or to the presence of another factor which had already been altered by N89-115Q prior to the isolation of the R6/1 forebrain nuclear extract. To distinguish between these two possibilities and to determine what caused the observed effects on *in vitro* transcription activity and protein-CMV promoter complex formation, we chose to add purified amino terminus of huntingtin with 87Q. To determine whether the effects were specifically caused by the expanded poly Q repeat or were caused by other regions of the

amino terminus of huntingtin, we compared the effects of huntingtin with 87Q to huntingtin with 23Q. We first produced N-terminus histidine-tagged fusion proteins of the N-terminus of human huntingtin (amino acids 1-171) with either 23 (His-23Q) or 87 (His-87Q) glutamines in the repeat region. The Dynabead-coupled CMV promoter was incubated with active HeLa nuclear extract or active HeLa nuclear extract supplemented with wild-type forebrain nuclear extract in the presence of either His-23Q or His-87Q. The presence of His-23Q and His-87Q did not alter the complement of proteins from active HeLa nuclear extract or active HeLa nuclear extract supplemented with wild-type forebrain nuclear extract that interacted with the Dynabead-coupled CMV promoter (Fig. 5-11A). The presence of His-87Q decreased the amount of proteins from active HeLa nuclear extract or active HeLa nuclear extract supplemented with wild-type forebrain nuclear extract that interacted with the Dynabead-coupled CMV promoter (Fig. 5-11A). The optical density of four single bands in the His-23Q and His-87Q reactions, normalized to the optical density of matched bands in the active HeLa nuclear extract or active HeLa nuclear extract supplemented with wild-type forebrain nuclear extract reactions were averaged (n=3, $P < 0.05$; Fig. 5-11B). The presence of His-87Q significantly decreased the amount of protein that interacted with the Dynabead-coupled CMV promoter (Fig. 5-11B). This indicated that, in this *in vitro* system, the protein complexes that interacted with the Dynabead-coupled CMV promoter were directly affected by His-87Q. His-23Q significantly increased the amount of proteins that interacted with the Dynabead-coupled CMV promoter in the reactions containing active HeLa nuclear extract supplemented with 15 μg of wild-type forebrain nuclear extract (Fig. 5-11B). This suggested that there are specific factors present in the wild-type

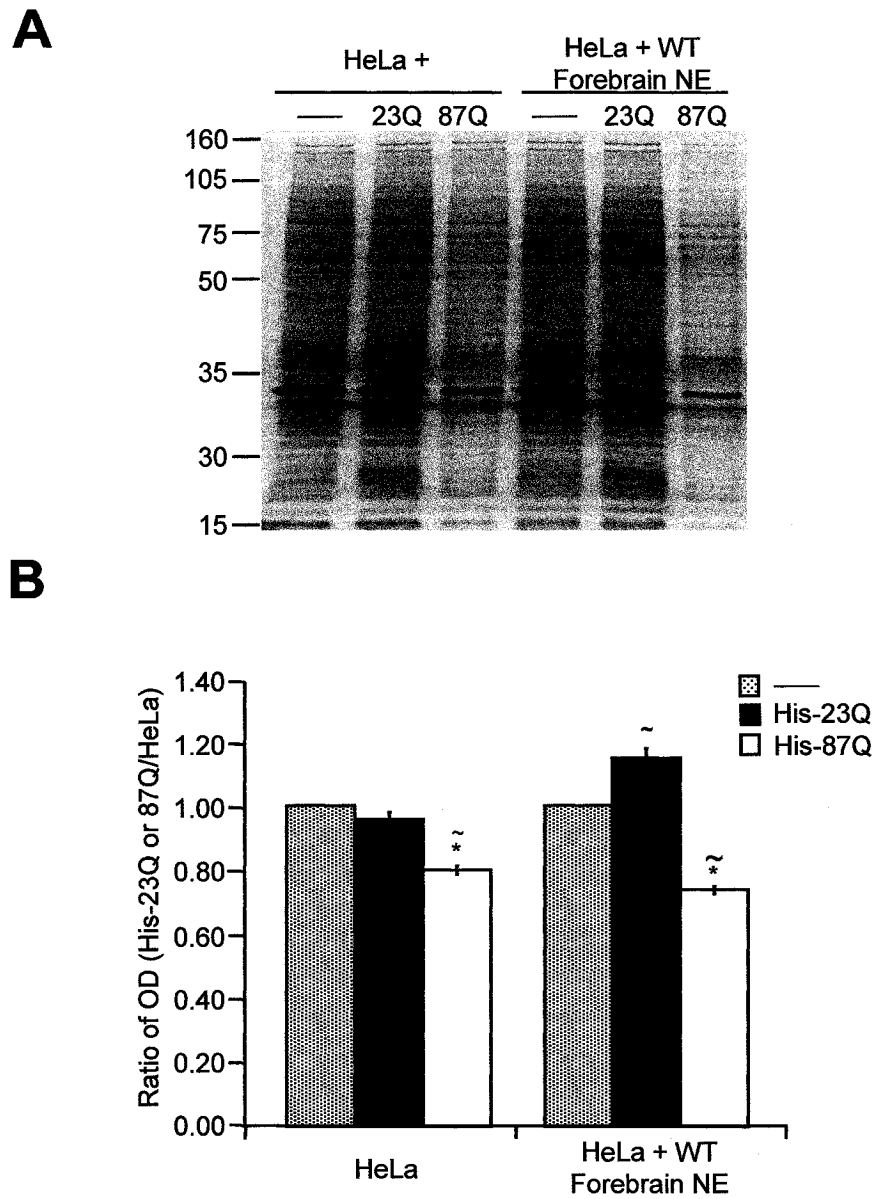

Figure 5-11. His-87Q in the presence of forebrain nuclear extract further decreased the proteins that were isolated with the Dynabead-coupled CMV promoter. Proteins from HeLa nuclear extract in the presence of wild-type (WT) forebrain nuclear extracts alone (—), or with 5.0 pmol of His-23Q (23Q) or His-87Q (87Q), that interact with the Dynabead-coupled CMV promoter, were isolated, separated on a 10% SDS-PAGE gel and then silver-stained (A). The relative mobility of the Full Range Rainbow™ Molecular Weight markers are indicated to the left of the panel. Histogram shows the mean OD (± SEM, n=3) of a single band normalized to the optical density of the band in the presence of HeLa nuclear extract or HeLa nuclear extract in the presence of wild-type forebrain nuclear extract (B). $*P < 0.05$, significantly different from the OD in the presence of His-23Q; $\sim P < 0.05$, significantly different from the OD in the presence of HeLa (two-way ANOVA).

forebrain nuclear extract that, in combination with the His-23Q, facilitate the interactions of proteins with the Dynabead-coupled CMV promoter. The ratio of the optical density of proteins that interacted with the Dynabead-coupled CMV promoter in the presence of His-87Q to His-23Q was approximately 0.8 in the presence of active HeLa nuclear extract and approximately 0.6 in the presence of active HeLa nuclear extract supplemented with wild-type forebrain nuclear extract. This implied that factors present in the wild-type forebrain nuclear extract enhanced the effects of the expanded polyglutamine region in His-87Q on the proteins that interacted with the Dynabead-coupled CMV promoter.

The effects of His-87Q on the proteins that interact with the Dynabead-coupled CMV promoter could be caused by changes in the rate of formation or the stability of these protein complexes. If the effects of His-87Q were due to a reduction in the rate of formation of the protein complexes, the difference in the amount of interacting protein would be greatest at early incubation times and become more similar to levels observed in the presence of His-23Q as the incubation time increased. However, increasing the preincubation time from 5, 10, 20 and 30 min did not alter the effect of the His-87Q on the proteins that interacted with the Dynabead-coupled CMV promoter in the presence of active HeLa nuclear extract supplemented with wild-type forebrain nuclear extract (Fig. 5-12A). The optical density of proteins from active HeLa nuclear extract supplemented with wild-type forebrain nuclear extract that interacted with the Dynabead-coupled CMV promoter after 5, 10, 20 and 30 min in the presence of His-87Q or His-23Q were measured. At each time point, the relative ratio of proteins that interacted with the Dynabead-coupled CMV promoter in the presence of His-87Q to His-23Q were constant

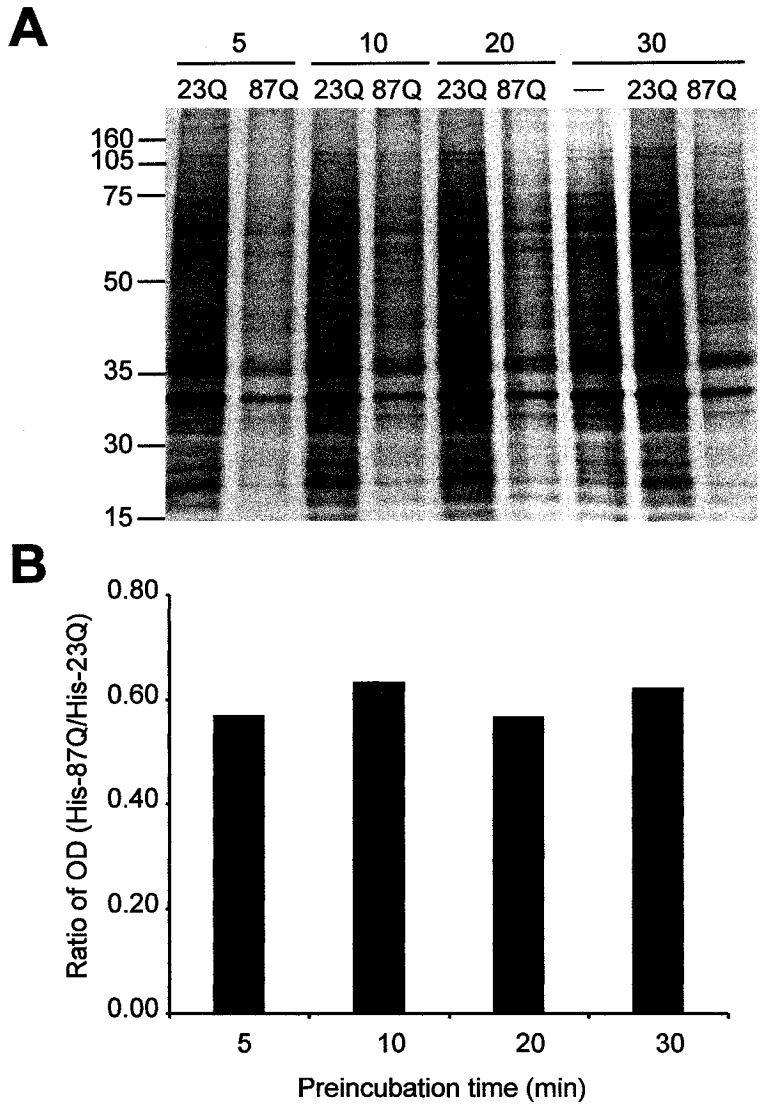

Figure 5-12. The effect of His-87Q were due to changes in the stability of the protein complexes rather than changes in the rate of formation of the protein complexes. Proteins from wild-type forebrain nuclear extracts in the presence of HeLa nuclear extract (—), or with HeLa nuclear extract supplemented with 5 pmol of His-23Q (23Q)/His-87Q (87Q), that interact with the Dynabead-coupled CMV promoter in 5, 10, 20 and 30 minutes were isolated, separated on a 7.5% SDS-PAGE gel and then silver-stained (A). The relative mobility of the Full Range Rainbow™ Molecular Weight markers are indicated to the left of the panel. The numbers above the panel indicate the incubation time in minutes. The ratio of the mean OD (His-87Q/His-23Q) of the isolated proteins after 5, 10, 20 and 30 minutes incubations are shown in panel B.

at approximately 0.6 (Fig. 5-12B). This indicated that the effects of His-87Q were caused by changes in the stability of the protein complexes rather than changes in the rate of formation of the protein complexes on the Dynabaead-coupled CMV promoter. His-87Q decreased the amount of proteins that interacted with the Dynabead-coupled CMV promoter in a dose-dependent manner. Increasing concentrations of His-87Q from 0.1, 0.5, 1.0 and 1.5 pmol decreased the amount of proteins isolated from the Dynabead-coupled CMV promoter compared to dose-matched His-23Q. The maximum effect on the proteins from the active HeLa nuclear extract supplemented with wild-type forebrain nuclear extract that interacted with the Dynabead-coupled CMV promoter was observed at 1.0 pmol of His-87Q (Fig. 5-13A). Addition of 1.0 pmol of His-87Q, compared to 1.0 pmol of His-23Q decreased the amount of transcript produced in *in vitro* transcription reactions from the CMV promoter in the presence of transcriptionally active HeLa nuclear extract supplemented with 5 μg of wild-type forebrain nuclear extract (Fig. 5-13B). This provided further evidence that the effects of His-87Q on the amount of proteins that interacted with the Dynabead-coupled CMV promoter were associated with the decrease in transcripts generated in the *in vitro* transcription reactions.

We demonstrated that His-87Q decreased *in vitro* transcription products generated from the CMV promoter and also decreased the amount of proteins that interacted with the Dynabead-coupled CMV promoter when incubated with active HeLa nuclear extract supplemented with wild-type forebrain nuclear extract. We then wanted to determine if His-23Q and His-87Q were part of the protein complexes that interact with the Dynabead-coupled CMV promoter. We isolated proteins from active HeLa nuclear extract supplemented with wild-type forebrain nuclear extract that interacted with the

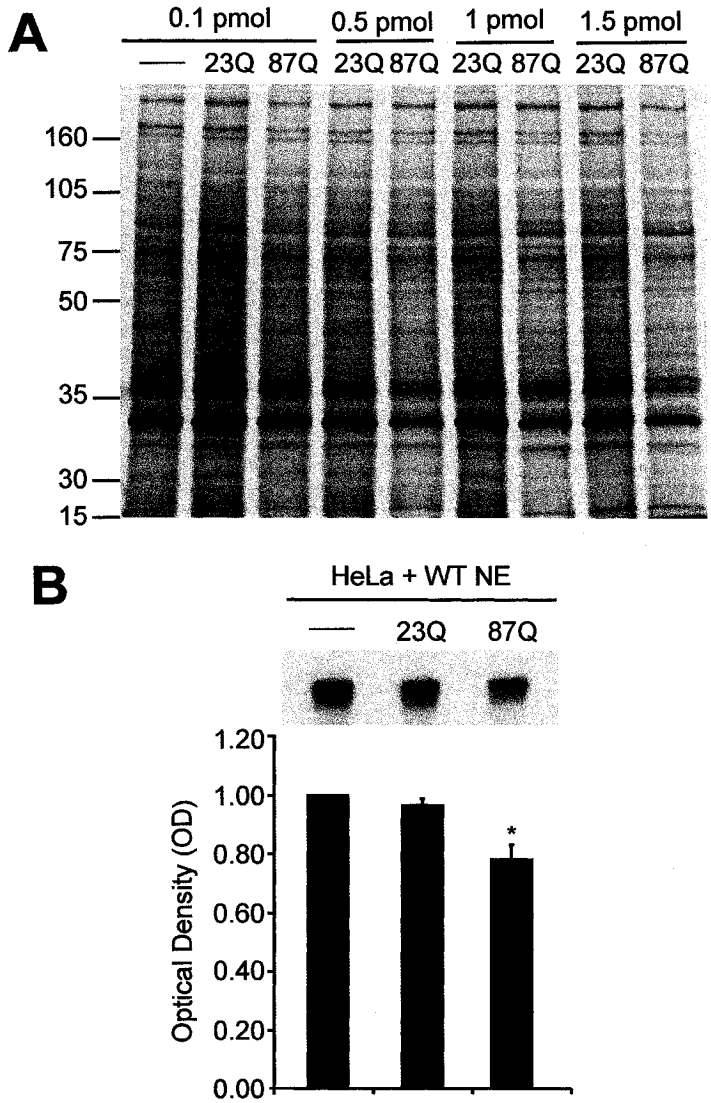

Figure 5-13. The presence of His-87Q decreased *in vitro* transcription of the CMV promoter in the presence of HeLa nuclear extract and 5 µg of wild-type forebrain nuclear extract. Proteins from wild-type forebrain nuclear extracts in the presence of HeLa nuclear extract (—), or HeLa nuclear extract supplemented with 0.1, 0.5, 1.0 or 1.5 pmol of His-23Q (23Q) or His-87Q (87Q), that interact with the Dynabead-coupled CMV promoter were isolated, separated on a 7.5% SDS-PAGE gel and then silver-stained (A). The relative mobility of the Full Range Rainbow™ Molecular Weight markers are indicated to the left of the panel. Panel B shows a representative autoradiogram of the 363 nt product generated from *in vitro* run-off transcription of the CMV promoter in the presence of HeLa nuclear extract and 5 µg of wild-type (WT) forebrain nuclear extracts (NE) alone (—), or with 1.0 pmol of His-23Q (23Q) or His-87Q (87Q). The histogram shows the mean optical density (± SEM, n=4) of the amount of transcription product produced normalized to the optical density of the product obtained in the presence of HeLa nuclear extract and 5 µg of wild-type forebrain nuclear extract. $*P < 0.05$, significant difference between the amount of CMV transcription product formed in the presence of 1.0 pmol of His-23Q (one-way ANOVA).

Dynabead-coupled CMV promoter and performed western analysis using the anti-histidine antibody to detect the histidine-tagged His-23Q and His-87Q fusion proteins (Fig. 5-14). The recombinant histidine-tagged His-23Q and His-87Q proteins were detected at 28 kDa and 38 kDa, respectively. This antibody also recognized a 75 kDa band in the lane containing purified His-87Q recombinant protein. This band could be attributed to dimerization of His-87Q proteins. This antibody also detected several other bands 40, 45, and 63 kDa in the lanes containing the proteins that interacted with the Dynabead-coupled CMV promoter in the presence of active HeLa nuclear extract supplemented with wild-type forebrain nuclear extract. These bands were also detected when His-23Q or His-87Q was added to these reactions. These three bands, therefore, are contained within HeLa or wild-type mouse extract and react with the anti-Histidine antibody. The 40 and 45 kDa bands were more abundant in HeLa and wild-type forebrain nuclear extracts containing either His-23Q or His-87Q. The band at 81 kDa was only detected in the lanes containing proteins from the HeLa and wild-type nuclear extract that interacted with the Dynabead-coupled CMV promoter in the presence of either His-23Q or His-87Q. This indicated that both His-23Q and His-87Q facilitated the interaction of these 40, 45 and 81 kDa proteins with the Dynabead-coupled CMV promoter. The band at 43 kDa was only detected in the lane containing the proteins from HeLa and wild-type nuclear extracts that interacted with the Dynabead-coupled CMV promoter in the presence of His-23Q. This implied that His-23Q facilitated the interaction of this protein with the Dynabead-coupled CMV promoter. We also detected His-23Q (28 kDa) and His-87Q (38 kDa) in the proteins that interacted with the Dynabead-coupled CMV promoter in the presence of active HeLa nuclear extract

supplemented with wild-type nuclear extract (Fig. 5-14). This indicated that both His-23Q and His-87Q were directly involved in the protein complexes that interacted with the Dynabead-coupled CMV promoter in the presence of HeLa and wild-type forebrain nuclear extract.

5.3 Discussion

We had previously determined that the N-terminal fragment of mutant huntingtin decreased transcription of the DARPP-32 and ppENK genes, but not the HPRT gene, *in vivo* and in cell culture models (Chapter 4). We had also determined that this decrease in transcription was an intracellular effect of the amino-terminus of mutant huntingtin (Chapter 4). However, it had yet to be determined whether N89-115Q directly affects transcription or alters the amount or state of other proteins that control expression of the DARPP-32 and ppENK promoters. Since N89-115Q affects transcription of the DARPP-32 promoter in a tissue-specific manner, we proposed that there was either a specific factor present in the brain that rendered the DARPP-32 promoter sensitive to N89-115Q, or a factor present in the kidney that protected DARPP-32 transcription from the effects of N89-115Q. To test these possibilities, we sought to develop an *in vitro* model of transcriptional repression induced by the amino-terminus of mutant huntingtin. In this *in vitro* system, the DARPP-32 promoter was weakly active and produced multiple low abundance transcripts. The HPRT promoter produced a distinct transcript at low levels *in vitro*. The ppENK promoter produced two distinct sized transcripts from two transcription start sites that could only be detected after an extended period of exposure of the gel to autoradiography film. This observation demonstrated that the ppENK

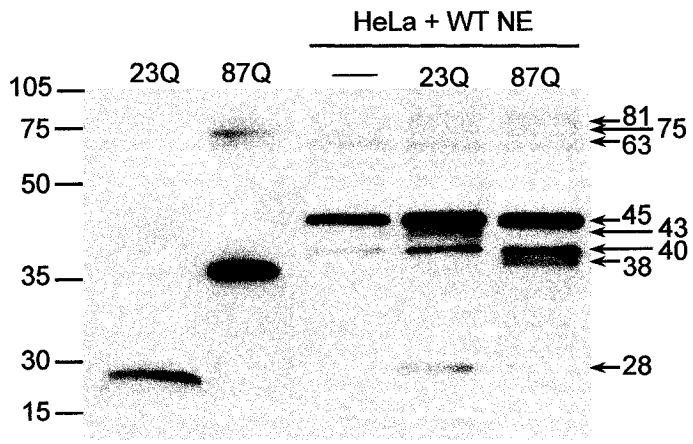

Figure 5-14. His-23Q and His-87Q proteins directly interacted with the Dynabead-coupled CMV promoter. Western blot analysis using an anti-histidine antibody is shown. 1.0 pmol of His-23Q (23Q) and His-87Q (87Q) were used as positive controls. Proteins from wild-type (WT) forebrain nuclear extracts in the presence of HeLa nuclear extract (—), or HeLa nuclear extract supplemented with 1.0 pmol of His-23Q (23Q) or His-87Q (87Q), that interact with the Dynabead-coupled CMV promoter were isolated, separated on a 7.5% SDS-PAGE gel, transferred to a membrane and probed with an anti-histidine antibody. Arrows and numbers to the right of the panel indicate bands of interest and their estimated molecular weight in kDa. The relative mobility of the Full Range Rainbow™ Molecular Weight markers are indicated to the left of the panel.

promoter was active *in vitro* from sites in proximity to those used *in vivo* but that the promoter was relatively weak *in vitro*. It is possible that upstream *cis*-elements or DNA conformation or both are needed to support transcription of the DARPP-32, ppENK and HPRT promoter *in* vitro. The DARPP-32, ppENK and HPRT promoters, therefore, could not be used as models in the adapted *in vitro* transcription system to examine the direct affect of the N-terminal fragment of mutant huntingtin on transcription. However, the CMV promoter was highly active in the *in vitro* transcription system and produced large amounts of transcripts from a single transcription start site. The CMV promoter was also affected by the stable expression of the N-terminus of mutant huntingtin in N548mu cells and by the transient expression of N89-115Q in ST14A cells. This provided us with a model promoter that we could use to study the effects of the amino-terminus of mutant huntingtin *in vitro*.

In vitro transcription from the CMV promoter was directly affected by the addition of nuclear extracts isolated from the R6/1 mice. The presence of 5 or 10 μg of forebrain nuclear extract from wild-type and R6/1 mice increased the activity of the HeLa nuclear extract to drive transcription of the CMV promoter but did not alter transcription start site selection demonstrating that these extracts contain proteins that enhanced the basal transcription provided by the active HeLa nuclear extract. When larger amounts of R6/1 nuclear extract were added to the *in vitro* transcription reaction, the amount of CMV-dependent product produced in the reaction was reduced compared to the levels of products produced in the presence of equivalent amounts of wild-type extract. Furthermore, adding kidney nuclear extracts to the system did not alleviate the repression on the transcriptional activity of the HeLa nuclear extract. This provides preliminary

evidence that a specific factor present in the brain renders the cells sensitive to N89-115Q rather than a kidney-specific factor that protects the cells from the effects of N89-115Q. These data also support the hypothesis that the transcriptional activity of this promoter is enhanced by a factor present in the forebrain extracts isolated from wild-type and R6/1 mice and that a second factor, which is present in extracts isolated from R6/1 mice, acts as a repressor. Increasing concentrations of wild-type nuclear extract did not increase the enhancement of the transcriptional activity of the CMV promoter suggesting that the maximal rate of HeLa-driven transcription had been reached or that factor(s) present in the nuclear extracts that enhanced the activity of the HeLa extract were at saturating concentrations. However, adding increasing levels of R6/1 forebrain nuclear extract repressed transcription to about 20% of the transcripts produced in reactions containing HeLa and wild-type forebrain nuclear extract. This suggested, but did not prove, that increasing the levels of the amino terminus of human huntingtin with 150 CAG repeats had a dose-dependent effect on transcription.

Currently there are several models that have been proposed to explain the transcriptional dysregulation observed in HD. It has been proposed that mutant huntingtin interacts with specific transcription factors, like Sp1, which are then incapable of binding to the promoter and enhancing the activity of the basal transcription machinery (Dunah *et al.*, 2002; Li *et al.*, 2002; Sugars & Rubinsztein, 2003). It has also been hypothesized that mutant huntingtin may interact with factors of the transcriptional complex, like CBP, that normally co-activate transcription by providing a protein bridge between specific transcription factors that bind DNA upstream of the core promoter and the basal transcriptional machinery (Kazantsev *et al.*, 1999; Steffan *et al.*, 2000; Sugars &

Rubinsztein, 2003). Yet another hypothesis is that the amino-terminus of mutant huntingtin interacts with components of the RNA polymerase II basal transcriptional machinery, like TFIID and TFIIF, sequesters these essential components and inhibits transcriptional activation (Dunah *et al.*, 2002; Zhai *et al.*, 2005; Luthi-Carter & Cha, 2003). Each of the hypotheses has limitations. For example, the transcription of the β-actin and HPRT genes are not affected by truncated N-terminal fragments of mutant huntingtin. However, both these promoters have potential Sp1 binding sites as do numerous promoters expressed in the brain and throughout tissues in the body. If the N-terminus of mutant huntingtin interacts with specific transcription factors, like Sp1 and CBP, which are widely expressed and involved in the regulation of a large number of genes, it is hard to explain the gene-specific effects of mutant huntingtin. The transcription factor TFIIF is a component of the core transcriptional machinery and is comprised of a heterodimer comprised of RNA polymerase II associating protein 30 (RAP30) and 74 (RAP74). It plays an important role in recruiting RNA polymerase II during preinitiation complex formation (Conaway *et al.*, 1991; Flores *et al.*, 1991; Orphanides *et al.*, 1996). Chromatin immunoprecipitation analysis showed a decrease in RAP30 levels on the dopamine D_2 receptor 2 (D_2) promoter and the ppENK promoter, which are known to be affected by N89-150Q, but not on the NMDA receptor 1 (NR1) promoter, which is not affected by N89-150Q in 10 week-old R6/2 mice when compared to their age-matched littermates (Zhai *et al.*, 2005). However, there is no difference in the RAP30 occupancy of the GAPDH promoter, which is known to be affected by N89-150Qin R6/2 transgenic HD mice (Luthi-Carter *et al.*, 2002a; McCaw *et al.*, 2004). It has been hypothesized that N89-150Q interacts with free RAP30 subunits, thereby competing

with its interaction with RAP74, and thus interferes with the formation of the active TFIIF. The transcription factor TFIID, another component of the core transcriptional machinery, contains various TBP-associating factors like $TAF_{II}130$. This protein is known to interact with the N-terminal fragment of mutant huntingtin (Dunah *et al.*, 2002) and the over expression of this transcription factor results in a rescue of the transcriptional repression of the amino-terminus of mutant huntingtin. However, if these components of the core basal transcriptional machinery are affected by the N-terminus of mutant huntingtin we would expect transcription from all genes including HPRT, β-actin and TK to be affected. Current hypotheses on the mechanism by which the N-terminual fragment of mutant huntingtin alters transcription focuses on interactions between mutant huntingtin and various transcription factors (Luthi-Carter & Cha, 2003; Sugars & Rubinsztein, 2003). However, there was no common transcription factor binding sites present on promoters like DARPP-32 and ppENK that were affected by the N-terminual fragment of mutant huntingtin that were absent from other non-affected promoters such as β-actin and HPRT. Furthermore, it has not yet been determined which aspect of the transcription cycle is affected by the presence of the N-terminal fragment of mutant huntingtin.

The assembly of the preinitiation complex is the first step in the transcription cycle. Therefore, we wanted to determine if the amino-terminus of mutant huntingtin altered this first step of transcription. We allowed the preinitiation complexes to form but did not allow initiation and elongation to occur. Initiation and elongation were blocked because we did not add rNTPs that are the necessary substrate for RNA synthesis and provide the ATP energy source to drive the reaction (Sawadogo & Roeder, 1984; Luse &

Jacob, 1987). We observed that there was no difference in the complexity of the proteins or the amount of proteins that interacted with the Dynabead-coupled CMV promoter in the presence of inactive wild-type or R6/1 forebrain nuclear extract. However, there was a decrease in the proteins that interacted with the Dynabead-coupled CMV promoter in the presence of active HeLa nuclear extract supplemented with R6/1 nuclear extract compared to wild-type nuclear extract. There was no difference in the complexity of proteins that interacted with the CMV promoter in the presence of active HeLa nuclear extract supplemented with either wild-type or R6/1 forebrain nuclear extract. The R6/1 nuclear extract contained factor(s) that altered the stability of HeLa proteins that interacted with the Dynabead-coupled CMV promoter.

N89-115Q in conjunction with a factor present in forebrain nuclear extract could directly alter the stability of the preinitiation complex formed and thus reduce the rate of transcription. Alternatively, it is also possible that N89-115Q modifies the abundance or state of a factor present in the mouse forebrain cells prior to the isolation of forebrain nuclear extract and that this factor then interferes with the formation of the preinitiation complex. Addition of the purified N-terminal fragment of mutant huntingtin (His-87Q) to the *in vitro* transcription system decreased the ability of active HeLa nuclear extract supplemented with wild-type forebrain nuclear extract to transcribe the CMV promoter. This indicated that N89-115Q in conjunction with a factor(s) present in forebrain tissue exerted its effects on *in vitro* transcription. The presence of His-87Q also decreased the stability of the proteins from the active HeLa nuclear extract that interacted with the Dynabead-coupled CMV promoter. This effect of His-87Q on the stability of the proteins that interacted with the Dynabead-coupled CMV promoter was enhanced when

HeLa nuclear extract was supplemented with wild-type forebrain nuclear extract. The effects of His-87Q on the stability of the proteins that interacted with the Dynabead-coupled CMV promoter could be correlated with the effects of His-87Q on transcription from the CMV promoter.

The presence of His-23Q increased the proteins from HeLa nuclear extract supplemented with wild-type nuclear extract that interacted with the Dynabead-coupled CMV promoter. This suggests that wild-type huntingtin increased the stability of proteins from the HeLa nuclear extract supplemented with wild-type forebrain nuclear extract that interacted with the Dynabead-coupled CMV promoter. This could be correlated with the observed increase in transcription from the CMV promoter in ST14A cells that transiently express wild-type huntingtin. Addition of His-23Q to the *in vitro* transcription reactions did not increase the ability of active HeLa nuclear extract supplemented with wild-type forebrain nuclear extract to transcribe the CMV promoter. However, it should be noted that the *in vitro* transcription reactions were performed in the presence of 5 μg of wild-type forebrain nuclear extract and it had been suggested earlier that the maximal rate of HeLa-driven transcription may have been reached after the addition of 5 μg of forebrain extract.

His-87Q could alter the stability of the preinitiation complex directly by being a part of the proteins that interact with the CMV promoter or indirectly by interacting with factors that are part of the preinitiation complex, rendering them inactive. His-87Q renders the factor from the preinitiation complex inactive by sequestering them or by altering the phosphorylation, acetylation or methylation state of the protein. Western blot analysis indicated that both His-23Q and His-87Q interacted with the Dynabead-coupled

CMV promoter. The presence of His-23Q and His-87Q enhanced the binding of specific proteins from the HeLa nuclear extract supplemented with wild-type nuclear extract to the Dynabead-coupled CMV promoter. This implies the both His-23Q and His-87Q are part of the preinitiation complex that forms on the Dynabead-coupled CMV promoter. His-23Q may directly interact with the Dynabead-coupled CMV promoter to enhance the stability of the proteins that form the preinitiation complex. This stabilized preinitiation complex could then be associated with the observed increase in transcription. Therefore, the observed decrease in the stability of the proteins that interact with the Dynabead-coupled CMV promoter and the potentially associated decrease in transcription could be attributed to the expanded polyglutamine region of the His-87Q protein.

Our data does not support the proposed sequestration models of mutant huntingtin. If the N-terminal fragment of mutant huntingtin was sequestering specific proteins away from the preinitiation complex, we would have also observed changes in the complexity of proteins that interacted with the Dynabead-coupled CMV promoter in the presence of wild-type or R6/1 forebrain nuclear extract. Furthermore, we have shown that the N-terminal fragment of mutant huntingtin itself is part of the preinitiation complex and alters the stability of proteins that form that complex. Therefore, we propose that the decrease in RAP30 occupancy on the D_2 and the ppENK promoters in R6/2 mice observed by Zhai *et al.* (2005) could be attributed to a decrease in the stability of the preinitiation complex at these promoters rather than sequestration of the RAP30 protein by the amino-terminual fragment of mutant huntingtin.

CHAPTER 6

Conclusion

6.1 General Discussion

A decrease in transcript levels of selected genes such as ppENK, DARPP-32, CB1, PDE10A and mGluR1 occurs prior to the earliest documented appearance of NIIs (DiFiglia *et al.*, 1997; Becher *et al.*, 1998; Hansson *et al.*, 2001), activation of caspases (Ona *et al.*, 1999; Chen *et al.*, 2000; Li *et al.*, 2000) and motor deficits (Mangiarini *et al.*, 1996; Carter *et al.*, 1999; Hansson *et al.*, 2001) in various transgenic HD mouse models and in the brain of HD patients. All of these changes occur prior to the wide-spread neurodegeneration of medium spiny projection neurons in the caudate and putamen that is a hallmark of HD (Davies *et al.*, 1997; Cha *et al.*, 1998; Carter *et al.*, 1999; Luthi-Carter *et al.*, 2000; Turmaine *et al.*, 2000; Luesse *et al.*, 2001; Hu *et al.*, 2004; McCaw *et al.*, 2004; Desplats *et al.*, 2006; Hodges *et al.*, 2006). Furthermore, positron emission tomography studies of patients that carry the HD gene but are clinically asymptomatic demonstrate that D_1 and D_2 receptors are decreased prior to the onset of symptoms (Andrews *et al.*, 1999). Some of the changes in gene expression may lead to secondary effects that are observed. Caspase-1 mRNA levels increase in 7 week-old R6/2 mice and as the disease progresses increases in caspase-3 mRNA are observed in 9 week-old mice (Chen *et al.*, 2000). Furthermore, mRNA levels of PGC-1α a transcriptional co-activator that regulates several metabolic processes including mitochondrial biogenesis and oxidative respiration (Puigserver & Spiegelman, 2003) is decreased in human HD brains, knock-in HD mouse models and in cell culture models of HD (Cui *et al.*, 2006). In the caudate nucleus of post-mortem human HD brains steady-state mRNA levels of 24 out of 26 PGC-1α target genes are reduced (Weydt *et al.*, 2006). Collectively, these data suggest that the decrease in steady-state mRNA levels of PGC-1α may cause

mitochondrial dysfunction observed in HD (McGill & Beal, 2006). Thus, the initial changes in gene expression may eventually lead to secondary changes that cause neuronal dysfunction and ultimately cell death. Mutant huntingtin may be directly responsible for the earliest changes in transcript levels, however, the mechanism by which that occurs has not yet been clearly defined.

The N-terminal fragments of mutant huntingtin in the R6 transgenic HD mice are known to accumulate in the nucleus (Davies *et al.*, 1997; DiFiglia *et al.*, 1997; Hackam *et al.*, 1998). These fragments include the first 17 amino acids of the huntingtin protein, the polyglutamine region (R6/1, N89-115Q; R6/2, N89-150Q) as well as the polyproline region. The first 17 amino acids contain the nuclear localization signal. It is known that the polyglutamine region and the polyproline region are involved in various protein-protein interactions (Sipione & Cattaneo, 2001; Li & Li, 2004). This is the smallest fragment of the huntingtin protein that is known to cause a decrease in the steady-state mRNA levels of specific genes. In humans, a larger N-terminal fragment containing the first 522 amino acids of huntingtin is present in the nucleus (Wellington *et al.*, 2002). The longer N-terminal fragment of mutant huntingtin in humans may confer additional cell- and tissue-specificity compared to the first 89 amino acids included in the R6 transgene.

N89-115Q affects transcription *in vivo* (Chapter 4 and Hu *et al.*, 2004; McCaw *et al.*, 2004) , in different cell culture models of HD (Chapter 4 and Dunah *et al.*, 2002; Li *et al.*, 2002; Cui *et al.*, 2006)) and *in vitro* (Chapter 5 and Zhai *et al.*, 2005). These observations indicated that the effects of N89-115Q on transcription were due to intracellular effects of the mutated protein rather than the effect of interneuronal

signaling. Moreover, the addition of purified N-terminal fragment of the mutant huntingtin protein altered both transcription and preinitiation complex formation *in vitro* (Chapter 5 and Zhai *et al.*, 2005) demonstrating that the amino-terminus of the mutant huntingtin protein and not the mutant huntingtin mRNA affected transcription. Generally, the mRNA and protein of mutant huntingtin are co-expressed in any cell-based system and, although, it has been assumed that the protein is causal to HD, it is known that nucleotide repeat diseases such as muscular dystrophy are caused by the presence of highly structured RNA (Ranum & Cooper, 2006).

There are several neurodegenerative diseases caused by expanded CAG repeat-encoded polyglutamine regions in proteins that are expressed in the brain. Each of these neurodegenerative disorders have a characteristic pattern of loss of neurons within specific regions of the brain and spinal cord depending on the protein that contains the expanded polyglutamine region (Ross, 1995a). Expanded polyglutamine tracts, in the absence of flanking protein sequence, can localize to the nucleus (Preisinger *et al.*, 1999). The constituents of the nuclear inclusions formed by the amino terminus of huntingtin with an expanded polyQ region and the specific pattern of neurodegeneration are dependent on the protein context of the polyglutamine region within the amino terminus of huntingtin (Chai *et al.*, 2001). Similarly, in the present study, we showed that the effects of the N-terminal fragment of mutant huntingtin on transcription in stably and transiently transfected immortalized striatal cells and in *in vitro* transcription assays were due to the expanded polyglutamine region in the context of the N-terminal fragment of the mutant huntingtin protein.

Soluble N-terminal fragment so mutant huntingtin rather than insoluble aggregates alters transcription. The addition of soluble recombinant N-terminal fragments of mutant huntingtin proteins decreased transcription in the *in vitro* transcription assay (Chapter 5 and Zhai *et al.*, 2005). This implies that transcriptional dysregulation occurs prior to the formation of insoluble aggregates. Similarly, DARPP-32 and ppENK mRNA levels *in vivo* start to decrease prior to when NIIs can be visualized in the R6/1 transgenic HD mice (Chapter 3). Furthermore, in the *in vitro* transcription assays increasing the concentration of soluble N-terminal fragments of mutant huntingtin present in the system increased the repression on transcription. *In vivo* it appears that after the initial decrease in transcript levels, DARPP-32 and ppENK continue to be expressed at lower steady-state levels (Chapter 5 and Zhai *et al.*, 2005). It is possible that following the initial accumulation of soluble N89-115Q in the nucleus, insoluble aggregates appear and increase in size while the levels of newly produced soluble N89-115Q in the nucleus remains constant.

N89-115Q altered transcription in a tissue-specific manner. Microarray analysis has shown decreases in transcript levels in different areas of the brain such as the cerebral cortex, cerebellum and striatum as well as skeletal muscle tissue in R6 transgenic HD mice (Luthi-Carter *et al.*, 2000; Luthi-Carter *et al.*, 2002a; Desplats *et al.*, 2006). Transcription from the DARPP-32 promoter was decreased in the striatum and cortex of the brain, but not in the renal medulla of the kidneys of R6 transgenic HD mice. Steady-state transcript levels of PDE10A mRNA levels are decreased in the brain but are not changed in the testis of transgenic HD mice (Hebb *et al.*, 2004). This indicates that N89-115Q alters transcription throughout the brain and in select tissues in the periphery and

that the effect is not localized to the striatum. Even within the striatum, there may be important differences between cells that alter the effect of N89-115Q. For example, CB1 is expressed at low levels throughout the brain and at relatively high levels in the lateral striatum and in isolated cells of the cortex. It appears that N89-115Q decreases expression of CB1 in the lateral striatum and isolated cells of the cortex without altering the constitutive low level expression of CB1 in the remainder of cells in the brain (Denovan-Wright & Robertson, 2000). This cell-specific effect was also observed in *ex vivo* models of HD. The presence of transiently transfected N-terminal fragment of mutant huntingtin transcription from the full-length DARPP-32 promoter was altered in immortalized ST14A cells but not HEK293 cells. The addition of wild-type kidney nuclear extract to *in vitro* transcription assays containing R6/1 transgenic HD nuclear extracts did not alleviate the repression on the CMV promoter activity whereas the presence of wild-type nuclear extract enhanced the effects of purified recombinant His-87Q protein on transcription and on the proteins that interacted with the Dynabead-coupled CMV promoter. These observations strongly support the hypothesis that a factor(s) present in the brain acts in concert with N89-115Q to affect transcription.

N89-115Q alters transcription in a gene-specific manner. Transcription from the DARPP-32, ppENK and CMV promoters were decreased while transcription from the β-actin, HPRT and TK promoters were unaffected in transiently transfected cell culture models of HD. Similarly, expression of DARPP-32 and ppENK, but not β-actin and HPRT, were affected in R6 transgenic mice. The DARPP-32 and ppENK genes are constitutively expressed in the striatum and this constitutive expression is affected in HD. The ppENK promoter was affected to the same extent in both the R6/1 and R6/2

transgenic HD model independent of the length of the CAG repeat and the expression of the transgene. However, the effect of N89-115Q and N89-150Q on transcription from the DARPP-32 promoter was more rapid in the R6/2 transgenic HD mice than in the R6/1 transgenic HD mice indicating that the N-terminal fragment of mutant huntingtin altered transcription from this promoter in a manner that was dependent on either the length of the polyglutamine or the concentration of the transgene-encoded protein or both. Similarly, the effects of transcription from the CB1, PDE10A and PDE1B genes occurred more rapidly in the R6/2 transgenic HD mice when compared to the R6/1 transgenic HD mice (Hebb *et al.*, 2004; Hu *et al.*, 2004; McCaw *et al.*, 2004). The ppENK and CB1 transcript levels start to decline prior to DARPP-32 transcript levels (this study and McCaw *et al.*, 2004). In all cases where expression has been followed over time, the steady-state levels of these transcripts decrease in the R6 mouse model and eventually reached a new equilibrium. This demonstrated that the repression of transcription by the N-terminal fragment of mutant huntingtin had a maximum effect that reduced transcription but did not block it. For the ppENK and CB1 transcripts, that started to decline early, this level was ~ 30% of the levels observed in wild-type mice, while for the DARPP-32 promoter, the levels are ~ 40-50% of those in wild-type mice (this study and McCaw *et al.*, 2004). This indicated that selective genes may be more sensitive to the effects of mutant huntingtin. The relative effect of the N-terminal fragment of mutant huntingtin on the maximal repression of each promoter were also observed in stably and transiently transfected cell culture models of HD as the activity of the ppENK promoter was affected to a greater extent than the activity of the DARPP-32 promoter.

N89-115Q exerts its effects in a promoter-specific manner. The DARPP-32 gene has multiple transcription start sites that can be grouped into the proximal and distal transcription initiation regions (Blau *et al.*, 1995). N89-115Q altered levels of all transcripts that initiated from the proximal but not the distal transcription initiation region that are both utilized to express this message in the brain. The promoter-specificity of N89-115Q cannot be attributed to the presence or absence of a TATA box sequence. The CB1 and DARPP-32 promoters do not contain TATA boxes and are affected by N89-115Q, while the HPRT promoter does not contain a TATA box but is resistant to the effects of N89-115Q. The TATA-less PDE10A2 promoter expressed in the brain has three transcription start sites and two start sites are affected by the expression of N89-115Q (Hu *et al.*, 2004). N89-115Q alters activity of the ppENK promoter, which contains a TATA-box at 28 bp upstream of the -289 transcription start site (Fig. 4-5) and the CMV promoter, which also contains a defined TATA box. The β-actin gene contains a defined TATA box but the levels of β-actin remain constant in HD transgenic mice. Therefore, N89-115Q alters DARPP-32 and ppENK transcription in a promoter-specific manner although the basis for susceptibility or resistance of this and other promoters to the action of N89-115Q remains to be determined.

The N-terminus of mutant huntingtin was hypothesized to alter transcription by interacting with HATs leading to a decrease in histone acetylation of the histone proteins that contribute to the formation of chromatin (Steffan *et al.*, 2001). A decrease in histone acetylation could result in the observed decreases in transcription (Steffan *et al.*, 2001; Cong *et al.*, 2005; Sadri-Vakili & Cha, 2006). While chromatin plays a key role in regulation of transcription in general, in this study, the effects of the N-terminal fragment

of mutant huntingtin on transcription were observed on extrachromosomal plasmids in transient transfections of cell culture models of HD and on purified, linearized promoter fragments in *in vitro* transcription assays. In both models, the effects of the amino-terminus of mutant huntingtin on promoter activity were separate from the effects of chromatin structure and chromatin remodeling (Smith & Hager, 1997).

The interaction of proteins with the Dynabead-coupled CMV promoter was decreased in the presence of active HeLa nuclear extract supplemented with nuclear extract from R6/1 transgenic HD mice containing mutant huntingtin. We assume that the ratio of the amino terminus of mutant huntingtin to other nuclear proteins is the same as the ratio *in vivo*. This relative concentration of mutant huntingtin, therefore, is physiologically relevant. In the absence of transcriptionally-competent HeLa extract, there was no difference in the amount of proteins that could interact with the Dynabead-coupled CMV promoter when inactive nuclear extracts from wild-type and R6/1 transgenic HD mice were added. The complement of proteins that bound to the promoter in the absence of HeLa were not decreased by N89-115Q within the R6/1 nuclear extract. It appeared that HeLa proteins preferentially bound the promoter compared to the DNA-binding proteins present in the mouse nuclear extracts. Moreover, the effect of purified His-87Q on the proteins that interacted with the Dynabead-coupled CMV promoter was enhanced in the presence of wild-type forebrain nuclear extract. These observations suggest that the amino terminus of mutant huntingtin in combination with a factor(s) present in the active HeLa nuclear extract alters the stability of the proteins that interact with the Dynabead-coupled CMV promoter and this interaction is enhanced by a factor(s)

present in the forebrain nuclear extract and inhibited by the polyQ repeat within the context of the amino terminus of mutant huntingtin.

There are several models that have been proposed to explain the transcriptional dysregulation observed in HD. The amino terminus of mutant huntingtin could interact with various sequence-specific DNA-binding transcription factors, like Sp1 and TBP, sequester these proteins and render them incapable of binding to DNA resulting in a lack of activation of transcription and lower levels of mRNA (Fig. 6-1A and Huang *et al.*, 1998; Suhr *et al.*, 2001; Dunah *et al.*, 2002; Li *et al.*, 2002). Alternatively, it has been proposed that the amino terminus of mutant huntingtin may interact with transcriptional co-activators like CBP and PGC-1α, that act as co-activators, sequester these factors and render them incapable of acting as a bridge between the sequence-specific transcription factors and the core basal transcription machinery, which usually increases the rate of transcription (Fig. 6-1B and Steffan *et al.*, 2000; Nucifora *et al.*, 2001; Dunah *et al.*, 2002; Cui *et al.*, 2006). Another hypothesis is that the N-terminal fragments of mutant huntingtin interacts with individual components of the basal transcriptional machinery, like TFIIF, sequester these components and decreases the formation of an active basal transcriptional complex (Fig. 6-1C and Zhai *et al.*, 2005). Protein-protein interactions between RAP30 and the amino terminus of mutant huntingtin blocks the interaction between RAP30 and RAP74, which constitutes the TFIIF subunit (Zhai *et al.*, 2005). The TFIIF subunit interacts with the RNA Pol II and helps recruit the enzyme to the preformed TFIID/TFIIB complex (Dvir *et al.*, 2001). Therefore the interaction of the N-terminal fragments of mutant huntingtin with RAP30 would decrease the formation of the TFIIF general transcription factor. This would ultimately interfere with the recruitment

Figure 6-1. Current hypothesis for the possible role of the amino terminus of mutant huntingtin in transcriptional dysregulation. The amino terminus of mutant huntingtin interacts with various sequence-specific transcription factors, sequesters them and renders them incapable of binding to the DNA (A). Mutant huntingtin interacts with various co-activators, sequesters them and renders them incapable acting as a bridge between the sequence-specific activators and the core basal transcriptional machinery (B). Mutant huntingtin interacts with components of the core transcriptional machinery, sequesters them and interferes with the formation of the active basal transcriptional machinery (C). Mutant huntingtin itself interacts with DNA and interferes with the binding of various transcription factors (D).

A

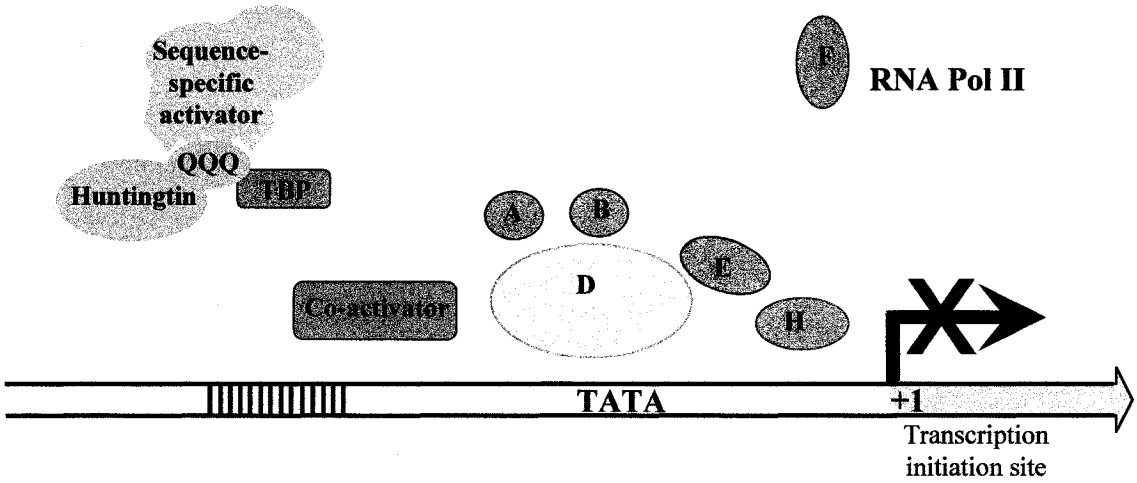
Sequence-specific activator
QQQ
Huntingtin
TBP
F
RNA Pol II
A
B
D
E
H
Co-activator
TATA
+1
Transcription initiation site

B

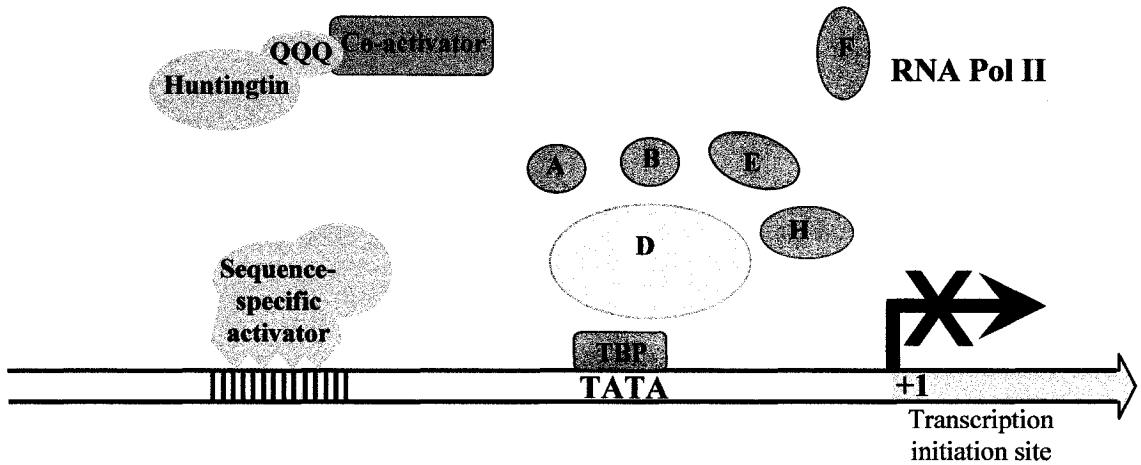
QQQ
Co-activator
Huntingtin
F
RNA Pol II
A
B
E
D
H
Sequence-specific activator
TBP
TATA
+1
Transcription initiation site

C

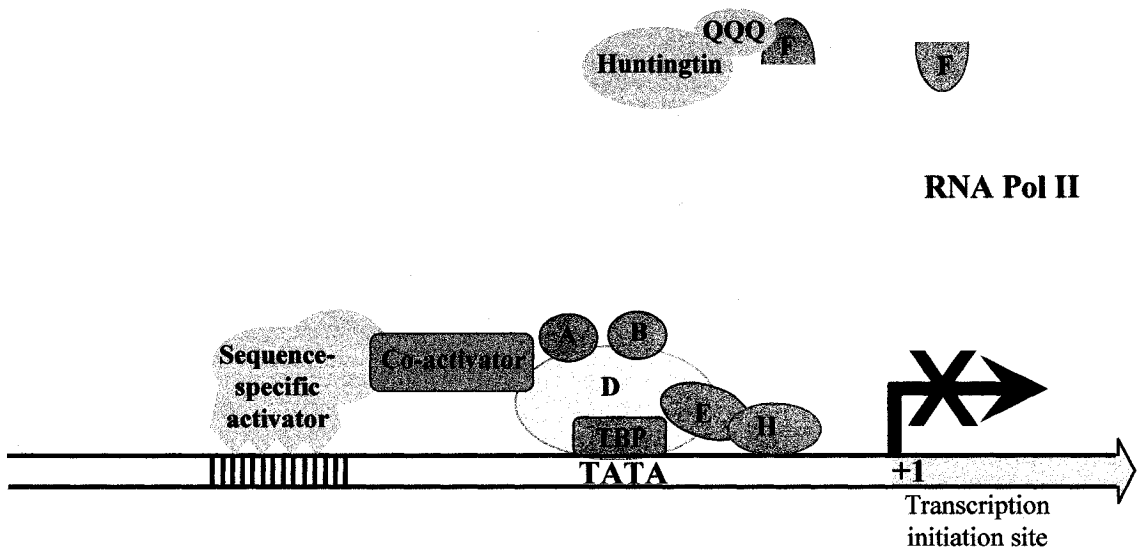
QQQ
Huntingtin
F
F
RNA Pol II
Sequence-
specific
activator
Co-activator
A
B
D
E
H
TBP
TATA
+1
Transcription
initiation site

D

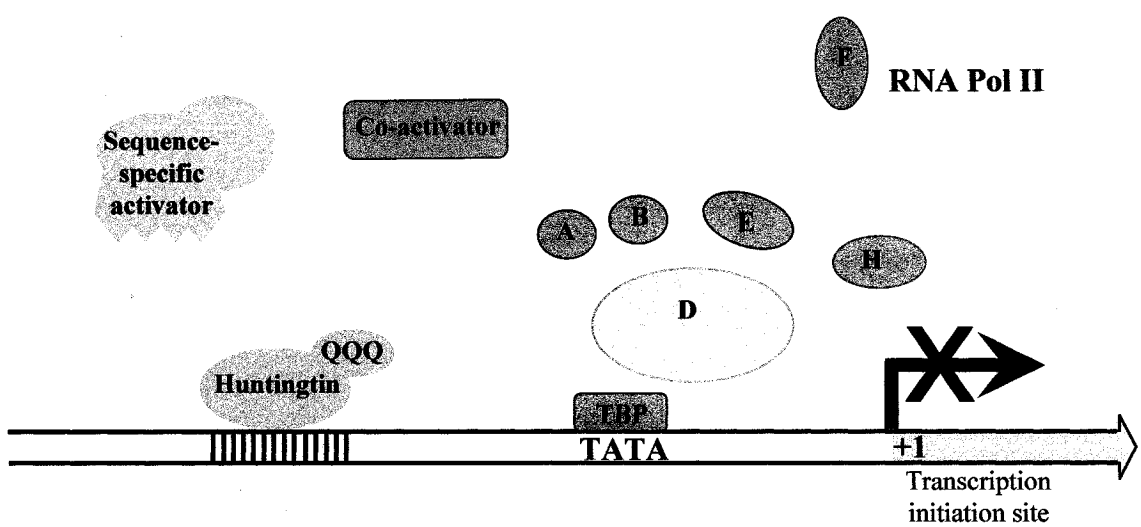
F
RNA Pol II
Sequence-
specific
activator
Co-activator
A
B
E
H
D
QQQ
Huntingtin
TBP
TATA
+1
Transcription
initiation site

of the RNA Pol II to the DNA to form the basal transcriptional complex. It has also been proposed that the amino-terminus of mutant huntingtin may itself interact with DNA and have a direct role as a transcription factor (Fig. 6-1D and Luthi-Carter & Cha, 2003).

Based on a large number of studies, the amino-terminus of mutant huntingtin can interact with many proteins that are involved in transcription and other cellular functions through protein-protein interactions (Sipione & Cattaneo, 2001; Harjes & Wanker, 2003; Li & Li, 2004). However, it is unclear which of these interactions occur *in vivo* or whether such interactions have been detected because the chemical properties of these interacting proteins allow for interactions during experimental manipulation. Furthermore, the presence of N89-115Q decreases the steady-state levels of a number of different genes in the striatum early in the progression of the disease (Augood *et al.*, 1996; Cha, 2000; Iannicola *et al.*, 2000; Luthi-Carter *et al.*, 2000; Luthi-Carter *et al.*, 2002a; Desplats *et al.*, 2006). However, it has not been determined if these changes are due to the direct effects of N89-115Q, or due to secondary compensatory changes. In order to determine if N89-115Q directly alters transcription and to aid in defining the mechanism by which this occurs, we developed an *in vitro* transcription assay system. Using this *in vitro* transcription assay we were able to study the effects of purified recombinant N-terminal mutant huntingtin protein and the effects of the mutant huntingtin protein in physiologically relevant concentrations from nuclear extracts of transgenic HD mice on transcription from promoters. Further modifications of this *in vitro* transcription assay will enable us to identify the proteins that directly interact with His-87Q in a functional system that recapitulates the effects of the amino-terminus of mutant huntingtin.

We propose that our data does not support the sequestration models or the model that the N-terminal fragments of mutant huntingtin itself interacts with DNA. We localized the effect to the smallest promoter fragments that had activity and did not find evidence that N89-115Q altered binding of proteins to DNA by sequestering factors away from the promoter, by increasing binding of repressor factors or acting directly as a DNA binding protein. Both His-87Q and His-23Q are components in the complex of proteins that interact with the Dynabead-coupled CMV promoter and their presence directly affects transcription and the stability of the protein-promoter interactions. Chromatin immunoprecipitation analysis on brain homogenates of wild-type and transgenic HD knock-in mice using an anti-huntingtin antibody indicated that the truncated N-terminal mutant huntingtin protein occupied the PGC-1α promoter region, while the presence of wild-type huntingtin on this promoter was not detected (Cui *et al.*, 2006). Therefore, it was recently proposed that the amino-terminus of mutant huntingtin associated with chromatin and interfered with the ability of sequence-specific transcription factors to activate transcription (Cui *et al.*, 2006). ChIP analysis cannot dissociate if the N-terminus of mutant huntingtin directly interacts with chromatin or interacts indirectly with chromatin by interacting with other DNA-binding proteins.

The presence of His-87Q does not completely stop transcription from the various promoters. It decreases the rate of transcription most likely by interfering with the formation of an active preinitiation complex. We did not observe any differences in the complex of proteins that interacted with the DNA in the presence of His-87Q. However, better resolution of these proteins may indicate unique factors from the forebrain nuclear extract that are present in these complexes, which enhance the effects of His-87Q. His-

87Q itself is a component in the complex of proteins that interacts with the DNA. This suggests that His-87Q may interact with factors in the preinitiation complex and alter the stability of the interaction of that protein complex with the DNA. His-87Q could interact with several components of the preinitiation complex. We hypothesize that the N-terminal fragments of mutant huntingtin may interact with sequence-specific activators and alter their activity, not by sequestering them away from the DNA, but by interfering with their interaction with various co-activators (Fig. 6-2). Because sequence-specific transcription factors recruit other proteins and RNA Pol II, interactions between His-87Q and these factors would decrease the frequency of the assembly of a competent transcription complex and result in lower levels of mRNA being produced. It is also possible that His-87Q may interact with co-activators that are assembled as part of the preinitiation complex. These co-activators act as a bridge between the sequence-specific activators and the basal transcriptional machinery, interactions between His-87Q and these factors could also destabilize the active transcriptional complex and result in a decrease in transcription. A third possibility is that His-87Q may interact with components of the basal transcriptional machinery and interfere with the formation of an active core basal transcriptional complex that has a stable interaction with the DNA. The three models proposed above take into account 1) the amino terminus of huntingtin is part of the preinitiation complex of proteins 2) the amino terminus of mutant huntingtin does not directly interact with DNA 3) specific factor(s) facilitates repression in the brain 4) factor(s) directs repression of specific promoters and 5) the expanded polyglutamine region in the N-terminus of mutant huntingtin destabilizes the complexes. Further comparisons of protein complexes isolated from the promoters of genes that are affected

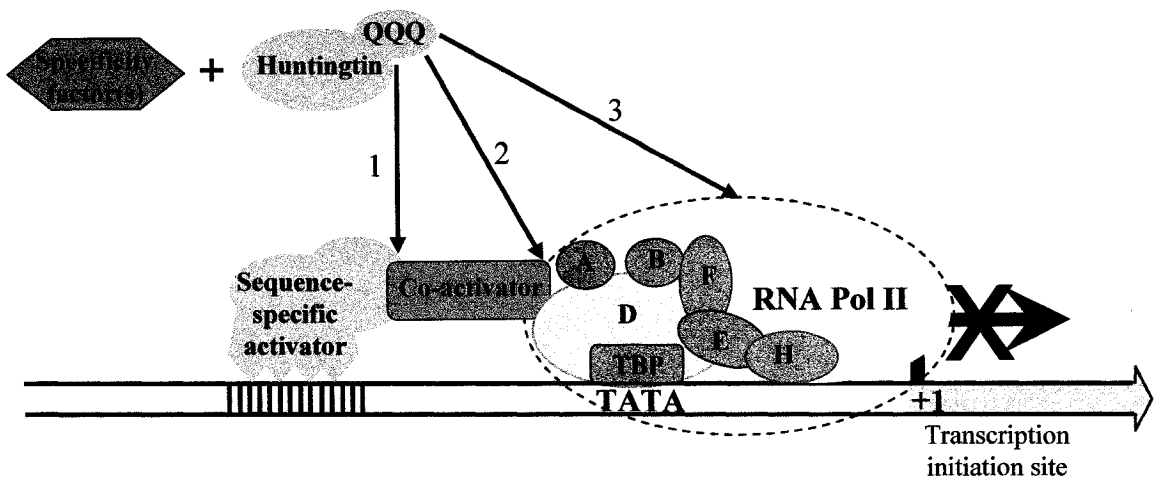

Figure 6-2. The possible role of amino terminus of mutant huntingtin in transcriptional dysregulation. The amino terminus of mutant huntingtin in combination with a factor(s) that confers tissue- and promoter-specificity (1) interferes with the interaction between the sequence-specific activators and the co-activators, (2) interferes with the interaction between the co-activator and components of the basal transcriptional machinery, or (3) interacts with components of the basal transcriptional machinery and inhibits the formation of the active core basal transcriptional complex.

and not affected by the N-terminus of mutant huntingtin in the presence of nuclear extract from different tissues would be required to reconcile the gene- and tissue-specific effects of the amino-terminus of mutant huntingtin.

6.2 Future Work

We have not yet identified the factor(s) present in the brain that confers the gene- and tissue-specific effects of the N-terminal fragment of mutant huntingtin. The *in vitro* assay that has been developed provides a system in which we can directly study the functional interactions of the N-terminus of mutant huntingtin and its effects on transcription. This *in vitro* assay can also be utilized to screen various compounds for their efficacy in alleviating the effects of the truncated N-terminal fragment of the mutant huntingtin protein on transcription. The *in vitro* assay provides a system in which we could analyze factors that could potentially block or even reverse the tissue-specific effects of truncated N-terminal fragment of mutant huntingtin on transcription.

The complement of proteins that interacted with the Dynabead-coupled CMV promoter was very complex. Differences in proteins that interact with the Dynabead-coupled CMV promoter in the presence of His-23Q and His-87Q were not observed on single dimension SDS-PAGE gels. However, two-dimensional SDS-PAGE gel analysis can be used to resolve differences in complex mixtures of proteins under different conditions (Issaq *et al.*, 2002). Conditions for two-dimensional SDS-PAGE analysis of proteins that interact with the Dynabeads have already been optimized (data not shown). Preliminary experiments indicate that sufficient protein can be obtained and resolved for comparison of the complexes that make up a functional transcription unit in the presence

of the amino terminus of huntingtin with and without an expanded polyglutamine region. Differences in proteins that interact with the Dynabead-coupled CMV promoter in the presence of His-23Q and His-87Q can be isolated and identified by mass spectrometry. Alternatively, proteins from the preinitiation complex formed on the Dynabead-coupled CMV promoter that interact directly with the His-87Q can be isolated using the Dynabead TALON™ (Invitrogen) technology. The Dynabead TALON™ magnetic beads can be used to isolate histidine-tagged His-87Q protein along with the proteins that interact with it. The isolated proteins can be resolved by two-dimensional SDS-PAGE analysis and identified by mass spectrometry. Both these approaches would enable us to identify factors from this subset of preinitiation complex proteins that interact directly with the amino terminus of mutant huntingtin and have a functional consequence *in vitro*. Once we identify huntingtin-interacting proteins that are components of a functional preinitiation complex, we can then observe how the amount of protein added to the *in vitro* system and in cell culture models alters the repressive effects of the N-terminus of mutant huntingtin on transcription from the CMV promoter. Furthermore, we could also observe the effects of over expressing the huntingtin-interacting proteins on other genes in cell culture models and *in vivo*. This would allow us to define how the amino terminus of mutant huntingtin selectively alters transcription of a small number of genes in specific tissues.

REFERENCES

Albin, R.L., Young, A.B., Penney, J.B., Handelin, B., Balfour, R., Anderson, K.D., Markel, D.S., Tourtellotte, W.W. & Reiner, A. (1990) Abnormalities of striatal projection neurons and N-methyl-D-aspartate receptors in presymptomatic Huntington's disease. *N Engl J Med*, **322**, 1293-1298.

Albin, R.L., Qin, Y., Young, A.B., Penney, J.B. & Chesselet, M.F. (1991) Preproenkephalin messenger RNA-containing neurons in striatum of patients with symptomatic and presymptomatic Huntington's disease: an in situ hybridization study. *Ann Neurol*, **30**, 542-549.

Albin, R.L. & Greenamyre, J.T. (1992) Alternative excitotoxic hypotheses. *Neurology*, **42**, 733-738.

Albright, S.R. & Tjian, R. (2000) TAFs revisited: more data reveal new twists and confirm old ideas. *Gene*, **242**, 1-13.

Altar, C.A., Cai, N., Bliven, T., Juhasz, M., Conner, J.M., Acheson, A.L., Lindsay, R.M. & Wiegand, S.J. (1997) Anterograde transport of brain-derived neurotrophic factor and its role in the brain. *Nature*, **389**, 856-860.

Ambrose, C.M., Duyao, M.P., Barnes, G., Bates, G.P., Lin, C.S., Srinidhi, J., Baxendale, S., Hummerich, H., Lehrach, H., Altherr, M. & et al. (1994) Structure and expression of the Huntington's disease gene: evidence against simple inactivation due to an expanded CAG repeat. *Somat Cell Mol Genet*, **20**, 27-38.

Andrade, M.A. & Bork, P. (1995) HEAT repeats in the Huntington's disease protein. *Nat Genet*, **11**, 115-116.

Andrews, T.C., Weeks, R.A., Turjanski, N., Gunn, R.N., Watkins, L.H., Sahakian, B., Hodges, J.R., Rosser, A.E., Wood, N.W. & Brooks, D.J. (1999) Huntington's disease progression. PET and clinical observations. *Brain*, **122 (Pt 12)**, 2353-2363.

Antonini, A., Leenders, K.L., Spiegel, R., Meier, D., Vontobel, P., Weigell-Weber, M., Sanchez-Pernaute, R., de Yebenez, J.G., Boesiger, P., Weindl, A. & Maguire, R.P. (1996) Striatal glucose metabolism and dopamine D_2 receptor binding in asymptomatic gene carriers and patients with Huntington's disease. *Brain*, **119 (Pt 6)**, 2085-2095.

Aronin, N., Chase, K., Young, C., Sapp, E., Schwarz, C., Matta, N., Kornreich, R., Landwehrmeyer, B., Bird, E., Beal, M.F. & et al. (1995) CAG expansion affects the expression of mutant Huntingtin in the Huntington's disease brain. *Neuron*, **15**, 1193-1201.

Arrasate, M., Mitra, S., Schweitzer, E.S., Segal, M.R. & Finkbeiner, S. (2004) Inclusion body formation reduces levels of mutant huntingtin and the risk of neuronal death. *Nature*, **431**, 805-810.

Asher, S.W. & Aminoff, M.J. (1981) Tetrabenazine and movement disorders. *Neurology*, **31**, 1051-1054.

Augood, S.J., Faull, R.L. & Emson, P.C. (1997) Dopamine D1 and D2 receptor gene expression in the striatum in Huntington's disease. *Ann Neurol*, **42**, 215-221.

Augood, S.J., Faull, R.L., Love, D.R. & Emson, P.C. (1996) Reduction in enkephalin and substance P messenger RNA in the striatum of early grade Huntington's disease: a detailed cellular in situ hybridization study. *Neuroscience*, **72**, 1023-1036.

Bachoud-Levi, A.C., Remy, P., Nguyen, J.P., Brugieres, P., Lefaucheur, J.P., Bourdet, C., Baudic, S., Gaura, V., Maison, P., Haddad, B., Boisse, M.F., Grandmougin, T., Jeny, R., Bartolomeo, P., Dalla Barba, G., Degos, J.D., Lisovoski, F., Ergis, A.M., Pailhous, E., Cesaro, P., Hantraye, P. & Peschanski, M. (2000) Motor and cognitive improvements in patients with Huntington's disease after neural transplantation. *Lancet*, **356**, 1975-1979.

Bachoud-Levi, A.C., Maison, P., Bartolomeo, P., Boisse, M.F., Dalla Barba, G., Ergis, A.M., Baudic, S., Degos, J.D., Cesaro, P. & Peschanski, M. (2001) Retest effects and cognitive decline in longitudinal follow-up of patients with early HD. *Neurology*, **56**, 1052-1058.

Bae, B.I., Xu, H., Igarashi, S., Fujimuro, M., Agrawal, N., Taya, Y., Hayward, S.D., Moran, T.H., Montell, C., Ross, C.A., Snyder, S.H. & Sawa, A. (2005) p53 mediates cellular dysfunction and behavioral abnormalities in Huntington's disease. *Neuron*, **47**, 29-41.

Bates, T.E., Strangward, M., Keelan, J., Davey, G.P., Munro, P.M. & Clark, J.B. (1996) Inhibition of N-acetylaspartate production: implications for 1H MRS studies *in vivo*. *Neuroreport*, **7**, 1397-1400.

Beal, M.F., Kowall, N.W., Ellison, D.W., Mazurek, M.F., Swartz, K.J. & Martin, J.B. (1986) Replication of the neurochemical characteristics of Huntington's disease by quinolinic acid. *Nature*, **321**, 168-171.

Beal, M.F., Kowall, N.W., Swartz, K.J., Ferrante, R.J. & Martin, J.B. (1989) Differential sparing of somatostatin-neuropeptide Y and cholinergic neurons following striatal excitotoxin lesions. *Synapse*, **3**, 38-47.

Beal, M.F., Ferrante, R.J., Swartz, K.J. & Kowall, N.W. (1991) Chronic quinolinic acid lesions in rats closely resemble Huntington's disease. *J Neurosci*, **11**, 1649-1659.

Beal, M.F. (1992) Does impairment of energy metabolism result in excitotoxic neuronal death in neurodegenerative illnesses? *Ann Neurol*, **31**, 119-130.

Beal, M.F., Brouillet, E., Jenkins, B.G., Ferrante, R.J., Kowall, N.W., Miller, J.M., Storey, E., Srivastava, R., Rosen, B.R. & Hyman, B.T. (1993) Neurochemical and histologic characterization of striatal excitotoxic lesions produced by the mitochondrial toxin 3-nitropropionic acid. *J Neurosci*, **13**, 4181-4192.

Beal, M.F. (2000) Energetics in the pathogenesis of neurodegenerative diseases. *Trends Neurosci*, **23**, 298-304.

Becher, M.W., Kotzuk, J.A., Sharp, A.H., Davies, S.W., Bates, G.P., Price, D.L. & Ross, C.A. (1998) Intranuclear neuronal inclusions in Huntington's disease and dentatorubral and pallidoluysian atrophy: correlation between the density of inclusions and IT15 CAG triplet repeat length. *Neurobiol Dis*, **4**, 387-397.

Beck, S. & Barrell, B.G. (1988) Human cytomegalovirus encodes a glycoprotein homologous to MHC class-I antigens. *Nature*, **331**, 269-272.

Bence, N.F., Sampat, R.M. & Kopito, R.R. (2001) Impairment of the ubiquitin-proteasome system by protein aggregation. *Science*, **292**, 1552-1555.

Bergemann, A.D., Cole, F. & Hirschhorn, K. (2005) The etiology of Wolf-Hirschhorn syndrome. *Trends Genet*, **21**, 188-195.

Bhide, P.G., Day, M., Sapp, E., Schwarz, C., Sheth, A., Kim, J., Young, A.B., Penney, J., Golden, J., Aronin, N. & DiFiglia, M. (1996) Expression of normal and mutant huntingtin in the developing brain. *J Neurosci*, **16**, 5523-5535.

Bibb, J.A., Yan, Z., Svenningsson, P., Snyder, G.L., Pieribone, V.A., Horiuchi, A., Nairn, A.C., Messer, A. & Greengard, P. (2000) Severe deficiencies in dopamine signaling in presymptomatic Huntington's disease mice. *Proc Natl Acad Sci U S A*, **97**, 6809-6814.

Blau, S., Daly, L., Fienberg, A., Teitelman, G. & Ehrlich, M.E. (1995) DARPP-32 promoter directs transgene expression to renal thick ascending limb of loop of Henle. *Am J Physiol*, **269**, F564-570.

Bonelli, R.M., Hodl, A.K., Hofmann, P. & Kapfhammer, H.P. (2004a) Neuroprotection in Huntington's disease: a 2-year study on minocycline. *Int Clin Psychopharmacol*, **19**, 337-342.

Bonelli, R.M., Wenning, G.K. & Kapfhammer, H.P. (2004b) Huntington's disease: present treatments and future therapeutic modalities. *Int Clin Psychopharmacol*, **19**, 51-62.

Borrell-Pages, M., Zala, D., Humbert, S. & Saudou, F. (2006) Huntington's disease: from huntingtin function and dysfunction to therapeutic strategies. *Cell Mol Life Sci.*

Borsook, D. & Hyman, S.E. (1995) Proenkephalin gene regulation in the neuroendocrine hypothalamus: a model of gene regulation in the CNS. *Am J Physiol*, **269**, E393-408.

Boshart, M., Weber, F., Jahn, G., Dorsch-Hasler, K., Fleckenstein, B. & Schaffner, W. (1985) A very strong enhancer is located upstream of an immediate early gene of human cytomegalovirus. *Cell*, **41**, 521-530.

Brouillet, E., Hantraye, P., Ferrante, R.J., Dolan, R., Leroy-Willig, A., Kowall, N.W. & Beal, M.F. (1995) Chronic mitochondrial energy impairment produces selective striatal degeneration and abnormal choreiform movements in primates. *Proc Natl Acad Sci U S A*, **92**, 7105-7109.

Burke, J.R., Enghild, J.J., Martin, M.E., Jou, Y.S., Myers, R.M., Roses, A.D., Vance, J.M. & Strittmatter, W.J. (1996) Huntingtin and DRPLA proteins selectively interact with the enzyme GAPDH. *Nat Med*, **2**, 347-350.

Carter, R.J., Lione, L.A., Humby, T., Mangiarini, L., Mahal, A., Bates, G.P., Dunnett, S.B. & Morton, A.J. (1999) Characterization of progressive motor deficits in mice transgenic for the human Huntington's disease mutation. *J Neurosci*, **19**, 3248-3257.

Cattaneo, E. & Conti, L. (1998) Generation and characterization of embryonic striatal conditionally immortalized ST14A cells. *J Neurosci Res*, **53**, 223-234.

Cattaneo, E., Rigamonti, D., Goffredo, D., Zuccato, C., Squitieri, F. & Sipione, S. (2001) Loss of normal huntingtin function: new developments in Huntington's disease research. *Trends Neurosci*, **24**, 182-188.

Cattaneo, E., Zuccato, C. & Tartari, M. (2005) Normal huntingtin function: an alternative approach to Huntington's disease. *Nat Rev Neurosci*, **6**, 919-930.

Cha, J.H., Kosinski, C.M., Kerner, J.A., Alsdorf, S.A., Mangiarini, L., Davies, S.W., Penney, J.B., Bates, G.P. & Young, A.B. (1998) Altered brain neurotransmitter receptors in transgenic mice expressing a portion of an abnormal human huntington disease gene. *Proc Natl Acad Sci U S A*, **95**, 6480-6485.

Cha, J.H., Frey, A.S., Alsdorf, S.A., Kerner, J.A., Kosinski, C.M., Mangiarini, L., Penney, J.B., Jr., Davies, S.W., Bates, G.P. & Young, A.B. (1999) Altered neurotransmitter receptor expression in transgenic mouse models of Huntington's disease. *Philos Trans R Soc Lond B Biol Sci*, **354**, 981-989.

Cha, J.H. (2000) Transcriptional dysregulation in Huntington's disease. *Trends Neurosci*, **23**, 387-392.

Chai, Y., Wu, L., Griffin, J.D. & Paulson, H.L. (2001) The role of protein composition in specifying nuclear inclusion formation in polyglutamine disease. *J Biol Chem*, **276**, 44889-44897.

Chan, E.Y., Luthi-Carter, R., Strand, A., Solano, S.M., Hanson, S.A., DeJohn, M.M., Kooperberg, C., Chase, K.O., DiFiglia, M., Young, A.B., Leavitt, B.R., Cha, J.H., Aronin, N., Hayden, M.R. & Olson, J.M. (2002) Increased huntingtin protein length reduces the number of polyglutamine-induced gene expression changes in mouse models of Huntington's disease. *Hum Mol Genet*, **11**, 1939-1951.

Charvin, D., Vanhoutte, P., Pages, C., Borrelli, E. & Caboche, J. (2005) Unraveling a role for dopamine in Huntington's disease: the dual role of reactive oxygen species and D_2 receptor stimulation. *Proc Natl Acad Sci U S A*, **102**, 12218-12223.

Chen, M., Ona, V.O., Li, M., Ferrante, R.J., Fink, K.B., Zhu, S., Bian, J., Guo, L., Farrell, L.A., Hersch, S.M., Hobbs, W., Vonsattel, J.P., Cha, J.H. & Friedlander, R.M. (2000) Minocycline inhibits caspase-1 and caspase-3 expression and delays mortality in a transgenic mouse model of Huntington disease. *Nat Med*, **6**, 797-801.

Chen-Plotkin, A.S., Sadri-Vakili, G., Yohrling, G.J., Braveman, M.W., Benn, C.L., Glajch, K.E., DiRocco, D.P., Farrell, L.A., Krainc, D., Gines, S., MacDonald, M.E. & Cha, J.H. (2006) Decreased association of the transcription factor Sp1 with genes downregulated in Huntington's disease. *Neurobiol Dis*, **22**, 233-241.

Chiang, M.C., Lee, Y.C., Huang, C.L. & Chern, Y. (2005) cAMP-response element-binding protein contributes to suppression of the A2A adenosine receptor promoter by mutant Huntingtin with expanded polyglutamine residues. *J Biol Chem*, **280**, 14331-14340.

Chinault, A.C. & Caskey, C.T. (1984) The hypoxanthine phosphoribosyltransferase gene: a model for the study of mutation in mammalian cells. *Prog Nucleic Acid Res Mol Biol*, **31**, 295-313.

Conaway, R.C., Garrett, K.P., Hanley, J.P. & Conaway, J.W. (1991) Mechanism of promoter selection by RNA polymerase II: mammalian transcription factors alpha and beta gamma promote entry of polymerase into the preinitiation complex. *Proc Natl Acad Sci U S A*, **88**, 6205-6209.

Cong, S.Y., Pepers, B.A., Evert, B.O., Rubinsztein, D.C., Roos, R.A., van Ommen, G.J. & Dorsman, J.C. (2005) Mutant huntingtin represses CBP, but not p300, by binding and protein degradation. *Mol Cell Neurosci*, **30**, 12-23.

Conner, J.M., Lauterborn, J.C., Yan, Q., Gall, C.M. & Varon, S. (1997) Distribution of brain-derived neurotrophic factor (BDNF) protein and mRNA in the normal adult rat CNS: evidence for anterograde axonal transport. *J Neurosci*, **17**, 2295-2313.

Cooper, J.K., Schilling, G., Peters, M.F., Herring, W.J., Sharp, A.H., Kaminsky, Z., Masone, J., Khan, F.A., Delanoy, M., Borchelt, D.R., Dawson, V.L., Dawson, T.M. & Ross, C.A. (1998) Truncated N-terminal fragments of huntingtin with expanded glutamine repeats form nuclear and cytoplasmic aggregates in cell culture. *Hum Mol Genet*, **7**, 783-790.

Courey, A.J. & Tjian, R. (1988) Analysis of Sp1 *in vivo* reveals multiple transcriptional domains, including a novel glutamine-rich activation motif. *Cell*, **55**, 887-898.

Courey, A.J., Holtzman, D.A., Jackson, S.P. & Tjian, R. (1989) Synergistic activation by the glutamine-rich domains of human transcription factor Sp1. *Cell*, **59**, 827-836.

Craufurd, D., Thompson, J.C. & Snowden, J.S. (2001) Behavioral changes in Huntington Disease. *Neuropsychiatry Neuropsychol Behav Neurol*, **14**, 219-226.

Cudkowicz, M. & Kowall, N.W. (1990) Degeneration of pyramidal projection neurons in Huntington's disease cortex. *Ann Neurol*, **27**, 200-204.

Cui, L., Jeong, H., Borovecki, F., Parkhurst, C.N., Tanese, N. & Krainc, D. (2006) Transcriptional repression of PGC-1alpha by mutant huntingtin leads to mitochondrial dysfunction and neurodegeneration. *Cell*, **127**, 59-69.

Davies, S.W., Turmaine, M., Cozens, B.A., DiFiglia, M., Sharp, A.H., Ross, C.A., Scherzinger, E., Wanker, E.E., Mangiarini, L. & Bates, G.P. (1997) Formation of neuronal intranuclear inclusions underlies the neurological dysfunction in mice transgenic for the HD mutation. *Cell*, **90**, 537-548.

Dawbarn, D., De Quidt, M.E. & Emson, P.C. (1985) Survival of basal ganglia neuropeptide Y-somatostatin neurones in Huntington's disease. *Brain Res*, **340**, 251-260.

de Almeida, L.P., Ross, C.A., Zala, D., Aebischer, P. & Deglon, N. (2002) Lentiviral-mediated delivery of mutant huntingtin in the striatum of rats induces a selective neuropathology modulated by polyglutamine repeat size, huntingtin expression levels, and protein length. *J Neurosci*, **22**, 3473-3483.

DeMars, R. (1971) Genetic studies of HG- PRT deficiency and the Lesch-Nyhan syndrome with cultured human cells. *Fed Proc*, **30**, 944-955.

Denovan-Wright, E.M. & Lee, R.W. (1994) Comparative structure and genomic organization of the discontinuous mitochondrial ribosomal RNA genes of Chlamydomonas eugametos and Chlamydomonas reinhardtii. *J Mol Biol*, **241**, 298-311.

Denovan-Wright, E.M., Newton, R.A., Armstrong, J.N., Babity, J.M. & Robertson, H.A. (1998) Acute administration of cocaine, but not amphetamine, increases the level of synaptotagmin IV mRNA in the dorsal striatum of rat. *Brain Res Mol Brain Res*, **55**, 350-354.

Denovan-Wright, E.M. & Robertson, H.A. (2000) Cannabinoid receptor messenger RNA levels decrease in a subset of neurons of the lateral striatum, cortex and hippocampus of transgenic Huntington's disease mice. *Neuroscience*, **98**, 705-713.

Denovan-Wright, E.M., Devarajan, S., Dursun, S.M. & Robertson, H.A. (2002) Maintained improvement with minocycline of a patient with advanced Huntington's disease. *J Psychopharmacol*, **16**, 393-394.

Desplats, P.A., Kass, K.E., Gilmartin, T., Stanwood, G.D., Woodward, E.L., Head, S.R., Sutcliffe, J.G. & Thomas, E.A. (2006) Selective deficits in the expression of striatal-enriched mRNAs in Huntington's disease. *J Neurochem*, **96**, 743-757.

DiFiglia, M., Sapp, E., Chase, K., Schwarz, C., Meloni, A., Young, C., Martin, E., Vonsattel, J.P., Carraway, R., Reeves, S.A. & et al. (1995) Huntingtin is a cytoplasmic protein associated with vesicles in human and rat brain neurons. *Neuron*, **14**, 1075-1081.

DiFiglia, M., Sapp, E., Chase, K.O., Davies, S.W., Bates, G.P., Vonsattel, J.P. & Aronin, N. (1997) Aggregation of huntingtin in neuronal intranuclear inclusions and dystrophic neurites in brain. *Science*, **277**, 1990-1993.

Dignam, J.D., Lebovitz, R.M. & Roeder, R.G. (1983) Accurate transcription initiation by RNA polymerase II in a soluble extract from isolated mammalian nuclei. *Nucleic Acids Res*, **11**, 1475-1489.

Dingledine, R., Borges, K., Bowie, D. & Traynelis, S.F. (1999) The glutamate receptor ion channels. *Pharmacol Rev*, **51**, 7-61.

Dragatsis, I., Levine, M.S. & Zeitlin, S. (2000) Inactivation of Hdh in the brain and testis results in progressive neurodegeneration and sterility in mice. *Nat Genet*, **26**, 300-306.

Dragunow, M., Faull, R.L., Lawlor, P., Beilharz, E.J., Singleton, K., Walker, E.B. & Mee, E. (1995) In situ evidence for DNA fragmentation in Huntington's disease striatum and Alzheimer's disease temporal lobes. *Neuroreport*, **6**, 1053-1057.

Drolet, G., Dumont, E.C., Gosselin, I., Kinkead, R., Laforest, S. & Trottier, J.F. (2001) Role of endogenous opioid system in the regulation of the stress response. *Prog Neuropsychopharmacol Biol Psychiatry*, **25**, 729-741.

Duan, W., Guo, Z., Jiang, H., Ware, M., Li, X.J. & Mattson, M.P. (2003) Dietary restriction normalizes glucose metabolism and BDNF levels, slows disease progression, and increases survival in huntingtin mutant mice. *Proc Natl Acad Sci U S A*, **100**, 2911-2916.

Dunah, A.W., Jeong, H., Griffin, A., Kim, Y.M., Standaert, D.G., Hersch, S.M., Mouradian, M.M., Young, A.B., Tanese, N. & Krainc, D. (2002) Sp1 and TAFII130 transcriptional activity disrupted in early Huntington's disease. *Science*, **296**, 2238-2243.

Duyao, M., Ambrose, C., Myers, R., Novelletto, A., Persichetti, F., Frontali, M., Folstein, S., Ross, C., Franz, M., Abbott, M. & et al. (1993) Trinucleotide repeat length instability and age of onset in Huntington's disease. *Nat Genet*, **4**, 387-392.

Duyao, M.P., Auerbach, A.B., Ryan, A., Persichetti, F., Barnes, G.T., McNeil, S.M., Ge, P., Vonsattel, J.P., Gusella, J.F., Joyner, A.L. & et al. (1995) Inactivation of the mouse Huntington's disease gene homolog Hdh. *Science*, **269**, 407-410.

Dvir, A., Conaway, J.W. & Conaway, R.C. (2001) Mechanism of transcription initiation and promoter escape by RNA polymerase II. *Curr Opin Genet Dev*, **11**, 209-214.

Ehrlich, M.E., Conti, L., Toselli, M., Taglietti, L., Fiorillo, E., Taglietti, V., Ivkovic, S., Guinea, B., Tranberg, A., Sipione, S., Rigamonti, D. & Cattaneo, E. (2001) ST14A cells have properties of a medium-size spiny neuron. *Exp Neurol*, **167**, 215-226.

Engqvist-Goldstein, A.E., Warren, R.A., Kessels, M.M., Keen, J.H., Heuser, J. & Drubin, D.G. (2001) The actin-binding protein Hip1R associates with clathrin during early stages of endocytosis and promotes clathrin assembly *in vitro*. *J Cell Biol*, **154**, 1209-1223.

Everett, C.M. & Wood, N.W. (2004) Trinucleotide repeats and neurodegenerative disease. *Brain*, **127**, 2385-2405.

Faber, P.W., Barnes, G.T., Srinidhi, J., Chen, J., Gusella, J.F. & MacDonald, M.E. (1998) Huntingtin interacts with a family of WW domain proteins. *Hum Mol Genet*, **7**, 1463-1474.

Ferrante, R.J., Kowall, N.W., Beal, M.F., Richardson, E.P., Jr., Bird, E.D. & Martin, J.B. (1985) Selective sparing of a class of striatal neurons in Huntington's disease. *Science*, **230**, 561-563.

Ferrante, R.J., Kowall, N.W., Richardson, E.P., Jr., Bird, E.D. & Martin, J.B. (1986) Topography of enkephalin, substance P and acetylcholinesterase staining in Huntington's disease striatum. *Neurosci Lett*, **71**, 283-288.

Ferrante, R.J., Kubilus, J.K., Lee, J., Ryu, H., Beesen, A., Zucker, B., Smith, K., Kowall, N.W., Ratan, R.R., Luthi-Carter, R. & Hersch, S.M. (2003) Histone deacetylase inhibition by sodium butyrate chemotherapy ameliorates the neurodegenerative phenotype in Huntington's disease mice. *J Neurosci*, **23**, 9418-9427.

Fienberg, A.A. & Greengard, P. (2000) The DARPP-32 knockout mouse. *Brain Res Brain Res Rev*, **31**, 313-319.

Flores, O., Lu, H., Killeen, M., Greenblatt, J., Burton, Z.F. & Reinberg, D. (1991) The small subunit of transcription factor IIF recruits RNA polymerase II into the preinitiation complex. *Proc Natl Acad Sci U S A*, **88**, 9999-10003.

Folstein, S.E., Leigh, R.J., Parhad, I.M. & Folstein, M.F. (1986) The diagnosis of Huntington's disease. *Neurology*, **36**, 1279-1283.

Franklin, K.B.J. & Paxinos, G. (1997) The Mouse Brain in Stereotaxic Coordinates. Academic Press, San Diego.

Freiman, R.N. & Tjian, R. (2002) Neurodegeneration. A glutamine-rich trail leads to transcription factors. *Science*, **296**, 2149-2150.

Gall, C. (1988) Seizures induce dramatic and distinctly different changes in enkephalin, dynorphin, and CCK immunoreactivities in mouse hippocampal mossy fibers. *J Neurosci*, **8**, 1852-1862.

Garrett, J.E., Collard, M.W. & Douglass, J.O. (1989) Translational control of germ cell-expressed mRNA imposed by alternative splicing: opioid peptide gene expression in rat testis. *Mol Cell Biol*, **9**, 4381-4389.

Gaura, V., Bachoud-Levi, A.C., Ribeiro, M.J., Nguyen, J.P., Frouin, V., Baudic, S., Brugieres, P., Mangin, J.F., Boisse, M.F., Palfi, S., Cesaro, P., Samson, Y., Hantraye, P., Peschanski, M. & Remy, P. (2004) Striatal neural grafting improves cortical metabolism in Huntington's disease patients. *Brain*, **127**, 65-72.

Gerfen, C.R. (1992) The neostriatal mosaic: multiple levels of compartmental organization. *J Neural Transm Suppl*, **36**, 43-59.

Glass, M., Dragunow, M. & Faull, R.L. (2000) The pattern of neurodegeneration in Huntington's disease: a comparative study of cannabinoid, dopamine, adenosine and GABA(A) receptor alterations in the human basal ganglia in Huntington's disease. *Neuroscience*, **97**, 505-519.

Glass, M., Faull, R.L. & Dragunow, M. (1993) Loss of cannabinoid receptors in the substantia nigra in Huntington's disease. *Neuroscience*, **56**, 523-527.

Goldberg, Y.P., Nicholson, D.W., Rasper, D.M., Kalchman, M.A., Koide, H.B., Graham, R.K., Bromm, M., Kazemi-Esfarjani, P., Thornberry, N.A., Vaillancourt, J.P. & Hayden, M.R. (1996) Cleavage of huntingtin by apopain, a proapoptotic cysteine protease, is modulated by the polyglutamine tract. *Nat Genet*, **13**, 442-449.

Greenamyre, J.T., Penney, J.B., Young, A.B., D'Amato, C.J., Hicks, S.P. & Shoulson, I. (1985) Alterations in L-glutamate binding in Alzheimer's and Huntington's diseases. *Science*, **227**, 1496-1499.

Greene, J.G., Porter, R.H., Eller, R.V. & Greenamyre, J.T. (1993) Inhibition of succinate dehydrogenase by malonic acid produces an "excitotoxic" lesion in rat striatum. *J Neurochem*, **61**, 1151-1154.

Greene, L.A. & Tischler, A.S. (1976) Establishment of a noradrenergic clonal line of rat adrenal pheochromocytoma cells which respond to nerve growth factor. *Proc Natl Acad Sci U S A*, **73**, 2424-2428.

Guidetti, P., Charles, V., Chen, E.Y., Reddy, P.H., Kordower, J.H., Whetsell, W.O., Jr., Schwarcz, R. & Tagle, D.A. (2001) Early degenerative changes in transgenic mice expressing mutant huntingtin involve dendritic abnormalities but no impairment of mitochondrial energy production. *Exp Neurol*, **169**, 340-350.

Gusella, J.F., MacDonald, M.E., Ambrose, C.M. & Duyao, M.P. (1993) Molecular genetics of Huntington's disease. *Arch Neurol*, **50**, 1157-1163.

Gusella, J.F., Wexler, N.S., Conneally, P.M., Naylor, S.L., Anderson, M.A., Tanzi, R.E., Watkins, P.C., Ottina, K., Wallace, M.R., Sakaguchi, A.Y. & et al. (1983) A polymorphic DNA marker genetically linked to Huntington's disease. *Nature*, **306**, 234-238.

Hackam, A.S., Singaraja, R., Wellington, C.L., Metzler, M., McCutcheon, K., Zhang, T., Kalchman, M. & Hayden, M.R. (1998) The influence of huntingtin protein size on nuclear localization and cellular toxicity. *J Cell Biol*, **141**, 1097-1105.

Handley, O.J., Naji, J.J., Dunnett, S.B. & Rosser, A.E. (2006) Pharmaceutical, cellular and genetic therapies for Huntington's disease. *Clin Sci (Lond)*, **110**, 73-88.

Hansson, O., Petersen, A., Leist, M., Nicotera, P., Castilho, R.F. & Brundin, P. (1999) Transgenic mice expressing a Huntington's disease mutation are resistant to quinolinic acid-induced striatal excitotoxicity. *Proc Natl Acad Sci U S A*, **96**, 8727-8732.

Hansson, O., Guatteo, E., Mercuri, N.B., Bernardi, G., Li, X.J., Castilho, R.F. & Brundin, P. (2001) Resistance to NMDA toxicity correlates with appearance of nuclear inclusions, behavioural deficits and changes in calcium homeostasis in mice transgenic for exon 1 of the huntington gene. *Eur J Neurosci*, **14**, 1492-1504.

Harjes, P. & Wanker, E.E. (2003) The hunt for huntingtin function: interaction partners tell many different stories. *Trends Biochem Sci*, **28**, 425-433.

Harper, P.S. (1992) The epidemiology of Huntington's disease. *Hum Genet*, **89**, 365-376.

Harper, S.Q., Staber, P.D., He, X., Eliason, S.L., Martins, I.H., Mao, Q., Yang, L., Kotin, R.M., Paulson, H.L. & Davidson, B.L. (2005) RNA interference improves motor and neuropathological abnormalities in a Huntington's disease mouse model. *Proc Natl Acad Sci U S A*, **102**, 5820-5825.

Hauser, R.A., Furtado, S., Cimino, C.R., Delgado, H., Eichler, S., Schwartz, S., Scott, D., Nauert, G.M., Soety, E., Sossi, V., Holt, D.A., Sanberg, P.R., Stoessl, A.J. & Freeman, T.B. (2002) Bilateral human fetal striatal transplantation in Huntington's disease. *Neurology*, **58**, 687-695.

Hebb, A.L., Robertson, H.A. & Denovan-Wright, E.M. (2004) Striatal phosphodiesterase mRNA and protein levels are reduced in Huntington's disease transgenic mice prior to the onset of motor symptoms. *Neuroscience*, **123**, 967-981.

Hedreen, J.C., Peyser, C.E., Folstein, S.E. & Ross, C.A. (1991) Neuronal loss in layers V and VI of cerebral cortex in Huntington's disease. *Neurosci Lett*, **133**, 257-261.

Hemmings, H.C., Jr., Girault, J.A., Nairn, A.C., Bertuzzi, G. & Greengard, P. (1992) Distribution of protein phosphatase inhibitor-1 in brain and peripheral tissues of various species: comparison with DARPP-32. *J Neurochem*, **59**, 1053-1061.

Hersch, S.M. & Ferrante, R.J. (2004) Translating therapies for Huntington's disease from genetic animal models to clinical trials. *NeuroRx*, **1**, 298-306.

Ho, L.W., Carmichael, J., Swartz, J., Wyttenbach, A., Rankin, J. & Rubinsztein, D.C. (2001) The molecular biology of Huntington's disease. *Psychol Med*, **31**, 3-14.

Hockly, E., Richon, V.M., Woodman, B., Smith, D.L., Zhou, X., Rosa, E., Sathasivam, K., Ghazi-Noori, S., Mahal, A., Lowden, P.A., Steffan, J.S., Marsh, J.L., Thompson, L.M., Lewis, C.M., Marks, P.A. & Bates, G.P. (2003) Suberoylanilide hydroxamic acid, a histone deacetylase inhibitor, ameliorates motor deficits in a mouse model of Huntington's disease. *Proc Natl Acad Sci U S A*, **100**, 2041-2046.

Hodges, A., Strand, A.D., Aragaki, A.K., Kuhn, A., Sengstag, T., Hughes, G., Elliston, L.A., Hartog, C., Goldstein, D.R., Thu, D., Hollingsworth, Z.R., Collin, F., Synek, B., Holmans, P.A., Young, A.B., Wexler, N.S., Delorenzi, M., Kooperberg, C., Augood, S.J., Faull, R.L., Olson, J.M., Jones, L. & Luthi-Carter, R. (2006) Regional and cellular gene expression changes in human Huntington's disease brain. *Hum Mol Genet*, **15**, 965-977.

Hodgson, J.G., Agopyan, N., Gutekunst, C.A., Leavitt, B.R., LePiane, F., Singaraja, R., Smith, D.J., Bissada, N., McCutcheon, K., Nasir, J., Jamot, L., Li, X.J., Stevens, M.E., Rosemond, E., Roder, J.C., Phillips, A.G., Rubin, E.M., Hersch, S.M. & Hayden, M.R. (1999) A YAC mouse model for Huntington's disease with full-length mutant huntingtin, cytoplasmic toxicity, and selective striatal neurodegeneration. *Neuron*, **23**, 181-192.

Hong, J.S., Wood, P.L., Gillin, J.C., Yang, H.Y. & Costa, E. (1980) Changes of hippocampal Met-enkephalin content after recurrent motor seizures. *Nature*, **285**, 231-232.

Housman, D. (1995) Gain of glutamines, gain of function? *Nat Genet*, **10**, 3-4.

Howlett, T.A. & Rees, L.H. (1986) Endogenous opioid peptides and hypothalamo-pituitary function. *Annu Rev Physiol*, **48**, 527-536.

Hu, H., McCaw, E.A., Hebb, A.L., Gomez, G.T. & Denovan-Wright, E.M. (2004) Mutant huntingtin affects the rate of transcription of striatum-specific isoforms of phosphodiesterase 10A. *Eur J Neurosci*, **20**, 3351-3363.

Huang, C.C., Faber, P.W., Persichetti, F., Mittal, V., Vonsattel, J.P., MacDonald, M.E. & Gusella, J.F. (1998) Amyloid formation by mutant huntingtin: threshold, progressivity and recruitment of normal polyglutamine proteins. *Somat Cell Mol Genet*, **24**, 217-233.

Huntington, G. (1872) On chorea. George Huntington, M.D. *The Medical and Surgical Reporter*, **26**, 317-321.

Huntington, G. (2003) On chorea. George Huntington, M.D. *J Neuropsychiatry Clin Neurosci*, **15**, 109-112.

Iadarola, M.J., Shin, C., McNamara, J.O. & Yang, H.Y. (1986) Changes in dynorphin, enkephalin and cholecystokinin content of hippocampus and substantia nigra after amygdala kindling. *Brain Res*, **365**, 185-191.

Iannicola, C., Moreno, S., Oliverio, S., Nardacci, R., Ciofi-Luzzatto, A. & Piacentini, M. (2000) Early alterations in gene expression and cell morphology in a mouse model of Huntington's disease. *J Neurochem*, **75**, 830-839.

Issaq, H.J., Conrads, T.P., Janini, G.M. & Veenstra, T.D. (2002) Methods for fractionation, separation and profiling of proteins and peptides. *Electrophoresis*, **23**, 3048-3061.

Jenkins, B.G., Koroshetz, W.J., Beal, M.F. & Rosen, B.R. (1993) Evidence for impairment of energy metabolism *in vivo* in Huntington's disease using localized 1H NMR spectroscopy. *Neurology*, **43**, 2689-2695.

Jenkins, B.G., Klivenyi, P., Kustermann, E., Andreassen, O.A., Ferrante, R.J., Rosen, B.R. & Beal, M.F. (2000) Nonlinear decrease over time in N-acetyl aspartate levels in the absence of neuronal loss and increases in glutamine and glucose in transgenic Huntington's disease mice. *J Neurochem*, **74**, 2108-2119.

Kahlem, P., Green, H. & Djian, P. (1998) Transglutaminase action imitates Huntington's disease: selective polymerization of Huntingtin containing expanded polyglutamine. *Mol Cell*, **1**, 595-601.

Kalchman, M.A., Koide, H.B., McCutcheon, K., Graham, R.K., Nichol, K., Nishiyama, K., Kazemi-Esfarjani, P., Lynn, F.C., Wellington, C., Metzler, M., Goldberg, Y.P., Kanazawa, I., Gietz, R.D. & Hayden, M.R. (1997) HIP1, a human homologue of S. cerevisiae Sla2p, interacts with membrane-associated huntingtin in the brain. *Nat Genet*, **16**, 44-53.

Katoh, A., Nabeshima, T. & Kameyama, T. (1990) Behavioral changes induced by stressful situations: effects of enkephalins, dynorphin, and their interactions. *J Pharmacol Exp Ther*, **253**, 600-607.

Kazantsev, A., Preisinger, E., Dranovsky, A., Goldgaber, D. & Housman, D. (1999) Insoluble detergent-resistant aggregates form between pathological and nonpathological lengths of polyglutamine in mammalian cells. *Proc Natl Acad Sci U S A*, **96**, 11404-11409.

Kegel, K.B., Meloni, A.R., Yi, Y., Kim, Y.J., Doyle, E., Cuiffo, B.G., Sapp, E., Wang, Y., Qin, Z.H., Chen, J.D., Nevins, J.R., Aronin, N. & DiFiglia, M. (2002) Huntingtin is present in the nucleus, interacts with the transcriptional corepressor C-terminal binding protein, and represses transcription. *J Biol Chem*, **277**, 7466-7476.

Kita, H., Carmichael, J., Swartz, J., Muro, S., Wyttenbach, A., Matsubara, K., Rubinsztein, D.C. & Kato, K. (2002) Modulation of polyglutamine-induced cell death by genes identified by expression profiling. *Hum Mol Genet*, **11**, 2279-2287.

Koroshetz, W.J., Jenkins, B.G., Rosen, B.R. & Beal, M.F. (1997) Energy metabolism defects in Huntington's disease and effects of coenzyme Q10. *Ann Neurol*, **41**, 160-165.

Kosinski, C.M., Cha, J.H., Young, A.B., Persichetti, F., MacDonald, M., Gusella, J.F., Penney, J.B., Jr. & Standaert, D.G. (1997) Huntingtin immunoreactivity in the rat neostriatum: differential accumulation in projection and interneurons. *Exp Neurol*, **144**, 239-247.

Kowalski, J. (1998) Immunologic action of [Met5]enkephalin fragments. *Eur J Pharmacol*, **347**, 95-99.

Landles, C. & Bates, G.P. (2004) Huntingtin and the molecular pathogenesis of Huntington's disease. Fourth in molecular medicine review series. *EMBO Rep*, **5**, 958-963.

Lastres-Becker, I., Gomez, M., De Miguel, R., Ramos, J.A. & Fernandez-Ruiz, J. (2002) Loss of cannabinoid CB(1) receptors in the basal ganglia in the late akinetic phase of rats with experimental Huntington's disease. *Neurotox Res*, **4**, 601-608.

Leegwater-Kim, J. & Cha, J.H. (2004) The paradigm of Huntington's disease: therapeutic opportunities in neurodegeneration. *NeuroRx*, **1**, 128-138.

Lemon, B. & Tjian, R. (2000) Orchestrated response: a symphony of transcription factors for gene control. *Genes Dev*, **14**, 2551-2569.

Leone, T.C., Lehman, J.J., Finck, B.N., Schaeffer, P.J., Wende, A.R., Boudina, S., Courtois, M., Wozniak, D.F., Sambandam, N., Bernal-Mizrachi, C., Chen, Z., Holloszy, J.O., Medeiros, D.M., Schmidt, R.E., Saffitz, J.E., Abel, E.D., Semenkovich, C.F. & Kelly, D.P. (2005) PGC-1alpha deficiency causes multi-system energy metabolic derangements: muscle dysfunction, abnormal weight control and hepatic steatosis. *PLoS Biol*, **3**, e101.

Lesch, M. & Nyhan, W.L. (1964) A Familial Disorder Of Uric Acid Metabolism And Central Nervous System Function. *Am J Med*, **36**, 561-570.

Levine, M.S., Klapstein, G.J., Koppel, A., Gruen, E., Cepeda, C., Vargas, M.E., Jokel, E.S., Carpenter, E.M., Zanjani, H., Hurst, R.S., Efstratiadis, A., Zeitlin, S. & Chesselet, M.F. (1999) Enhanced sensitivity to N-methyl-D-aspartate receptor activation in transgenic and knockin mouse models of Huntington's disease. *J Neurosci Res*, **58**, 515-532.

Li, J.L., Hayden, M.R., Almqvist, E.W., Brinkman, R.R., Durr, A., Dode, C., Morrison, P.J., Suchowersky, O., Ross, C.A., Margolis, R.L., Rosenblatt, A., Gomez-Tortosa, E., Cabrero, D.M., Novelletto, A., Frontali, M., Nance, M., Trent, R.J., McCusker, E., Jones, R., Paulsen, J.S., Harrison, M., Zanko, A., Abramson, R.K., Russ, A.L., Knowlton, B., Djousse, L., Mysore, J.S., Tariot, S., Gusella, M.F., Wheeler, V.C., Atwood, L.D., Cupples, L.A., Saint-Hilaire, M., Cha, J.H., Hersch, S.M., Koroshetz, W.J., Gusella, J.F., MacDonald, M.E. & Myers, R.H. (2003) A genome scan for modifiers of age at onset in Huntington disease: The HD MAPS study. *Am J Hum Genet*, **73**, 682-687.

Li, J.Y., Popovic, N. & Brundin, P. (2005) The use of the R6 transgenic mouse models of Huntington's disease in attempts to develop novel therapeutic strategies. *NeuroRx*, **2**, 447-464.

Li, S.H., Schilling, G., Young, W.S., 3rd, Li, X.J., Margolis, R.L., Stine, O.C., Wagster, M.V., Abbott, M.H., Franz, M.L., Ranen, N.G. & et al. (1993) Huntington's disease gene (IT15) is widely expressed in human and rat tissues. *Neuron*, **11**, 985-993.

Li, S.H., Cheng, A.L., Li, H. & Li, X.J. (1999a) Cellular defects and altered gene expression in PC12 cells stably expressing mutant huntingtin. *J Neurosci*, **19**, 5159-5172.

Li, S.H., Lam, S., Cheng, A.L. & Li, X.J. (2000) Intranuclear huntingtin increases the expression of caspase-1 and induces apoptosis. *Hum Mol Genet*, **9**, 2859-2867.

Li, S.H., Cheng, A.L., Zhou, H., Lam, S., Rao, M., Li, H. & Li, X.J. (2002) Interaction of Huntington disease protein with transcriptional activator Sp1. *Mol Cell Biol*, **22**, 1277-1287.

Li, S.H. & Li, X.J. (2004) Huntingtin-protein interactions and the pathogenesis of Huntington's disease. *Trends Genet*, **20**, 146-154.

Li, Z., Karlovich, C.A., Fish, M.P., Scott, M.P. & Myers, R.M. (1999b) A putative Drosophila homolog of the Huntington's disease gene. *Hum Mol Genet*, **8**, 1807-1815.

Lievens, J.C., Rival, T., Iche, M., Chneiweiss, H. & Birman, S. (2005) Expanded polyglutamine peptides disrupt EGF receptor signaling and glutamate transporter expression in Drosophila. *Hum Mol Genet*, **14**, 713-724.

Lightman, S.L. & Young, W.S., 3rd (1987) Changes in hypothalamic preproenkephalin A mRNA following stress and opiate withdrawal. *Nature*, **328**, 643-645.

Lin, C.H., Tallaksen-Greene, S., Chien, W.M., Cearley, J.A., Jackson, W.S., Crouse, A.B., Ren, S., Li, X.J., Albin, R.L. & Detloff, P.J. (2001) Neurological abnormalities in a knock-in mouse model of Huntington's disease. *Hum Mol Genet*, **10**, 137-144.

Lin, J., Wu, P.H., Tarr, P.T., Lindenberg, K.S., St-Pierre, J., Zhang, C.Y., Mootha, V.K., Jager, S., Vianna, C.R., Reznick, R.M., Cui, L., Manieri, M., Donovan, M.X., Wu, Z., Cooper, M.P., Fan, M.C., Rohas, L.M., Zavacki, A.M., Cinti, S., Shulman, G.I., Lowell, B.B., Krainc, D. & Spiegelman, B.M. (2004) Defects in adaptive energy metabolism with CNS-linked hyperactivity in PGC-1alpha null mice. *Cell*, **119**, 121-135.

Lipton, S.A. & Rosenberg, P.A. (1994) Excitatory amino acids as a final common pathway for neurologic disorders. *N Engl J Med*, **330**, 613-622.

Lodi, R., Schapira, A.H., Manners, D., Styles, P., Wood, N.W., Taylor, D.J. & Warner, T.T. (2000) Abnormal *in vivo* skeletal muscle energy metabolism in Huntington's disease and dentatorubropallidoluysian atrophy. *Ann Neurol*, **48**, 72-76.

Lonze, B.E. & Ginty, D.D. (2002) Function and regulation of CREB family transcription factors in the nervous system. *Neuron*, **35**, 605-623.

Luesse, H.G., Schiefer, J., Spruenken, A., Puls, C., Block, F. & Kosinski, C.M. (2001) Evaluation of R6/2 HD transgenic mice for therapeutic studies in Huntington's disease: behavioral testing and impact of diabetes mellitus. *Behav Brain Res*, **126**, 185-195.

Lunkes, A. & Mandel, J.L. (1998) A cellular model that recapitulates major pathogenic steps of Huntington's disease. *Hum Mol Genet*, **7**, 1355-1361.

Lunkes, A., Trottier, Y., Fagart, J., Schultz, P., Zeder-Lutz, G., Moras, D. & Mandel, J.L. (1999) Properties of polyglutamine expansion *in vitro* and in a cellular model for Huntington's disease. *Philos Trans R Soc Lond B Biol Sci*, **354**, 1013-1019.

Luse, D.S. & Jacob, G.A. (1987) Abortive initiation by RNA polymerase II *in vitro* at the adenovirus 2 major late promoter. *J Biol Chem*, **262**, 14990-14997.

Luthi-Carter, R., Strand, A., Peters, N.L., Solano, S.M., Hollingsworth, Z.R., Menon, A.S., Frey, A.S., Spektor, B.S., Penney, E.B., Schilling, G., Ross, C.A., Borchelt, D.R., Tapscott, S.J., Young, A.B., Cha, J.H. & Olson, J.M. (2000) Decreased expression of striatal signaling genes in a mouse model of Huntington's disease. *Hum Mol Genet*, **9**, 1259-1271.

Luthi-Carter, R., Hanson, S.A., Strand, A.D., Bergstrom, D.A., Chun, W., Peters, N.L., Woods, A.M., Chan, E.Y., Kooperberg, C., Krainc, D., Young, A.B., Tapscott, S.J. & Olson, J.M. (2002a) Dysregulation of gene expression in the R6/2 model of polyglutamine disease: parallel changes in muscle and brain. *Hum Mol Genet*, **11**, 1911-1926.

Luthi-Carter, R., Strand, A.D., Hanson, S.A., Kooperberg, C., Schilling, G., La Spada, A.R., Merry, D.E., Young, A.B., Ross, C.A., Borchelt, D.R. & Olson, J.M. (2002b) Polyglutamine and transcription: gene expression changes shared by DRPLA and Huntington's disease mouse models reveal context-independent effects. *Hum Mol Genet*, **11**, 1927-1937.

Luthi-Carter, R. & Cha, J.H. (2003) Mechanisms of transcriptional dysregulation in Huntington's disease. *Clin Neurosci Res*, **3**, 165-177.

Mangiarini, L., Sathasivam, K., Seller, M., Cozens, B., Harper, A., Hetherington, C., Lawton, M., Trottier, Y., Lehrach, H., Davies, S.W. & Bates, G.P. (1996) Exon 1 of the HD gene with an expanded CAG repeat is sufficient to cause a progressive neurological phenotype in transgenic mice. *Cell*, **87**, 493-506.

Marcora, E., Gowan, K. & Lee, J.E. (2003) Stimulation of NeuroD activity by huntingtin and huntingtin-associated proteins HAP1 and MLK2. *Proc Natl Acad Sci U S A*, **100**, 9578-9583.

Marks, P.A., Richon, V.M., Breslow, R. & Rifkind, R.A. (2001) Histone deacetylase inhibitors as new cancer drugs. *Curr Opin Oncol*, **13**, 477-483.

Martindale, D., Hackam, A., Wieczorek, A., Ellerby, L., Wellington, C., McCutcheon, K., Singaraja, R., Kazemi-Esfarjani, P., Devon, R., Kim, S.U., Bredesen, D.E., Tufaro, F. & Hayden, M.R. (1998) Length of huntingtin and its polyglutamine tract influences localization and frequency of intracellular aggregates. *Nat Genet*, **18**, 150-154.

McCaw, E.A., Hu, H., Gomez, G.T., Hebb, A.L., Kelly, M.E. & Denovan-Wright, E.M. (2004) Structure, expression and regulation of the cannabinoid receptor gene (CB1) in Huntington's disease transgenic mice. *Eur J Biochem*, **271**, 4909-4920.

McGill, J.K. & Beal, M.F. (2006) PGC-1alpha, a New Therapeutic Target in Huntington's Disease? *Cell*, **127**, 465-468.

Meade, C.A., Deng, Y.P., Fusco, F.R., Del Mar, N., Hersch, S., Goldowitz, D. & Reiner, A. (2002) Cellular localization and development of neuronal intranuclear inclusions in striatal and cortical neurons in R6/2 transgenic mice. *J Comp Neurol*, **449**, 241-269.

Meister, B., Fryckstedt, J., Schalling, M., Cortes, R., Hokfelt, T., Aperia, A., Hemmings, H.C., Jr., Nairn, A.C., Ehrlich, M. & Greengard, P. (1989) Dopamine- and cAMP-regulated phosphoprotein (DARPP-32) and dopamine DA1 agonist-sensitive Na+,K+-ATPase in renal tubule cells. *Proc Natl Acad Sci U S A*, **86**, 8068-8072.

Melton, D.W., Konecki, D.S., Ledbetter, D.H., Hejtmancik, J.F. & Caskey, C.T. (1981) *In vitro* translation of hypoxanthine/guanine phosphoribosyltransferase mRNA: characterization of a mouse neuroblastoma cell line that has elevated levels of hypoxanthine/guanine phosphoribosyltransferase protein. *Proc Natl Acad Sci U S A*, **78**, 6977-6980.

Melton, D.W., McEwan, C., McKie, A.B. & Reid, A.M. (1986) Expression of the mouse HPRT gene: deletional analysis of the promoter region of an X-chromosome linked housekeeping gene. *Cell*, **44**, 319-328.

Menalled, L., Zanjani, H., MacKenzie, L., Koppel, A., Carpenter, E., Zeitlin, S. & Chesselet, M.F. (2000) Decrease in striatal enkephalin mRNA in mouse models of Huntington's disease. *Exp Neurol*, **162**, 328-342.

Menalled, L.B. & Chesselet, M.F. (2002) Mouse models of Huntington's disease. *Trends Pharmacol Sci*, **23**, 32-39.

Metzler, M., Legendre-Guillemin, V., Gan, L., Chopra, V., Kwok, A., McPherson, P.S. & Hayden, M.R. (2001) HIP1 functions in clathrin-mediated endocytosis through binding to clathrin and adaptor protein 2. *J Biol Chem*, **276**, 39271-39276.

Mills, I.G., Gaughan, L., Robson, C., Ross, T., McCracken, S., Kelly, J. & Neal, D.E. (2005) Huntingtin interacting protein 1 modulates the transcriptional activity of nuclear hormone receptors. *J Cell Biol*, **170**, 191-200.

Morton, A.J., Lagan, M.A., Skepper, J.N. & Dunnett, S.B. (2000) Progressive formation of inclusions in the striatum and hippocampus of mice transgenic for the human Huntington's disease mutation. *J Neurocytol*, **29**, 679-702.

Myers, R.H., Leavitt, J., Farrer, L.A., Jagadeesh, J., McFarlane, H., Mastromauro, C.A., Mark, R.J. & Gusella, J.F. (1989) Homozygote for Huntington disease. *Am J Hum Genet*, **45**, 615-618.

Nasir, J., Floresco, S.B., O'Kusky, J.R., Diewert, V.M., Richman, J.M., Zeisler, J., Borowski, A., Marth, J.D., Phillips, A.G. & Hayden, M.R. (1995) Targeted disruption of the Huntington's disease gene results in embryonic lethality and behavioral and morphological changes in heterozygotes. *Cell*, **81**, 811-823.

Naver, B., Stub, C., Moller, M., Fenger, K., Hansen, A.K., Hasholt, L. & Sorensen, S.A. (2003) Molecular and behavioral analysis of the R6/1 Huntington's disease transgenic mouse. *Neuroscience*, **122**, 1049-1057.

Nucifora, F.C., Jr., Sasaki, M., Peters, M.F., Huang, H., Cooper, J.K., Yamada, M., Takahashi, H., Tsuji, S., Troncoso, J., Dawson, V.L., Dawson, T.M. & Ross, C.A. (2001) Interference by huntingtin and atrophin-1 with cbp-mediated transcription leading to cellular toxicity. *Science*, **291**, 2423-2428.

Obrietan, K. & Hoyt, K.R. (2004) CRE-mediated transcription is increased in Huntington's disease transgenic mice. *J Neurosci*, **24**, 791-796.

Okazawa, H., Sudol, M. & Rich, T. (2001) PQBP-1 (Np/PQ): a polyglutamine tract-binding and nuclear inclusion-forming protein. *Brain Res Bull*, **56**, 273-280.

Ona, V.O., Li, M., Vonsattel, J.P., Andrews, L.J., Khan, S.Q., Chung, W.M., Frey, A.S., Menon, A.S., Li, X.J., Stieg, P.E., Yuan, J., Penney, J.B., Young, A.B., Cha, J.H. & Friedlander, R.M. (1999) Inhibition of caspase-1 slows disease progression in a mouse model of Huntington's disease. *Nature*, **399**, 263-267.

Ordway, J.M., Tallaksen-Greene, S., Gutekunst, C.A., Bernstein, E.M., Cearley, J.A., Wiener, H.W., Dure, L.S.t., Lindsey, R., Hersch, S.M., Jope, R.S., Albin, R.L. & Detloff, P.J. (1997) Ectopically expressed CAG repeats cause intranuclear inclusions and a progressive late onset neurological phenotype in the mouse. *Cell*, **91**, 753-763.

Orphanides, G., Lagrange, T. & Reinberg, D. (1996) The general transcription factors of RNA polymerase II. *Genes Dev*, **10**, 2657-2683.

Ouimet, C.C., Miller, P.E., Hemmings, H.C., Jr., Walaas, S.I. & Greengard, P. (1984) DARPP-32, a dopamine- and adenosine 3':5'-monophosphate-regulated phosphoprotein enriched in dopamine-innervated brain regions. III. Immunocytochemical localization. *J Neurosci*, **4**, 111-124.

Palfi, S., Ferrante, R.J., Brouillet, E., Beal, M.F., Dolan, R., Guyot, M.C., Peschanski, M. & Hantraye, P. (1996) Chronic 3-nitropropionic acid treatment in baboons replicates the cognitive and motor deficits of Huntington's disease. *J Neurosci*, **16**, 3019-3025.

Panov, A.V., Gutekunst, C.A., Leavitt, B.R., Hayden, M.R., Burke, J.R., Strittmatter, W.J. & Greenamyre, J.T. (2002) Early mitochondrial calcium defects in Huntington's disease are a direct effect of polyglutamines. *Nat Neurosci*, **5**, 731-736.

Pechnick, R.N. (1993) Effects of opioids on the hypothalamo-pituitary-adrenal axis. *Annu Rev Pharmacol Toxicol*, **33**, 353-382.

Perutz, M.F. (1995) Polar zippers: their role in human disease. *Pharm Acta Helv*, **69**, 213-224.

Peters, M.F., Nucifora, F.C., Jr., Kushi, J., Seaman, H.C., Cooper, J.K., Herring, W.J., Dawson, V.L., Dawson, T.M. & Ross, C.A. (1999) Nuclear targeting of mutant Huntingtin increases toxicity. *Mol Cell Neurosci*, **14**, 121-128.

Poirier, M.A., Jiang, H. & Ross, C.A. (2005) A structure-based analysis of huntingtin mutant polyglutamine aggregation and toxicity: evidence for a compact beta-sheet structure. *Hum Mol Genet*, **14**, 765-774.

Portera-Cailliau, C., Hedreen, J.C., Price, D.L. & Koliatsos, V.E. (1995) Evidence for apoptotic cell death in Huntington disease and excitotoxic animal models. *J Neurosci*, **15**, 3775-3787.

Preisinger, E., Jordan, B.M., Kazantsev, A. & Housman, D. (1999) Evidence for a recruitment and sequestration mechanism in Huntington's disease. *Philos Trans R Soc Lond B Biol Sci*, **354**, 1029-1034.

Pugh, B.F. & Tjian, R. (1990) Mechanism of transcriptional activation by Sp1: evidence for coactivators. *Cell*, **61**, 1187-1197.

Puigserver, P. & Spiegelman, B.M. (2003) Peroxisome proliferator-activated receptor-gamma coactivator 1 alpha (PGC-1 alpha): transcriptional coactivator and metabolic regulator. *Endocr Rev*, **24**, 78-90.

Qiu, Z., Norflus, F., Singh, B., Swindell, M.K., Buzescu, R., Bejarano, M., Chopra, R., Zucker, B., Benn, C.L., DiRocco, D.P., Cha, J.H., Ferrante, R.J. & Hersch, S.M. (2006) Sp1 is up-regulated in cellular and transgenic models of Huntington disease, and its reduction is neuroprotective. *J Biol Chem*, **281**, 16672-16680.

Ranum, L.P. & Cooper, T.A. (2006) RNA-mediated neuromuscular disorders. *Annu Rev Neurosci*, **29**, 259-277.

Raymond, L.A. (2003) Excitotoxicity in Huntington disease. *Clin Neurosci Res*, **3**, 121-128.

Reddy, P.H., Williams, M., Charles, V., Garrett, L., Pike-Buchanan, L., Whetsell, W.O., Jr., Miller, G. & Tagle, D.A. (1998) Behavioural abnormalities and selective neuronal loss in HD transgenic mice expressing mutated full-length HD cDNA. *Nat Genet*, **20**, 198-202.

Richfield, E.K., Maguire-Zeiss, K.A., Cox, C., Gilmore, J. & Voorn, P. (1995) Reduced expression of preproenkephalin in striatal neurons from Huntington's disease patients. *Ann Neurol*, **37**, 335-343.

Rigamonti, D., Bauer, J.H., De-Fraja, C., Conti, L., Sipione, S., Sciorati, C., Clementi, E., Hackam, A., Hayden, M.R., Li, Y., Cooper, J.K., Ross, C.A., Govoni, S., Vincenz, C. & Cattaneo, E. (2000) Wild-type huntingtin protects from apoptosis upstream of caspase-3. *J Neurosci*, **20**, 3705-3713.

Rincon-Limas, D.E., Krueger, D.A. & Patel, P.I. (1991) Functional characterization of the human hypoxanthine phosphoribosyltransferase gene promoter: evidence for a negative regulatory element. *Mol Cell Biol*, **11**, 4157-4164.

Rodriguez-Lebron, E., Denovan-Wright, E.M., Nash, K., Lewin, A.S. & Mandel, R.J. (2005) Intrastriatal rAAV-mediated delivery of anti-huntingtin shRNAs induces partial reversal of disease progression in R6/1 Huntington's disease transgenic mice. *Mol Ther*, **12**, 618-633.

Ross, C.A. (1995a) When more is less: pathogenesis of glutamine repeat neurodegenerative diseases. *Neuron*, **15**, 493-496.

Ross, C.A. (1997) Intranuclear neuronal inclusions: a common pathogenic mechanism for glutamine-repeat neurodegenerative diseases? *Neuron*, **19**, 1147-1150.

Ross, J. (1995b) mRNA stability in mammalian cells. *Microbiol Rev*, **59**, 423-450.

Rubinsztein, D.C. (2002) Lessons from animal models of Huntington's disease. *Trends Genet*, **18**, 202-209.

Rubinsztein, D.C., Leggo, J., Coles, R., Almqvist, E., Biancalana, V., Cassiman, J.J., Chotai, K., Connarty, M., Crauford, D., Curtis, A., Curtis, D., Davidson, M.J., Differ, A.M., Dode, C., Dodge, A., Frontali, M., Ranen, N.G., Stine, O.C., Sherr, M., Abbott, M.H., Franz, M.L., Graham, C.A., Harper, P.S., Hedreen, J.C., Hayden, M.R. & et al. (1996) Phenotypic characterization of individuals with 30-40 CAG repeats in the Huntington disease (HD) gene reveals HD cases with 36 repeats and apparently normal elderly individuals with 36-39 repeats. *Am J Hum Genet*, **59**, 16-22.

Sabol, S.L., Yoshikawa, K. & Hong, J.S. (1983) Regulation of methionine-enkephalin precursor messenger RNA in rat striatum by haloperidol and lithium. *Biochem Biophys Res Commun*, **113**, 391-399.

Sadri-Vakili, G. & Cha, J.H. (2006) Mechanisms of disease: Histone modifications in Huntington's disease. *Nat Clin Pract Neurol*, **2**, 330-338.

Salzet, M., Vieau, D. & Day, R. (2000) Crosstalk between nervous and immune systems through the animal kingdom: focus on opioids. *Trends Neurosci*, **23**, 550-555.

Sambrook, J., Fritsch, E.F. & Maniatis, T. (2000) Molecular Cloning: a Laboratory Manual, 3rd ed. Cold Spring Harbor Laboratory Press, Cold Spring Harbor, New York.

Sanchez, I., Xu, C.J., Juo, P., Kakizaka, A., Blenis, J. & Yuan, J. (1999) Caspase-8 is required for cell death induced by expanded polyglutamine repeats. *Neuron*, **22**, 623-633.

Sathasivam, K., Hobbs, C., Turmaine, M., Mangiarini, L., Mahal, A., Bertaux, F., Wanker, E.E., Doherty, P., Davies, S.W. & Bates, G.P. (1999) Formation of polyglutamine inclusions in non-CNS tissue. *Hum Mol Genet*, **8**, 813-822.

Saudou, F., Finkbeiner, S., Devys, D. & Greenberg, M.E. (1998) Huntingtin acts in the nucleus to induce apoptosis but death does not correlate with the formation of intranuclear inclusions. *Cell*, **95**, 55-66.

Sawadogo, M. & Roeder, R.G. (1984) Energy requirement for specific transcription initiation by the human RNA polymerase II system. *J Biol Chem*, **259**, 5321-5326.

Schaffar, G., Breuer, P., Boteva, R., Behrends, C., Tzvetkov, N., Strippel, N., Sakahira, H., Siegers, K., Hayer-Hartl, M. & Hartl, F.U. (2004) Cellular toxicity of polyglutamine expansion proteins: mechanism of transcription factor deactivation. *Mol Cell*, **15**, 95-105.

Schalling, M., Djurfeldt, M., Hokfelt, T., Ehrlich, M., Kurihara, T. & Greengard, P. (1990) Distribution and cellular localization of DARPP-32 mRNA in rat brain. *Brain Res Mol Brain Res*, **7**, 139-149.

Schilling, G., Sharp, A.H., Loev, S.J., Wagster, M.V., Li, S.H., Stine, O.C. & Ross, C.A. (1995) Expression of the Huntington's disease (IT15) protein product in HD patients. *Hum Mol Genet*, **4**, 1365-1371.

Schilling, G., Becher, M.W., Sharp, A.H., Jinnah, H.A., Duan, K., Kotzuk, J.A., Slunt, H.H., Ratovitski, T., Cooper, J.K., Jenkins, N.A., Copeland, N.G., Price, D.L., Ross, C.A. & Borchelt, D.R. (1999) Intranuclear inclusions and neuritic aggregates in transgenic mice expressing a mutant N-terminal fragment of huntingtin. *Hum Mol Genet*, **8**, 397-407.

Schmidt, E.V., Christoph, G., Zeller, R. & Leder, P. (1990) The cytomegalovirus enhancer: a pan-active control element in transgenic mice. *Mol Cell Biol*, **10**, 4406-4411.

Sharp, A.H., Loev, S.J., Schilling, G., Li, S.H., Li, X.J., Bao, J., Wagster, M.V., Kotzuk, J.A., Steiner, J.P., Lo, A. & et al. (1995) Widespread expression of Huntington's disease gene (IT15) protein product. *Neuron*, **14**, 1065-1074.

Shelbourne, P.F., Killeen, N., Hevner, R.F., Johnston, H.M., Tecott, L., Lewandoski, M., Ennis, M., Ramirez, L., Li, Z., Iannicola, C., Littman, D.R. & Myers, R.M. (1999) A Huntington's disease CAG expansion at the murine Hdh locus is unstable and associated with behavioural abnormalities in mice. *Hum Mol Genet*, **8**, 763-774.

Shimohata, T., Nakajima, T., Yamada, M., Uchida, C., Onodera, O., Naruse, S., Kimura, T., Koide, R., Nozaki, K., Sano, Y., Ishiguro, H., Sakoe, K., Ooshima, T., Sato, A., Ikeuchi, T., Oyake, M., Sato, T., Aoyagi, Y., Hozumi, I., Nagatsu, T., Takiyama, Y., Nishizawa, M., Goto, J., Kanazawa, I., Davidson, I., Tanese, N., Takahashi, H. & Tsuji, S. (2000) Expanded polyglutamine stretches interact with TAFII130, interfering with CREB-dependent transcription. *Nat Genet*, **26**, 29-36.

Sipione, S. & Cattaneo, E. (2001) Modeling Huntington's disease in cells, flies, and mice. *Mol Neurobiol*, **23**, 21-51.

Sipione, S., Rigamonti, D., Valenza, M., Zuccato, C., Conti, L., Pritchard, J., Kooperberg, C., Olson, J.M. & Cattaneo, E. (2002) Early transcriptional profiles in huntingtin-inducible striatal cells by microarray analyses. *Hum Mol Genet*, **11**, 1953-1965.

Sisodia, S.S. (1998) Nuclear inclusions in glutamine repeat disorders: are they pernicious, coincidental, or beneficial? *Cell*, **95**, 1-4.

Smith, C.L. & Hager, G.L. (1997) Transcriptional regulation of mammalian genes *in vivo*. A tale of two templates. *J Biol Chem*, **272**, 27493-27496.

Snell, R.G., MacMillan, J.C., Cheadle, J.P., Fenton, I., Lazarou, L.P., Davies, P., MacDonald, M.E., Gusella, J.F., Harper, P.S. & Shaw, D.J. (1993) Relationship between trinucleotide repeat expansion and phenotypic variation in Huntington's disease. *Nat Genet*, **4**, 393-397.

Sorensen, A.N. & Claesson, M.H. (1998) Effect of the opioid methionine enkephalinamide on signal transduction in human T-lymphocytes. *Life Sci*, **62**, 1251-1259.

Steffan, J.S., Kazantsev, A., Spasic-Boskovic, O., Greenwald, M., Zhu, Y.Z., Gohler, H., Wanker, E.E., Bates, G.P., Housman, D.E. & Thompson, L.M. (2000) The Huntington's disease protein interacts with p53 and CREB-binding protein and represses transcription. *Proc Natl Acad Sci U S A*, **97**, 6763-6768.

Steffan, J.S., Bodai, L., Pallos, J., Poelman, M., McCampbell, A., Apostol, B.L., Kazantsev, A., Schmidt, E., Zhu, Y.Z., Greenwald, M., Kurokawa, R., Housman, D.E., Jackson, G.R., Marsh, J.L. & Thompson, L.M. (2001) Histone deacetylase inhibitors arrest polyglutamine-dependent neurodegeneration in Drosophila. *Nature*, **413**, 739-743.

Stenberg, R.M., Thomsen, D.R. & Stinski, M.F. (1984) Structural analysis of the major immediate early gene of human cytomegalovirus. *J Virol*, **49**, 190-199.

Stinski, M.F., Thomsen, D.R. & Rodriguez, J.E. (1982) Synthesis of human cytomegalovirus-specified RNA and protein in interferon-treated cells at early times after infection. *J Gen Virol*, **60**, 261-270.

Stinski, M.F., Thomsen, D.R., Stenberg, R.M. & Goldstein, L.C. (1983) Organization and expression of the immediate early genes of human cytomegalovirus. *J Virol*, **46**, 1-14.

St-Pierre, J., Drori, S., Uldry, M., Silvaggi, J.M., Rhee, J., Jager, S., Handschin, C., Zheng, K., Lin, J., Yang, W., Simon, D.K., Bachoo, R. & Spiegelman, B.M. (2006) Suppression of reactive oxygen species and neurodegeneration by the PGC-1 transcriptional coactivators. *Cell*, **127**, 397-408.

Sugars, K.L. & Rubinsztein, D.C. (2003) Transcriptional abnormalities in Huntington disease. *Trends Genet*, **19**, 233-238.

Sugars, K.L., Brown, R., Cook, L.J., Swartz, J. & Rubinsztein, D.C. (2004) Decreased cAMP response element-mediated transcription: an early event in exon 1 and full-length cell models of Huntington's disease that contributes to polyglutamine pathogenesis. *J Biol Chem*, **279**, 4988-4999.

Suhr, S.T., Senut, M.C., Whitelegge, J.P., Faull, K.F., Cuizon, D.B. & Gage, F.H. (2001) Identities of sequestered proteins in aggregates from cells with induced polyglutamine expression. *J Cell Biol*, **153**, 283-294.

Sun, Y., Savanenin, A., Reddy, P.H. & Liu, Y.F. (2001) Polyglutamine-expanded huntingtin promotes sensitization of N-methyl-D-aspartate receptors via post-synaptic density 95. *J Biol Chem*, **276**, 24713-24718.

Sun, Z., Del Mar, N., Meade, C., Goldowitz, D. & Reiner, A. (2002) Differential changes in striatal projection neurons in R6/2 transgenic mice for Huntington's disease. *Neurobiol Dis*, **11**, 369-385.

Szekely, J.I. (1990) Opioid peptides and stress. *Crit Rev Neurobiol*, **6**, 1-12.

Takano, H. & Gusella, J.F. (2002) The predominantly HEAT-like motif structure of huntingtin and its association and coincident nuclear entry with dorsal, an NF-kB/Rel/dorsal family transcription factor. *BMC Neurosci*, **3**, 15.

Tang, F., Costa, E. & Schwartz, J.P. (1983) Increase of proenkephalin mRNA and enkephalin content of rat striatum after daily injection of haloperidol for 2 to 3 weeks. *Proc Natl Acad Sci U S A*, **80**, 3841-3844.

Telenius, H., Kremer, H.P., Theilmann, J., Andrew, S.E., Almqvist, E., Anvret, M., Greenberg, C., Greenberg, J., Lucotte, G., Squitieri, F. & et al. (1993) Molecular analysis of juvenile Huntington disease: the major influence on (CAG)n repeat length is the sex of the affected parent. *Hum Mol Genet*, **2**, 1535-1540.

Telenius, H., Almqvist, E., Kremer, B., Spence, N., Squitieri, F., Nichol, K., Grandell, U., Starr, E., Benjamin, C., Castaldo, I. & et al. (1995) Somatic mosaicism in sperm is associated with intergenerational (CAG)n changes in Huntington disease. *Hum Mol Genet*, **4**, 189-195.

Terrence, C.F. (1976) Fluphenazine decanoate in the treatment of chorea: a double-blind study. *Curr Ther Res Clin Exp*, **20**, 177-183.

The Huntington's Disease Collaborative Research Group. (1993) A novel gene containing a trinucleotide repeat that is expanded and unstable on Huntington's disease chromosomes. *Cell*, **72**, 971-983.

Thomas, E.A. (2006) Striatal specificity of gene expression dysregulation in Huntington's disease. *J Neurosci Res*, **84**, 1151-1164.

Thomsen, D.R., Stenberg, R.M., Goins, W.F. & Stinski, M.F. (1984) Promoter-regulatory region of the major immediate early gene of human cytomegalovirus. *Proc Natl Acad Sci U S A*, **81**, 659-663.

Tjian, R. (1996) The biochemistry of transcription in eukaryotes: a paradigm for multisubunit regulatory complexes. *Philos Trans R Soc Lond B Biol Sci*, **351**, 491-499.

Tokunaga, K., Taniguchi, H., Yoda, K., Shimizu, M. & Sakiyama, S. (1986) Nucleotide sequence of a full-length cDNA for mouse cytoskeletal beta-actin mRNA. *Nucleic Acids Res*, **14**, 2829.

Trettel, F., Rigamonti, D., Hilditch-Maguire, P., Wheeler, V.C., Sharp, A.H., Persichetti, F., Cattaneo, E. & MacDonald, M.E. (2000) Dominant phenotypes produced by the HD mutation in STHdh(Q111) striatal cells. *Hum Mol Genet*, **9**, 2799-2809.

Truant, R. (2003) Nucleocytoplasmic transport of huntingtin and Huntington's disease. *Clin Neurosci Res*, **3**, 157-164.

Turmaine, M., Raza, A., Mahal, A., Mangiarini, L., Bates, G.P. & Davies, S.W. (2000) Nonapoptotic neurodegeneration in a transgenic mouse model of Huntington's disease. *Proc Natl Acad Sci U S A*, **97**, 8093-8097.

Udenfriend, S. & Kilpatrick, D.L. (1983) Biochemistry of the enkephalins and enkephalin-containing peptides. *Arch Biochem Biophys*, **221**, 309-323.

van Dellen, A., Welch, J., Dixon, R.M., Cordery, P., York, D., Styles, P., Blakemore, C. & Hannan, A.J. (2000) N-Acetylaspartate and DARPP-32 levels decrease in the corpus striatum of Huntington's disease mice. *Neuroreport*, **11**, 3751-3757.

Van Raamsdonk, J.M., Pearson, J., Rogers, D.A., Lu, G., Barakauskas, V.E., Barr, A.M., Honer, W.G., Hayden, M.R. & Leavitt, B.R. (2005) Ethyl-EPA treatment improves motor dysfunction, but not neurodegeneration in the YAC128 mouse model of Huntington disease. *Exp Neurol*, **196**, 266-272.

Vogelauer, M., Wu, J., Suka, N. & Grunstein, M. (2000) Global histone acetylation and deacetylation in yeast. *Nature*, **408**, 495-498.

Vonsattel, J.P., Myers, R.H., Stevens, T.J., Ferrante, R.J., Bird, E.D. & Richardson, E.P., Jr. (1985) Neuropathological classification of Huntington's disease. *J Neuropathol Exp Neurol*, **44**, 559-577.

Vonsattel, J.P. & DiFiglia, M. (1998) Huntington disease. *J Neuropathol Exp Neurol*, **57**, 369-384.

Waelter, S., Boeddrich, A., Lurz, R., Scherzinger, E., Lueder, G., Lehrach, H. & Wanker, E.E. (2001a) Accumulation of mutant huntingtin fragments in aggresome-like inclusion bodies as a result of insufficient protein degradation. *Mol Biol Cell*, **12**, 1393-1407.

Waelter, S., Scherzinger, E., Hasenbank, R., Nordhoff, E., Lurz, R., Goehler, H., Gauss, C., Sathasivam, K., Bates, G.P., Lehrach, H. & Wanker, E.E. (2001b) The huntingtin interacting protein HIP1 is a clathrin and alpha-adaptin-binding protein involved in receptor-mediated endocytosis. *Hum Mol Genet*, **10**, 1807-1817.

Walaas, S.I. & Greengard, P. (1984) DARPP-32, a dopamine- and adenosine 3':5'-monophosphate-regulated phosphoprotein enriched in dopamine-innervated brain regions. I. Regional and cellular distribution in the rat brain. *J Neurosci*, **4**, 84-98.

Wanker, E.E., Rovira, C., Scherzinger, E., Hasenbank, R., Walter, S., Tait, D., Colicelli, J. & Lehrach, H. (1997) HIP-I: a huntingtin interacting protein isolated by the yeast two-hybrid system. *Hum Mol Genet*, **6**, 487-495.

Waragai, M., Lammers, C.H., Takeuchi, S., Imafuku, I., Udagawa, Y., Kanazawa, I., Kawabata, M., Mouradian, M.M. & Okazawa, H. (1999) PQBP-1, a novel polyglutamine tract-binding protein, inhibits transcription activation by Brn-2 and affects cell survival. *Hum Mol Genet*, **8**, 977-987.

Watts, R.W., Harkness, R.A., Spellacy, E. & Taylor, N.F. (1987) Lesch-Nyhan syndrome: growth delay, testicular atrophy and a partial failure of the 11 beta-hydroxylation of steroids. *J Inherit Metab Dis*, **10**, 210-223.

Weisinger, G., DeCristofaro, J.D. & LaGamma, E.F. (1990) Multiple preproenkephalin transcriptional start sites are induced by stress and cholinergic pathways. *J Biol Chem*, **265**, 17389-17392.

Wellington, C.L., Ellerby, L.M., Hackam, A.S., Margolis, R.L., Trifiro, M.A., Singaraja, R., McCutcheon, K., Salvesen, G.S., Propp, S.S., Bromm, M., Rowland, K.J., Zhang, T., Rasper, D., Roy, S., Thornberry, N., Pinsky, L., Kakizuka, A., Ross, C.A., Nicholson, D.W., Bredesen, D.E. & Hayden, M.R. (1998) Caspase cleavage of gene products associated with triplet expansion disorders generates truncated fragments containing the polyglutamine tract. *J Biol Chem*, **273**, 9158-9167.

Wellington, C.L., Singaraja, R., Ellerby, L., Savill, J., Roy, S., Leavitt, B., Cattaneo, E., Hackam, A., Sharp, A., Thornberry, N., Nicholson, D.W., Bredesen, D.E. & Hayden, M.R. (2000) Inhibiting caspase cleavage of huntingtin reduces toxicity and aggregate formation in neuronal and nonneuronal cells. *J Biol Chem*, **275**, 19831-19838.

Wellington, C.L., Ellerby, L.M., Gutekunst, C.A., Rogers, D., Warby, S., Graham, R.K., Loubser, O., van Raamsdonk, J., Singaraja, R., Yang, Y.Z., Gafni, J., Bredesen, D., Hersch, S.M., Leavitt, B.R., Roy, S., Nicholson, D.W. & Hayden, M.R. (2002) Caspase cleavage of mutant huntingtin precedes neurodegeneration in Huntington's disease. *J Neurosci*, **22**, 7862-7872.

Wexler, N.S., Young, A.B., Tanzi, R.E., Travers, H., Starosta-Rubinstein, S., Penney, J.B., Snodgrass, S.R., Shoulson, I., Gomez, F., Ramos Arroyo, M.A. & et al. (1987) Homozygotes for Huntington's disease. *Nature*, **326**, 194-197.

Wexler, N.S., Lorimer, J., Porter, J., Gomez, F., Moskowitz, C., Shackell, E., Marder, K., Penchaszadeh, G., Roberts, S.A., Gayan, J., Brocklebank, D., Cherny, S.S., Cardon, L.R., Gray, J., Dlouhy, S.R., Wiktorski, S., Hodes, M.E., Conneally, P.M., Penney, J.B., Gusella, J., Cha, J.H., Irizarry, M., Rosas, D., Hersch, S., Hollingsworth, Z., MacDonald, M., Young, A.B., Andresen, J.M., Housman, D.E., De Young, M.M., Bonilla, E., Stillings, T., Negrette, A., Snodgrass, S.R., Martinez-Jaurrieta, M.D., Ramos-Arroyo, M.A., Bickham, J., Ramos, J.S., Marshall, F., Shoulson, I., Rey, G.J., Feigin, A., Arnheim, N., Acevedo-Cruz, A., Acosta, L., Alvir, J., Fischbeck, K., Thompson, L.M., Young, A., Dure, L., O'Brien, C.J., Paulsen, J., Brickman, A., Krch, D., Peery, S., Hogarth, P., Higgins, D.S., Jr. & Landwehrmeyer, B. (2004) Venezuelan kindreds reveal that genetic and environmental factors modulate Huntington's disease age of onset. *Proc Natl Acad Sci U S A*, **101**, 3498-3503.

Weydt, P., Pineda, V.V., Torrence, A.E., Libby, R.T., Satterfield, T.F., Lazarowski, E.R., Gilbert, M.L., Morton, G.J., Bammler, T.K., Strand, A.D., Cui, L., Beyer, R.P., Easley, C.N., Smith, A.C., Krainc, D., Luquet, S., Sweet, I.R., Schwartz, M.W. & La Spada, A.R. (2006) Thermoregulatory and metabolic defects in Huntington's disease transgenic mice implicate PGC-1alpha in Huntington's disease neurodegeneration. *Cell Metab*, **4**, 349-362.

Wheeler, V.C., Auerbach, W., White, J.K., Srinidhi, J., Auerbach, A., Ryan, A., Duyao, M.P., Vrbanac, V., Weaver, M., Gusella, J.F., Joyner, A.L. & MacDonald, M.E. (1999) Length-dependent gametic CAG repeat instability in the Huntington's disease knock-in mouse. *Hum Mol Genet*, **8**, 115-122.

Wheeler, V.C., White, J.K., Gutekunst, C.A., Vrbanac, V., Weaver, M., Li, X.J., Li, S.H., Yi, H., Vonsattel, J.P., Gusella, J.F., Hersch, S., Auerbach, W., Joyner, A.L. & MacDonald, M.E. (2000) Long glutamine tracts cause nuclear localization of a novel form of huntingtin in medium spiny striatal neurons in HdhQ92 and HdhQ111 knock-in mice. *Hum Mol Genet*, **9**, 503-513.

White, J.K., Auerbach, W., Duyao, M.P., Vonsattel, J.P., Gusella, J.F., Joyner, A.L. & MacDonald, M.E. (1997) Huntingtin is required for neurogenesis and is not impaired by the Huntington's disease CAG expansion. *Nat Genet*, **17**, 404-410.

Wyttenbach, A., Swartz, J., Kita, H., Thykjaer, T., Carmichael, J., Bradley, J., Brown, R., Maxwell, M., Schapira, A., Orntoft, T.F., Kato, K. & Rubinsztein, D.C. (2001) Polyglutamine expansions cause decreased CRE-mediated transcription and early gene expression changes prior to cell death in an inducible cell model of Huntington's disease. *Hum Mol Genet*, **10**, 1829-1845.

Xia, J., Lee, D.H., Taylor, J., Vandelft, M. & Truant, R. (2003) Huntingtin contains a highly conserved nuclear export signal. *Hum Mol Genet*, **12**, 1393-1403.

Yamamoto, A., Lucas, J.J. & Hen, R. (2000) Reversal of neuropathology and motor dysfunction in a conditional model of Huntington's disease. *Cell*, **101**, 57-66.

Yohrling, G.J., Farrell, L.A., Hollenberg, A.N. & Cha, J.H. (2003) Mutant huntingtin increases nuclear corepressor function and enhances ligand-dependent nuclear hormone receptor activation. *Mol Cell Neurosci*, **23**, 28-38.

Young, A.B., Greenamyre, J.T., Hollingsworth, Z., Albin, R., D'Amato, C., Shoulson, I. & Penney, J.B. (1988) NMDA receptor losses in putamen from patients with Huntington's disease. *Science*, **241**, 981-983.

Zeitlin, S., Liu, J.P., Chapman, D.L., Papaioannou, V.E. & Efstratiadis, A. (1995) Increased apoptosis and early embryonic lethality in mice nullizygous for the Huntington's disease gene homologue. *Nat Genet*, **11**, 155-163.

Zeron, M.M., Chen, N., Moshaver, A., Lee, A.T., Wellington, C.L., Hayden, M.R. & Raymond, L.A. (2001) Mutant huntingtin enhances excitotoxic cell death. *Mol Cell Neurosci*, **17**, 41-53.

Zhai, W., Jeong, H., Cui, L., Krainc, D. & Tjian, R. (2005) *In vitro* analysis of huntingtin-mediated transcriptional repression reveals multiple transcription factor targets. *Cell*, **123**, 1241-1253.

Zhong, F., Li, X.Y., Yang, S.L., Stefano, G.B., Fimiani, C. & Bilfinger, T.V. (1998) Methionine-enkephalin stimulates interleukin-6 mRNA expression: human plasma levels in coronary artery bypass grafting. *Int J Cardiol*, **64 Suppl 1**, S53-59.

Zuccato, C., Ciammola, A., Rigamonti, D., Leavitt, B.R., Goffredo, D., Conti, L., MacDonald, M.E., Friedlander, R.M., Silani, V., Hayden, M.R., Timmusk, T., Sipione, S. & Cattaneo, E. (2001) Loss of huntingtin-mediated BDNF gene transcription in Huntington's disease. *Science*, **293**, 493-498.

Zuccato, C., Tartari, M., Crotti, A., Goffredo, D., Valenza, M., Conti, L., Cataudella, T., Leavitt, B.R., Hayden, M.R., Timmusk, T., Rigamonti, D. & Cattaneo, E. (2003) Huntingtin interacts with REST/NRSF to modulate the transcription of NRSE-controlled neuronal genes. *Nat Genet*, **35**, 76-83.

Zuccato, C., Liber, D., Ramos, C., Tarditi, A., Rigamonti, D., Tartari, M., Valenza, M. & Cattaneo, E. (2005) Progressive loss of BDNF in a mouse model of Huntington's disease and rescue by BDNF delivery. *Pharmacol Res*, **52**, 133-139.